
Synthesis and Evaluation of Novel Antifungal Agents targeting the Fungal Plasma Membrane H⁺-ATPase

Dhruvnesht Vijaykumar Patel

*A thesis submitted to the University of Hertfordshire in partial fulfilment
of the requirements for the degree award of:*

Doctor of Philosophy

February 2020

DECLARATION

I, Dhruvnesh Vijaykumar Patel, confirm that the work presented in this thesis is my own.

Where information has been derived from other sources, I confirm that this has been indicated in the thesis.

ABSTRACT

Fungal infections now contribute significantly to microbe-related morbidity and mortality due to there being a limited number of available antifungal agents and limited modes of delivery. Over the past two decades, many pathogenic fungi have developed various modes of resistance to commonly used antifungals. Thus there is a need for novel antifungal agents with novel mechanisms of action. Inhibition of the essential plasma membrane (PM) H⁺-ATPase of fungi is a potentially effective therapeutic approach in antifungal drug discovery. In order to investigate this, three series (A-C) consisting of a total of thirty-three symmetrical 1,4-diene-3-one (**22a-v**, **23a-h** and **24a-c**) compounds have been synthesized.

In vitro macro-broth susceptibility testing of 1,4-diene-3-ones showed wide range of inhibition against *Saccharomyces cerevisiae* (0.2 - 99%) and *Candida albicans* (0 - 99%). Compounds **22f**, **22m**, **22n** and **22s** exhibited highest potency than other compounds from the library against *S. cerevisiae* (IC₅₀ = 1.21, 2.22, 0.62 and 1.87 μM), however these compounds demonstrated limited activity against *C. albicans* (IC₅₀ = 114, 525, 474 and 666 μM). In contrast, compounds **23f**, **23g** and **23h** exhibited a higher degree of antifungal activity against *C. albicans* (IC₅₀ = 68.5, 57.6 and 50.7 μM) and these compounds also showed good potency against *S. cerevisiae* (IC₅₀ = 8.46, 5.52 and 6.25 μM).

To gain an understanding about the mechanism of action of 1,4-diene-3-ones, the H⁺-ATPase mediated proton pumping by *S. cerevisiae* was investigated by measuring the pH of the glucose-induced acidification of the external medium. The bis-pyridylidene derivatives of N-methylpiperidin-4-one (**23a-c**, 60 μM) were determined to be the most potent inhibitors of H⁺ efflux from *S. cerevisiae* and the steady state of proton flux from *S. cerevisiae* was achieved

within 10 minutes of medium acidification. A similar result was observed with N-ethylmaleimide (NEM, 60 μ M, positive control). Additionally, **23a**, **23b** and **23c** have shown good potency in the macro broth susceptibility assay of *S. cerevisiae* (IC_{50} = 12.6, 8.84 and 9.45 μ M). Moreover, the most potent compounds **22n** and **23h** in macro broth susceptibility assay against *S. cerevisiae* and *C. albicans* exhibited limited activity to inhibit the proton efflux from *S. cerevisiae*.

To further elucidate the mechanism of action, preliminary structure-activity relationship (SAR) studies was performed. SAR of bis-benzylidene derivatives of N-methylpiperidin-4-one displayed reasonable correlation coefficient (R^2 = 0.6746) between the inhibitory activity expressed as $\log(1/IC_{50})$ and an electronic parameter, the 1H -NMR δ -values of proton on the β -carbon. Conversely, SAR of $\log(1/IC_{50})$ and a lipophilic parameter, calculated $\log P$ (clogP) of bis-benzylidene derivatives of N-methylpiperidin-4-one showed R^2 of 0.4138. This indicates that the inhibitory activity of compounds is due to the influence of electronic property rather than the lipophilic property. In conclusion, the inhibitory action of 1,4-diene-3-ones on yeast suggests a membrane-bound enzyme target for its action. It is hypothesized that these compounds form a covalent C-S thio-ether bond with cysteine residues of proteins of the plasma membrane and eventually inhibit the H^+ -ATPase.

ACKNOWLEDGEMENTS

I would like to thank my primary supervisor Dr. David Griffiths for sharing his enormous knowledge, providing his support and guidance during my entire research project. His passion for the research had encouraged me to develop my research skills and become a pro-active researcher. I would also like to thank my co-supervisor Dr. Jatinder Paul Bassin for helping me with synthetic chemistry, NMR, Mass Spectrometry and his guidance on my research project.

I would like to express my gratitude to Dr. Mark Scott for training me on analytical equipment including the NMR and Mass Spectrometers. I would also like to thank Mr. James Stanley and Mr. Virendra Shah for their support and assistance in the chemistry research laboratory. In addition, I am very pleased to have great friends like Hassan Farah, Kathryn Kellett and Pushpendra Goswami in my research office who supported me and encouraged me to make this journey more enjoyable.

I would like to acknowledge my aunt Mrs. Chandrikaben Jitendra Patel for providing me financial support which enabled me to study this research programme. I would like to thank my family Mr. Vijaykumar Patel, Mrs. Kalpanaben Patel, my brother Mr. Harshil Patel, my wife Mrs. Rima Patel and recent arrival in my family Ms. Vihaa Patel who have kept their patience with me and provided their emotional support during my research project. I would like to dedicate this thesis to my late father Mr. Vijaykumar Patel, as it was his wish that I will complete this Ph.D. I am very grateful to have a caring and responsible wife Mrs. Rima Patel who has supported me in the final two years of my Ph.D. and during my thesis-write up period.

Abbreviations

2-D	Two-dimensional
3-D	Three-dimensional
A-ATPase	Archaea ATPase
ABC	ATP-binding cassette transporter
ADME	Absorption, distribution, metabolism and excretion
A-domain	Actuator domain
ADP	Adenosine diphosphate
Al ³⁺	Aluminium cation
AMP	Adenosine monophosphate
ANN	Artificial neural network
ANOVA	Analysis of variance
A _s	Slope factor
ATCC	American Type Culture Collection
ATP	Adenosine triphosphate
AUC	Area under the curve
br	Broad
BRANN	Bayesian-regulated artificial neural network
C=O	Carbonyl
Ca ²⁺	Calcium cation
Cd ²⁺	Cadmium cation
CDCl ₃	Deuterated chloroform
CDR1	Cerebellar degeneration related protein
CFU	Colony forming unit
CH=	Olefinic group
CLSI	Clinical and Laboratory Standards Institute
CoMFA	Comparative Molecular Field Analysis
COMT	Catechol-O-methyltransferase
COOH	Carboxylic acid
Cu ²⁺	Copper cation
CYP51	Cytochrome P450 14 α -sterol demethylase
D	Deuterium
d	Doublet
DCM	Dichloromethane
dd	Doublet of doublets
DEPT	Distortionless Enhancement by Polarization Transfer
DMSO	Dimethyl sulfoxide
DNA	Deoxyribonucleic acid
E-ATPase	Extracellular ATPase
EF2	Elongation factor 2

ERG11	Lanosterol 14 α -demethylase encoded by ergosterol biosynthesis gene
ESI	Electrospray ionisation
EtOH	Ethanol
EUCAST	European Committee on Antimicrobial Susceptibility Testing
F-ATPase	ATP synthase / F ₀ F ₁ -ATPase
Fe ³⁺	Iron (ferric) cation
FITC	Fluorescein isothiocyanate
FTIR	Fourier Transform Infrared
h	Hill slope
H	Hydrogen
HCl	Hydrochloric acid
Hill slope	Slope factor in sigmoidal dose response curves or Hill coefficient
HIV	Human Immune-deficiency Virus
HPLC	High Pressure (or performance) Liquid Chromatography
HSV	Herpes simplex virus
Hz	Hertz
I ₅₀	Asymptotic 50% inhibitory concentration at point of inflection of a sigmoidal dose response curve
IC _{10, 25, 50, 90}	Inhibitory concentrations at 10%, 25%, 50% and 90% of a dose-response curve
IMPS	Invalid metabolic panaceas compounds
IFIs	Invasive fungal infections
J values	Coupling constant in NMR spectra
K ⁺	Potassium cation
KCl	Potassium chloride
LC-MS	Liquid Chromatography Mass Spectrometry
log <i>P</i>	Measure of lipophilicity
MALDI-TOF	Matrix-assisted laser desorption or ionization time of flight
MALDI-MS	Matrix-assisted laser desorption or ionization mass spectrometry
m	Multiplet
M.Pt	Melting point
m/z	Mass ionization
MB	Methylene blue
MEA	Malt extract agar
MEB	Malt extract broth
MFC	Minimal fungicidal concentration
MFS pump	Major facilitator pump
Mg ²⁺	Magnesium cation
MIC	Minimal inhibitory concentration
MLC	Minimal lethal concentration
MLR	Multiple linear regression
MOE	Molecular Orbital Environment

MDR1	Multidrug resistance gene 1
MRA	Multiple regression analysis
MRR1	Multidrug resistance regulator 1
N/R	Did not reach a specific level of inhibition
Na ²⁺	Sodium cation
NaOH	Sodium hydroxide
NCYC	National Collection of Yeast Cultures
N-domain	Nucleotide binding domain
NEM	N-ethyl maleimide
NH ₂	Amine
NMR	Nuclear Magnetic Resonance Spectroscopy
OH	Hydroxyl
P-450 _{DM}	Cytochrome P-4540-dependent 14 α -sterol demethylase enzyme
PAINS	Pan-assay interference compounds
P-ATPase	Phosphorylated ATPase
Pb ²⁺	Lead cation
PCA	Principal component analysis
PCR	Polymerase chain reaction
P-domain	Phosphorylation domain
pH _i	Internal pH (of a cell)
P _i	Free phosphate
PM	Plasma membrane
ppm	Parts per million
psi	Atmospheric pressure (pounds per square inch) used in moist heat autoclave
q	Quartet
QSAR	Quantitative Structure-Activity Relationship
R ²	Coefficient of determination
RIF	Relative inhibition factor
RNA	Ribonucleic acid
s	Singlet
SAR	Structure-Activity Relationship
SD	Standard deviation
S-domain	Specific support domain
SERCA	Sarcoplasmic reticulum Ca ²⁺ -ATPase
SFIs	Superficial fungal infections
SH	Sulfhydryl group
spp	Species
t	triplet
T-domain	Transport domain
TLC	Thin-layer chromatography
TM	Transmembrane
UH	University of Hertfordshire

UV	Ultraviolet
UV-Vis	Ultraviolet visible spectroscopy
V-ATPase	Vacuolar ATPase
YPD	Bacteriological peptone, yeast extract and glucose
Zn ²⁺	Zinc cation
ΔpH	Difference in the pH across a cell membrane or pH gradient
$\Delta\text{pH}_{\text{ir}}$	Change in pH in terms of the initial rate after 1 min
$\Delta\text{pH}_{\text{max}}$	Change in pH in terms of the total extent after 30 mins
$\Delta\Psi_{\text{H}^+}$	Electrical potential due to protons
$\Delta\Psi_{\text{K}^+}$	Electrical potential due to Potassium ions
Π	QSAR descriptor lipophilicity index
σ	Hammett substituent constant

Contents

DECLARATION	I
ABSTRACT	II
ACKNOWLEDGEMENTS.....	IV
ABBREVIATIONS	V
CONTENTS.....	IX
LIST OF TABLES.....	XIII
LIST OF FIGURES.....	XIV
1 GENERAL INTRODUCTION	2
1.1 Introduction	2
1.2 Fungi	2
1.2.1 The genus <i>Saccharomyces</i>	3
1.2.2 The genus <i>Candida</i>	5
1.3 Fungal infections.....	6
1.3.1 Superficial fungal infections	7
1.3.2 Invasive fungal infections.....	9
1.4 Background to antifungal agents and drug targets.....	11
1.4.1 Overview of the classes of currently available antifungal agents.....	14
1.4.1.1 Polyenes and macrolides.....	14
1.4.1.2 Azoles and triazoles	15
1.4.1.3 Allylamines.....	18
1.4.1.4 Echinocandins	19
1.4.1.5 Other antifungal agents.....	21
1.5 Drug resistance in fungi.....	22
1.6 Identification of novel antifungal drug target	24
1.6 ATPase and ATP synthase enzymes	27
1.7.1 Types of ATPases	28
1.7.1.1 F-type ATPases.....	28

1.7.1.2 A-type ATPases	29
1.7.1.3 V-type ATPases	29
1.7.1.4 E-type ATPases	30
1.7.1.5 P-type ATPases	30
1.7.1.5.1 Reaction mechanism of the plasma membrane H ⁺ -ATPase	33
1.8 Compounds known to react with cellular thiols	34
1.8.1 Maleimides	35
1.8.2 Omeprazole	36
1.8.3 Curcumin	38
1.8.4 Chalcones	39
1.8.5 Ebselen	39
1.8.6 Caffeic acid	40
1.8.7 Other sulfhydryl reactive natural products	41
1.9 Structure-activity relationship (SAR)	43
1. 10 Aims and scope	49
1.10.1 Objectives	49
2 SYNTHESIS AND CHARACTERIZATION OF 1,4-DIENE-3-ONES.....	52
2.1 Introduction	52
2.2 Materials and Methods.....	54
2.2.1 Materials	54
2.2.2 Experimental section.....	56
2.2.2.1 General method for the synthesis of ring substituted bis(benzylidene) derivatives of methylpiperidin-4-one, cyclopentanone and cyclohexanone.....	56
2.2.2.2 Preparation of bis-pyridylidene derivatives of N-methylpiperidin-4-one and cycloalkanones.....	59
2.2.2.3 Preparation of bis-thienylidene derivatives of N-methylpiperidin-4-one and cycloalkanones.....	61
2.3 Results – Spectral data of synthesized 1,4-diene-3-ones	63
2.3.1 Spectral data of bis-(benzylidene)-1-methylpiperidin-4-one	63
2.3.2 Spectral data of bis-(benzylidene)cycloalkanones	67
2.3.3 Spectral data of bis-pyridylidene derivatives of N-methylpiperidin-4-one and cycloalkanones	67
2.3.4 Spectral data of bis-thienylidene derivatives of N-methylpiperidin-4-one and cycloalkanones	69
2.4 Discussion of bis-benzylidene, bis-pyridylidene and bis-thienylidene derivatives of N-methylpiperidin-4-one, cyclopentanone and cyclohexanone	70

2.5 Conclusions	73
3 EVALUATION OF ANTIFUNGAL ACTIVITY	75
3.1 Introduction	75
3.1.1 Theory of dose-response curves	76
3.2 Materials and Methods.....	80
3.2.1 Macro-broth susceptibility assay	80
3.2.1.1 Cell cultures	80
3.2.1.2 Growth medium and materials	80
3.2.1.3 Stock solution of the antifungal agent	81
3.2.1.4 Stock solutions of the synthesized compounds	81
3.2.1.5 Growth of yeast cells for macro-broth susceptibility assay	81
3.2.1.6 Macro-broth susceptibility testing of 1,4-diene-3-ones	82
3.2.1.7 Data processing for macro-broth susceptibility assay	83
3.3 Results – Investigation of Antifungal activity	86
3.3.1 Growth curves of <i>S. cerevisiae</i> and <i>C. albicans</i>	86
3.3.2 Investigation of the inhibitory activity of 1,4-diene-3-ones using a macro-broth susceptibility assay	89
3.3.2.1 Susceptibility of <i>S. cerevisiae</i> to 1,4-diene-3-ones	89
3.3.2.2 Susceptibility of <i>C. albicans</i> to 1,4-diene-3-ones	106
3.4 Discussion of macro-broth susceptibility assay	120
3.4.1 Discussion of susceptibility assay of <i>S. cerevisiae</i>	120
3.4.2 Discussion of susceptibility assay of <i>C. albicans</i>	127
3.5 Conclusions	131
4 PROTON EXTRUSION ASSAY	134
4.1 Introduction	134
4.2 Materials and Methods.....	137
4.2.1 Materials, growth medium and growth condition for proton extrusion assay	137
4.2.2 Stock solution of test compounds and controls	138
4.2.3 Measurement of glucose-induced acidification of the external medium	139
4.3 Results of proton extrusion assay.....	141
4.3.1 Effect of N-ethyl maleimide on the proton pumping activity by <i>S. cerevisiae</i>	141
4.3.2 Investigation of the effect of curcumin and miconazole on the H ⁺ pumping activity by <i>S. cerevisiae</i>	144
4.3.3 Effect of 1,4-diene-3-ones on the H ⁺ pumping activity by <i>S. cerevisiae</i>	146

4.3.4 Effect of (3 <i>E</i> , 5 <i>E</i>)-1-methyl-3,5-bis(pyridine-3-ylmethylene)piperidin-4-one on the proton pumping activity by <i>S. cerevisiae</i>	154
4.4 Discussion of H⁺ extrusion assay.....	159
4.5 Conclusions	166
5 STRUCTURE-ACTIVITY RELATIONSHIP	169
5.1 Introduction - Structure-activity relationship.....	169
5.2 Methods – Structure activity-relationship	172
5.2.1 Structure-activity relationships of 1,4-diene-3-ones	172
5.3 Results – Structure activity-relationship	180
5.4 Discussion – Structure-activity relationship	199
5.5 Conclusions – Structure-activity relationship.....	204
6 GENERAL DISCUSSIONS AND CONCLUSIONS	207
7 SPECULATIONS ON FUTURE WORK AND DEVELOPMENT	224
BIBLIOGRAPHY.....	228
APPENDIX 1 - FULL SPECTRA OF SYNTHESIZED DIENONES	241
APPENDIX 2 LIST OF SYNTHESIZED 1,4-DIENE-3-ONES WITH THEIR CHEMICAL NAMES, STRUCTURES AND MOLECULAR WEIGHT	274
COMMUNICATIONS.....	277
Publication	277
Oral Presentation	277
Posters	277

List of Tables

Table 2. 1. List of various R-substituted bis-benzylidene derivatives of N-methylpiperidin-4-one and cycloalkanones (22a-v).....	58
Table 2. 2. List of bis-pyridylidene derivatives of N-methylpiperidin-4-one, cyclopentanone and cyclohexanone (23a-h).....	60
Table 2. 3. List of bis-thienylidene derivatives of N-methylpiperidin-4-one, cyclopentanone, and cyclohexanone (24a-c).	61
Table 3. 1. The antifungal activity of various 1,4-diene-3-ones against <i>S. cerevisiae</i>	105
Table 3. 2. The antifungal activity of various 1,4-diene-3-ones against <i>C. albicans</i>	119
Table 3. 3. Ranking of bis-benzylidene derivatives of N-methylpiperidin-4-one, cyclopentanone and cyclohexanone based on their inhibitory activity against <i>S. cerevisiae</i>	125
Table 4. 1. Effect of NEM and various 1,4-diene-3-ones on the H ⁺ pumping by <i>S. cerevisiae</i>	158
Table 5. 1. Electronic and lipophilic properties of bis-benzylidene, bis-pyridylidene and bis-thienylidene derivatives of N-methylpiperidin-4-ones and their anti-fungal activity against <i>S. cerevisiae</i>	174
Table 5. 2. Electronic and lipophilic properties of bis-benzylidene, bis-pyridylidene and bis-thienylidene derivatives of cyclopentanone and cyclohexanone and their anti-fungal activity against <i>S. cerevisiae</i>	176
Table 5. 3. Comparison of the correlation coefficients of the lipophilic and electronic parameters of various 1,4-diene-3-ones with the inhibitory activities obtained from <i>S. cerevisiae</i> study.	198
Table 6. 1. Comparison of the inhibitory activity of para substituted bis-benzylidene derivatives of N-methylpiperidin-4-ones against <i>S. cerevisiae</i>	211
Table 6. 2. Discrimination ratio of the inhibitory activities of various 1,4-diene-3-ones against <i>S. cerevisiae</i> and <i>C. albicans</i>	217
Table 7. 1. Appendix. List of synthesized 1,4-diene-3-ones with detailed information about their chemical structures, chemical names and molecular weight.	274

List of Figures

Figure 1. 1. Electron micrograph view of <i>S. cerevisiae</i> cells.	4
Figure 1. 2. Various examples of superficial fungal infections.	8
Figure 1. 3. Structure of a fungal cell with various antifungal drug targets.	11
Figure 1. 4. Biosynthetic pathway of ergosterol.	13
Figure 1. 5. Structure of Amphotericin B (1).	14
Figure 1. 6. Structures of azole antifungal agents that includes ketoconazole (2), clotrimazole (3), miconazole (4) and econazole (5).	17
Figure 1. 7. Structures of allylamines that includes naftifine (6) and terbinafine (7).	18
Figure 1. 8. Structure of Echinocandin B (8).	19
Figure 1. 9. The structural organization of P-type ATPases.	31
Figure 1. 10. Reaction cycle of P-type ATPases according to Post-Albers scheme.	34
Figure 1. 11. General N-substituted maleimide structure (9) and N-ethyl maleimide (9a). ...	35
Figure 1. 12. Structure of acid-activated omeprazole (10).	36
Figure 1. 13. The topology of the yeast plasma membrane H ⁺ -ATPase with extracytoplasmic and cytoplasmic binding sites.	37
Figure 1. 14. Structure of curcumin (11).	38
Figure 1. 15. Structure of chalcone (12).	39
Figure 1. 16. Structure of ebselen (13).	40
Figure 1. 17. Structure of caffeic acid (14a) and its oxidised form (14b).	40
Figure 1. 18. Structures of ellagic acid (15), salvianolic acid (16) and plectrinone A (17).	41
Figure 1. 19. Mechanism of cysteine proteinase inactivation with acyloxy methyl ketone. Such compounds could potentially react with PMA1 cysteines if designed correctly.	48
Figure 2. 1. Structures of keto and enol intermediates.	53
Figure 2. 2. Structures of various aldehydes and ketones.	54
Figure 2. 3. Synthesis of bis-benzylidene derivatives of N-methylpiperidin-4-one or cyclopentanone or cyclohexanone (22a-v).	56
Figure 2. 4. Synthesis of bis-pyridylidene derivatives of N-methylpiperidin-4-one or cyclopentanone or cyclohexanone (23a-h).	59
Figure 2. 5. Synthesis of thienylidene derivatives of N-methylpiperidin-4-one and cycloalkanones (24a-c).	61
Figure 2. 6. Structures of synthesized 1,4-diene-3-ones.	62
Figure 3. 1. Schematic representation of dose-response curves.	77
Figure 3. 2. Example of the dose-response curves of three drugs.	79
Figure 3. 3. Growth curves of the two fungal strains over 24 hours.	86
Figure 3. 4. Correlation plots of absorbance and cell counts of fungal species.	87
Figure 3. 5. Dose-dependent inhibition of <i>S. cerevisiae</i> growth by various para-substituted bis-benzylidene derivatives of N-methylpiperidin-4-one after 24 hours.	90
Figure 3. 6. Dose-response curves of the meta- substituted bis-benzylidene derivatives of N-methylpiperidin-4-one against <i>S. cerevisiae</i> after 24 hours.	93

Figure 3. 7. Dose-response curves of the ortho-substituted [a] and dichloro substituted [b] bis-benzylidene derivatives of N-methylpiperidin-4-one against <i>S. cerevisiae</i> after 24 hours.	95
Figure 3. 8. Dose-response curves of the bis-benzylidene and bis-pyridylidene derivatives of N-methylpiperidin-4-one against <i>S. cerevisiae</i> after 24 hours.	97
Figure 3. 9. Dose-response curves of the bis-pyridylidene derivatives of cycloalkanones against <i>S. cerevisiae</i> after 24 hours.	99
Figure 3. 10. Dose-response curves of the bis-thienylidene derivatives of N-methylpiperidin-4-one and cycloalkanones against <i>S. cerevisiae</i> after 24 hours.	102
Figure 3. 11. Dose-response curves of the para-substituted bis-benzylidene derivatives of N-methylpiperidin-4-one against <i>C. albicans</i>	107
Figure 3. 12. Dose-response curves of the meta-substituted bis-benzylidene derivatives of N-methylpiperidin-4-one against <i>C. albicans</i>	109
Figure 3. 13. Dose-response curves of the ortho-substituted [a] and dichloro substituted [b] bis-benzylidene derivatives of N-methylpiperidin-4-one against <i>C. albicans</i>	111
Figure 3. 14. Dose-response curves of the bis-pyridylidene derivatives of N-methylpiperidin-4-one against <i>C. albicans</i> after 24 hours.	112
Figure 3. 15. Dose-response curves of bis-benzylidene and bis-pyridylidene derivatives of cycloalkanones against <i>C. albicans</i> after 24 hours.	114
Figure 3. 16. Dose-response curves of the bis-benzylidene and bis-thienylidene derivatives of N-methylpiperidin-4-one and cycloalkanones against <i>C. albicans</i> after 24 hours.	116
Figure 3. 17. A representative example of a compound which shows an increase in the electrophilicity of β -carbon of the bis-benzylidene derivative of N-methylpiperidin-4-one.	122
Figure 4. 1. Set up of the proton extrusion assay.	139
Figure 4. 2. Effect of N-ethyl maleimide on the H^+ pumping ability of <i>S. cerevisiae</i>	141
Figure 4. 3. Effect of N-ethyl maleimide on proton pumping of <i>S. cerevisiae</i>	143
Figure 4. 4. Analysis of miconazole [a] and curcumin [b] susceptibility of the H^+ pumping in <i>S. cerevisiae</i>	145
Figure 4. 5. Effect of bis-benzylidene derivatives of N-methylpiperidin-4-one on the H^+ pumping by <i>S. cerevisiae</i>	148
Figure 4. 6. Effect of bis-pyridylidene derivatives of N-methylpiperidin-4-one on the H^+ pumping by <i>S. cerevisiae</i>	150
Figure 4. 7. Effect of bis-pyridylidene derivatives of cyclopentanone and cyclohexanone on the H^+ pumping by <i>S. cerevisiae</i>	152
Figure 4. 8. Effect of bis-benzylidene or thienylidene derivatives of N-methylpiperidin-4-one, cyclopentanone and cyclohexanone on the H^+ pumping by <i>S. cerevisiae</i>	153
Figure 4. 9. Effect of Bis-(pyridine-3ylmethylene)-1-methylpiperidin-4-one on the H^+ pumping by <i>S. cerevisiae</i>	155
Figure 5. 1. A representative example of potential interaction of ortho-substituent with either olefinic proton or protons of central pyridyl ring.	178
Figure 5. 2. SAR of $\log (1/IC_{50})$ against clogP [a] and $\log (1/IC_{50})$ against the δ -values of the protons on the β -carbon [b] of the 1,4-diene-3-ones.	181

Figure 5. 3. SAR of $\log(1/IC_{50})$ against clogP [a] and $\log(1/IC_{50})$ against the δ -values of protons on the β -carbon [b] of the 1,4-diene-3-ones (excluding ortho-substituents).	183
Figure 5. 4. SAR of $\log(1/IC_{50})$ against clogP [a] and $\log(1/IC_{50})$ against the δ -values of protons on the β -carbon [b] of bis-benzylidene derivatives of N-methylpiperidin-4-one.....	185
Figure 5. 5. SAR of $\log(1/IC_{50})$ against clogP [a] and $\log(1/IC_{50})$ against the δ -values of proton on the β -carbon [b] of bis-benzylidene derivatives of N-methylpiperidin-4-one (excluding ortho-substituents).	187
Figure 5. 6. SAR of $\log(1/IC_{50})$ against clogP [a] and $\log(1/IC_{50})$ against the δ -values of the proton on the β -carbon [b] of bis-pyridylidene derivatives of N-methylpiperidin-4-one and cycloalkanones.	189
Figure 5. 7. SAR of $\log(1/IC_{50})$ against the δ -values of the carbon atom of the carbonyl [a] and $\log(1/AUC)$ against the δ -values of the carbon atom of the carbonyl [b] of bis-pyridylidene derivatives of N-methylpiperidin-4-one and cycloalkanones.	191
Figure 5. 8. Comparison of $\log(1/AUC)$ with $\log(1/IC_{50})$ of the 1,4-diene-3-ones against <i>S. cerevisiae</i> (full data set containing 31 compounds).	192
Figure 5. 9. Comparison of the δ -values of the carbon atom of the carbonyl with the δ -values of the proton on the β -carbons; full data [a], bis-pyridylidene derivatives of N-methylpiperidin-4-one [b] and bis-pyridylidene derivatives of N-methylpiperidin-4-one and cycloalkanones [c].	194
Figure 6. 1. A possible mechanism of cysteine and 3,5-(E)-bis-(4-trifluoromethylbenzylidene)-1-methylpiperidin-4-one (22n) reaction kinetics.	212
Figure 7. 1. A potential example of the mechanism for a reverse Michael reaction.....	225
Figure 7. 2. A potential example of attachment of dienone or phosphoramidate to the ATP.	227

CHAPTER ONE

GENERAL INTRODUCTION

1 General introduction

1.1 Introduction

In the recent years, the P-type H⁺-ATPase enzyme has received significant interest as a target for the discovery and development of novel antifungal agents (Monk & Perlin, 1994; Tung *et al.*, 2017; Otilie *et al.*, 2018). The P-type H⁺-ATPase exhibits a vital role in the maintenance of the electrochemical proton gradient which facilitates the uptake of nutrients and ions into fungal cells (Monk *et al.*, 1995). The PM H⁺-ATPase is restricted to fungi, plants, protists (Monk *et al.*, 1995) and bacteria such as *Lactococcus lactis* and *Pseudomonas aeruginosa* (Andrés & Fierro, 2010); which makes this enzyme a potential target for drug discovery and the development of novel drugs. The essential role of this enzyme in cell growth and division was demonstrated using a Glucose-Galactose promoter exchange experiment by Portillo & Serrano, (1989). Additionally in various research articles it has been mentioned that α,β -unsaturated carbonyls inhibited the PM H⁺-ATPase (Manavathu, Vashishtha, Alangaden, & Dimmock, 1998; Dao *et al.*, 2016; Kjellerup *et al.*, 2017). In this research work, the benzylidene/pyridylidene/thienylidene derivatives of N-methylpiperidin-4-one and cycloalkanones were synthesised and tested for their antifungal activity.

1.2 Fungi

There are estimated to be more than 1.5 million fungal species in the world (Hawksworth, 2001). However, only a few hundred are considered pathogenic to humans. Fungi can be identified based on their shape, size, structure and nutritional requirements. They are often visible as their mature (fruiting) forms such as found in moulds (Moore, 2003). Fungi may be either single-celled or multicellular. Unicellular fungi are the yeasts which exist in a planktonic

form. However, multicellular fungi comprise networks of long hollow tubes termed hyphae. Hyphae are elongated, branched filamentous structures of fungi. Some species of pathogenic fungi are dimorphic exhibiting both yeast and mycelial forms of growth e.g. *Candida* spp. whilst other human pathogenic fungi only exist in mycelial form e.g. *Aspergillus* spp. (Moore, 2003).

In the current taxonomic arrangement, fungi are classified into several phyla based on their sexual reproduction, these being *Ascomycota*, *Basidiomycota*, *Chytridiomycota*, *Deuteromycota* and *Zygomycota*. However in this chapter, only *Ascomycota* is described because the majority of pathogenic fungi belong to this phylum, which is characterised by the key structure the ascus, a sac like structure which contains haploid ascospores (Deacon, 2013). Many ascomycetes (e.g. *Saccharomyces species*) are used commercially in fermentation process to produce bread, beer or wine (Walker *et al.*, 2014) and some are used in the production of antibiotics (e.g. *Penicillium species*) to treat various bacterial infections (Li *et al.*, 2019). However, some ascomycetes are pathogenic, which can cause infections e.g. species of *Candida*, *Aspergillus*, and *Trichoderma* (Deacon, 2013). Additionally, some species of ascomycetes are used as model organisms in laboratory research including *S. cerevisiae* (example of non-pathogenic yeast) and *C. albicans* (pathogenic yeast). Therefore, in the later section the genera *Saccharomyces* and *Candida* are describe in more detail.

1.2.1 The genus *Saccharomyces*

The genus *Saccharomyces* contains several species of yeasts including *S. cerevisiae* (Figure 1.1), *S. pastorianus*, *S. eubayanus*, *S. cariocus*, etc. (Buckley, 1989). Although non-pathogenic some of these are opportunistic pathogens, particularly in individuals who are significantly immunocompromised (Pérez-Torrado & Querol, 2016). *S. cerevisiae* is the most

extensively studied yeast in terms of both its molecular and cell biology, and biochemistry. The yeast *S. cerevisiae* can easily be grown, and the maintenance of mutant strains is also relatively easy compared to other fungi (Cherry *et al.*, 2012). A significant reason for the use of *S. cerevisiae* is that it is available in both haploid and diploid variants. Thus the generation of mutant strains is relatively simple unlike other yeasts such as *Candida* spp., which are generally believed to be obligate diploid (Odds, 1988).

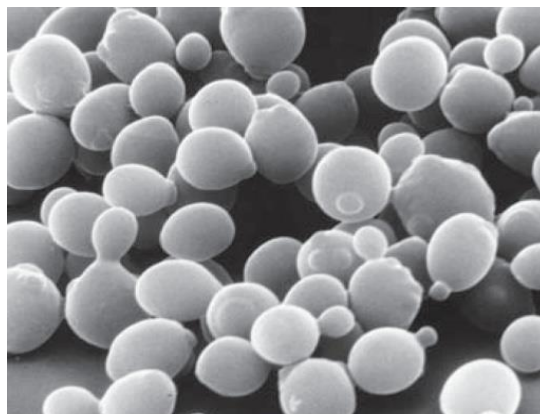


Figure 1. 1. Electron micrograph view of *S. cerevisiae* cells.

The cells of *S. cerevisiae* are round or ovoid in shape with their size being about 5-10 μm in diameter. *S. cerevisiae* cells reproduce by the budding process. Cytokinesis facilitates *S. cerevisiae* cells to divide into two daughter cells by producing bud scars. Image is taken from Milo & Phillips, (2015).

Model organisms are useful for research since they offer a framework on which methods can be developed and standardized. Karathia, Vilaprinyo, Sorribas, & Alves, (2011) have compared *S. cerevisiae* with 704 other organisms from various phyla and suggested that *S. cerevisiae* is a good model organism to study various biological processes. Study using a model organism can provide a framework on which methods can be developed and standardised and compared to species, which are difficult to study. Additionally, model organisms are chosen as they are often considered representative of living beings. *S. cerevisiae* is one of the most commonly used eukaryotic model organisms and has been used in studies of the regulation

of gene expression, cell ageing, signal transduction, metabolism, cell cycle activity, apoptosis and various other biological processes (Karathia *et al.*, 2011).

1.2.2 The genus *Candida*

The genus *Candida* is composed of a diverse group of species of yeast in which the cells commonly vary in shape. There are presently 166 species allocated to the genus *Candida* (Sullivan *et al.*, 1996) although this number continues to rise. The different species of *Candida* can be characterised on the basis of their biochemical, physiological or morphological properties (Lehmann, Lin, & Lasker, 1992). Identification of the genus *Candida* by physical profile includes analysis of cell wall properties, the ability to produce: germ tubes, true hyphae or pseudohyphae, chlamydospores; and by physiological profiles such as the capacity to consume a range of compounds as a single source of nitrogen or carbon (Kim *et al.*, 2002). *Candidal* species can also be differentiated based variously on DNA fingerprinting, DNA-DNA re-association, and Southern blot analyses (Lehmann *et al.*, 1992).

In the 1990s, several research groups studied diverse features of yeasts such as *C. albicans*. By 1996, the genomic sequence of this pathogen was completed with more than 80% of *C. albicans* genes being similar to *S. cerevisiae* (Kabir, Hussain, & Ahmad, 2012). A eukaryotic pathogen, in nature *C. albicans* exists genetically as a diploid, and exhibits morphologically dimorphic forms of growth in response to diverse environmental conditions and signals (Moore, 2003). *C. albicans* is generally a harmless endosymbiont of human epithelial tissues. However it can rapidly adapt to changes in the host's environment even though nutrient bioavailability may be limited and develop into a significant pathological infection (Sexton, Brown, & Johnston, 2007).

1.3 Fungal infections

In recent years, the incidence of fungal infections has increased significantly particularly in immunocompromised patients such as individuals on prolonged cancer chemotherapy or patients having undergone organ transplantation surgery (Neelofar *et al.*, 2011; Brown *et al.*, 2012). Such fungal infections can be described as either superficial or invasive (Parker, 2009). Fungal infections have become widespread in immunocompromised patients and have become a significant problem in disease management (Sardi, Scorzoni, Bernardi, Fusco-Almeida, & Mendes Giannini, 2013). Additionally infections of the bloodstream caused by *Candida* spp. termed candidaemia, is the fourth most recurrent infection in hospitalized patients in the USA (Edmond *et al.*, 1999) and the sixth leading cause of bloodstream infections in Europe (Canela *et al.*, 2018). It has been reported that more than 90% deaths related to fungal infections are due to species belonging to the genera *Aspergillus*, *Candida* and *Cryptococcus* (Cowen, Sanglard, Howard, Rogers, & Perlin, 2015).

During the past 20 years, there has been an expansion of diagnostic methods including the immunoassay of specific antigen detection in clinical samples or polymerase chain reaction in molecular diagnostics. This had led to better diagnosis of both species and strain identification of *Candida* species and new strategies to counteract candidaemia (Kozel & Wickes, 2014). However, the incidence of candidaemia continuous to increase due to reduced susceptibility to azoles and echinocandins in *Candida* species caused by an increase incidence of resistance (Guinea, 2014).

Species of *Candida* often cause gastrointestinal, subcutaneous or nasal infections especially in immunocompromised individuals (Richardson & Warnock, 2012). *Candidal* infections in immunocompromised individuals can give rise to mortality rates of about 30% (Sexton *et al.*,

2007). Certain species of the genus *Candida* (*C. albicans*, *C. tropicalis*, *C. glabrata*, *C. guillemondii*, *C. krusei* and *C. parapsilosis*) are the most common cause of yeast infections worldwide accounting for 62% of cases (Dadar *et al.*, 2018). Although other species are increasing in their incidence e.g. *Candida auris*. Out of the 62% of cases, about 80% of *Candidal* infections are due to *C. albicans* (because *C. albicans* is part of our natural microflora), whilst a further 12% is accounted for by *C. tropicalis*. The remaining 8% of fungal infections are due to *C. krusei* and various other species of *Candida* (Di Santo, 2010).

1.3.1 Superficial fungal infections

Superficial fungal infections (SFIs, Figure 1.2) includes superficial candidiasis and dermatophytosis which affects tissues such as skin or mucous membranes. Dermatophytic fungi usually digest keratin (Ameen, 2010). Infections of the skin, hair or nails caused by the genera *Trichophyton*, *Microsporum* or *Epidermophyton* is termed 'dermatophytosis' (Hay, 2017). SFIs can be diagnosed and usually treated with ease using currently available antifungal drugs such as (tri)-azoles or allylamines although treatments may require long term (3 – 10 months) treatment depending on the severity of the infections. Such SFIs affect up to 25% of the world's population and the incidence of such SFIs continues to increase (Ameen, 2010).



Figure 1. 2. Various examples of superficial fungal infections.

Examples of superficial fungal infections. Oral thrush (a) commonly due to *Candida spp.* appears as white spots on the tongue. Ringworm (b) appears as round scaly, swollen, red patch on the body due to *C. albicans*. Nail infection (c) and athlete's foot (d) infections develop due to the moist and warm environment and are commonly caused by *Trichophyton spp.*

The most common mucosal infection caused by *Candida* is thrush (which is the appearance of white spots on the infected membranes) and is generally observed on oropharyngeal mucosa, vaginal mucosa or gastrointestinal epithelial cells (Richardson & Warnock, 2012). Oral thrush (Figure 1.2a) is caused by elevated levels of *C. albicans* that appears as white spots on an erythematous background. SFIs also include ringworm of the body (*Tinea corporis*), nail infections (*Tinea unguium*), athlete's foot (*Tinea pedis*) and ringworm of the groin (*Tinea cruris*). Several topical antifungal drugs are available for the treatment of superficial fungal infections including amorolfin or terbinafine (from the allylamine class), and clotrimazole, econazole, miconazole or ketoconazole (from the azole class). Fungal nail infections require long-term treatment with amorolfin as a topical application normally applied weekly as a

lacour (which may require 6 – 9 months treatment) or systemic treatment with terbinafine 250 mg daily for 6-12 weeks (Hay, 2017).

1.3.2 Invasive fungal infections

The occurrence of opportunistic invasive fungal infections has gradually increased in China (Liao, Chen, Thomas, Yang, & Liao, 2013) and across the world predominantly due to infections with *Candida* species (McCarthy, Kontoyiannis, Cornely, Perfect, & Walsh, 2017; Pemán & Zaragoza, 2010). Invasive fungal infections (IFIs) have high levels of mortality and morbidity, often exhibiting greater than 50% morbidity especially in immunocompromised patients, individuals on long-term steroid therapy or chemotherapy and those undergoing organ transplantation or blood transfusions (Manavathu, Dimmock, Vashishtha, & Chandrasekar, 1999). These individuals are at high risk for many opportunistic fungal infections such as aspergillosis, candidiasis, cryptococcosis and pneumocystosis (Chakrabarti, 2011).

IFIs are most commonly caused by species of *Candida* or *Cryptococcus* followed by *Aspergillus* or *Mucor spp* (Kjellerup *et al.*, 2017). The infections caused by *C. neoformans*, *Pneumocystis jiroveci*, *Histoplasma capsulatum* and *Penicillium marneffeii* are most commonly reported in Africa, Southeast Asia and South America. Individuals suffering from these infections are difficult to diagnose and treat due to lack of specificity and sensitivity in the diagnostic methods (Kozel & Wickes, 2014). *H. capsulatum* is the causative agent of a globally distributed systemic disease that affects lungs of humans (Mora-Montes & Gacser, 2016). *C. neoformans* often affects immunocompromised individuals whereas *Cryptococcus gattii* can affect healthy individuals however demonstrated a diminished reaction to the central nervous system (Mora-Montes & Gacser, 2016).

C. auris an emerging fungal pathogen, is responsible for nosocomial invasive infections (Bidaud, Chowdhary, & Dannaoui, 2018). A significant outbreak of *C. auris* infection was reported in London's Cardio-thoracic Center between April 2015 and July 2016 (Schelenz *et al.*, 2016). It is difficult to detect *C. auris* using conventional biochemical methods of detection hence its incidence and prevalence rate is not yet available. Due to this, infection with *C. auris* is difficult to treat. Additionally *C. auris* is resistant to commonly used anti-fungal agents such as fluconazole. Additionally *C. auris* has shown variable susceptibility to both amphotericin and echinocandins (Chowdhary, Voss, & Meis, 2016). Yeast identification methods currently in use in clinical laboratories include matrix-assisted laser desorption/ionisation – time of flight mass spectrometry (MALDI-TOF MS), polymerase chain reaction (PCR), sequencing analysis and DNA fingerprinting (Bidaud *et al.*, 2018).

Other diseases such as asthma, an inflammatory disease of the airways, can be aggravated by *Aspergillus* spp. especially *Aspergillus niger* (Agarwal & Gupta, 2011). In recent years, there has been an increase in the incidence of invasive infections caused by filamentous fungi (both *Aspergillus* and non-*Aspergillus* spp.), particularly in patients suffering from cystic fibrosis (Sudfeld, Dasenbrook, Merz, Carroll, & Boyle, 2010). Invasive aspergillosis, usually caused by *A. fumigatus*, which is most commonly reported in patients with compromised immune system (Mora-Montes & Gacser, 2016).

1.4 Background to antifungal agents and drug targets

The structure of the fungal cell and the potential sites of action of available antifungal agents is shown in Figure 1.3.

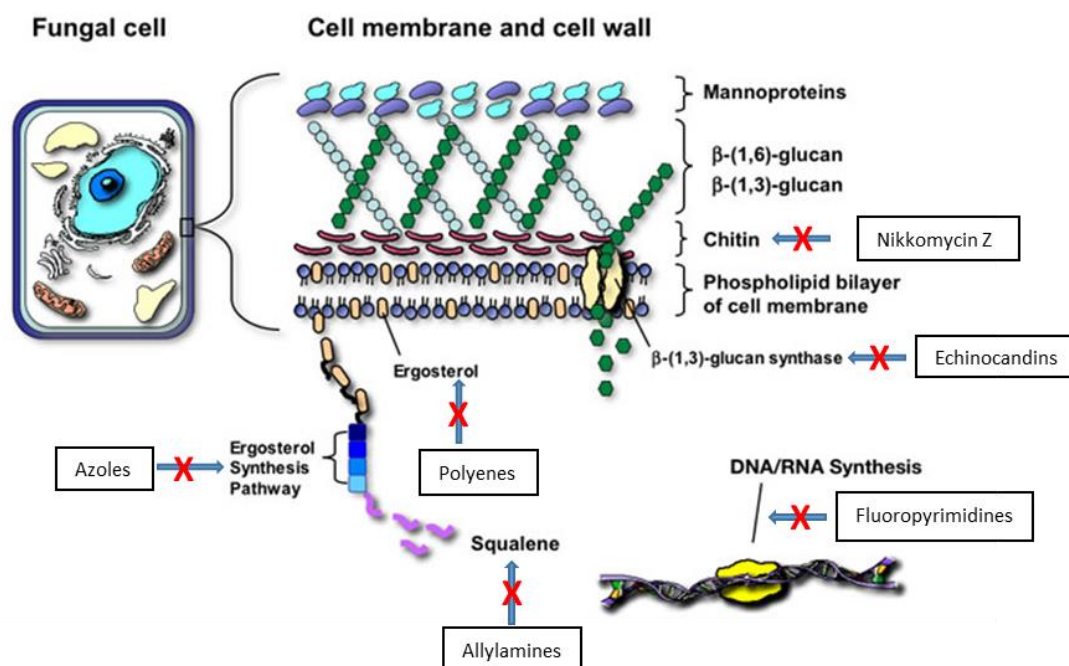


Figure 1. 3. Structure of a fungal cell with various antifungal drug targets.

Schematic outlining the topology of a fungal cell, cell membrane and cell wall. The fungal cell wall is composed of chitin, mannoproteins, β -1,3-glucan and β -1,6-glucan. Fungal cell membrane composed of a phospholipid bilayer, which contains ergosterol. Ergosterol plays an essential role in membrane fluidity and sterol biosynthesis in fungi. Ergosterol and its precursor are the key targets for many of the currently available antifungals. Image taken from (Ashley, Lewis, Lewis, Martin, & Andes, 2006).

Ergosterol is a sterol found specifically in fungi, particularly (but not exclusively) in the plasma and vacuolar membranes of fungi, and is responsible for stabilizing these membranes (Zhang *et al.*, 2010) which is in contrast to cholesterol the main steroid found in animal cells, whereas phytosterols, brassicasterols and stanosterols, which are found in plant cells. Animal and plant sterols have a similar role in membranes to ergosterol in fungi which is to stabilise and increase or control the membrane's rigidity. The biosynthetic pathway of ergosterol is

presented in Figure 1.4. Thus the enzymes involved in ergosterol synthesis represent an excellent target for the development of anti-fungal drug therapies since most of the enzymes involved in the synthesis of ergosterol are unique to fungi (Bhattacharya, Esquivel, & White, 2018).

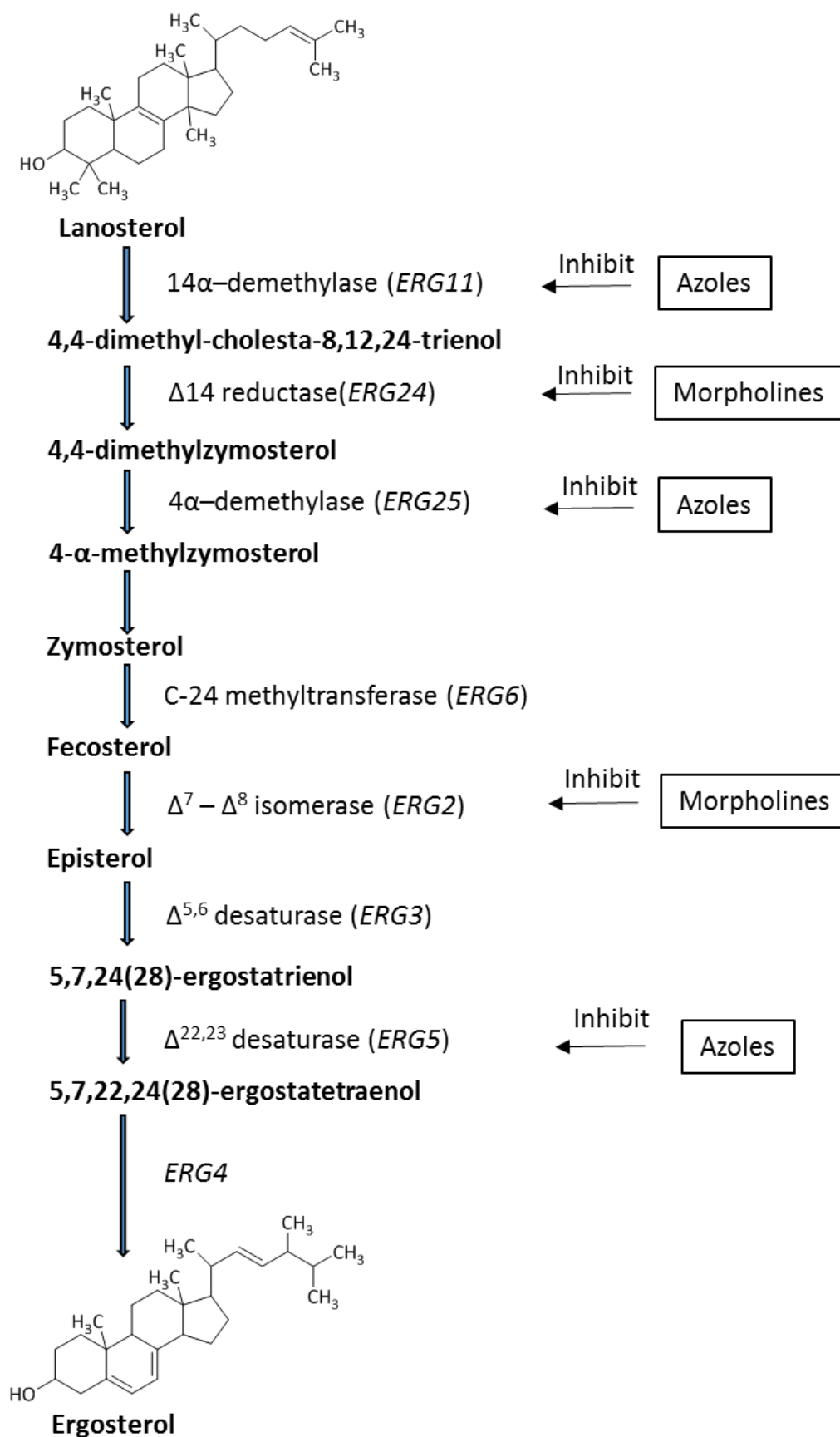


Figure 1. 4. Biosynthetic pathway of ergosterol.

1.4.1 Overview of the classes of currently available antifungal agents

1.4.1.1 Polyenes and macrolides

Polyenes are antifungal agents that bind to ergosterol resulting in the destabilisation of the fungal plasma membrane. This destabilisation results in the consequent leakage, especially of Na^+ , K^+ and H^+ ions, which eventually leads to cell death (Sheehan, Hitchcock, & Carol, 1999). Examples of polyenes include amphotericin B and nystatin. Since the 1950s, Amphotericin B (**1**) has been considered to be the 'gold standard' antifungal therapy when treating severe, life-threatening, fungal infections (Groll, De Lucca, & Walsh, 1998). Amphotericin B, originally isolated from *Streptomyces nodosus*, possesses a wide spectrum of antifungal activity. Nevertheless, the use of amphotericin B is limited due its narrow therapeutic index, poor oral absorption and notorious nephrotoxicity. Consequently the preferred route of administration is clinically controlled intravenous infusion (Sheehan *et al.*, 1999).

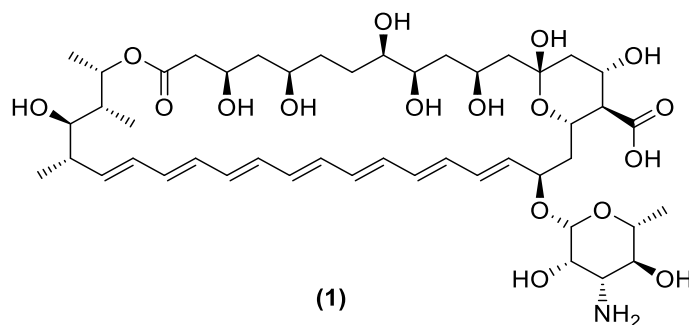


Figure 1. 5. Structure of Amphotericin B (1).

In the 1950s, nystatin was identified as a further polyene antifungal. Nystatin works in a similar fashion to amphotericin B by causing the leakage of ions such as Na^+ , K^+ or H^+ ions, leading to cell death. Nystatin is not absorbed after oral administration. However it is very effective in the treatment of oropharyngeal candidiasis (Kathiravan *et al.*, 2012). Systemic use

of nystatin is limited due to adverse effects including itching, burning, irritation, nausea and diarrhoea. Other macrolides, such as Candicidin, are used in the topical treatment of vulvovaginal candidiasis (Ghannoum & Rice, 1999).

Until the 1970s, treatment options for systemic fungal infections were limited to either griseofulvin or amphotericin B. For invasive fungal infections, the treatment option was limited to amphotericin B until 1979. However Flucytosine, a pyrimidine analog originally developed as an anti-cancer agent, was introduced in the late 1970s and early 1980s, which acts as a prodrug by blocking cell division (Sheehan *et al.*, 1999). Flucytosine is converted to 5-fluorouracil which is able to inhibit the enzyme thymidylate synthase an enzyme involved in the replication of DNA in the fungal cell (Polak & Scholer, 1975). However, flucytosine is rarely used due to it rapidly giving rise to drug resistance. It does however continue to be used in combination therapies of various types of fungal infections.

1.4.1.2 Azoles and triazoles

In the 1970s it was observed that alkyl imidazoles had an antifungal effect, leading to the development of various azole containing drugs. The first systemic azoles for the treatment of systemic infections were introduced clinically in the 1980s including ketoconazole (**2**), which include two nitrogens in the azole ring and itraconazole which include three nitrogens in the azole ring (Groll *et al.*, 1998). Subsequently the azole ring was substituted by a triazole ring, the first-generation tri-azoles included itraconazole and fluconazole. Ketoconazole shows a wide spectrum of antifungal activity against blastomycosis, candidiasis, coccidioidomycosis, paracoccidioidomycosis and histoplasmosis (Shao, Huang, & Hsueh, 2007). Conversely itraconazole is effective against *Aspergillus* spp (Groll *et al.*, 1998). However, there are

significant adverse side effects reported with some (tri)azoles such as ketoconazole including fatal toxic hepatitis (Kathiravan *et al.*, 2012).

Cytochrome P450 is found in all biological kingdoms and it is the most commonly disseminated CYP gene family (Lepesheva & Waterman, 2004). However therapeutic concentrations of azoles have a greater affinity towards fungal P-450_{DM} (cytochrome P-450-dependent 14 α -sterol demethylase enzyme) than the mammalian sterol-demethylating enzyme (Sheehan *et al.*, 1999). Many azoles/triazoles does not cause major problems with mammalian CYP although reversible male impotence has been reported in some cases (Zakhem, Goldberg, Motosko, Cohen, & Ho, 2019).

Antifungal azoles inhibit various enzymes in (pathogenic) fungi involved in ergosterol synthesis especially the cytochrome P450 enzymes 4 α -demethylase, 14 α -demethylase and sterol-C-24-methyltransferase (Kathiravan *et al.*, 2012). Inhibition of one or more of these enzymes leads to the impairment of ergosterol synthesis in fungi (resulting in the destabilization of various ionic gradients such as ΔpH , ΔK^+ or the electrochemical potential due to the protons $\Delta\Psi_{\text{H}^+}$). In the 1990s further azole analogues were introduced including clotrimazole (**3**), miconazole (**4**), econazole (**5**), fluconazole, voriconazole, posaconazole, isavuconazole and ravuconazole (Sheehan *et al.*, 1999). Fluconazole and itraconazole are the only two azole drugs which are currently available as oral formulations. Fluconazole has both a high water solubility and low affinity for plasma proteins, which makes it a unique antifungal agent in the azole class (Andriole, 2000). Fluconazole is used in the treatment of both superficial and invasive *Candida* infections.

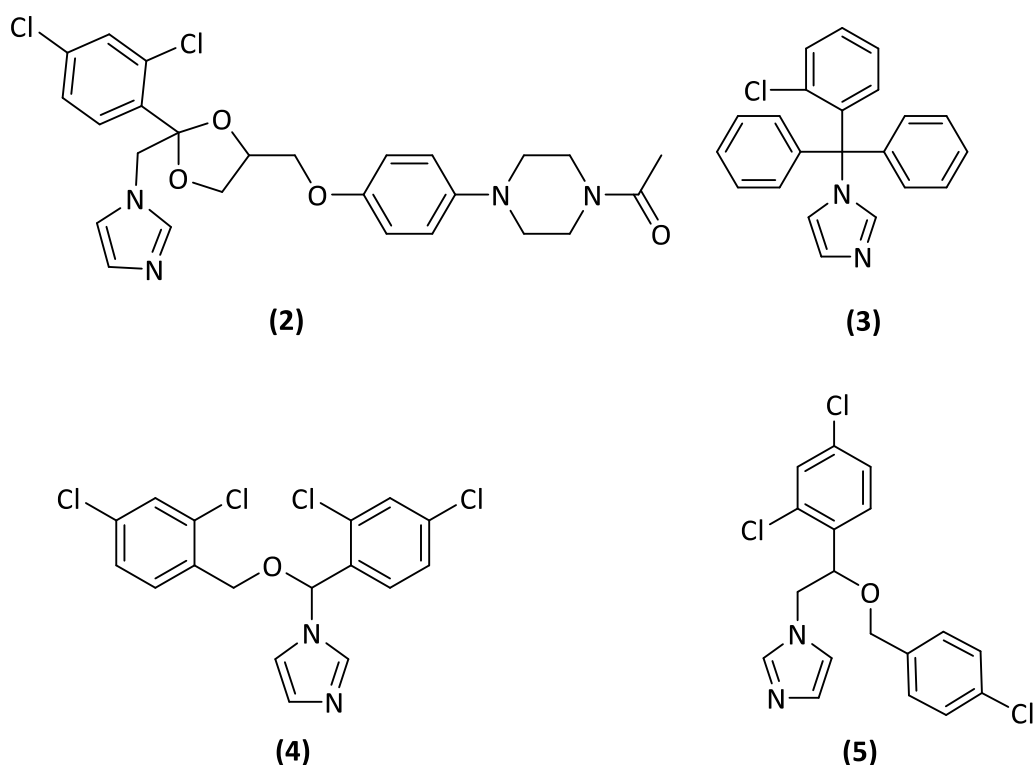


Figure 1. 6. Structures of azole antifungal agents that includes ketoconazole (2), clotrimazole (3), miconazole (4) and econazole (5).

Second-generation triazoles include voriconazole, posaconazole, isavuconazole and ravuconazole. Voriconazole is a low molecular weight, water-soluble triazole having a wide spectrum of activity and is effective against *Aspergillus* spp, *Candida* spp, *Fusarium* spp. and *Scedosporium* infections (Pemán & Zaragoza, 2010). Posaconazole is a lipophilic antifungal triazole, which is effective against *Aspergillus*, *Candida* spp, *Cryptococcus* spp and *Histoplasma* spp. However, there are various common side effects reported with the use of posaconazole including: headache, nausea, abdominal pain, vomiting and skin rashes (Kathiravan *et al.*, 2012). Ravuconazole has shown a broad spectrum of antifungal activity even against some isolates that displayed resistance to fluconazole (Kathiravan *et al.*, 2012). The development of this class of antifungal continues with other molecule of this type in clinical development.

1.4.1.4 Echinocandins

In 2001, a novel class of antifungal agent, first echinocandin, Caspofungin, was introduced (Ashley *et al.*, 2006). Subsequent addition to this class includes micafungin, anidulafungin and echinocandin-B (**8**).

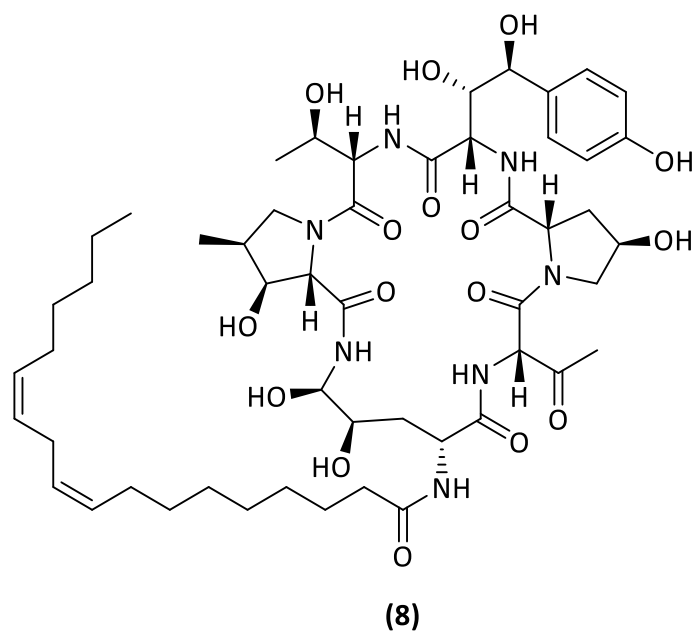


Figure 1. 8. Structure of Echinocandin B (8).

Echinocandins inhibit the synthesis of glucan by targeting the enzyme β -(1,3)-glucan synthase, a major component in the fungal cell wall. Inhibition of this enzyme leads to disruption of the cell wall of the growing cell, causing osmotic instability leading to lysis of susceptible yeast cells (Ashley *et al.*, 2006). This class of compounds were a significant addition to the antifungal armoury due to their inhibiting a different enzyme system compared to the (tri)-azoles.

Caspofungin is very effective against *Aspergillus* spp. However it has only moderate activity against *B. dermatitidis*, *H. Capsulatum* and *C. immitis*, and has no activity against *Fusarium* spp, *Trichosporon* spp, *C. neoformans*, Hyalohyphomycetes or Zygomycetes (Akins, 2005). In

addition, they are ineffective against pseudo-fungi due to the different components of the cell walls where many pseudo fungal cell walls are made from cellulose (Akins, 2005). A study conducted by van Burik *et al.*, (2004) demonstrated that prophylactic treatment with micafungin in stem cell transplantation patients during neutropenia displayed better potency compared to fluconazole. Additionally, micafungin is very effective in the treatment of candidiasis (Kathiravan *et al.*, 2012).

Echinocandins are considered an effective alternative to azole antifungals due to their different mode of action, decreased side effects and having higher fungicidal activity against many species of *Candida*. The fungicidal activity of echinocandins against several *Candida* species makes it an effective alternative for the treatment of azole-resistant strains (Cannon & Holmes, 2015).

Additionally the toxicity profile of echinocandins is significantly lower than many of the (tri)azoles (Cannon & Holmes, 2015). This may be due, in part, to the fact they target the enzyme involved in the cell wall synthesis and mammalian cells do not contain a homologue of this enzyme whereas (tri)azoles may interact with a variety of P450 type enzymes in mammalian cells and tissues. Unfortunately, echinocandin has poor oral bioavailability partly due to its high molecular weight. Consequently, it can be used only via intravenous administration. In addition, there are some side effects associated with echinocandins including fever, nausea, vomiting, diarrhoea, rash, phlebitis, headache, hypotension, leukopenia and hypokalemia. The use of echinocandins is also limited due to both cost and their interactions with antihistamine medications such as diphenhydramine (Ashley *et al.*, 2006).

1.4.1.5 Other antifungal agents

Other agents having antifungal activity include griseofulvin, nikkomycin, polyoxins, ciclopirox, sordarins, tolnaftate and benzoic acid. Griseofulvin inhibits the formation of mitotic spindles by inhibition of microtubule polymerization and is effective in the treatment of cutaneous mycoses (Sheehan *et al.*, 1999). The main adverse effect of griseofulvin is a headache, although it may also cause aplastic anaemia or liver toxicity (Odds, Brown, & Gow, 2003).

Other compounds under development as clinical agents include nikkomycin and polyoxins which are inhibitors of chitin synthesis. Nikkomycin is effective when used in combination with caspofungin against *A. fumigates*. Polyoxins are effective against phytopathogenic fungi (Kathiravan *et al.*, 2012). The Sordarins are a group of inhibitors of protein synthesis which act by inhibiting fungal translation by impairing the function of the fungal elongation factor 2 (eF2) (Kathiravan *et al.*, 2012; Chakraborty, Sengupta, & Mukherjee, 2013).

Ciclopirox is a broad-spectrum antifungal medication, available as a topical solution, which exhibits both fungistatic and fungicidal activities due to its high affinity for trivalent cations such as Fe^{3+} or Al^{3+} (Ghannoum & Rice, 1999). Ciclopirox inhibit the availability of important mineral co-factors for proteins or enzymes such as iron for cytochromes or P450 type enzymes involved in ergosterol biosynthesis. Ciclopirox thus causes instability in the fungal membrane and interferes with amino acid transport across the cell membrane (Piraccini & Tosti, 2019). However there are some adverse effects associated with the use of ciclopirox including redness of the skin, burning, irritation and swelling at the site of application (Ghannoum & Rice, 1999).

1.5 Drug resistance in fungi

Antifungal drug resistance is an ongoing problem in the fight against invasive fungal infections (Chakrabarti, 2011). Antifungal resistance is a major concern in individuals with suppressed immune system due to extensive use of antifungals, antibiotics and chemotherapy (Sardi *et al.*, 2013). The extensive use of antifungal agents and growing numbers of individuals with opportunistic infections has led to the development of resistance to currently available antifungals (Scorzoni *et al.*, 2017). Evolution of organisms resistant to multiple example and classes of antifungal drugs especially among *Candida* species (Cowen *et al.*, 2015). Resistance can be categorised in two ways; clinical resistance and *in vitro* resistance. Clinical resistance is defined as the progression of the fungal infection even after administration of adequate doses of antifungal drugs. Conversely, *in vitro* resistance is a laboratory measurement, which relates to clinical involvement and the range of fungal species are resistant to antifungal drugs (Rogers, 2006).

In vitro resistance may be sub-divided into primary and secondary resistance. In primary resistance, fungi are intrinsically resistant prior to drug exposure, an example of which is *C. auris*, which is intrinsically resistant to many clinically used antifungal agents (Chowdhary *et al.*, 2016) whereas in secondary resistance fungi develop resistance following exposure to the drug (Rogers, 2006). Such resistance may be due to environmental or genetic changes in the fungal cell. It is difficult to manage infections caused by certain fungi such as *C. auris*, *C. krusei*, *C. parapsilosis* and *C. glabrata* due to their inherent drug resistance (Rogers, 2006; Schelenz *et al.*, 2016). *C. auris* shows high level of resistance against azoles, echinocandins and amphotericin (Schelenz *et al.*, 2016). The mechanism of resistance in *C. auris* is still unclear. However, it is possible that the occurrence of resistance is due to enzymes being

intrinsically resistant due to poor binding of the drug or the drug being taken up slowly or the efflux pumps being very effective against these drugs even in the wild type strains of *C. auris* (Chowdhary *et al.*, 2016).

Molecular mechanisms of resistance in fungi may also be associated with the formation of biofilms. Overexpression or increased expression of drug target metabolising or transporting enzymes (e.g. 4 α -demethylase, 14 α -demethylase). Due to changes in the efflux pumps such as the ABC transporters (ATP-binding cassette transporter) or MFS pump (major facilitator) both result in a reduction of intracellular drug levels (Cowen *et al.*, 2015). Certain fungi (e.g. *C. albicans*, *C. tropicalis*, *C. krusei*, *C. parapsilosis* and *C. glabrata*) develops resistance by the formation of biofilms on synthetic or natural surfaces (Emami, Ghobadi, Saednia, & Hashemi, 2019). Biofilms are a thick layer of cells (i.e. cells are clumped together), which form a physical barrier thus making it difficult for a drug to penetrate into the cells (Cowen *et al.*, 2015).

It has also been shown that *C. parapsilosis* develops resistance to fluconazole by overexpression of efflux pumps encoded by multidrug resistance regulator 1 (MRR1) that alongside cause overexpression of cerebellar degeneration related protein (CDR1) and the multidrug resistance gene 1 (MDR1) (Zhang *et al.*, 2015).

Genetic factors associated with a resistance in certain fungal strains such as genetic modification of enzymes in the targeted biosynthetic pathway give rise to structural, kinetic and/or drug binding changes in the target enzyme (Sangamwar, Deshpande, & Pekamwar, 2008). Additionally environmental factors affect the inability of antifungals to effectively treat diseases (Scorzoni *et al.*, 2017).

The occurrence of azole resistance in certain fungi (e.g. *C. albicans*) may also be due to degradation of the drug, a decrease in drug import or an alteration of ergosterol biosynthesis

associated with molecular changes in the ERG11 gene (Cannon & Holmes, 2015). Additionally azoles not only interact with CYP51 but also affect xenobiotic-metabolizing CYP enzymes in mammals which may affect the pharmacodynamics or pharmacokinetics of a wide range of the (tri)azole drugs (Mishra *et al.*, 2007).

Even though there has been an increase in the number of antifungal drugs, the choice of different classes of antifungal drug remains limited. Additionally, variations in drug bioavailability and drug toxicity in immunocompromised individuals compared to the normal individual are known (Chakrabarti, 2011). Furthermore, many agrochemically relevant fungi some of which are opportunistic human pathogens have become resistant to various antifungal drugs and agrochemicals. There is thus an increased interest and need for the identification of novel clinical drug and agrochemical targets within the mycota.

1.6 Identification of novel antifungal drug target

Identification of appropriate novel enzyme or receptor targets is necessary in order to develop new antifungal agents with improved absorption, distribution, metabolism and excretion (ADME) profiles along with reduced toxicity and the ability to overcome resistance in drug resistance strains (Scorzoni *et al.*, 2017). Therefore, when selecting a drug target, one of the most important factors to consider is that the synthesized compounds should selectively target fungal cells without causing any damage to the host organism or cell. However the antifungal market is relatively small and there are many azoles/tri-azoles available (Chakrabarti, 2011). Pharmaceutical companies commonly expand their range of antifungals by looking at X-ray structures and computer-generated models of proteins involved in the pathway for ergosterol synthesis and expanding existing drug structures along

the azole binding groove in e.g. 14 α -demethylase enzyme rather than identifying novel enzyme target (Scorzoni *et al.*, 2017).

To bring new antifungal drugs into development, academic researchers have focused on finding new lead molecules targeting novel target enzymes. High throughput screening (HTS) is a discipline used by pharmaceutical companies as part of effective drug discovery programmes (Pouliot & Jeanmart, 2016). It is predictable that hits from HTS campaigns include many false positives among the real hits. The activity of many hits does not depend on a specific drug-like interaction between the molecule and protein (Baell & Holloway, 2010).

In recent years many researchers have published papers claiming their compounds have good antifungal property but many of them act as either pan-assay interference compounds (PAINS) or promiscuous aggregating compounds (Pouliot & Jeanmart, 2016). Where molecules commonly form dimers or higher multimer complexes, one key reason for PAINS compounds is the inadequate quality of the data for some of these new inhibitors reported in the antifungal literature. Many of them contain undesirable structural features such as the presence of 1,2-dihydroxyl groups, which can be oxidise to a 1,2-di-carbonyl structure which is able to react with arginine (Murakami *et al.*, 1990).

Also some covalent modifier compounds which are able to produce hydrogen peroxide, which inactivates the target protein in a non-specific fashion (Baell & Walters, 2014). Examples of covalent modifiers includes 1,3-dicarbonyls such as curcumin, enones, ene-rhodanine, isothiazolones, hydroxyphenyl hydrazones, quinones and catechols. "Most PAINS works as reactive chemicals rather than discriminating drugs" (Baell & Walters, 2014). However many researchers have been attracted by the activity of certain PAINS compounds and continue

their work although it has been published in some reports that covalent modifiers may interfere with assays (Baell & Walters, 2014).

However a review by De Cesco *et al.*, (2017) mentioned that about 30% of marketed drugs which target enzymes act as covalent inhibitors. One such example is omeprazole, which was discovered in the 1970s and subsequently, in 1988, licenced for use as a H⁺/K⁺-ATPase inhibitor for the treatment of ulcerative disease. In 1986, Lindberg, Nordberg, Alminger, Brandstrom, & Wallmark found that omeprazole acts as a pro-drug and that, in its acid activated form, is a sulfinamide, a molecular class that Baell suggested should not be developed as drugs (De Cesco *et al.*, 2017). Therefore, it is suggested that this class of compounds and other compounds having similar modes of action may be reassessed considering the historic achievements of covalent drugs in becoming clinically useful agents.

The binding of covalent drugs to the target enzyme has significant consequences for their efficacy such as prolonged duration of action, increased potency and decoupled pharmacokinetic and pharmacodynamics profiles (Singh, Petter, Baillie, & Whitty, 2011). Although some companies and lead investigators had concerns over the last 20 years targeting drugs to the nucleotide binding sites of various enzymes such as protein kinases, this has not stopped the development of various compounds that covalently modify the target at nucleotide binding sites and which have been licensed in recent years for clinical use.

Reviews by various authors have commented in favour of the development of novel covalent drugs, especially targeting the ATP binding site of protein kinases (Singh *et al.*, 2011; Barf & Kaptein, 2012; Jackson, Widen, Harki, & Brummond, 2017; Dalton *et al.*, 2018). Although ATP binding sites have been disparaged as target sites due to the high cellular concentration of ATP and relatively high K_m and K_{eq} values and there has been a resurgence of interest in targeting

such sites in recent years (Škedelj, Tomašić, Mašič, & Zega, 2011). In recent years there has been an increase in the study and development of covalent modifiers as drugs, resulting in the development and licensing of various irreversible protein kinase inhibitors (Barf & Kaptein, 2012). Greater efficacy and functional selectivity of irreversible protein kinase inhibitors makes them popular over reversible drugs (Barf & Kaptein, 2012). The covalent conjugation of a drug molecule with lysine is less common due to the protonation of the side chain NH_2 under physiological conditions. Therefore kinome-conserved lysine residues are considered to be a good alternative target to cysteine (Dahal *et al.*, 2016). Dalton *et al.*, (2018) described a novel approach to accomplish irreversible kinase inhibition by targeting the preserved catalytic lysine residue. By this method, selective covalent chemical probes can be created for selected kinases at the nucleotide (ATP) binding site.

Using various molecular biological techniques, it has been identified that the plasma membrane H^+ -ATPase of fungi and plants could be a potential new antifungal drug target due to its genetic and biochemical properties, and the fact that this enzyme is absent from mammalian cells (Serrano, 1980; Monk *et al.*, 1995; Portillo, 2000). The fungal plasma membrane (PM) is composed of phospholipids and sterols as their main lipid constituents, which acts as a permeability barrier to transport molecules across the membrane. Chemical modification of membrane-embedded PM proteins could lead to the disruption of cellular functions and thus cell death, thus potentially acting as a new drug target (Sangamwar *et al.*, 2008; Otilie *et al.*, 2018).

1.6 ATPase and ATP synthase enzymes

ATPases (adenosine triphosphatases) are a class of enzymes that catalyze the hydrolysis of ATP to ADP and free phosphate (P_i). The F_0F_1 ATP synthase is found in the inner membrane of

mitochondria in eukaryotes, and the plasma membrane of many prokaryotes, and is involved in the synthesis of ATP using the (mitochondrial) proton electrochemical potential composed of a proton gradient ($\Delta p\text{H}$) and electrical potential ($\Delta\Psi_{\text{H}^+}$). The electrical field influences the movement of protons and a higher concentration of protons present on one side leads to higher driving force for the transport of protons across the membrane. In the past 60 years, various membrane bound ATPases from various classes have been discovered and studied to solve the specific demands of the cells. The different types of ATPases discovered include F-, A-, V-, P- and E-ATPases based on their cellular function and location (Becher & Muller, 1994).

1.7.1 Types of ATPases

1.7.1.1 F-type ATPases

F-type ATPases, more commonly termed ATP synthases are found in (eu)bacteria, chloroplasts and mitochondria. F-ATPases are composed of two multi-protein complexes, these being: F_0 which is present in the membrane and F_1 which is present in the lumen/cytoplasm and is attached to the F_0 sector. F_1 is responsible for the hydrolysis or synthesis of ATP, whilst the F_0 complex facilitates the translocation of protons. In eukaryotes, the F-ATPase transports three or four protons into mitochondria for each ATP synthesized. In bacteria, the F-ATPase pumps three to four H^+ or Na^+ in (or out) of the cell for each ATP synthesized or hydrolyzed (Becher & Muller, 1994).

Eukaryotic and prokaryotic classes of F-ATPases can be differentiated based on their sensitivity towards inhibitors such as oligomycin. The bacterial F_0F_1 -ATPase is not sensitive to oligomycin whereas eukaryotic F_0F_1 -ATPases are very sensitive to oligomycin (Perlin, Latchney, & Senior, 1985). In other inhibitor studies undertaken by Gledhill, Montgomery, Leslie, & Walker, (2007) it has been shown that resveratrol and related stilbene

polyphenols inhibit the F_1 ATPase from bovine heart mitochondria. Resveratrol blocks the synthesis and hydrolysis of ATP by the ATP synthase (F_1F_0 -ATPase) enzyme found in mitochondria (Gledhill *et al*, 2007). The inhibitors bind to the F_1 -ATPase and act as non-competitive inhibitors. The stilbene nucleus found in molecules such as resveratrol, binds via hydrophobic interactions whilst the substituents on the benzene rings of the stilbene such as hydroxyl (-OH) may bind via H-bonds (Gledhill *et al*, 2007). Additionally, stilbenes such as resveratrol also block the transport of H^+ through the F_0 channel (Dadi, Ahmad, & Ahmad, 2009).

1.7.1.2 A-type ATPases

A-type ATPases (A_0A_1) are found in archaea and function in a similar fashion to the F-type ATPases. Some of the A-type ATPases are known to utilize Na^+ rather than H^+ gradients (Becher & Muller, 1994).

1.7.1.3 V-type ATPases

Vacuolar (V_0V_1) or V-type ATPases act as proton pumps in eukaryotic vacuolar membranes. A V-type ATPase is found in various eukaryotic vacuolar membranes including the human lysosomal and fungal membranes. Similar enzymes are also found in neuronal synaptic vesicles of humans and plasma membranes of plants (Becher & Muller, 1994). The V-ATPase is comprised of a V_0 complex consisting of six different types of subunit and is responsible for proton translocation. V_1 is a soluble complex composed of eight types of subunit that hydrolyses ATP. This enzyme is linked to controlling the uptake and concentration of various neurotransmitters in vesicles in mammalian cells (Becher & Muller, 1994).

In fungal cells, V-ATPases acidify vacuoles by hydrolysing ATP, with the consequent pumping of protons from the cytoplasm into the vacuole, the Golgi body or endosomes (Becher &

Muller, 1994). Treatment of the V-ATPase with β -methylcyclodextrin showed a loss of vesicular acidification in mammalian cells (Yoshinaka, Kumanogoh, Nakamura, & Maekawa, 2004). The ergosterol synthesis inhibitor, fluconazole has also been shown to decrease vacuolar acidification in both *C. albicans* and *S. cerevisiae* (Zhang *et al.*, 2010). Vesicular ergosterol thus appears to be important for optimal functioning of the V-ATPase (Zhang *et al.*, 2010). Fluconazole thus appears to reduce the flow of cytosolic H^+ and Ca^{2+} ions and impairs the storage of Ca^{2+} ions in purified vacuolar vesicles (Zhang *et al.*, 2010).

1.7.1.4 E-type ATPases

Ecto, or E-type, ATPases are membrane-associated proteins found in many eukaryotic cells (Zhong & Guidotti, 1999). They play an essential role in many biological processes such as prevention of intravascular thrombosis, glycosylation of proteins or modulation of neural cell activity. E-ATPases have the ability to hydrolyze both di- or tri-phosphate nucleotides when activated by Mg^{2+} or Ca^{2+} ions (Zhong & Guidotti, 1999).

1.7.1.5 P-type ATPases

P-type ATPases (Figure 1.9) are found in both plasma and endoplasmic reticulum membranes of eukaryotes such as fungi, plants, protists and in the cytoplasmic membrane of prokaryotes. (Monk *et al.*, 1995). Their function is to transport a wide variety of ions such as H^+ , Ca^{2+} , Cu^{2+} , K^+ , Na^+ , NH_4^+ , Zn^{2+} and heavy metals or phospholipids across membranes with the associated hydrolysis of ATP.

Axelsen & Palmgren, (1998) classified P-ATPases into five classes. P-type ATPases are grouped together in a phylogenetic tree according to their substrate specificities regardless of the evolutionary distance between the parental species (Axelsen & Palmgren, 1998). Type I ATPases includes those pumping heavy metals and other potentially toxic ions out of cells

such as Cu^{2+} , Cd^{2+} , Pb^{2+} and Zn^{2+} . The type II family includes the Na^+/K^+ -ATPase, Ca^{2+} -ATPase (both plasma membrane and endoplasmic reticulum) and the H^+/K^+ -ATPase and relates to mammalian ATPases, which are the most extensively studied P-type ATPases. Type III P-type ATPases includes the H^+ -ATPase that appears in fungi and plants, and Mg^{2+} pumps. The type IV P-type ATPases include the aminophospholipid pumps and are also involved in the transport of other hydrophobic compounds. Type V P-type ATPases includes a group of pumps with no known substrate specificity (Lecchi & Slayman, 2004).

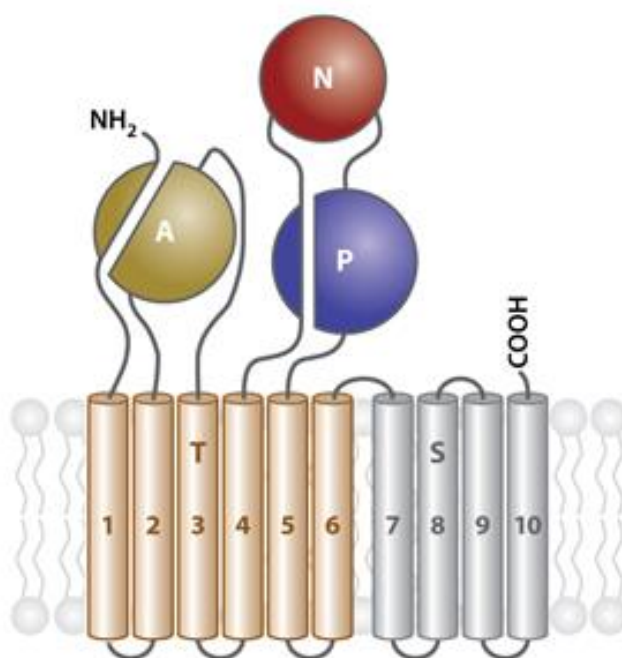


Figure 1. 9. The structural organization of P-type ATPases.

P-type ATPases contains five domains, two of these are membrane-embedded domains (S–class specific support domain and T–transport domain) and along with other three other cytoplasmic domains (A–actuator, N–nucleotide binding and P–phosphorylation). The P-domain is phosphorylated by the activity of the N-domain which is then dephosphorylated by the A-domain during each catalytic cycle. In this system, the P-domain acts as the site for both phosphatase and kinase activities, whereas the N-domain acts as a protein kinase and the A-domain acts as a protein phosphatase. Image is taken from (Palmgren & Nissen, 2011).

The plasma membrane (PM) H^+ -ATPase belongs to the type III P-type ATPase family of ion translocating ATPases. The PM H^+ -ATPase is encoded by the genes PMA1 and PMA2 in

S. cerevisiae and other fungi, and AHA1 to 10 in plants such as *Arabidopsis thaliana*. Some species of fungi contain only one PMA gene. The PM H⁺-ATPase is an essential enzyme for the growth of fungi where it generates an electrochemical proton gradient across the fungal plasma membrane that drives the uptake of nutrients such as amino acids, sugars, ions, etc. by secondary transporters and to regulate the intracellular pH (Portillo, 2000). Both glucose and pH are responsible for the regulation of the PM H⁺-ATPase (Mazon, Eraso, & Portillo, 2015).

Mammalian type II P-type ATPases are involved in the exchange of various cations such as the Na⁺/K⁺ or H⁺/K⁺-ATPases but fungal and plant P-type H⁺-ATPases (type III ATPases) are not involved in the cation exchange process. P-type ATPases particularly the H⁺, Na⁺/K⁺ and Cu²⁺ play an important role in the regulation of cell metabolism in their respective organisms, such that their malfunctioning could potentially cause number of diseases or cell death. The P-type ATPase enzymes such as the Na⁺/K⁺-ATPase and H⁺/K⁺-ATPase are well-defined targets for surface-active cardiac glycosides such as digitoxin and anti-ulcer treatments such as omeprazole (Monk & Perlin, 1994). In view of the proton ATPase being present in fungi and not in animals, the PMA P-type ATPase is considered as a useful target for the development and identification of new classes of antifungal agent (Kongstad *et al.*, 2014).

It has been shown that vanadate is a potent inhibitor of many P-type ATPases (Clausen *et al.*, 2016). Nevertheless, the structural details of its inhibitory action have remained elusive although it is believed to act as a transition state analogue of phosphate (Clausen *et al.*, 2016). Clausen *et al.*, (2016) have solved the crystal structure of the sarcoplasmic reticulum (SERCA) Ca²⁺-ATPase bound to vanadate. The Ca²⁺-ATPase is inhibited by decavanadate competing with TNP-8N₃-ATP at the nucleotide binding site whereas orthovanadate is characterised as a

trigonal bipyramidal transition state intermediate of the SERCA Ca²⁺-ATPase dephosphorylation process (Clausen *et al.*, 2016).

Many studies have been conducted using a wide variety of inhibitors to elucidate the structure, organisation and mechanism of Pma1 (Monk *et al.*, 1995; Petrov & Slayman, 1995; Dao *et al.*, 2016; Otilie *et al.*, 2018). To date, only ebselen and the peptide BM₂ have been shown to inhibit fungal growth in the low micromolar range (Kjellerup *et al.*, 2017).

1.7.1.5.1 Reaction mechanism of the plasma membrane H⁺-ATPase

The P-type H⁺-ATPase pumps protons out of the cell which results in an increase in the internal pH (pH_i) causing cytoplasmic alkalization which stimulates cell growth (Serrano, 1993; Kjellerup *et al.*, 2017) The H⁺-ATPase acts as a master transporter to facilitate uptake of nutrients such as sugars, amino acids or mineral ions into the cells via series of 'slave' transporters. These 'slave' transporters require energy which is supplied from the plasma membrane ΔpH much of which is generated by the master transporter H⁺-ATPase (Palmgren & Nissen, 2011).

The P-type H⁺-ATPase undergoes covalent *trans*-phosphorylation via the formation of an aspartyl phosphate intermediate during each catalytic cycle hence the term phosphorylated ATPase or P-type ATPase, also known as E₁-E₂ ATPases. This formation of a near thermodynamically neutral phospho-carboxyl mixed anhydride intermediate is the key mechanism that separates P-type ATPase from the other A-, E-, V- or F-type ATPases (Yatime *et al.*, 2009). The reaction mechanism of P-type H⁺-ATPase in Figure 1.10 is described by the Post-Albers scheme (Lecchi & Slayman, 2004). This mechanism describes two conformational states, E₁ and E₂ (later sometimes called open and closed states) associated with either ATP or the phosphate ion.

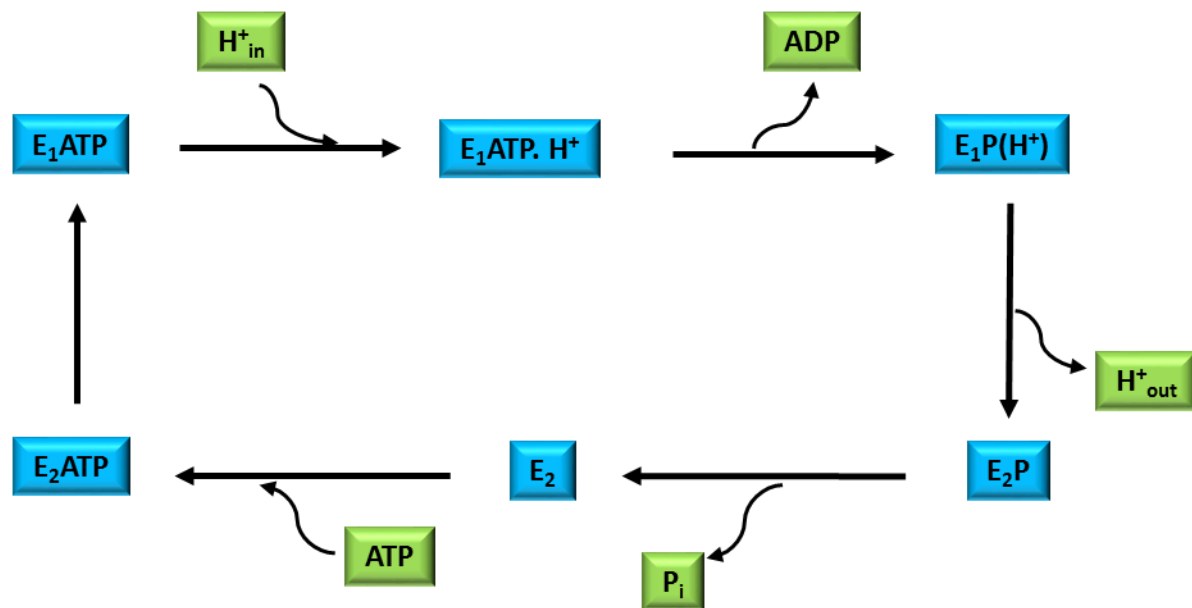


Figure 1. 10. Reaction cycle of P-type ATPases according to Post-Albers scheme.

(Lecchi & Slayman, 2004).

ATP first binds to the E_1 form of the enzyme in the nucleotide-binding domain which is then followed by the binding of intracellular H^+ ions to E_1ATP as shown in figure 1.10. Following binding of the hydronium ion, the transfer of the γ -phosphate from ATP to the enzyme produces a 'high-energy' β -aspartyl phosphate intermediate (E_1PH^+). The phosphorylated carboxylated group then undergoes hydrolysis with concomitant transfer of a proton through the enzyme to the extracellular space. In the process of exporting the H^+ , the E_1P form shifts to the E_2P conformation. However, the protein remains phosphorylated. The enzyme then dephosphorylates to form the E_2 state to which ATP binds thus re-generating the E_2 -ATP conformational state (Lecchi & Slayman, 2004; Yatime *et al.*, 2009; Palmgren & Nissen, 2011).

1.8 Compounds known to react with cellular thiols

Over the last 50 years, researchers have shown interest in compounds which are known to react with cellular thiols particularly compounds containing an α,β -unsaturated carbonyl group (Manavathu *et al.*, 1999). Compounds containing an α,β -unsaturated carbonyl group

markedly inhibit the plasma membrane H⁺-ATPase and exhibited antifungal activity (Dimmock *et al.*, 1998; Manavathu *et al.*, 1999; Nakhjiri *et al.*, 2012). Such activities are of interest since α,β -unsaturated carbonyl groups may not cause any genotoxic effects since thiols are not present in nucleic acids. However sulfhydryl reactive compounds react with a wide variety of proteins which contain reduced cysteine residues (Winslow, 1981).

Several studies have demonstrated that inhibition of Na⁺/K⁺, Ca²⁺ and H⁺/K⁺-ATPase can be achieved by a covalent interaction with group-specific chemical probes such as sulfhydryl reagents (Katz & Sussman, 1987). The PM H⁺-ATPase enzyme has been shown to be inhibited by maleimides (**9**) (e.g. N-ethyl maleimide, which binds to Cysteine 532), sulphinimides (e.g. omeprazole (**10**)), curcumin (**11**), chalcones (**12**), caffeic acid (**13**), ebselen (**14**) and α,β -unsaturated carbonyls such as 1,4-diene-3-ones (Figure 2.6) (Manavathu *et al.*, 1999).

1.8.1 Maleimides

A series of N-substituted imides were synthesized by Zentz *et al.*, (2002) who demonstrated that N-substituted maleimides (Figure 1.11) were highly active against various bacterial species including *Escherichia coli*, *Enterococcus faecalis*, *Staphylococcus aureus* and *Pseudomonas aeruginosa*.

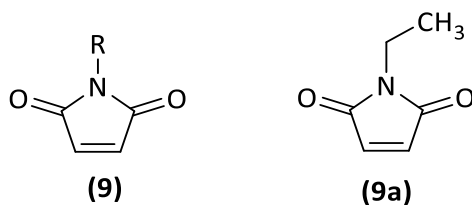


Figure 1. 11. General N-substituted maleimide structure (9) and N-ethyl maleimide (9a).

Maleimides (**9**) have also been shown to inhibit mitosis in fungal cells (Brooker & Slayman, 1982). They also demonstrated that N-ethyl maleimide (NEM) (**9a**) inhibits the H⁺-ATPase of

Neurospora crassa and that it can be used as a probe to examine the nature of enzyme-ligand interactions in PMA1. NEM binds to cysteine-532 in the cytoplasmic region causing inhibition of the PM H⁺-ATPase. NEM, a covalent modifier of protein sulfhydryl groups also exhibited inhibitory activity against the PM H⁺-ATPase (AHA) of *Avena sativa* root cells (Katz & Sussman, 1987).

1.8.2 Omeprazole

The PM H⁺-ATPase is a critical target that has been studied using the sulfhydryl-reactive reagent omeprazole (Seto-Young, Monk, Mason, & Perlin, 1997). Omeprazole (**10**) is used clinically as an anti-ulcerative drug, which following acid activation, is known to inhibit the gastrointestinal H⁺/K⁺-ATPase by reacting with a protein SH/thiol to form an asymmetric disulphide (Schultz *et al.*, 2007). The structure of acid-activated omeprazole is shown in Figure 1.12.

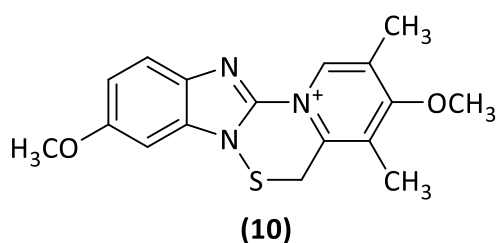


Figure 1. 12. Structure of acid-activated omeprazole (10).

Omeprazole has also shown inhibitory activity against the fungal plasma membrane H⁺-ATPase by the formation of a covalent (disulfide) bond within the first two transmembrane segments M₁ & M₂ in Figure 1.13 (Monk *et al.*, 1995). Specifically, acid activated omeprazole reacts with PMA1 to form a disulphide S-S bond between omeprazole and cysteine-148 in the M₂ loop.

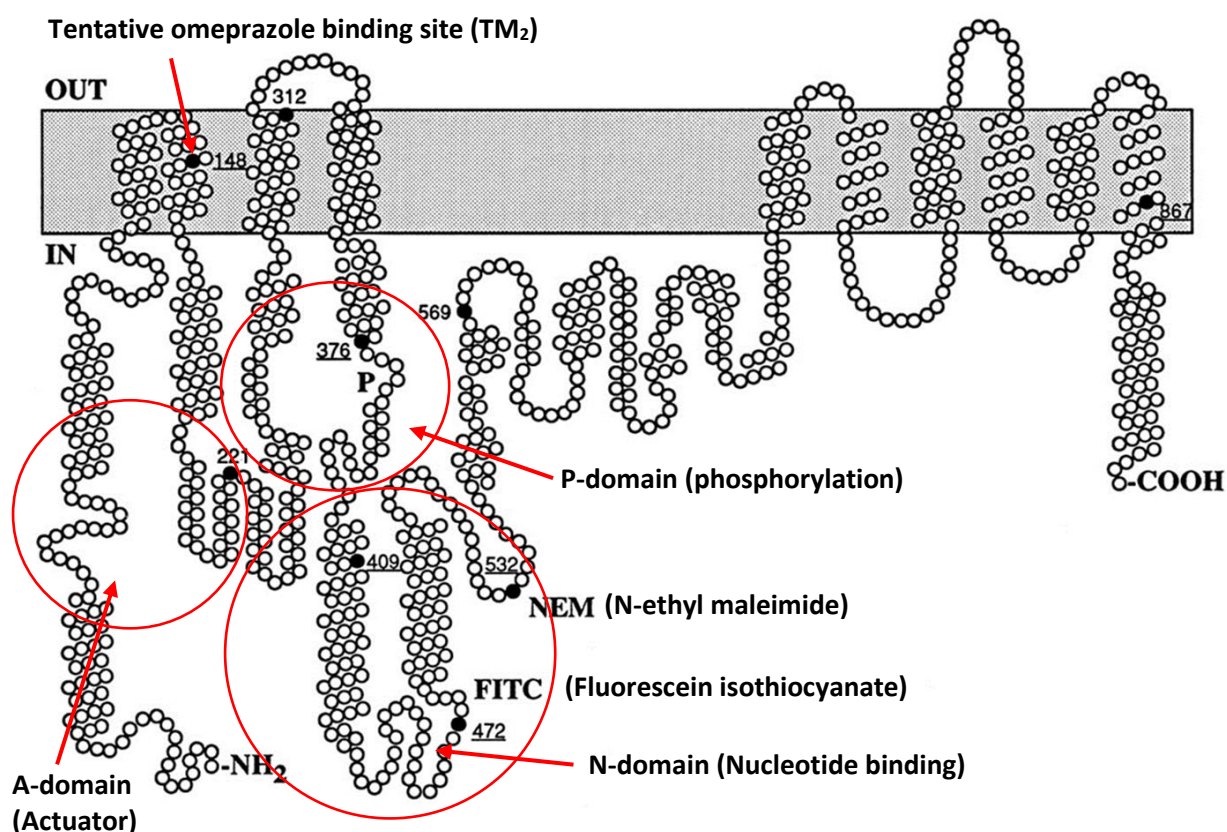


Figure 1. 13. The topology of the yeast plasma membrane H⁺-ATPase with extracytoplasmic and cytoplasmic binding sites.

The yeast plasma membrane H⁺-ATPase contains three cysteine residue in the transmembrane segment (C-148, C-312 and C-867) and six-cysteine residue in the cytoplasmic segment (C-221, C-376, C-409, C-472, C-532 and C-569). Omeprazole binds at the TM₂ region whereas N-ethyl maleimide binds in the N-domain region of the plasma membrane H⁺-ATPase. Image is taken from *Petrov & Slayman, 1995*.

Seto-Young *et al.*, (1997) have also studied the molecular interaction of omeprazole with the H⁺-ATPase of various *S. cerevisiae pma1* mutants. They have identified that modification of amino acid side groups (e.g. cysteine) at various positions in the membrane sector shown little effect. Site directed mutations at M128C and D140A or D140C enhanced the sensitivity of cells to omeprazole whilst G158D and G156C shown insensitivity to omeprazole. They have also shown that M128C, D140A or D140C did not show direct interaction with omeprazole. It

thus appears likely that inhibition by omeprazole is the result of some form of disruptive conformational changes following formation of the disulfide adduct.

1.8.3 Curcumin

Curcumin (**11a and b**) is a natural product obtained from the rhizome of the plant *Curcuma longa* and is most commonly used in Asian cooking. In solution curcumin commonly adopts a 'carbonyl and keto-enol' (**11b**) form rather than the di-carbonyl or di-keto form (**11a**). Many studies have shown that curcumin exhibits a wide range of biological activities including antifungal activity (Martins *et al.*, 2009), antioxidant, anti-tumour and anti-mutagenic (Neelofar *et al.*, 2011), antimicrobial, and anti-HIV protease activity (Sahu, Sahu, Gupta, Thavaselvam, & Agarwal, 2012).

Recent investigations concerning the antifungal activity of curcumin have shown that curcumin is more effective than fluconazole against various *Candida* species (Martins *et al.*, 2009). Curcumin has also shown inhibitory activity against the Ca^{2+} -ATPase (Logan-Smith, Lockyer, East, & Lee, 2001) and Na^+/K^+ -ATPase (Mahmmoud, 2005) and therefore it may be expected to have activity against the fungal plasma membrane H^+ -ATPase.

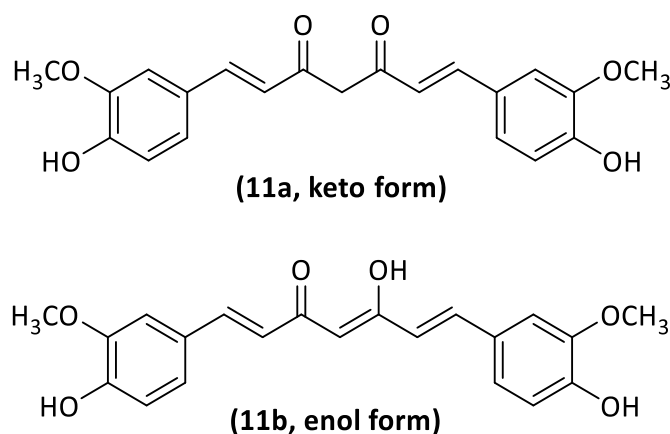
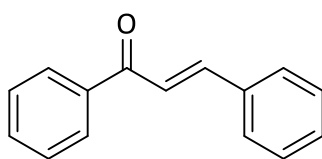


Figure 1. 14. Structure of curcumin (11).

Commercially available curcumin preparations contain several curcuminoids including curcumin (80%), demethoxycurcumin (15%) and about 5% of bisdemethoxycurcumin with various others being present in small amounts (Dao *et al.*, 2016). According to Dao *et al.*, (2016) demethoxycurcumin was an effective non-competitive ATP inhibitor of the fungal P-type ATPase (Pma1p; H⁺-ATPase). Additionally, it was also identified to be non-toxic to mammalian cells. However in vivo testing has shown that curcumin has very low bioavailability especially over the medium to long term.

1.8.4 Chalcones

Chalcones (**12**) are precursors of flavonoids, which are polyphenolic antioxidants found in many fruits, vegetables, nuts and red wine. Chalcones (Figure 1.15) contain two aromatic rings linked by a three-carbon α , β -unsaturated carbonyl structure and have been shown to inhibit the growth of *C. albicans* based on their ability to interact with sulfhydryl groups (Batovska *et al.*, 2007). They are also known to inhibit the synthesis of the fungal cell wall by inhibiting the $\beta(1,3)$ -glucan synthase enzyme (Lopez *et al.*, 2001; Chen, Zheng, Sun, and Piao, 2010).



(12)

Figure 1. 15. Structure of chalcone (12).

1.8.5 Ebselen

Ebselen (**14**) is a selenium-containing compound, known for its anti-oxidative, anti-inflammatory and anti-atherosclerotic properties (Figure 1.16). It has also been shown to

have antifungal properties (Soteropoulos *et al.*, 2000). More specifically ebselen has been shown to inhibit the H⁺-ATPase in *S. cerevisiae* in a concentration-dependent manner by interacting with a sulfhydryl group of cysteine (Chan, Hardej, Santoro, Lau-Cam, & Billack, 2007). Medium acidification by *S. cerevisiae* Pma1 appears to be blocked by ebselen in both haploid and diploid strains (Chan *et al.*, 2007).

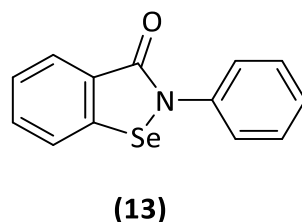


Figure 1. 16. Structure of ebselen (13).

1.8.6 Caffeic acid

Other α,β -ketones exhibiting antimicrobial activities include caffeic acids (**14a**). Sardi *et al.*, (2016) investigated their antifungal activity against *Candida* species and identified structure-activity relationships derived from various caffeic acids derivatives.

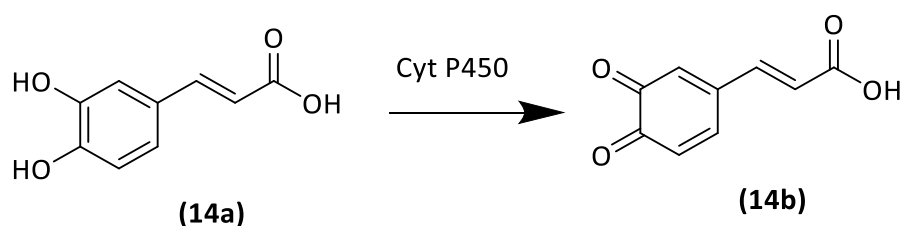


Figure 1. 17. Structure of caffeic acid (14a) and its oxidised form (14b).

However, it is also the case that oxidation of caffeic acids by cytochrome P450 may lead to the formation of various enzyme inhibitors. Since caffeic acids contains a 1,2-dihydroxy or catchol structure it is possible that caffeic acids may oxidise to 1,2-diones (**14b**) which will

react non-specifically with arginine residues. Such 1,2-diones structure of caffeic acid have been shown to be potentially toxic (Murakami *et al.*, 1990).

1.8.7 Other sulfhydryl reactive natural products

Other natural products found in vegetables and soft fruits such as the plant phenols ellagic acid (15), salvianolic acid (16) and plectrinone A (17) have been shown to inhibit the gastric H^+/K^+ -ATPase (Figure 1.18). Ellagic acid blocks the formation of phosphoenzyme in the H^+/K^+ -ATPase by competing with ATP at the ATP hydrolysis site (Murakami *et al.*, 1990). A study conducted on *Plectranthus barbatus* leaves has shown that the molecule Plectrinone A is also capable of inhibiting the gastric H^+/K^+ -ATPase acting as both an antiulcerative and antisecretory molecule (Schultz *et al.*, 2007). However, Plectrinone A also contains a quinoid sub-structure which may be associated with the generation of toxic free radicals such as hydroxyl or peroxy.

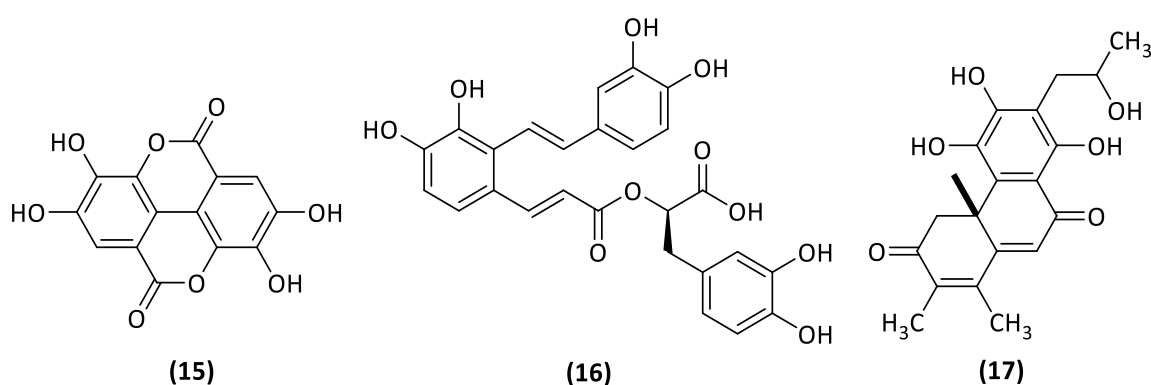


Figure 1. 18. Structures of ellagic acid (15), salvianolic acid (16) and plectrinone A (17).

The gastric H^+/K^+ -ATPase inhibitors such as ellagic acid, salvianolic acid and plectrinone A. These three compounds have ortho-catechol structure and a poly hydroxyl stilbene structure both of 1,2-dihydroxy moiety. However, salvianolic acid also contains an α,β -unsaturated carbonyl group which may interact with H^+/K^+ -ATPase.

Although containing α,β -unsaturated ketones the phenolic hydroxyl groups of both ellagic and salvianolic acids appear to be essential for their interaction with the ATPase (Murakami

et al., 1990). Salvianolic acid A and ellagic acid binds to the ATPase on the cytosolic side and inhibits the synthesis of the phosphoenzyme intermediate thus inhibiting the H⁺/K⁺-ATPase (Murakami *et al.*, 1990). As indicated for caffeic acid all of the compounds salvianolic acid, ellagic acid and plectrinone A contain an ortho catecholic structure which may possibly be oxidised to a 1,2-dicarbonyl. Such 1,2-dicarbonyls are well known to be toxic due to non-specific interactions with protein arginine residues (Murakami *et al.*, 1990).

Recently an article published by Tung *et al.*, (2017) demonstrated that benzo[d]thiazoles containing a 3,4-dihydroxyphenyl moiety acts as a potent inhibitors of PM H⁺-ATPase. However, their synthesized compounds are unlikely to be drugable due to the presence of the 3,4-dihydroxybenzene moiety, present within the whole structure which will probably oxidise to the arginine reactive 3,4-dicarbonyl structure. Alternatively it may be methylated via catechol-O-methyltransferase (COMT) which has a low substrate specificity regarding methylation of the hydroxyl (-OH) group probably at ring position-3, or alternatively sulphated by phenol-o-sulphatase (Tung *et al.*, 2017).

In a recent review on drug development, curcumin was classified as a pan-assay interference compound (PAINS) and invalid metabolic panaceas (IMPS) based on the presence of a reactive Michael acceptor, its susceptibility to aggregation and its fluorescence activity (Nelson *et al.*, 2017). Furthermore, curcumin itself is not considered as a potential drug candidate due to its toxic effects under certain circumstances, low efficacy in several disease models, poor solubility and low bioavailability (Nelson *et al.*, 2017).

Similarly due to the requirement for prior acid activation and pH dependence of omeprazole action (Monk *et al.*, 1995; Tung *et al.*, 2017), its weak inhibitory effect against the plasma membrane H⁺-ATPase, the general toxicity of ebselen makes all of these molecules poor

starting points for developing novel anti-fungal drugs targeting the H⁺-ATPase (Tung *et al.*, 2018). Hence, these compounds are not considered for further investigation in the discovery and development of H⁺-ATPase inhibitors as new antifungal agents.

Studies have shown that α,β -unsaturated ketones (chalcones, acrylic acid, etc) undergo Michael reactions with protein thiols such as cysteine (Pati *et al.*, 2009). The nucleophilic attack would be anticipated to occur on the β -carbon of the enones due to the electron-withdrawing effect of the carbonyl group (Manavathu *et al.*, 1999). However various drugs containing this enone structure have been licensed in recent years for the treatment of various diseases, which are regulated by ATP binding proteins such as protein kinases (Chène, 2002; Barf & Kaptein, 2012; Haruta, Gray, & Sussman, 2015).

1.9 Structure-activity relationship (SAR)

One of the first examples of the development of a structure-activity relationship is the established work of Meyer and Overton. They investigated the physicochemical and structural parameters that lead them to predict potencies of anaesthetics (Meyer, 1901; Overton, 1991). From various *in vivo* and *in vitro* experiments, they were able to plot anaesthetic potency against the same consistent set of octanol/water partition coefficients (logP). The results proposed that the potencies of anaesthetics were due to their lipophilic properties (Schwilden & Schuttler, 2008).

Subsequently in the 1930s Hammett introduced the concept of substituent constants (σ) to predict how the introduction of either electron withdrawing groups or electron donating groups onto a benzene ring would alter the rate constants of chemical reactions using a linear free-energy relationship (Mager, 2006). In this work Hammett characterised the electronic influence of the various substituent groups in a series of benzoic acids on the reaction

equilibrium dissociation constant (Mager, 2006). This constant now termed the Hammett substituent constant (σ) is one of the best-known and utilised parameters used to measure electrostatic interaction forces between molecules. It provides a quantitative assessment of the electron-withdrawing or -donating properties of different functional groups relative to hydrogen.

In the 1960s, Hansch & Fujita, (1964) developed a Quantitative structure-activity relationship (QSAR) model. They correlated structure and biological activity based on the concept of linear free energy relationship by incorporating the Hammett constant (σ) and the lipophilicity index (π), a term derived from the water/octanol partition coefficient, a descriptor in the Hansch equation (Hansch & Fujita, 1964). This (now called) Hansch equation is used to analyze chemical and biological data using linear regression or pattern recognition techniques. General practice in the drug discovery process is to optimize the SAR of functional groups with regard to their role in biological activities and perform analyses using complex computer-based techniques involving multivariate analysis.

Modern technique in QSAR may use up to six different physicochemical descriptors, from then now more than one thousand properties that may be measured or calculated to analyze the relationships between chemical and biological activities for small data sets or more descriptors for large datasets. A QSAR model provides information about the correlation of physiochemical and structural properties of compounds with their biological properties, such as protein binding, or enzyme or receptor affinity. This relationship is then used to estimate and predict the biological properties of new molecules prior to their chemical synthesis.

A modification in the chemical structure of a compound may result in changes in its properties and thus a change to its biological activity. By comparing the molecular properties with the

biological activity of the compounds, QSAR modelling predicts the most promising structural derivatives that might be synthesized to obtain the greatest efficacy for a potential drug. Additionally, there is no totally accurate or definitive method for predicting ADME properties such as binding of novel molecules or drugs to plasma proteins. However, it is possible to measure protein binding using techniques such as Surface Plasmon Resonance (SPR) or fluorescence (polarisation) using a fluorescently labelled analogue of the molecule set in order to investigate binding (Giannetti, Koch, & Browner, 2008; Leonova *et al.*, 2013; Tung *et al.*, 2017).

In order to analyse the data resulting from such experiments, sets of inhibitor molecules are analysed using QSAR. This methodology is used to determine which combinations of a wide variety of molecular descriptors may be used to construct a mathematical relationship using the statistical algebraic technique of regression analysis to biological activity. Such techniques include multi variate and non-linear regression analysis. By using commercial statistical software packages for QSAR modelling it is possible to obtain either a two or three-dimensional (2D or 3D) arrangement of chemical groups that are potentially involved in defining the biological response to a given molecule. Such analyses may be used to optimise or maximise biological responses including ADME, pharmacokinetics and pharmacodynamics, etc (Yap & Chen, 2005).

In the early stages of QSAR, modelling was used in the analysis of chemical structures in order to determine any relationships between properties such as lipophilicity ($\log P$, (octanol/water)); π , the Hammett substituent constant (σ) and the Taft steric parameter (T_s) and biological responses such as inhibition of growth or enzyme/receptor binding. Molecular structures could be then devised prior to their synthesis that would hopefully have a set of

desired properties such as target binding, residency time, plasma half-life, etc. that could be further modified to produce drug candidates optimised in terms of their structure and mapping to the probable drug binding site(s). Such modelling would potentially optimise and minimise the number of molecules required to be synthesized.

Therefore, QSAR modelling is used as a guide to modify the molecular structures of potential drugs in order to alter their physicochemical properties in some defined fashion. There are now in excess of 1202 physicochemical and molecular descriptors of which some 284 descriptors are listed in the computer programme MOE that may be used to correlate with some response or (bio) assay (e.g. dose required to elicit 50% of the maximum activity, EC_{50} , IC_{50} , K_i , MIC, etc).

Many reviews and articles have been published regarding QSAR modelling and antifungal activity. However most researchers have focused on ligand-receptor interactions. For example Caballero & Fernández, (2006) predicted the antifungal activity of 96 heterocyclic ring derivatives against *C. albicans* using Bayesian-regularized neural networks along with multiple linear regression of 2-substituted benzothiazoles, 2,5-disubstituted benzimidazoles, 2,5,6-trisubstituted benz-oxazoles and 2-substituted oxazole(4,5-b)pyridines. They have shown that the molecular mass, polarizability and compound volume have an important relationship with the potency of compounds.

In other studies a QSAR model for antifungal activity of heterocyclic compounds was developed by using principal component analysis (PCA) and multiple regression analysis (MRA) on benzoxazoles, benzimidazoles, benzothiazoles and oxazolo[4,5-b]pyridines against *C. albicans* (Ursu, Costescu, Diudea, & Parv, 2006). A further study conducted by Duchowicz, Vitale, Castro, Fernández, & Caballero, (2007) described how QSAR modelling using linear

regression analysis on 1202 descriptors, including electronic, geometrical or topological parameters was used on a library of heterocyclic compounds in order to determine optimal structures for antifungal activity.

In yet a further study, Katritzky, Slavov, Dobchev, & Karelson, (2008) used a set of measured antifungal activities of a library of disparate molecular structures in order to determine the best physicochemical descriptors in order to develop a general QSAR for antifungal activity. They have generated a QSAR using CODESSA PRO software to generate descriptors (electronic, topological, geometrical and hybrid) and subsequently correlated them with the MIC values of a diverse set of 83 compounds obtained from susceptibility assay on *C. albicans*. They have seen an increase in the antifungal activity when a molecule acts as a stronger electrophile and identified that generated models showed a fundamental influence of electrostatic properties over both steric and transport abilities. The presence of heteroatoms in a molecule is usually related to their electronegativity or electron pairing which is often responsible for the surface recognition and creating acceptor-donor bonds. They have also shown that proposed molecules with higher logP values tends to show a decrease in the antifungal activity. The models generated by Katritzky *et al.*, (2008) shows similar trend between individual and general model indicating the main influence was due to the electrostatic effects compared to the steric effects or transport abilities.

Based on this theory it is believed it would be useful to synthesize a library of molecules containing electrophiles containing the 1,4-diene-3-one pharmacophore which contains the α,β -unsaturated carbonyl and determine their ability to act as antifungal agents. Subsequently *in silico* SAR could be used to analyse the possible relationships between mechanism(s) of action of such compounds or structures and biological activity. The

synthesized compounds should have a noticeable affinity or reactivity towards thiols, but not for hydroxyl or amino groups such as are found in nucleic acids.

Other potential SH reactive pharmacophores could include sulphenamide (Yatime *et al.*, 2009) or R-substituted acyloxy methyl ketone (Figure 1.19) (Krantz, Copp, Coles, Smith, & Heard, 1991). Where R is a fragment that may have an affinity for docking to the nucleotide-binding site or the omeprazole binding site of PMA1. By targeting specific binding sites and generating molecules of high (nanomolar to low micromolar) affinities along with them being reactive to cysteine residues within or close to the binding site they are less likely to have carcinogenic or mutagenic effects.

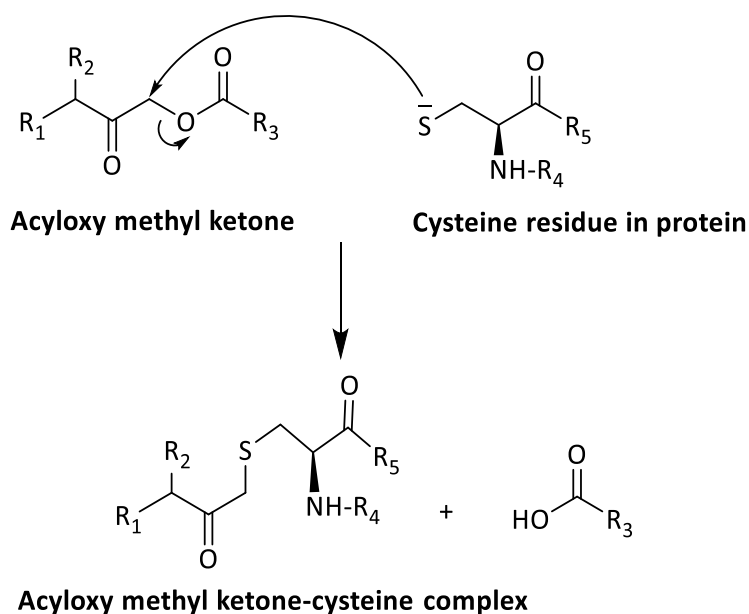


Figure 1. 19. Mechanism of cysteine proteinase inactivation with acyloxy methyl ketone. Such compounds could potentially react with PMA1 cysteines if designed correctly.

It is anticipated that the synthesized compounds will react with either the sulfhydryl-containing region (S⁻ or SH) of the PM H⁺-ATPase either in the extra-cytoplasmic region i.e the omeprazole binding region or alternatively the cysteine present in the nucleotide binding site in the cytoplasmic region where NEM has been shown to bind (Brooker & Slayman, 1982).

1. 10 Aims and scope

The plasma membrane H⁺-ATPase is an essential fungal protein and an anticipated therapeutic target for the discovery of novel antifungal agents. Cysteine reactive pharmacophores may prove useful in PMA-targeted drugs as many of the nucleotide-binding sites of protein kinases lack cysteine residue (Krishnan *et al.*, 2014). This lack of cysteine potentially gives the drugs a higher degree of selectivity if targeting ATP binding sites in fungi along with lower toxicities or side effects (Zhao, Liu, Bliven, Xie, & Bourne, 2017). It was believed that derivatives of bis-benzylidienones might be useful bio-chemical probes to determine some of the structural requirements for drugs targeted to cysteine residues found in transmembrane segments M₁ and M₂ or in the nucleotide-binding (N) domain of the cytoplasmic site of PMA1. Given the generally accepted safety of benzylidenes, chalcones and related compounds, a library of 1,4-diene-3-ones containing an α,β -unsaturated carbonyl group has been synthesised using standard synthetic procedures. The intent of this study was to explore 1,4-diene-3-ones and identify if they are capable of inhibiting the export of protons from the fungal cell, thus changing the plasma membrane Δ pH and decreasing the cytoplasmic pH. These results lead to a decrease in cell growth and cell division (Monk *et al.*, 1995).

1.10.1 Objectives

- 1) To synthesize a library of dienones comprising bis-benzylidene, bis-pyridylidene and bis-thienylidene derivatives of N-methylpiperidin-4-one, cyclopentanone and cyclohexanone;
- 2) To characterize the synthesized compounds using ¹H- and ¹³C-NMR, mass spectrometry, FT-IR spectroscopy, Thin-layer chromatography (TLC) and melting points;

- 3) To determine the potency of the synthesized 1,4-diene-3-ones against *S. cerevisiae* and *C. albicans*;
- 4) To determine the mechanism of action of the synthesized 1,4-diene-3-ones by conducting the proton extrusion assays on carbon starved *S. cerevisiae* cells;
- 5) To perform a preliminary structure-activity relationship of the 1,4-diene-3-ones antifungal activity with their electronic and lipophilic properties.

CHAPTER TWO

SYNTHESIS AND CHARACTERIZATION OF 1,4-DIENE-3-ONES

2 Synthesis and characterization of 1,4-diene-3-ones

2.1 Introduction

Several studies have shown that α,β -unsaturated carbonyl compounds are able to undergo a Michael addition with cellular or protein thiols (Das *et al.*, 2007). The Michael addition is the nucleophilic addition to the electrophilic β -carbon of an α,β -unsaturated carbonyl compound (Pati *et al.*, 2009). An α,β -unsaturated carbonyl group is electrophilic in nature, therefore, it is easily attacked by a nucleophile at the β -carbon atom. These compounds have noticeable reactivities towards thiols but not for hydroxyl or amino groups such as those found in nucleic acids (Leonova *et al.*, 2013). Thus they are less likely to have carcinogenic or mutagenic effects (Pati *et al.*, 2009). Thus, a possible mechanism of action of the dienones is by the reaction of one or more of the sulfhydryl groups found in the various cysteine residues present in the fungal plasma membrane PMA1 protein with the dienone (Pati *et al.*, 2009; Tung *et al.*, 2018).

These α,β -unsaturated carbonyl compounds can be synthesised using the Claisen-Schmidt reaction. The Claisen-Schmidt reaction plays an indispensable role in organic chemistry. It is a condensation reaction of an (aromatic) aldehyde with a ketone containing a methylene α to the carbonyl to generate α,β -unsaturated carbonyl compounds (Rahman, Ali, Jahng, & Kadi, 2012). This reaction requires a strong base (e.g. sodium hydroxide) in the presence of alcoholic or aqueous solvent. Alternatively the reaction can occur using a strong acid like hydrochloric acid in glacial acetic acid (Leonova *et al.*, 2010). Ketones containing ' α ' methylene groups have a tendency to undergo tautomerisation due to the formation of keto/enol-tautomers (Figure 2.1). Sodium hydroxide solution is not basic enough to completely form an enolate ion therefore carbanion attack another molecule of aldehyde and

form a bond. This allows coupling of (benz) aldehydes with such ketones to form benzylidene structures.

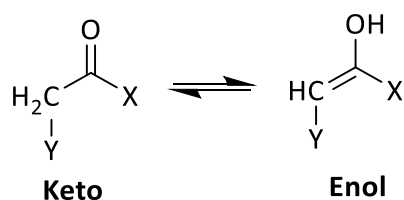


Figure 2. 1. Structures of keto and enol intermediates.

Curcumin a yellow carotenoid, natural product can be isolated from turmeric and which along with other α,β -unsaturated enones such as caffeic acid have shown promise as antifungal agents (Martins *et al.*, 2009). It has been suggested that this small molecule is an encouraging lead compound for structural modification. Therefore, in this study, the 1,3-dicarbonyl structure of curcumin (**11a**) was modified by removing the CH₂-CO section (to eliminate dicarbonyl metal binding) and various analogs were generated as “dienones” which are the mono-carbonyl homologs of curcumin, hereafter referred to as 1,4-diene-3-ones. A library of thirty-three symmetrical 1,4-diene-3-ones was synthesized using the Claisen-Schmidt reaction.

In this study, the coupling of ketones, such as N-methylpiperidin-4-one (**18c**), with ring-substituted benzaldehydes (**19**) at carbons 3 and 5 of the ketone was accomplished using the Claisen-Schmidt reaction in the presence of a base catalyst, usually aqueous ethanolic sodium hydroxide to yield compounds **22a-t** (Leonova *et al.*, 2010). Various substituents on aromatic rings were introduced to vary the magnitude of their hydrophobic, electronic or (iso)steric properties. Common steric effects include steric hindrance and Vander Waals repulsion. The library of compounds was further extended by reacting heterocyclic aldehydes such as pyridinecarboxaldehydes (which contain a nitrogen atom at either the *ortho*-, *meta*- or *para*-

positions; **20a**, **20b**, **20c**). Alternatively, the pseudo-aromatic 2-thiophenecarboxaldehyde (**21**) was coupled with the appropriate ketone; cyclopentanone (**18a**), cyclohexanone (**18b**) or N-methylpiperidin-4-one (**18c**).

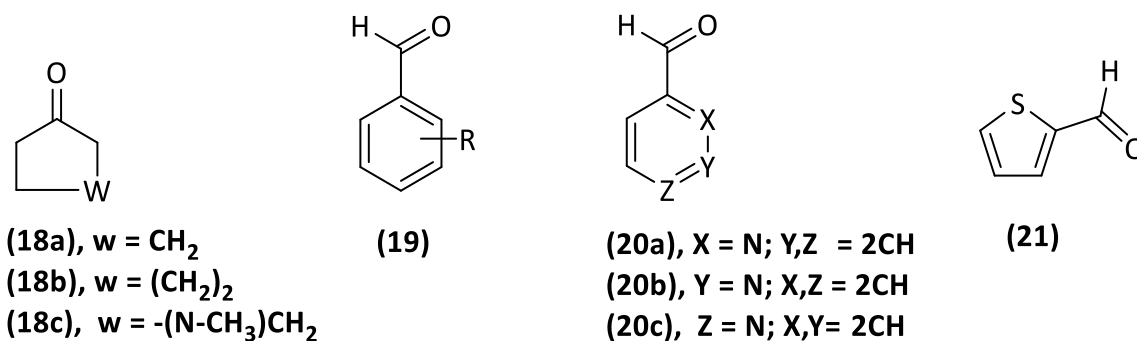


Figure 2. 2. Structures of various aldehydes and ketones.

Parent cyclopentanone (**18a**) and cyclohexanone (**18b**), N-methylpiperidin-4-one (**18c**), ring substituted benzaldehyde (**19**), 2-pyridinecarboxaldehyde (**20a**), 3-pyridinecarboxaldehyde (**20b**), 4-pyridinecarboxaldehyde (**20c**) and 2-thiophenecarboxaldehyde (**21**), respectively.

2.2 Materials and Methods

2.2.1 Materials

Chemical reagents were purchased from either Sigma-Aldrich (UK) or Maybridge Chemicals and were used without further purification. Solvents were purchased from Fisher Scientific (UK). Silica gel plates for thin-layer chromatography (TLC) were obtained from Macherey-Nagel, Germany: DC-Fertigfolien POLYGRAM SIL G/UV₂₅₄. TLC was used to monitor the reaction and the purity of the compounds. TLCs were visualized using a UVGL-58 handheld ultra-violet (UV) lamp (UVP, Cambridge, UK). Melting points (m.pt) were determined using an open capillary tube in the heating block of a Griffin melting point apparatus (EDU-LAB: EN61010-1) and are uncorrected.

Proton, carbon and DEPT (Distortionless Enhancement by Polarization Transfer) NMR spectra were recorded using a JEOL ECA400 spectrometer, CDCl₃ (deuterated chloroform) was used to dissolve the compounds unless otherwise indicated, in which case dimethyl sulfoxide (DMSO) was used. Chemical shifts were measured in ppm (δ) for both proton and ¹³C-NMR. Abbreviations used to identify the splitting or coupling patterns were described as s (singlet), d (doublet), dd (doublet of doublets), t (triplet), q (quartet), m (multiplet) and br (broad). The coupling constant, J values (Hz) were used to measure the interaction between a pair of protons.

Infrared spectra were obtained using a Perkin-Elmer Fourier Transform Infrared Spectrometer (SA-LR 64912C) using a golden gate plate attachment point. The IR peaks were measured in wavenumbers (cm⁻¹) over the region 4000–400 cm⁻¹. Liquid chromatography-Mass spectrometry (LC-MS) analysis was performed to obtain both molecular mass and molecular fragments of synthesized compounds using both positive and negative modes. Unless indicated otherwise acetonitrile was used as a solvent to dissolve the compounds. LC-MS data were recorded using a VG Micromass V15 spectrometer operating at 70 eV (Varian: 210 LC pumps x 2, 1200L Quadrupole MS/MS, 410 autosampler). The LC-MS was equipped with a Varian Pursuit C18 column (3000 – 050 x 020 mm, 5 μ m) and eluted using a gradient method containing water with 0.1% formic acid and acetonitrile with 0.1% formic acid (90:10 - 10:90 - 90:10) at a flow rate of 1 ml/min.

2.2.2 Experimental section

2.2.2.1 General method for the synthesis of ring substituted bis(benzylidene) derivatives of methylpiperidin-4-one, cyclopentanone and cyclohexanone

Method A: The synthetic route to compounds (**22a-v**) is shown in Figure 2.3. The appropriate ketone [cyclopentanone (**18a**), cyclohexanone (**18b**) or N-methyl-4-piperidone (**18c**), 10 mmol] was dissolved in 25 ml of 95% ethanol in a 100 ml round bottom flask. Subsequently, a ring substituted benzaldehyde (**19**, 20 mmol, **Table 2.1**) was added and stirred, with cooling, to 5 °C. An aqueous solution of sodium hydroxide (10% w/v, 10 ml) was added dropwise with vigorous stirring. The reaction mixture was stirred for 120 minutes at room temperature until a precipitate was obtained. The reaction mixture was monitored using TLC to check the progress of the reaction using ethyl acetate/cyclohexane (1:1) as developing solvents.

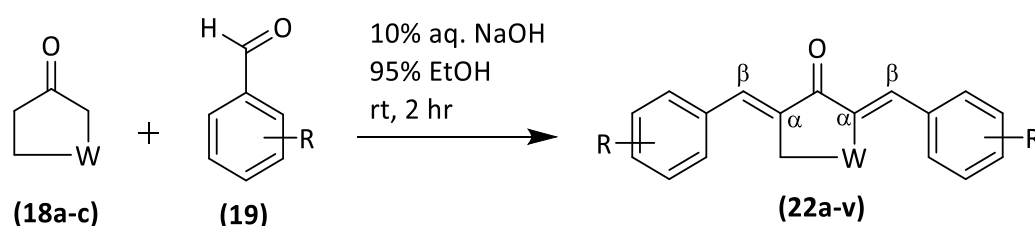
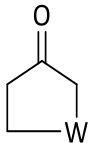
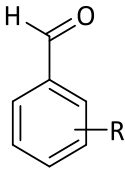


Figure 2. 3. Synthesis of bis-benzylidene derivatives of N-methylpiperidin-4-one or cyclopentanone or cyclohexanone (22a-v).

The precipitate was filtered under vacuum, rinsed with cold 95% ethanol (normally 3 ml) and dried using a vacuum pistol (50 °C) to a constant weight. The crude product was recrystallized from dichloromethane (approximately 5 ml) and 95% hot ethanol (approx. 12 ml). The resultant crystalline products ranging from white to yellow/ orange or brown in colour depending on the ring substituent(s) were filtered under vacuum, rinsed with ice-cold 95% ethanol (usually approx. 3 ml) and finally dried to a constant weight using a vacuum pistol (50 °C). The purity of each synthesized compound was initially analysed by TLC on silica using ethyl acetate/cyclohexane (1:1) as developing solvents, followed by NMR. Due to the cost and

limited amount of starting material available, compounds **22q** and **22r** were prepared on a small-scale utilising one mmol of N-methylpiperidin-4-one and two mmol of the relevant iodo-benzaldehyde.

Table 2. 1. List of various R-substituted bis-benzylidene derivatives of N-methylpiperidin-4-one and cycloalkanones (22a-v).

Compound		
	(18a-c) Where W=	(19) Where R=
22a	-(N-CH ₃)-CH ₂ -	H
22b	-(N-CH ₃)-CH ₂ -	2-OCH ₃
22c	-(N-CH ₃)-CH ₂ -	3-OCH ₃
22d	-(N-CH ₃)-CH ₂ -	4-OCH ₃
22e	-(N-CH ₃)-CH ₂ -	2-Cl
22f	-(N-CH ₃)-CH ₂ -	3-Cl
22g	-(N-CH ₃)-CH ₂ -	4-Cl
22h	-(N-CH ₃)-CH ₂ -	2, 4-diCl
22i	-(N-CH ₃)-CH ₂ -	3, 4-diCl
22j	-(N-CH ₃)-CH ₂ -	2-COOH
22k	-(N-CH ₃)-CH ₂ -	4-COOH
22l	-(N-CH ₃)-CH ₂ -	4-CH ₃
22m	-(N-CH ₃)-CH ₂ -	3-CF ₃
22n	-(N-CH ₃)-CH ₂ -	4-CF ₃
22o	-(N-CH ₃)-CH ₂ -	3-OCF ₃
22p	-(N-CH ₃)-CH ₂ -	4-OCF ₃
22q	-(N-CH ₃)-CH ₂ -	2-I
22r	-(N-CH ₃)-CH ₂ -	3-I
22s	-(N-CH ₃)-CH ₂ -	3-NO ₂
22t	-(N-CH ₃)-CH ₂ -	4-NO ₂
22u	-CH ₂ -	H
22v	-(CH ₂) ₂ -	H

2.2.2.2 Preparation of bis-pyridylidene derivatives of N-methylpiperidin-4-one and cycloalkanones

Method B: The synthetic route to the bis-pyridylidene derivative of N-methylpiperidin-4-one or cyclopentanone or cyclohexanone (**22a-h**) is shown in Figure 2.4. Briefly, a solution containing 10 mmol of ketone (cyclopentanone (**18a**), cyclohexanone (**18b**) or N-methyl-4-piperidone (**18c**)) was prepared in distilled water (40 ml). Subsequently, isomers of pyridine carboxaldehyde (**20**, 20 mmol, **Table 2.2**) were added (to different reactions) and stirred, with cooling, to 5 °C. An aqueous solution of NaOH 10% w/v (2 ml) was added with vigorous stirring. The reaction mixture was stirred for 10 hours at room temperature (Vatsadze *et al.*, 2006). TLC using ethyl acetate/cyclohexane (1:1) as developing solvents was used to monitor the progress of the reaction. The reaction mixture was neutralized using a dilute solution of hydrochloric acid (≈ 1 ml). The resultant yellow precipitate was filtered under vacuum, rinsed with cold 95% ethanol (usually 3 ml) and dried using a vacuum pistol (50 °C) to a constant weight. The crude product was purified using the recrystallization method detailed in **section**

2.2.2.1.

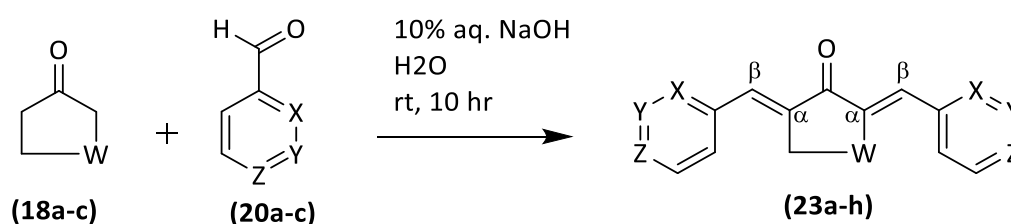
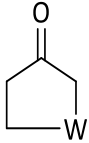
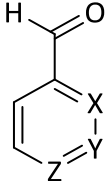


Figure 2. 4. Synthesis of bis-pyridylidene derivatives of N-methylpiperidin-4-one or cyclopentanone or cyclohexanone (23a-h).

Table 2. 2. List of bis-pyridylidene derivatives of N-methylpiperidin-4-one, cyclopentanone and cyclohexanone (23a-h).

Compound	 (18a-c)	 (20a-c)
	Where W=	
23a	-(N-CH ₃)-CH ₂ -	X=N, Y=H, Z=H
23b	-(N-CH ₃)-CH ₂ -	X=H, Y=N, Z=H
23c	-(N-CH ₃)-CH ₂ -	X=H, Y=H, Z=N
23d	-CH ₂ -	X=N, Y=H, Z=H
23e	-CH ₂ -	X=H, Y=N, Z=H
23f	-CH ₂ -	X=H, Y=H, Z=N
23g	-(CH ₂) ₂ -	X=H, Y=N, Z=H
23h	-(CH ₂) ₂ -	X=H, Y=H, Z=N

2.2.2.3 Preparation of bis-thienylidene derivatives of N-methylpiperidin-4-one and cycloalkanones

Compounds **24a-c** were prepared using a modification from the method described in **section**

2.2.2.2 Method B and their synthetic route is displayed in Figure 2.5.

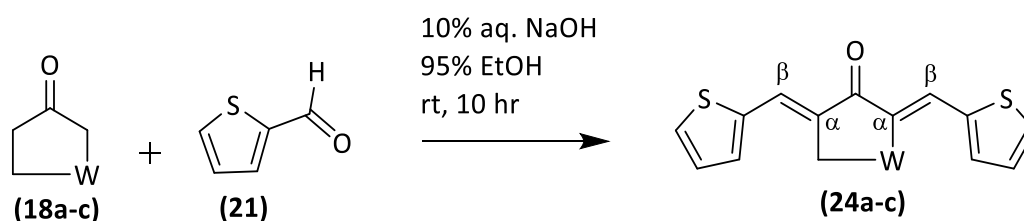
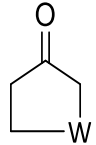
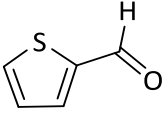


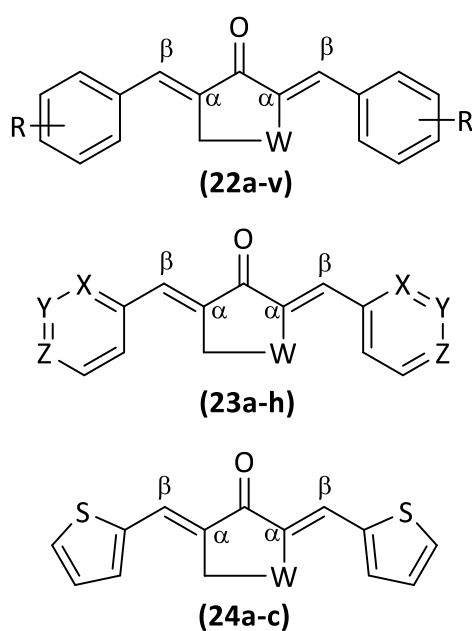
Figure 2. 5. Synthesis of thienylidene derivatives of N-methylpiperidin-4-one and cycloalkanones (24a-c).

Ketone (10 mmol; **18a**, **18b** or **18c**, **Table 2.3**) was dissolved in 95% ethanol (15 ml) followed by the addition of 20 mmol of 2-thiophenecarboxaldehyde (**21**), stirred with cooling, to 5 °C. An aqueous sodium hydroxide solution (10% w/v, 0.4 ml) was added dropwise with vigorous stirring. The reaction mixture was stirred for 10 hours until a yellow precipitate was obtained. The progress of the reaction was monitored using TLC with acetate/cyclohexane (1:1) as developing solvents. Crude products were recrystallized by following the method described above in **section 2.2.2.1** Method A.

Table 2. 3. List of bis-thienylidene derivatives of N-methylpiperidin-4-one, cyclopentanone, and cyclohexanone (24a-c).

Compound	 (18a-c) Where W=	 (21)
24a	-(N-CH ₃)-CH ₂ -	2-thiophene-carboxaldehyde
24b	-CH ₂ -	2-thiophene-carboxaldehyde
24c	-(CH ₂) ₂ -	2-thiophene-carboxaldehyde

A library of thirty-three symmetric 1,4-diene-3-ones (Figure 2.6) contains three groups of molecules, namely; bis-benzylidene, bis-pyridylidene or bis-thienylidene derivatives of N-methylpiperidin-4-one, cyclopentanone and cyclohexanone. All of these compounds contain the dienone pharmacophore with an α,β -unsaturated carbonyl group in the centre.



Where, R = F, Cl, Br, I, COOH, CH₃, OCH₃, CF₃, OCF₃, NO₂

X = N; Y, Z = H

Y = N; Z, Z = H

Z = N; X, Y = H

W = -(CH₂), -(CH₂)₂, -(NCH₃)CH₂

Figure 2. 6. Structures of synthesized 1,4-diene-3-ones.

Thirty-three symmetric 1,4-diene-3-ones were synthesized using the Claisen-Schmidt reaction. Within the molecular classes, R-substituted bis-benzylidene derivatives of N-methylpiperidin-4-one and cycloalkanones (**22a-v**), bis-pyridylidene derivatives of N-methylpiperidin-4-one and cycloalkanones (**23a-h**) and bis-thienylidene derivatives of N-methylpiperidin-4-one and cycloalkanones (**24a-c**).

2.3 Results – Spectral data of synthesized 1,4-diene-3-ones

2.3.1 Spectral data of bis-(benzylidene)-1-methylpiperidin-4-one

3,5-Bis[(E)benzylidene]-1-methylpiperidin-4-one (22a)

Yellow powder, 77% yield; m.pt. 110-111 °C, (literature (Pati *et al.*, 2009) m.pt. 110 °C). ¹H NMR (400 MHz, CDCl₃) δ ppm: 2.49 (s, 3 H), 3.87 (s, 4 H), 7.38 - 7.45 (m, 10 H), 7.88 (s, 2 H). ¹³C NMR (400 MHz, CDCl₃) δ ppm: 45.90, 57.16, 128.32, 128.65, 129.10, 130.48, 133.21, 135.36, 136.53, 187.02 (C=O). IR (V_{max}): 1671.72 (C=O), 1615.41 (C=C, olefinic), 1585.52 (C=C, aromatic) cm⁻¹. LC-MS (ESI): *m/z* calculated for C₂₀H₁₉NO [M+H]⁺: 289.37; found: 290.6.

3,5-bis[(E)-2-methoxybenzylidene]- 1-methylpiperidin-4-one (22b)

Yellow crystals, 72% yield; m.pt. 111-113 °C, (literature (Wu *et al.*, 2013) m.pt. 108.2 – 110.9 °C). ¹H NMR (400 MHz, CDCl₃) δ ppm: 2.37 (s, 3 H), 3.66 (d, *J*=1.74 Hz, 4 H), 3.83 (s, 6 H), 6.90 – 6.98 (m, 4 H), 7.18 - 7.20 (dd, *J*=7.60, 1.56 Hz, 2 H), 7.31 - 7.35 (m, *J*=1.65 Hz, 2 H), 8.06 (s, 2 H). ¹³C NMR (400 MHz, CDCl₃) δ ppm: 45.62, 55.71, 57.24, 110.72, 110.98, 119.93, 120.23, 124.59, 130.14, 130.30, 130.62, 132.22, 133.13, 158.56, 187.05 (C=O). IR (V_{max}): 1667.9 (C=O), 1606 (C=C, olefinic), 1575.1 (C=C, aromatic) cm⁻¹. LC-MS (ESI): *m/z* calculated for C₂₂H₂₃NO₃, [M+H]⁺: 349.43; found: 350.5.

3,5-bis[(E)-3-methoxybenzylidene]- 1-methylpiperidin-4-one (22c)

Yellow crystals, 84% yield; m.pt. 115-117 °C. ¹H NMR (400 MHz, CDCl₃) δ ppm: 2.44 (s, 3 H), 3.75 (d, *J*=1.56 Hz, 4 H), 3.83 (s, 6 H), 6.89 – 6.92 (m, 4 H), 6.96 - 6.99 (d, 4 H), 7.32 - 7.33 (m, 2 H), 7.77 (s, 2 H). ¹³C NMR (400 MHz, CDCl₃) δ ppm: 45.91, 55.41, 57.15, 114.65, 115.97, 122.86, 129.64, 133.39, 136.48, 136.62, 159.60, 186.97 (C=O). IR (V_{max}): 1670.81 (C=O), 1603.12 (C=C, olefinic), 1575.81 (C=C, aromatic) cm⁻¹. LC-MS (ESI): *m/z* calculated for C₂₂H₂₃NO₃, [M+H]⁺: 349.43; found: 350.5.

3,5-bis[(E)-4-methoxybenzylidene]-1-methylpiperidin-4-one (22d)

Yellow crystals, 95% yield; m.pt. 187-188°C, (literature (Pati *et al.*, 2009) m.pt. 186°C). ¹H NMR (400 MHz, CDCl₃) δ ppm: 2.48 (s, 3 H), 3.77 (s, *J*=1.56 Hz, 4 H), 3.84 (s, 6 H), 6.93 - 6.95 (d, 4 H), 7.35 - 7.37 (d, 4 H), 7.77 (s, 2 H). ¹³C-NMR (400 MHz, CDCl₃) δ ppm: 45.55, 55.46, 56.97, 114.20, 127.92, 130.62, 132.46, 136.69, 160.42, 186.51 (C=O). IR (V_{max}): 1669.91 (C=O), 1596.12 (C=C, olefinic), 1515.11 (C=C, aromatic) cm⁻¹. LC-MS (ESI): *m/z* calculated for C₂₂H₂₃NO₃, [M+H]⁺: 349.43; found: 350.4.

3,5-bis[(E)-2-chlorobenzylidene]-1-methylpiperidin-4-one (22e)

Yellow crystals, 75% yield; m.pt. 142-143.5°C, (literature (Wu *et al.*, 2013) m.pt. 143-145.2°C). ¹H NMR (400 MHz, CDCl₃) δ ppm: 2.38 (s, 3 H), 3.65 (d, *J*=1.56 Hz, 4 H), 7.21 – 7.23 (m, 2 H), 7.27 – 7.33 (m, 4 H), 7.43 – 7.46 (m, 2 H), 8.02 (s, 4 H). ¹³C-NMR (400 MHz, CDCl₃) δ ppm: 45.27, 56.54, 126.56, 130.06, 130.22, 130.42, 133.56, 133.80, 134.63, 135.25, 185.95 (C=O). IR (V_{max}): 1679.91 (C=O), 1586.12 (C=C, olefinic), 1459.11 (C=C, aromatic) cm⁻¹. LC-MS (ESI): *m/z* calculated for C₂₀H₁₇Cl₂NO, [M+H]⁺: 358.26; found: 359.5.

3,5-bis[(E)-3-chlorobenzylidene]-1-methylpiperidin-4-one (22f)

Pale yellow powder, yield: 79%, m.pt. 152-154°C. ¹H NMR (400 MHz, CDCl₃) δ ppm: 2.48 (s, 3 H), 3.76 (d, *J*=1.56 Hz, 4 H), 7.24 – 7.27 (m, 2 H), 7.33 – 7.38 (m, 6 H), 7.73 (s, 4 H). ¹³C-NMR (400 MHz, CDCl₃) δ ppm: 45.61, 56.68, 128.53, 129.27, 129.99, 130.06, 133.54, 134.66, 135.61, 136.81, 186.21 (C=O). IR (V_{max}): 1679.01 (C=O), 1576.11 (C=C, olefinic), 1489.61 (C=C, aromatic) cm⁻¹. LC-MS (ESI): *m/z* calculated for C₂₀H₁₇Cl₂NO, [M+H]⁺: 358.26; found: 359.5.

3,5-bis[(E)-4-chlorobenzylidene]-1-methylpiperidin-4-one (22g)

Pale yellow powder, yield: 81%; m.pt. 170-171°C, (literature (Leonard & Locke, 1955) m.pt. 174-176°C). ¹H NMR (400 MHz, CDCl₃) δ ppm: 2.47 (s, 3 H), 3.75 (d, *J*=1.56 Hz, 4 H), 7.29 – 7.32 (m, 4 H), 7.37 – 7.40 (m, 4 H), 7.76 (s, 4 H). ¹³C-NMR (400 MHz, CDCl₃) δ ppm: 45.60, 56.79, 129.02, 131.70, 132.82, 133.50, 135.36, 135.83, 186.22 (C=O). IR (V_{max}): 1676.31 (C=O), 1578.31 (C=C, olefinic), 1499.42 (C=C, aromatic) cm⁻¹. LC-MS (ESI): *m/z* calculated for C₂₀H₁₇Cl₂NO, [M+H]⁺: 358.26; found: 359.1.

3,5-bis[(E)-2,4-dichlorobenzylidene]-1-methylpiperidin-4-one (22h)

Yellow crystals, 71% yield; m.pt. 146-147 °C, (literature (Wu *et al.*, 2013) m.pt. 145.9-147.6 °C). ¹H NMR (400 MHz, CDCl₃) δ ppm: 2.37 (s, 3 H), 3.56 (d, *J*=1.46 Hz, 4 H), 7.16 (d, *J*=8.33 Hz, 2 H), 7.27 – 7.29 (m, 2 H), 7.47 (d, *J*=2.11 Hz, 2 H), 7.90 (s, 2 H). ¹³C NMR (400 MHz, CDCl₃) δ ppm: 45.72, 56.71, 126.98, 130.02, 131.09, 132.13, 133.07, 134.62, 135.46, 136.06, 185.86 (C=O). IR (V_{max}): 1676.41 (C=O), 1621.83 (C=C, olefinic), 1580.81 (C=C, aromatic) cm⁻¹. LC-MS (ESI): *m/z* calculated for C₂₀H₁₅Cl₄NO, [M+H]⁺: 427.15; found: 428.3.

3,5-bis[(E)-3,4-dichlorobenzylidene]-1-methylpiperidin-4-one (22i)

Yellow crystals 74% yield; m.pt. 162-164 °C. ¹H NMR (400 MHz, CDCl₃) δ ppm: 2.47 (s, 3 H), 3.70 (d, *J*=1.83 Hz, 4 H), 7.19 (d, *J*=2.11 Hz, 1 H), 7.21 (d, *J*=2.11 Hz, 1 H), 7.45 (d, *J*=2.11 Hz, 2 H), 7.47 (s, 1 H), 7.50 (s, 1 H), 7.65 (s, 2 H). ¹³C NMR (400 MHz, CDCl₃) δ ppm: 45.97, 56.82, 129.49, 130.73, 131.83, 133.00, 133.40, 134.11, 134.29, 135.08, 186.18 (C=O). IR (V_{max}): 1676.41 (C=O), 1617.23 (C=C, olefinic), 1585.42 (C=C, aromatic) cm⁻¹. LC-MS (ESI): *m/z* calculated for C₂₀H₁₅Cl₄NO, [M+H]⁺: 427.15; found: 428.3.

2,2'-((1E, 1'E)-(1-methyl-4-oxopiperidine-3,5-diylidene)bis(methaneylylidene))dibenzoic acid (22j)

White powder, 71% yield; m.pt. 227-229 °C. ¹H NMR (400 MHz, DMSO-*d*₆) δ ppm 2.65 (s, 3 H), 3.09 (br s, 2 H), 4.15 (br s, 2 H), 6.26 - 6.27 (d, 2 H), 7.65 - 7.72 (d, *J*=8.51 Hz, 4 H), 7.89 - 7.91 (d, *J*=8.33 Hz, 4 H). ¹³C NMR (400 MHz, DMSO-*d*₆) δ ppm: 49.00, 51.64, 76.60, 123.63, 125.82, 130.50, 135.50, 147.70, 169.95 (C=O). IR (V_{max}): 1767.42 (C=O), 1731.11 (C=C, olefinic), 1641.14 (C=C, aromatic) cm⁻¹. LC-MS (ESI): *m/z* calculated for C₂₂H₁₉NO₅, [M+H]⁺: 377.41; found: 378.4.

4,4'-((1E, 1'E)-(1-methyl-4-oxopiperidine-3,5-diylidene)bis(methaneylylidene))dibenzoic acid (22k)

Pale yellow powder, 74% yield; m.pt. 254-256 °C. ¹H NMR (400 MHz, DMSO-*d*₆) δ ppm: 2.93 (s, 3 H), 4.61 (br s, 4 H), 7.66 (d, *J*=8.51 Hz, 4 H), 7.91 (s, 2 H), 8.05 (d, *J*=8.33 Hz, 4 H), 10.11 (s, 2 H). ¹³C NMR (400 MHz, DMSO-*d*₆) δ ppm: 43.03, 53.90, 130.19, 131.35, 132.19, 138.17, 138.72, 167.29 (C=O). IR (V_{max}): 1703.72 (C=O), 1676.43 (C=C, olefinic), 1617.24 (C=C, aromatic) cm⁻¹. LC-MS (ESI): *m/z* calculated for C₂₂H₁₉NO₅, [M+H]⁺: 377.41; found: 378.4.

3,5-bis[(E)-4-methylbenzylidene]-1-methylpiperidin-4-one (22l)

Yellow crystals, 91% yield; m.pt. 192-193 °C, (literature (Leonard & Locke, 1955) m.pt. 192-195 °C). ¹H NMR (400 MHz, CDCl₃) δ ppm 2.38 (s, 6 H), 2.46 (s, 3 H), 3.75 - 3.76 (m, 4 H), 7.21 - 7.24 (m, 4 H), 7.29 - 7.31 (m, 4 H), 7.79 (s, 2 H). ¹³C NMR (400 MHz, CDCl₃) δ ppm: 21.55, 46.00, 57.29, 129.40, 130.61, 132.52, 136.49, 139.41, 187.08 (C=O). IR (V_{max}): 1676.41 (C=O), 1617.22 (C=C, olefinic), 1605.11 (C=C, aromatic) cm⁻¹. LC-MS (ESI): *m/z* calculated for C₂₂H₂₃NO, [M+H]⁺: 317.43; found 318.5.

3,5-bis[(E)-3-trifluoromethylbenzylidene]-1-methylpiperidin-4-one (22m)

Yellow crystals, 71% yield; m.pt. 122-123 °C. ¹H NMR (400 MHz, CDCl₃) δ ppm 2.47 (s, 3 H), 3.73 (d, *J*=1.74 Hz, 4 H), 7.25 (s, 2 H), 7.27 (s, 2 H), 7.39 - 7.43 (d, 4 H), 7.76 (s, 2 H). ¹³C NMR (400 MHz, CDCl₃) δ ppm: 46.06, 57.02, 120.65, 121.24, 131.67, 133.66, 133.80, 135.21, 149.52, 186.58 (C=O). IR (V_{max}): 1676.41 (C=O), 1617.22 (C=C, olefinic), 1580.84 (C=C, aromatic) cm⁻¹. LC-MS (ESI): *m/z* calculated for C₂₂H₁₇F₆NO, [M+H]⁺: 425.37; found 426.4.

3,5-bis[(E)-4-trifluoromethylbenzylidene]-1-methylpiperidin-4-one (22n)

Yellow crystals, 78% yield; m.pt. 123-124 °C. ¹H NMR (400 MHz, CDCl₃) δ ppm 2.46 (s, 3 H), 3.74 (d, *J*=1.83 Hz, 4 H), 7.47 - 7.50 (d, 4 H), 7.67 - 7.69 (d, 4 H), 7.80 (s, 2 H). ¹³C-NMR (400 MHz, CDCl₃) δ ppm: 45.42, 56.12, 124.22, 125.72, 126.22, 130.29, 131.23, 133.29, 134.77, 135.28, 138.63, 186.42 (C=O). IR (V_{max}): 1676.41 (C=O), 1612.12 (C=C, olefinic), 1590.21 (C=C, aromatic) cm⁻¹. LC-MS (ESI): *m/z* calculated for C₂₂H₁₇F₆NO, [M+H]⁺: 425.37; found 426.4.

3,5-bis[(E)-3-trifluoromethoxybenzylidene]-1-methylpiperidin-4-one (22o)

Yellow crystals, 73% yield; m.pt. 98-99 °C. ¹H NMR (400 MHz, CDCl₃) δ ppm 2.46 (s, 3 H), 3.73 (d, *J*=1.83 Hz, 4 H), 7.22 (d, 4 H), 7.30 – 7.32 (d, 2 H), 7.43 – 7.47 (m, 2 H), 7.75 (s, 2 H). ¹³C NMR (400 MHz, CDCl₃) δ ppm: 45.89, 56.89, 121.39, 122.48, 128.66, 130.09, 134.32, 134.89, 137.15, 149.38, 186.46 (C=O). IR (V_{max}): 1675.21 (C=O), 1620.52 (C=C, olefinic), 1588.62 (C=C, aromatic) cm⁻¹. LC-MS (ESI): *m/z* calculated for C₂₂H₁₇F₆NO, [M+H]⁺: 457.30; found 458.4.

3,5-bis[(E)-4-trifluoromethoxybenzylidene]-1-methylpiperidin-4-one (22p)

Yellow crystals, 71% yield; m.pt. 95-97 °C. ¹H NMR (400 MHz, CDCl₃) δ ppm 2.46 (s, 3 H), 3.75 (d, *J*=1.65 Hz, 4 H), 7.22 (d, 4 H), 7.55 – 7.56 (m, 4 H), 7.62 – 7.64 (d, 4 H), 7.81 (s, 2 H). ¹³C-NMR (400 MHz, CDCl₃) δ: 45.42, 56.12, 125.62, 127.01, 127.34, 128.11, 129.19, 133.29, 134.41, 135.28, 135.92, 186.11 (C=O). IR (V_{max}): 1676.41 (C=O), 1617.22 (C=C, olefinic), 1590.21 (C=C, aromatic) cm⁻¹. LC-MS (ESI): *m/z* calculated for C₂₂H₁₇F₆NO, [M+H]⁺: 457.30; found 458.4.

3,5-bis[(E)-2-iodobenzylidene]-1-methylpiperidin-4-one (22q)

Yellow powder, 68% yield; m.pt. 141-143 °C. ¹H NMR (400 MHz, CDCl₃) δ ppm: 2.34 (s, 3 H), 3.54 (d, *J*=1.74 Hz, 4 H), 7.01 – 7.06 (t, *J*=1.65 Hz, 2 H), 7.17 – 7.20 (d, *J*=1.65 Hz, 2 H), 7.36 – 7.40 (t, *J*=1.65 Hz, 2 H), 7.81 (s, 2 H), 7.92 (d, *J*=1.65 Hz, 2 H). ¹³C NMR (400 MHz, CDCl₃) δ ppm: 45.57, 56.52, 100.60, 127.94, 129.67, 130.11, 133.63, 139.08, 139.67, 140.50, 185.98 (C=O). IR (V_{max}): 1676.8 (C=O), 1618.6 (C=C, olefinic), 1584.6 (C=C, aromatic) cm⁻¹. LC-MS (ESI): *m/z* calculated for, C₂₀H₁₇I₂NO, [M+H]⁺: 540.84; found 542.3.

3,5-bis[(E)-3-iodobenzylidene]-1-methylpiperidin-4-one (22r)

Pale yellow crystals, 53% yield; m.pt. 139-140 °C. ¹H NMR (400 MHz, CDCl₃) δ ppm: 2.46 (s, 3 H), 3.70 (d, *J*=1.74 Hz, 4 H), 7.15 (t, 2 H), 7.32 (d, 2 H), 7.68 (d, 2 H), 7.71 (m, 4 H). ¹³C NMR (400 MHz, CDCl₃) δ ppm: 45.84, 56.81, 94.46, 129.36, 130.25, 134.06, 134.96, 137.39, 137.93, 138.94, 186.44 (C=O). IR (V_{max}): 1672 (C=O), 1613.7 (C=C, olefinic), 1589.5 (C=C, aromatic) cm⁻¹. LC-MS (ESI): *m/z* calculated for, C₂₀H₁₇I₂NO, [M+H]⁺: 540.84; found 542.3.

3,5-bis[(E)-3-nitrobenzylidene]-1-methylpiperidin-4-one (22s)

Pale yellow powder, 60% yield; m.pt. 158-160 °C. ¹H NMR (400 MHz, CDCl₃) δ ppm: 2.49 (s, 3 H), 3.78 (d, *J*=1.65 Hz, 4 H), 7.60 – 7.65 (t, 2 H), 7.70 – 7.72 (d, 2 H), 7.81 (s, 2 H), 8.22 – 8.24 (d, *J*=1.28 Hz, 4 H). ¹³C NMR (400 MHz, CDCl₃) δ ppm: 45.97, 56.71, 123.77, 124.54, 129.85, 134.06, 135.08, 136.10, 136.64, 148.44, 186.03 (C=O). IR (V_{max}): 1672 (C=O), 1595 (C=C, olefinic), 1347 (NO₂) cm⁻¹. LC-MS (ESI): *m/z* calculated for C₂₀H₁₇N₃O₅, [M+H]⁺: 379.04; found 380.3.

3,5-bis[(E)-4-nitrobenzylidene]-1-methylpiperidin-4-one (22t)

Brownish orange powder, 48% yield; m.pt. 203-205 °C, (literature (El-Subbagh, Abu-Zaid, Mahran, Badria, & Al-Obaid, 2000) m.pt. 204-205 °C). ¹H NMR (400 MHz, CDCl₃) δ ppm: 2.47 (s, 3 H), 3.75 (d, *J*=1.83 Hz, 4 H), 7.52 – 7.54 (d, 4 H), 7.81 (s, 2 H), 8.27 – 8.29 (d, 4 H). ¹³C NMR (400 MHz, CDCl₃) δ ppm: 45.97, 56.92, 94.46, 123.93, 130.91, 134.18, 135.74, 141.40, 147.72, 186.06 (C=O). IR (V_{max}): 1652.8 (C=O), 1598.2 (C=C, olefinic), 1346.8 (NO₂) cm⁻¹. LC-MS (ESI): *m/z* calculated for C₂₀H₁₇N₃O₅, [M+H]⁺: 379.04; found 380.5.

2.3.2 Spectral data of bis-(benzylidene)cycloalkanones**2,5-bis[(E)-(benzylidene)cyclopentanone (22u)**

Yellow crystals, 83% yield; m.pt. 190-192 °C, (literature (Vatsadze *et al.*, 2006) m.pt. 196 °C). ¹H NMR (400 MHz, CDCl₃) δ ppm: 3.12 (t, 4 H), 7.36 - 7.40 (m, 2 H), 7.42 – 7.46 (m, 4 H), 7.59 – 7.60 (m, 4 H), 7.61 (br s, 2 H). ¹³C NMR (400 MHz, CDCl₃) δ ppm: 26.65, 128.87, 129.49, 130.86, 133.97, 135.89, 137.39, 196.55 (C=O). IR (V_{max}): 1689.39 (C=O), 1621.48 (C=C, olefinic), 1597.14 (C=C, aromatic) cm⁻¹. LC-MS (ESI): *m/z* calculated for C₁₉H₁₆O, [M+H]⁺: 260.12; found 261.1.

2,6-Bis[(E)-(benzylidene)cyclohexanone (22v)

Yellow crystals, 79% yield; m.pt. 119-120 °C, (literature (Vatsadze *et al.*, 2006) m.pt. 118 °C). ¹H NMR (400 MHz, CDCl₃) δ ppm: 1.75 – 1.82 (p, 2 H), 2.91 – 2.95 (td, 4 H), 7.31 - 7.35 (m, 2 H), 7.38 – 7.42 (m, 4 H), 7.45 – 7.47 (m, 4 H), 7.80 (s, 2 H). ¹³C NMR (400 MHz, CDCl₃) δ ppm: 23.11, 28.56, 128.48, 128.69, 130.48, 136.06, 136.27, 137.06, 190.55 (C=O). IR (V_{max}): 1682.32 (C=O), 1617.34 (C=C, olefinic), 1591.41 (C=C, aromatic) cm⁻¹. LC-MS (ESI): *m/z* calculated for C₂₀H₁₈O, [M+H]⁺: 274.14; found 275.5.

2.3.3 Spectral data of bis-pyridylidene derivatives of N-methylpiperidin-4-one and cycloalkanones**(3E,5E)-1-methyl-3,5-bis(pyridine-2-ylmethylene)piperidin-4-one (23a)**

Yellow crystals, 87% yield; m.pt. 148-150 °C, (literature (Moore, Zhu, Randolph, Shoji, & Snyder, 2014) m.pt. 148-150 °C). ¹H NMR (400 MHz, CDCl₃) δ ppm: 2.44 (s, 3 H), 3.72 (br d, *J*=1.83 Hz, 4 H), 7.32 – 7.35 (dd, *J*=7.96, 4.85 Hz, 2 H), 7.65 – 7.67 (dt, *J*=8.06, 1.92 Hz, 2 H), 7.73 (s, 2 H), 8.55 - 8.57 (dd, *J*=4.85, 1.56 Hz, 2 H) 8.63 (d, *J*=2.20 Hz, 2 H). ¹³C NMR (400 MHz, CDCl₃) δ ppm: 45.94, 56.97, 123.55, 131.05, 132.95, 134.76, 137.19, 149.82, 151.08, 186.01 (C=O). IR (V_{max}): 1676.8 (C=O), 1613.7 (C=C, olefinic), 1597.9 (C=C, aromatic) cm⁻¹. LC-MS (ESI): *m/z* calculated for C₁₈H₁₇N₃O, [M+H]⁺: 291.35; found 292.4.

(3E,5E)-1-methyl-3,5-bis(pyridine-3-ylmethylene)piperidin-4-one (23b)

Yellow crystals, 76% yield; m.pt. 140-141 °C, (literature (Vatsadze *et al.*, 2006) m.pt. 139 °C). ¹H NMR (400 MHz, CDCl₃) δ ppm: 2.40 (s, 3 H), 3.70 (d, *J*=1.74 Hz, 4 H), 7.29 – 7.32 (ddd, *J*=7.92, 4.81, 0.82 Hz, 2 H), 7.61 – 7.64 (tt, *J*=7.91 Hz, 2 H), 7.69 (s, 2 H), 8.51 - 8.53 (dd, *J*=4.85, 1.65 Hz, 2 H) 8.58 - 8.58 (d, *J*=2.29 Hz, 2 H). ¹³C NMR (400 MHz, CDCl₃) δ ppm: 45.86, 56.89, 123.54, 130.99, 132.97, 134.66, 137.16, 149.79, 151.06, 185.91 (C=O). IR (V_{max}): 1672 (C=O), 1615.6 (C=C, olefinic), 1579.7 (C=C, aromatic) cm⁻¹. LC-MS (ESI): *m/z* calculated for C₁₈H₁₇N₃O, [M+H]⁺: 291.35; found 292.4.

(3E,5E)-1-methyl-3,5-bis(pyridine-4-ylmethylene)piperidin-4-one (23c)

Yellow crystals, 46% yield; m.pt. 180-182 °C, (literature (Dimmock *et al.*, 1992) m.pt. 188-190 °C). ¹H NMR (400 MHz, CDCl₃) δ ppm: 2.46 (s, 3 H), 3.75 (d, *J*=1.83 Hz, 4 H), 7.22 – 7.24 (dd, *J*=7.92 Hz, 4 H), 7.68 (s, 2 H), 8.67 - 8.69 (dd, *J*=7.92 Hz, 4 H). ¹³C NMR (400 MHz, CDCl₃) δ ppm: 45.72, 56.67, 124.03, 134.00, 135.99, 142.36, 150.29, 185.94 (C=O). IR (V_{max}): 1676.8 (C=O), 1620 (C=C, olefinic), 1587.9 (C=C, aromatic) cm⁻¹. LC-MS (ESI): *m/z* calculated for C₁₈H₁₇N₃O, [M+H]⁺: 291.35; found 292.4.

(2E,5E)-2,5-bis(pyridin-2-ylmethylene)cyclopentan-1-one (23d)

Pale yellow powder, 94% yield; m.pt. 190-192 °C, (literature (Vatsadze *et al.*, 2006) m.pt. 195 °C). ¹H NMR (400 MHz, CDCl₃) δ ppm: 3.35 (t, 4 H), 7.21 - 7.24 (m, 2 H), 7.51 – 7.53 (d, 2 H), 7.55 (s, 2 H), 7.71 – 7.75 (m, 2 H), 8.73 – 8.75 (d, 2 H). ¹³C NMR (400 MHz, CDCl₃) δ ppm: 27.25, 122.88, 127.23, 131.61, 136.36, 141.97, 150.09, 155.23, 197.83 (C=O). IR (V_{max}): 1699.6 (C=O), 1636.6 (C=C, olefinic), 1617.2 (C=C, aromatic) cm⁻¹. LC-MS (ESI): *m/z* calculated for C₁₇H₁₄N₂O, [M+H]⁺: 262.31; found 263.4.

(2E,5E)-2,5-bis(pyridin-3-ylmethylene)cyclopentan-1-one (23e)

Pale yellow powder, 81% yield; m.pt. 216-218 °C, (literature (Vatsadze *et al.*, 2006) m.pt. 216 °C). ¹H NMR (400 MHz, CDCl₃) δ ppm: 3.12 (t, 4 H), 7.34 – 7.37 (m, 2 H), 7.53 (s, 2 H), 7.84 – 7.87 (dt, *J*=7.99, 1.91 Hz, 2 H), 8.56 – 8.58 (dd, *J*=4.81, 1.60 Hz, 2 H), 8.81 - 8.82 (d, *J*=2.20 Hz, 2 H). ¹³C NMR (400 MHz, CDCl₃) δ ppm: 26.50, 123.75, 130.71, 131.57, 137.12, 138.89, 149.98, 151.74, 195.31 (C=O). IR (V_{max}): 1685 (C=O), 1622 (C=C, olefinic), 1602.6 (C=C, aromatic) cm⁻¹. LC-MS (ESI): *m/z* calculated for C₁₇H₁₄N₂O, [M+H]⁺: 262.31; found 263.4.

(2E,5E)-2,5-bis(pyridin-4-ylmethylene)cyclopentan-1-one (23f)

Pale yellow powder, 84% yield; m.pt. 236-238 °C, (literature (Vatsadze *et al.*, 2006) m.pt. 239 °C). ¹H NMR (400 MHz, CDCl₃) δ ppm: 3.14 (t, 4 H), 7.38 – 7.40 (dd, 4 H), 7.47 (s, 2 H), 8.67 – 8.69 (dd, 4 H). ¹³C NMR (400 MHz, CDCl₃) δ ppm: 26.45, 124.18, 131.63, 140.91, 142.58, 150.48, 195.43 (C=O). IR (V_{max}): 1694.8 (C=O), 1636.6 (C=C, olefinic), 1597.9 (C=C, aromatic) cm⁻¹. LC-MS (ESI): *m/z* calculated for C₁₇H₁₄N₂O, [M+H]⁺: 262.31; found 263.4.

(2E,6E)-2,6-bis(pyridin-3-ylmethylene)cyclohexan-1-one (23g)

Yellow crystals, 93% yield; m.pt. 140-142 °C, (literature (Vatsadze *et al.*, 2006) m.pt. 139 °C). ¹H NMR (400 MHz, CDCl₃) δ ppm: 1.80 – 1.86 (p, 2 H), 2.91 – 2.94 (td, 4 H), 7.36 - 7.38 (dd, 2 H), 7.74 (s, 2 H), 7.76 – 7.78 (t, 2 H), 8.55 – 8.57 (dd, 2 H), 8.70 – 8.71 (d, 2 H). ¹³C NMR (400 MHz, CDCl₃) δ ppm: 22.80, 28.44, 123.51, 131.86, 133.59, 137.45, 137.88, 149.03, 149.18, 150.82, 150.97, 189.27 (C=O). IR (V_{max}): 1665.9 (C=O), 1607.3 (C=C, olefinic), 1578 (C=C, aromatic) cm⁻¹. LC-MS (ESI): *m/z* calculated for C₁₈H₁₆N₂O, [M+H]⁺: 276.33; for 277.4.

(2E,6E)-2,6-bis(pyridine-4-ylmethylene)cyclohexan-1-one (23h)

Yellow powder, 86% yield; m.pt. 145-146 °C, (literature (Vatsadze *et al.*, 2006) m.pt. 150 °C). ¹H (400 MHz, CDCl₃) δ ppm: 1.82 – 1.88 (p, 2 H), 2.92 – 2.95 (td, 4 H), 7.39 - 7.40 (dd, 4 H), 7.68 (s, 2 H), 8.67 – 8.69 (dd, 4 H). ¹³C NMR (400 MHz, CDCl₃) δ ppm: 22.80, 28.44, 123.51, 131.86, 133.59, 137.45, 137.88, 149.03, 149.18, 150.82, 150.97, 189.27 (C=O). IR (V_{max}): 1665.9 (C=O), 1601 (C=C, olefinic), 1592.7 (C=C, aromatic) cm⁻¹. LC-MS (ESI): *m/z* calculated for C₁₈H₁₆N₂O, [M+H]⁺: 276.33; for 277.4.

2.3.4 Spectral data of bis-thienylidene derivatives of N-methylpiperidin-4-one and cycloalkanones

(3E,5E)-1-methyl-3,5-bis(thiophen-2-ylmethylene)piperidin-4-one (24a)

Yellow crystals, 89% yield; m.pt. 109-110 °C, (literature (El-Subbagh *et al.*, 2000) m.pt. 114-115 °C). ¹H NMR (400 MHz, CDCl₃) δ ppm: 2.63 (s, 3 H), 3.92 (br s, 4 H), 7.15 – 7.17 (dd, 2 H), 7.34 – 7.35 (d, 2 H), 7.57 – 7.58 (d, 2 H), 7.98 (s, 2 H). ¹³C NMR (400 MHz, CDCl₃) δ ppm: 45.88, 56.60, 128.08, 128.72, 130.02, 130.63, 133.26, 138.72, 185.97 (C=O). IR (V_{max}): 1663.6 (C=O), 1601.3 (C=C, olefinic), 1572.6 (C=C, aromatic) cm⁻¹. LC-MS (ESI): *m/z* calculated for C₁₆H₁₅NOS₂, [M+H]⁺: 301.43; found 302.3.

(2E,5E)-2,5-bis(thiophen-2-ylmethylene)cyclopentan-1-one (24b)

Yellow crystals, 93% yield; m.pt. 224-225 °C, (literature (Vatsadze *et al.*, 2006) m.pt. 222 °C). ¹H NMR (400 MHz, CDCl₃) δ ppm: 3.03 (t, 4 H), 7.15 – 7.17 (dd, 2 H), 7.39 – 7.40 (d, 2 H), 7.56 – 7.70 (d, 2 H), 7.797 (s, 2 H). ¹³C NMR (400 MHz, CDCl₃) δ ppm: 26.12, 126.38, 128.23, 130.48, 132.76, 135.89, 140.50, 195.17 (C=O). IR (V_{max}): 1682.8 (C=O), 1596.5 (C=C, olefinic), 1508 (C=C, aromatic) cm⁻¹. LC-MS (ESI): *m/z* calculated for C₁₅H₁₂OS₂, M.Wt: 272.39; found 273.3.

(2E,6E)-2,6-bis(thiophen-2-ylmethylene)cyclohexan-1-one (24c)

Yellow powder, 90% yield; m.pt. 169-170 °C, (literature (Vatsadze *et al.*, 2006) m.pt. 169 °C). ¹H NMR (400 MHz, CDCl₃) δ ppm: 1.91 – 1.97 (p, 2 H), 2.88 - 2.92 (td, 4 H), 7.11 – 7.13 (dd, *J*=5.13, 3.66 Hz, 2 H), 7.35 – 7.36 (d, *J*=3.66 Hz, 2 H), 7.50 – 7.51 (d, *J*=5.12 Hz, 2 H), 7.97 (s, 2 H). ¹³C NMR (400 MHz, CDCl₃) δ ppm: 21.74, 28.21, 127.72, 129.84, 130.06, 132.94, 133.12, 139.60, 189.08 (C=O). IR (V_{max}): 1649.2 (C=O), 1582.2 (C=C, olefinic), 1543.8 (C=C, aromatic) cm⁻¹. LC-MS (ESI): *m/z* calculated for C₁₆H₁₄OS₂, [M+H]⁺: 286.41; found 287.3.

2.4 Discussion of bis-benzylidene, bis-pyridylidene and bis-thienylidene derivatives of N-methylpiperidin-4-one, cyclopentanone and cyclohexanone

Several methods have been developed to synthesize bis-benzylidene-piperidone/cyclohexanone (containing 1,4-diene-3-one pharmacophore), which differ in the nature of the catalyst or solvent use for the reaction (Dong, Jian, Zhenghao, Kai, & Zuliang, 2008; Wu *et al.*, 2013; Moore *et al.*, 2014). Some researchers have mentioned the use of dry hydrogen chloride and acetic acid as a catalyst to facilitate the reaction e.g. bis-benzylidene-cyclohexanone (Das *et al.*, 2008; Pati *et al.*, 2009).

In the present study, a Claisen-Schmidt condensation of cyclopentanone, cyclohexanone or N-methyl-piperidin-4-one with aromatic and heteroaromatic aldehydes was performed and a series of symmetrical 1,4-diene-3-one compounds were synthesized. The bis-benzylidene and bis-thienylidene derivatives of N-methylpiperidin-4-one, cyclopentanone and cyclohexanones (**22a-v** and **24a-c**) were synthesized using basic catalyst in aqueous-ethanolic media whereas bis-pyridylidene derivatives of N-methylpiperidin-4-one, cyclopentanone or cyclohexanone (**23a-h**) were synthesized using basic catalyst in aqueous media using a modification of a previously reported method described by Vatsadze *et al.*, (2006). Heterocyclic aromatic compounds were synthesized to increase the solubility of the compounds (Moore *et al.*, 2014). As pyridine improves the aqueous solubility due to its weak basicity (Hamada, 2018).

The synthesized compounds were purified by recrystallization method using dichloromethane and 95% hot ethanol. Yields of the synthesized 1,4-diene-3-ones ranged from 48 to 95%. The purity of 1,4-diene-3-ones was analysed by melting point, TLC and NMR whereas their structures were established using FT-IR, LC-MS, ¹H and ¹³C-NMR analysis and their structural

details mentioned in **section 2.3**. The melting point of compounds **22a**, **22b**, **22d**, **22e**, **22g**, **22h**, **22l**, **22t**, **22u**, **22v**, **23a-h** and **24a-c** agreed with those quoted in the literature (Leonard & Locke, 1955; Dimmock *et al.*, 1992; El-Subbagh *et al.*, 2000; Vatsadze *et al.*, 2006; Pati *et al.*, 2009; Wu *et al.*, 2013; Moore *et al.*, 2014). Moreover, compounds **22c**, **22f**, **22i**, **22j**, **22k**, and **22m-s** were novel synthesized compounds. The melting point of all synthesized compounds was within 1-3 °C range, which is consistent with these compounds being pure.

The molecular mass of each of the synthesized 1,4-diene-3-one was calculated using the ChemDraw Professional 16.0 software (Perkin Elmer). The mass spectra of all the synthesized compounds showed their molecular ion peak at the expected value, corresponding to the molecular mass ion measured under positive ion mode. Therefore, the mass to charge ratio (m/z) of each compound was $M+1$ which is expressed as $M+H$. FT-IR spectroscopic analysis of all 1,4-diene-3-ones gave a peak corresponding to an unsaturated carbonyl (C=O) group in the region of 1600 cm^{-1} signifying the presence of a carbonyl group. In addition, an IR peak between the region of $1390\text{-}1595\text{ cm}^{-1}$, represents the presence of an olefinic (C=C) double bonds in all compounds.

The presence of carbonyl (C=O) is further confirmed by ^{13}C -NMR resonances between 180 and 198 ppm for compounds **22a-l**, **22l-v**, **23a-h** and **24a-c** whereas compounds **22j** and **22k** gave resonances at 170 and 167 ppm respectively. This shift in the resonance is possibly due to the use of different solvent for NMR analysis as both compounds **22j** and **22k** were not soluble in CDCl_3 and therefore DMSO-d_6 was used. Alternatively this could be due to the presence of carboxylic acid group attached to the aromatic rings. Compound **22j** has a carboxylic acid group at the *ortho*-position whereas **22k** has a carboxyl group at the *para*-position of the aromatic rings.

The $^1\text{H-NMR}$ spectra of 1,4-diene-3-ones containing a central piperidyl ring with nitrogen atom (**22a-t**, **23a-c** and **24a**) displayed the presence of aliphatic protons ($-\text{CH}_3$) with a singlet peak between δ 2.38 to 2.48 ppm for the methyl protons. Other aliphatic methylene protons $-\text{CH}_2$, one each attached to the nitrogen atom of the various piperidine dienone derivatives exhibit a singlet peak ranging between δ 3.56 to 3.84 ppm depending on the derivative. In contrast the derivatives of cyclopentanone and cyclohexanone have multiple CH_2 groups these being two in the case of cyclopentanone and three in the case of cyclohexanone. The $^1\text{H-NMR}$ spectra of bis-benzylidene derivatives of cyclopentanone (**22u**), bis-pyridylidene derivatives of cyclopentanone (**23d-f**) and bis-thienylidene derivative of cyclopentanone (**24b**) showed an aliphatic protons ($-\text{CH}_2$) with a triplet peak between δ 3.03 and 3.35 ppm. Likewise, the $^1\text{H-NMR}$ spectra of bis-benzylidene derivatives of cyclohexanone (**22v**), bis-pyridylidene derivatives of cyclohexanone (**23g-h**) and bis-thienylidene derivative of cyclohexanone (**24c**) displayed the presence of an three sets of aliphatic protons; first ($-\text{CH}_2$) showed a pentet peak between δ 1.80 and 1.97 ppm and second $(-\text{CH}_2)_2$ showed three doublet peaks between δ 2.88 and 2.95 ppm.

The $^1\text{H-NMR}$ spectra of 1,4-diene-3-one compounds (bis-benzylidene, bis-pyridylidene and bis-thienylidene derivatives of N-methylpiperidin-4-one and cycloalkanones) revealed the presence of (two) olefinic protons (attached at the β -carbon) between δ 7.47 – 7.89 ppm, which is characteristic of *E* isomers (Das *et al.*, 2008). The synthesized 1,4-diene-3-ones can exist in either *E,E*, *E,Z* or *Z,Z* tautomers. It has been shown that olefinic protons in the *E*-isomers exhibit NMR peaks at δ 7.5 ppm whereas *Z*-isomers exhibit peaks in the region of 6.80 ppm (Vatsadze *et al.*, 2006). No peaks were observed in the 6.80 ppm region thus all synthesized compounds were deemed to be the *E,E*-isomers. The $^1\text{H-NMR}$ and $^{13}\text{C-NMR}$ spectra of all compounds are presented in **Appendix 1**, Page 241-273.

2.5 Conclusions

In conclusion, a series of previously synthesized and novel bis-benzylidene, bis-pyridylidene and bis-thienylidene derivatives of N-methyl-piperidin-4-one, cyclopentanone and cyclohexanone with various substituents on rings were synthesized using the Claisen-Schmidt condensation method. The value of this methodology is that it is simple and efficient. The spectral data of the synthesized compounds reveal that all synthesized 1,4-diene-3-ones were isomerically pure at the time of synthesis and after first recrystallization.

CHAPTER THREE

EVALUATION OF ANTIFUNGAL ACTIVITY

3 Evaluation of antifungal activity

3.1 Introduction

The increasing occurrence of fungal infections and regular use of available antifungal agents have strengthened the need for useful and reliable antifungal susceptibility test methods. Various standardised methods have been developed to investigate the antifungal activity of drugs including protocols developed by the European Committee of Antifungal Susceptibility Testing (EUCAST), the Clinical Laboratory and Standards Institute (CLSI) and the British Society for Antimicrobial Chemotherapy. The CLSI has developed and approved several methods for determining the drug susceptibility of yeasts in both biofilm and planktonic form (Fothergill, 2012). However, these methods are time-consuming and less suitable for high throughput screening of compound libraries for antifungal susceptibility testing. Conversely Galgiani & Stevens, (1976) have developed both macro- and micro-dilution broth susceptibility testing methods, which are reproducible and independent of inoculum size.

Antifungal susceptibility screening of the compound library synthesized as described in Chapter-2 was performed using the method described by Galgiani & Stevens, (1976). The parameters described by Galgiani and co-workers were: an inoculum size of 2.0 to 2.5×10^4 cells/ml and malt extract broth (MEB) as a medium. An incubation time of 24 hours was used, as optimized by Hussain, (2014) and which depends on the fungal species being screened.

The antifungal activity of a drug can be described as either fungistatic or fungicidal at a known concentration. The ability of the drug to inhibit the growth of yeast cells can be obtained by measuring the absorbance at 600 nm of the cell growths with and without the test compounds. The inhibitory activity of the antifungal agents can be determined using various

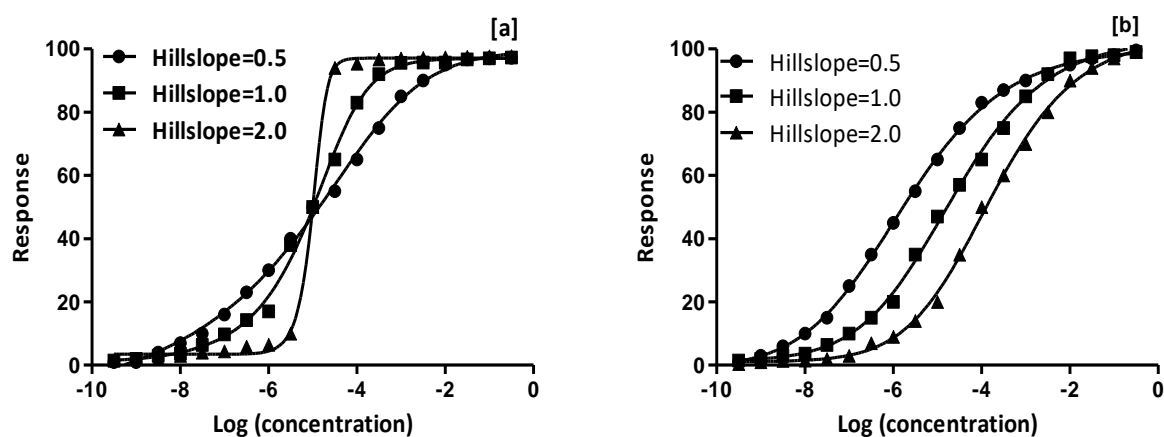
analyses of the dose-response curve (percentage inhibition of the cell growth compared to control) against a range of drug concentrations, although primary high throughput screening has often used a single inhibitor concentration value, such as a concentration in the low (10 - 60) micromolar region (Giacometti *et al.*, 2000). The inhibitory activity of the drug can be evaluated using various parameters such as IC_{10} , IC_{25} , IC_{50} , IC_{90} , area under the curve (AUC) and the Hill slope sometime termed the Hill coefficient or slope factor.

3.1.1 Theory of dose-response curves

A dose-response curve reveals the potency of a compound. By observing what happens to a dose-response curve over time, it is possible to differentiate between fungicidal and fungistatic activity (Rautenbach, Gerstner, Vlok, Kulenkampff, & Westerhoff, 2006). Dose-response curves from bioassays, radioimmunoassays or radioreceptor assays may be either symmetrical in shape (reflection around the point of inflection), smooth or sigmoidal when the drug concentration is expressed on a logarithmic scale. These curves are well defined by Gaussian cumulative distribution or logistic models (DeLean, Munson, & Rodbard, 1978). Gaussian cumulative distribution is also called a normal distribution or bell curve. It is used to characterize real values of inhibitory concentration random variables whose distributions are not known. The logistic model is a predictive analysis, which is commonly used to describe the relationship between dependent binary variables with one or more nominal independent variables (DeLean *et al.*, 1978).

Until recently the dose-response curve as used in drug development studies utilised a four-parameter logistic model (Figure 3.1a) which fits the minimum and maximum plateaus of the curve. From this curve, the Hill slope and point of inflection (IC_{50}) could be determined. However, unless 100% inhibition of growth is observed the point of inflection will be different

from the 50% reduction in antimicrobial growth assays. In addition, a four-parameter logistic model cannot effectively model asymmetric data (Rautenbach *et al.*, 2006). The maximum information can be obtained from the dose-response curve at a point where there is the maximum change in the shape of the curve. The main purpose of fitting the dose-response curve is to determine the best fit value of a drug at known concentration (DeLean *et al.*, 1978).



(DeLean *et al.*, 1978)(DeLean *et al.*, 1978)(DeLean *et al.*, 1978)

Figure 3. 1. Schematic representation of dose-response curves.

The dose-response curve of response against drug concentration fitted using a four-parameter [a] and five-parameter [b] logistic model. The curve is symmetrical around its midpoint in four-parameter whereas a five-parameter logistic equation curves are asymmetrical. A five-parameter equation also includes an additional parameter 'S' which measures the asymmetry of the curve.

The Hill slope (h) commonly referred to as the slope factor (A_5) or Hill coefficient may be suggestive of an underlying mechanism and is valuable in comparison of drug potencies (Rautenbach *et al.*, 2006). However this term has limited utility in cell growth assays due to the complexity of such systems. Hill coefficients provides information about the number of interacting sites in a receptor or enzyme but cannot differentiate between competitive or non-competitive mechanisms (Prinz, 2010). Hill coefficient is best understood as an

interaction coefficient, reflecting the level of cooperativity among multiple ligand binding sites when studying isolated receptors or enzymes.

Prism software calculates the Hill slope using the Levenberg-Marquardt algorithm for non-linear least square minimization. In Figure 3.1[a], Hill slope defines the steepness of the curve; if the Hill slope is 1.0 then the curve is a standard slope. The dose-response curve is steep when a Hill slope is >1.0 which suggests a greater chance of correspondence between desired and undesired effects of a drug. Hill slope is >1.0 also indicate high order of concentration dependence, this can sometimes be explained by high levels of aggregating molecules. In contrast, if the curve is shallow then a Hill slope is <1.0 which suggests no problem of aggregation of the molecule. In recent years a further term has been introduced to reflect the symmetry of the sigmoidal curve (Gottschalk & Dunn, 2005). In a five-parameter logistic model 'S' is an extra, unitless, parameter reflecting the symmetry of the curve around its point of inflection (Figure 3.1b). If $S=1$, the curve is symmetrical and identical to the standard four parameter dose-response equation. If S is not equal to 1.0, then the curve is asymmetric. The advantage of a five-parameter logistic model is that it eliminates the 'lack-of-fit' error, which usually occurs in a four-parameter logistic model.

Other studies have used the concept of area under the curve as a measure of the inhibitory potency of antimalarial or antifungal agents since using MICs or IC_{50} s can often give ambiguous results (Odds & Abbott, 1984). Consequently Odds & Abbott, (1984) developed a new parameter which measures the area under the dose-response curve (AUC) using an indefinite, or unbounded, integral between two different concentrations common to all of the inhibitors being tested. Better reproducibility of the inhibitory activity of the compounds between two log dose concentrations can be obtained from the AUC (Figure 3.2). Odds &

Abbott, (1984) also stated that accurate assessment of the activity of various drugs can be achieved by comparing the AUC with the other inhibitory parameters such as IC_{50} or IC_{90} .

The AUC between C_1 and C_2 can be presented as a percentage of the theoretical maximum area to provide a relative inhibition factor (RIF). A RIF close to 0% means the yeast is susceptible to a particular drug whereas RIF close to 100% means the yeast is resistant to that drug. The areas are measured and presented as a percentage of the area of the rectangle between C_1 and C_2 , and 0% and 100%.

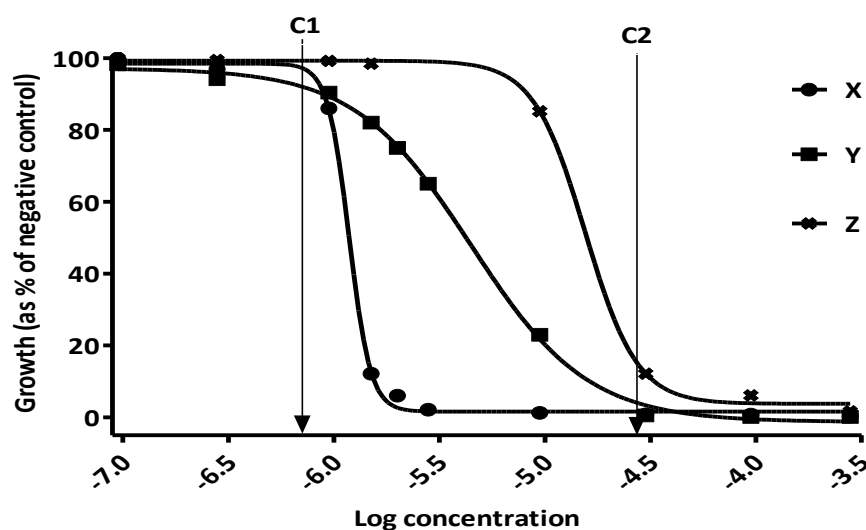


Figure 3. 2. Example of the dose-response curves of three drugs.

An example of the dose-response curve of three drugs, growth stated as a percentage of negative control cultures against log concentration. The drugs X and Z shows a clear minimum inhibitory concentration (MIC) end-points but drug Y shows partial inhibitory activity. The AUC was obtained by selecting two concentrations, C_1 and C_2 , which specifies the upper and lower limits of the test range. The AUC of Z is high and therefore it is considered to be least inhibitory antifungal agent whereas, low AUC of X denotes most inhibitory activity and drug Y indicates the intermediate value of AUC indicates partial inhibitory activity (Odds & Abbott, 1984).

The aim of the work described in this chapter was to identify and analyse the (potential) and relative anti-fungal activities of the thirty-three synthesized 1,4-diene-3-one compounds. This was accomplished by performing the *in vitro* macro-broth susceptibility assays against both *S. cerevisiae* and *C. albicans*.

3.2 Materials and Methods

3.2.1 Macro-broth susceptibility assay

3.2.1.1 Cell cultures

Yeasts *S. cerevisiae* ATCC 46182 (UH fungal culture collection strain code Y13a) and *C. albicans* NCYC 854 (UH fungal culture collection strain code Y100) were obtained from the University of Hertfordshire fungal culture collection.

3.2.1.2 Growth medium and materials

Malt Extract Agar (Malt extract 30 g/l, Mycological peptone 5 g/l and agar 15 g/l) was purchased from Oxoid microbiological products, CM0059, Lot-1671689. Malt extract agar (MEA) was used to culture the yeasts in Petri dishes to obtain individual colonies derived from single cells. MEA powder (20 g) was dissolved in distilled water to a final volume of 400 ml. The pH of MEA was adjusted to 5.4 using either 1M hydrochloric acid or 1M NaOH solution, followed by autoclaving at 121 °C/15 psi for 15 minutes. Petri dishes containing approximately 20 ml of MEA were prepared from freshly autoclaved medium. Yeast cultures were sub-cultured every two weeks. Cultured plates were incubated at 30 °C for 48 hours and then stored at 4 °C until needed.

Malt extract broth (Malt extract 17 g/l, Mycological peptone 3 g/l) was purchased from Oxoid microbiology products, CM057, Lot-1350078. Malt extract broth (MEB) was used to grow the yeast in liquid medium. MEB powder (20 g) was dissolved in distilled water just under final volume then adjusted the pH to 5.4 using 1M HCl or 1M NaOH, then to the final volume of 1 Litre. All glassware used for antifungal studies was acid washed overnight followed by rinsing with distilled water, drained and allowed to dry to eliminate any traces of organic or

interfering materials. Aliquots of MEB (2.0 ml and 80 ml) were prepared in 5 ml bijous or 250 ml conical flasks respectively, followed by autoclaving as described above and stored at 4 °C until used.

3.2.1.3 Stock solution of the antifungal agent

Miconazole nitrate powder (**4**) (Sigma-Life Science, M3512, Lot: BCBD5966V) was used as a positive reference control. Miconazole nitrate (4.8 mg) was dissolved in dimethyl sulfoxide (Hybri-Max; D2650, Sigma-Life Science) to obtain a final concentration of 1.92 mM. A stock solution of miconazole in DMSO was prepared freshly daily. Stock solution was diluted with DMSO to obtain range of standard concentrations between 0.91 nM and 27.4 µM.

3.2.1.4 Stock solutions of the synthesized compounds

Stock solutions of synthesized compounds were prepared at 0.1 M concentration in DMSO. The stock solution was sonicated for 10 minutes to dissolve the compound completely. The stock solutions were diluted appropriately in DMSO (Hybri-Max; D2650) to obtain concentrations ranging from 2×10^{-2} to 2×10^{-5} M. Solutions were prepared fresh daily. DMSO was used as a negative control (0.5% and 1.5%) when treating yeast cells with a solution of the test compound. A 'blank' control was also used for macro-broth susceptibility assay to determine the effect of MEB medium on the test compounds (composition: 2.1 ml MEB, 10 µl or 30 µl of test compound).

3.2.1.5 Growth of yeast cells for macro-broth susceptibility assay

A few colonies of yeast (*S. cerevisiae* or *C. albicans*) were aseptically inoculated into MEB (80 ml). This cell suspension was incubated in an orbital shaker overnight at 32 °C, 100 rpm. The absorbances of the fungal cultures were measured at 600 nm using a Cecil (CE1011) UV-Visible spectrophotometer. Subsequently, cell counts were performed using a Naubauer haemocytometer to identify the number

of cells present in the cell suspension. A cell suspension (1.0 ml) containing approximately 1×10^8 cells/ml from an overnight culture was re-suspended in a 250 ml sterile conical flask containing MEB (80 ml) and incubated at 32 °C, 100 rpm until the cells reached the mid-log phase (approximately 5-7 hours). Absorbance measurements at 600 nm and cell counts were performed each hour between 1 to 8 hours and finally after 24 hours (Galgiani & Stevens, 1976; Fothergill, 2012).

3.2.1.6 Macro-broth susceptibility testing of 1,4-diene-3-ones

The library of 1,4-diene-3-ones was investigated for their *in-vitro* antifungal activity against *C. albicans* and *S. cerevisiae* using a macro-broth dilution method (Galgiani & Stevens, 1976).

The reason for choosing this method is due to its reproducibility and that results are independent of cell inoculum size e.g. 2.0×10^4 or 2.0×10^5 cells/ml. The fungal strains of both *C. albicans* and *S. cerevisiae* were grown to mid-log phase (5 hours) as described in **section**

3.2.1.5. The cell counts and absorbance at 600 nm measurements were performed to determine the number of cells present. Cell viability was determined by adding Methylene blue (MB) dye to the cell suspension. Cell suspensions containing mid-log phase cells were diluted first with MEB medium (1/10; 100 μ l of cell suspension added to 900 μ l of MEB) then with MB (1:1; 100 μ l of diluted cell suspension added to 100 μ l MB) to obtain the overall dilution of 1/20. Cell suspensions were diluted with MEB to obtain stock cell concentrations of $4.2\text{-}5.2 \times 10^5$ cells/ml for *C. albicans* cells, and $4.2\text{-}5.2 \times 10^6$ cells/ml for *S. cerevisiae* cells.

For the macro-broth susceptibility assay, 10 or 30 μ l volumes from stock or standard dilutions of either the synthesized 1,4-diene-3-one, miconazole nitrate or DMSO were added to each bijou containing MEB (2.0 ml). The final concentrations of 1,4-diene-3-ones ranged between 0.10 and 3000 μ M. The final concentration of miconazole ranged between 9 nM and 27.4 μ M.

For *C. albicans* susceptibility assays, a cell suspension (100 μ l) containing $4.2 - 5.2 \times 10^5$

cells/ml was inoculated into each bijou. Similarly for *S. cerevisiae* susceptibility assays, a cell suspension (100 µl) containing $4.2 - 5.2 \times 10^6$ cells/ml was inoculated into each bijou.

The final concentration of the *C. albicans* or *S. cerevisiae* cells in each bijou was $2.0 - 2.5 \times 10^4$ cells/ml and $2.0 - 2.5 \times 10^5$ cells/ml respectively. All bijous were prepared in duplicate and incubated for 24 hours at 32 °C, 100 rpm. Each experiment was performed with three different growths of cells for *S. cerevisiae* susceptibility assays and twice for *C. albicans* susceptibility assays. The inhibitory activities of the various 1,4-diene-3-ones against *C. albicans* and *S. cerevisiae* were obtained by measuring the optical density (600 nm) of each sample after incubating for 24 hours.

3.2.1.7 Data processing for macro-broth susceptibility assay

Absorbance values of the yeast cell suspensions (*S. cerevisiae* and *C. albicans*), test compounds and controls were recorded using a Cecil (CE1011) UV-Vis spectrophotometer at 600 nm. The absorbance of the cell suspension containing the test compound was converted to the percentage growth of treated *S. cerevisiae* or *C. albicans* cells as compared to the control (DMSO 1.5%) using **Equation 1**.

Cell growth (% of control) =

$$\frac{\text{Absorbance of cell suspension with Drug} \times 100}{\text{Absorbance of cell suspension without drug (negative control with DMSO 1.5\%)}} \quad (\text{Eq. 1})$$

The inhibitory activities of the 1,4-diene-3-ones were analyzed using the software GraphPad Prism 5. Non-linear regression model fitted to response (variable on Y axis) vs log (inhibitor concentration) was performed on the dose-response data acquired from the macro-broth susceptibility assays (Rautenbach *et al.*, 2006). A sigmoidal curve with variable slope (Figure 3.1a) and continuous variation of 100 between the top (inhibition at high drug

concentrations) and bottom (response with no inhibition) were fixed to each datasets using the four-parameter model, **Equation 2**.

$$\mathbf{Growth\ inhibition} = \mathbf{Bottom} + \frac{\mathbf{Top} - \mathbf{Bottom}}{\mathbf{1} + \mathbf{10}^{(\log(\mathbf{conc.}) - \mathbf{X}) \times \mathbf{Hill\ slope}}} \quad (\mathbf{Eq. 2})$$

Where X represents the log (base 10) of 1,4-diene-3-one concentrations in terms of molarity. The concentration of drug at the point of inflection 50% inhibitory concentration (IC₅₀) was obtained from the x value equivalent to a response halfway between the top and bottom plateaus. The 10% and 25% inhibitory concentration (IC₁₀ and IC₂₅) of each 1,4-diene-3-one was the calculated x value at the intercept between the bottom plateau and maximum slope (Figure 3.1b). The 90% inhibitory concentration (IC₉₀) was the calculated x value at the intercept between the top plateau and maximum slope. The Hill slope or slope factor was calculated from the dose-response curve using **Equation 2**.

The dose-response curves were also analyzed using a five-parameter logistic (**Eq. 3**). This equation contains an additional parameter 'S' that quantifies the asymmetry of the curve (Figure 3.1b):

$$\mathbf{Growth\ inhibition} = \mathbf{Bottom} + \frac{\mathbf{Top} - \mathbf{Bottom}}{\mathbf{1} + \mathbf{10}^{(\log(\mathbf{conc.}) - \mathbf{X}) \times \mathbf{Hill\ slope})^{\mathbf{S}}}} \quad (\mathbf{Eq. 3})$$

Data was also analysed by plotting the dose-response curve of growth of cells as percentage of control. Areas under the dose-response curve (AUC, Figure 3.2) was obtained by selecting two concentrations and applying the following formula:

$$\mathbf{AUC} = \int_{\mathbf{c1}}^{\mathbf{c2}} \mathbf{f(x)} \mathbf{dx} \quad (\mathbf{Eq. 4})$$

Where, C₁ = concentration (1400 μM; *S. cerevisiae* and *C. albicans*)

C_2 = concentration (0.1 μM ; *S. cerevisiae* and *C. albicans*)

$$\int_{C_1}^{C_2} f(x)dx = \text{area under the curve from concentration } C_1 \text{ to } C_2.$$

All synthesized 1,4-diene-3-one compounds showed turbidity in the cell suspension at concentrations $>1400 \mu\text{M}$, this may be due to the problem of solubility at high concentration. Therefore, the AUCs were obtained by selecting $1400 \mu\text{M}$ as C_1 and $0.1 \mu\text{M}$ as C_2 for both *S. cerevisiae* and *C. albicans* susceptibility assays. Concentrations C_1 to C_2 represents the lower and upper limits of a test range to identify the area under the dose-response curves (Odds & Abbott, 1984).

The antifungal activity of each compound was stated in terms of specific percentage Inhibitory concentrations (IC). The relevant IC_{10} , IC_{25} , IC_{50} and IC_{90} values for compounds giving 10, 25, 50 or 90 % levels of inhibition were obtained manually at the point of intersection between the intercept value and the corresponding log concentration value. The 'point of inflection' IC_{50} values obtained from GraphPad was described as the asymptotic I_{50} values. The values of asymptotic I_{50} (i.e. 50% of the curve according to the shape of the curve generated with Prism 5) and manually calculated IC_{50} (by plotting a line across 50% inhibition of growth) were compared to identify the difference in the inhibitory activity of these 1,4-diene-3-ones (**Tables 3.1 and 3.2**, pages 105 and 119).

3.3 Results – Investigation of Antifungal activity

3.3.1 Growth curves of *S. cerevisiae* and *C. albicans*

The growth of *S. cerevisiae* and *C. albicans* was determined by plotting absorbance at 600 nm against time (Figure 3.3). The point at which the cells proliferate at their maximal rate is termed the mid-exponential or mid-log phase.

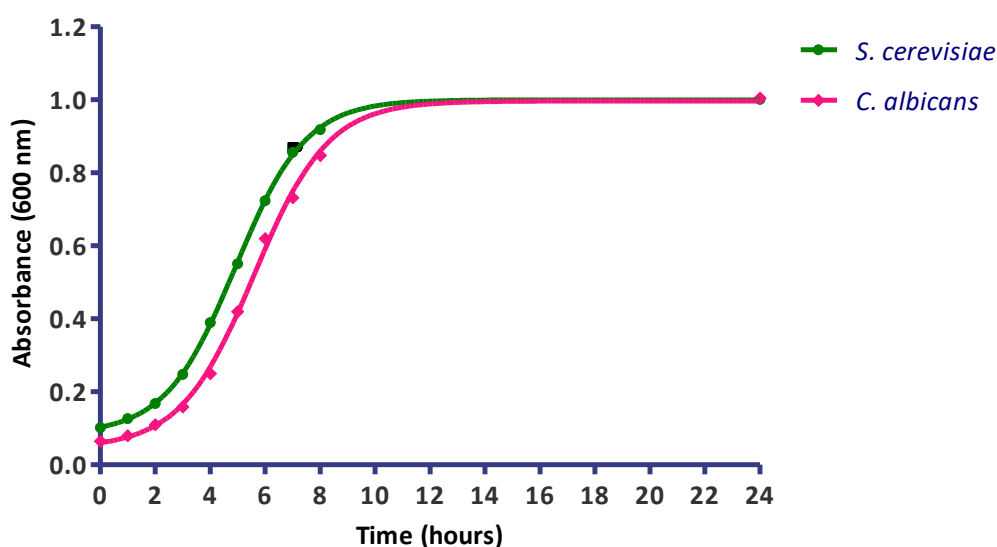


Figure 3. 3. Growth curves of the two fungal strains over 24 hours.

The growth curves of the absorbance (600 nm) against time of *C. albicans* and *S. cerevisiae*. Each data point represents the mean \pm SD of the two individual experiment each conducted in duplicate, $n=4$. Error bars were difficult to observe on the plots due to very low standard deviation value.

The exponential phase was observed to be between 5-7 hours for both *C. albicans* and *S. cerevisiae*. The yeast cells enter the deceleration or late log phase after 7 hours of incubation followed by entry to the stationary phase by 24 hours. Although the absorbance of *S. cerevisiae* and *C. albicans* were relatively similar to each other, there was a difference in the absolute cell numbers. Therefore, individual calibration between absorbance and cell numbers is necessary. Hence, correlation plots of absorbance of the cell suspension with the

number of cells present in the suspension of *S. cerevisiae* and *C. albicans* were implemented to identify the relationship between them (Figure 3.4).

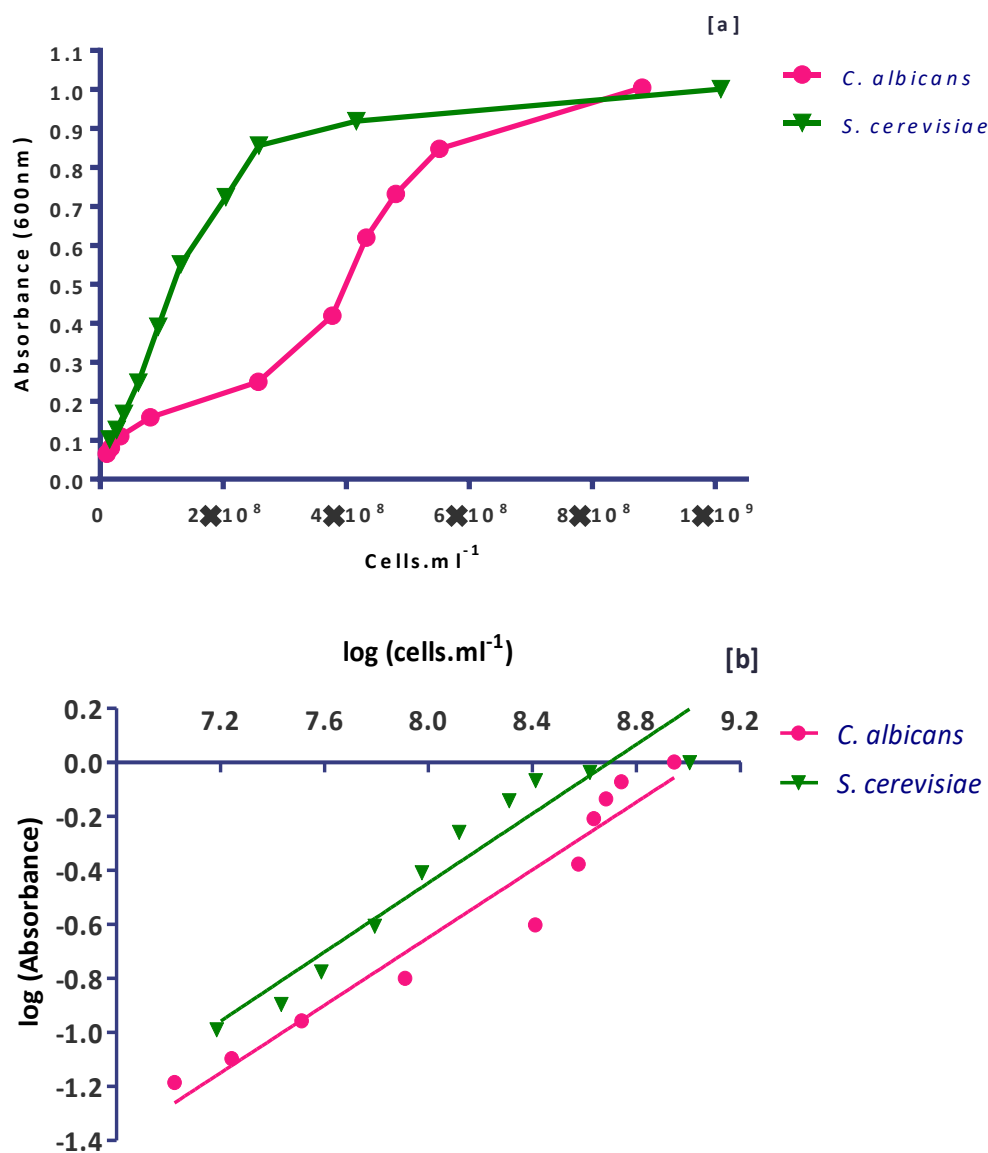


Figure 3. 4. Correlation plots of absorbance and cell counts of fungal species.

Absorbance against cell.ml⁻¹ [a] and its derivative logarithmic absorbance values against cells.ml⁻¹ of both *S. cerevisiae* and *C. albicans* [b]. Each data point represents the mean of the two individual experiments each conducted in duplicate, n=4. Error bars were difficult to observe on the plots due to very low standard deviation value.

S. cerevisiae depicted a linear relationship between the absorbance values of 0 to 0.9 with the cell counts whereas *C. albicans* displayed limited correlation between the absorbance and the cell counts especially at high cell concentrations (Figure 3.4a). This could be possibly due

to environmental stress such as changes in the pH during the cell growth (Francois *et al.*, 2005). In addition, both *S. cerevisiae* and *C. albicans* shows deviation in their values after reaching an absorbance of 0.9. This may be because absorbance is a log function for the general transmission of light. Therefore, log transformation of absorbance and cells.ml⁻¹ for both fungal species have been performed to stabilise the variances of the data points. Correlation plots of log (absorbance) and log (cells.ml⁻¹) for both *S. cerevisiae* and *C. albicans* were fitted using linear equation (Fig 3.4b). The plots of logarithmic transformed values displayed good correlation coefficient values for both *S. cerevisiae* and *C. albicans*, these being R² = 0.948 and 0.927 respectively.

3.3.2 Investigation of the inhibitory activity of 1,4-diene-3-ones using a macro-broth susceptibility assay

3.3.2.1 Susceptibility of *S. cerevisiae* to 1,4-diene-3-ones

The potency of each synthesized 1,4-diene-3-one compound was determined by comparing the IC_{10} , IC_{25} , IC_{50} , IC_{90} , asymptotic I_{50} values, slope factors (Hill slopes) and the area under the curve (AUC) values. The latter values were obtained from the dose-response curves using the five-parameter logistic model (GraphPad, Prism 5) and an indefinite integral between two common concentrations, C_1 and C_2 . Standard deviation (SD) of the latter values was calculated from the dose-response curves of three individual experiments each assayed in duplicate.

The asymptotic I_{50} value depends on the shape of the curve and the overall degree of inhibition exhibited. In this study, the dose-response curve of 1,4-diene-3-one compounds vary in shape. For example, some compounds show a maximum response of 90% inhibition whereas some only show 20% inhibition of the growth. An asymptotic I_{50} value usually takes an account of the shape and nature of the curve and determines the I_{50} value based on 50% inhibition of that curve.

Therefore an asymptotic I_{50} value could lead to a false interpretation of the results. It is thus important to compare the manually obtained IC_{10} , IC_{25} , IC_{50} and IC_{90} values from the dose-response curve along with the I_{50} and AUC values. The dose-dependent curve of bis-benzylidene, bis-pyridylidene and bis-thienylidene derivatives of N-methylpiperidin-4-one and cycloalkanones against *S. cerevisiae* were shown in figures 3.5 to 3.9.

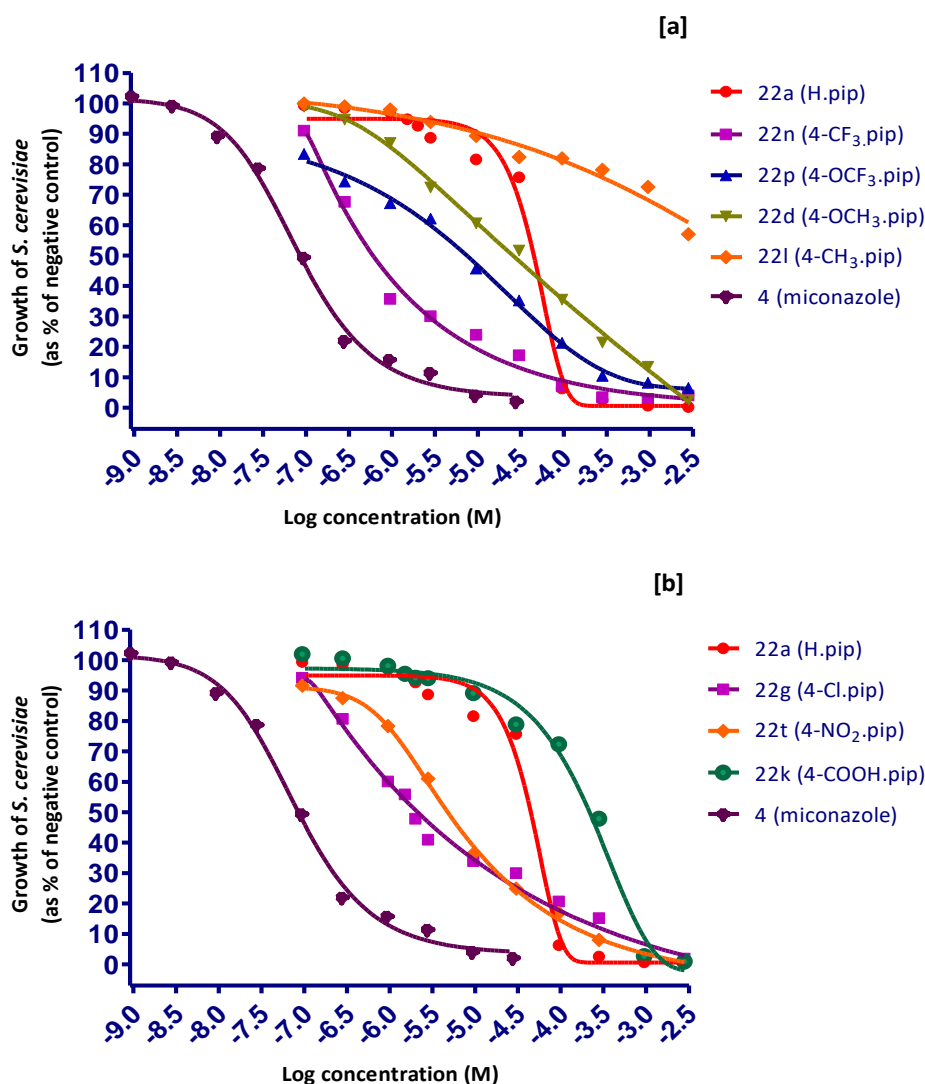


Figure 3. 5. Dose-dependent inhibition of *S. cerevisiae* growth by various *para*-substituted bis-benzylidene derivatives of *N*-methylpiperidin-4-one after 24 hours.

Dose-dependent inhibition of *S. cerevisiae* growth by the bis-benzylidene derivatives of *N*-methylpiperidin-4-one with various substituents attached to the *para*-position of the aromatic ring. The *para*-substituent groups include hydrogen, trifluoromethyl, trifluoromethoxy, methoxy and methyl [a]; hydrogen, chloro, nitro and carboxylic acid [b]. The inhibitory activity was expressed as the growth of *S. cerevisiae* in the presence of a compound as a percentage of the negative drug-free control after 24 hours. All assays contained 1.5% DMSO. The dose-response curve was fitted using the five-parameter logistic model on GraphPad, Prism 5. Data were presented as the mean of three individual growth experiments. Each assay was performed in duplicate. SD values were omitted for clarity of graphs.

The various dose-dependent curves in figure 3.5 show that increasing the concentrations of compounds results in increased inhibition as measured after treatment for 24 hours. The

para-trifluoromethyl substituted bis-benzylidene derivative of N-methylpiperidin-4-one (**22n**) was found to be the most potent inhibitor of *S. cerevisiae* growth ($IC_{50} = 0.62 \mu\text{M}$) amongst the group of *para*-substituted compounds (Figure 3.5a). Compound **22n** shows a shallow dose-response curve with low Hill slope (0.63) which suggests this compound does not have a problem regarding molecular aggregation (Seidler, McGovern, Doman, & Shoichet, 2003).

Compounds **22d** and **22p** also showed shallow dose-response curve with low Hill slopes values (0.56 and 0.71 respectively) suggests no formation of aggregates (Seidler *et al.*, 2003). In addition, compounds **22d** and **22p** both exhibited good activity by inhibiting the growth of *S. cerevisiae* with IC_{50} values of 27.9 and 12.9 μM . The difference in the activity of compounds **22d** and **22p** was only 2.16-fold this being due to the difference in their R-group on the rings, **22d** has methoxy group as electron donating group (EDG) whereas **22p** has an electron withdrawing (EWG) trifluoromethoxy group. Due to the presence of the EWG **22p** exhibited slightly better activity than **22d**. The *para*-methyl substituted bis-benzylidene-N-methylpiperidin-4-one (**22i**) in Figure 3.5[a] was identified as the least active compound in the 1,4-diene-3-ones library.

Compounds **22a** and **22k** both showed more than 90% inhibition at concentrations above 100 μM (Fig. 3.5b). The dose-response curve of **22a** was slightly steeper than **22k** and their Hill slopes were identified as 2.80 and 0.97, respectively suggesting aggregation of the former molecule. However in terms of the IC_{50} values, **22a** (40.7 μM) showed better potency than **22k** (218 μM). The higher inhibitory activity of **22a** could possibly be due to promiscuous aggregation (Seidler *et al.*, 2003). On the other hand, compounds **22g** and **22t** exhibited good potency with low IC_{50} values (5.56 and 3.37 μM respectively). Both **22g** and **22t** showed shallow curve with low Hill slope values (0.25 and 0.56). This may be due to factors associated

with compound solubility (Seidler *et al.*, 2003). The inhibitory potency of **22g** and **22t** was 46 and 28-fold lower than miconazole nitrate. Based on the above information the group potency order in the *para*-substituted compounds, in terms of their IC₅₀ values was identified as CF₃ >NO₂ >Cl >OCF₃ >OCH₃ >H > COOH >CH₃.

Furthermore, the dose-response curves of bis-benzylidene derivatives of N-methylpiperidin-4-one and its *meta*- substituents on the benzene ring is shown in Figure 3.6.

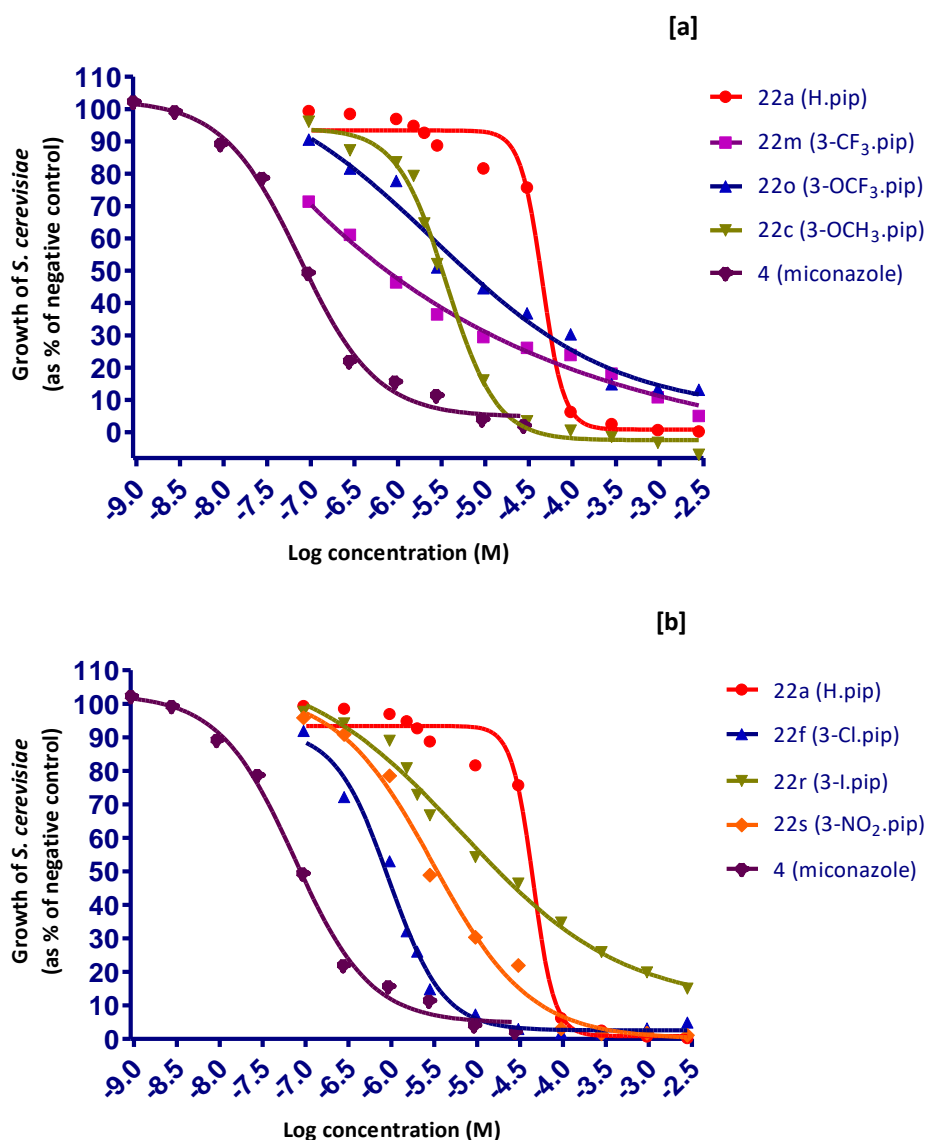


Figure 3. 6. Dose-response curves of the meta- substituted bis-benzylidene derivatives of N-methylpiperidin-4-one against *S. cerevisiae* after 24 hours.

Dose-dependent inhibition of *S. cerevisiae* growth by the bis-benzylidene derivatives of N-methylpiperidin-4-one with various substituents attached to the *meta*- position of the aromatic ring. The *meta*- substituent groups include hydrogen, trifluoromethyl, trifluoromethoxy, methoxy [a]; hydrogen, chloro, iodo and nitro [b]. The inhibitory activity was expressed as the growth of *S. cerevisiae* in the presence of a compound as a percentage of the negative drug-free control (DMSO 1.5%) after 24 hours. The dose-response curve was fitted using the five-parameter logistic model on GraphPad, Prism 5. Data was recorded as the mean of three individual growth experiments. Each assay was performed in duplicate. SD values were omitted for clarity of graphs.

Compounds **22c**, **22m** and **22o** exhibited good inhibitory activity by inhibiting the growth of *S. cerevisiae* with low IC₅₀ values 3.24, 2.22 and 2.83 μ M, respectively (Figure 3.6a).

Compounds **22m** and **22o** both showed shallow curves with low Hill slope values (0.43 and 0.85 respectively) whereas **22c** gave a steep curve with Hill slope of 1.65. High hill slope of **22c** suggesting aggregation of the molecule and consequently increase in the activity of this compound due to promiscuous aggregation. While **22m** and **22o** have low Hill slope (<1) indicating their potency is not linked to aggregation. In contrast, compound **22a** displays a very steep dose-response curve between concentrations of 30 and 100 μM with a high Hill slope (2.80), which indicates that the inhibitory action could possibly be due to drug aggregation at higher concentrations (Seidler *et al.*, 2003).

Compounds **22f**, **22r** and **22s** all exhibited good inhibitory activities against *S. cerevisiae* with IC_{50} values of 1.21, 7.64 and 1.87 respectively. In addition, compounds **22f** and **22s** displayed fairly steep curves with high Hill slopes (1.73 and 2.90), whereas **22r** gave a shallow curve with Hill slope of 0.65. Although **22f** and **22s** gave better potency than **22r**, the high Hill slope values of **22f** and **22s** again suggesting promiscuous inhibition due to aggregation. In conclusion the iodo-substituent was identified as the least active inhibitor compared to other *meta*-substituent groups. This may be due to the size of the iodine atom compared to the other substituents. Based on the results the order of potency for groups in the *meta*-substituted compounds, in terms of their IC_{50} values was identified as $\text{Cl} > \text{NO}_2 > \text{CF}_3 > \text{OCF}_3 > \text{OCH}_3 > \text{I} > \text{H}$. The dose-response curve of *ortho*-substituted and di-chloro substituted bis-benzylidene derivative of N-methylpiperidin-4-one is shown in Figure 3.7.

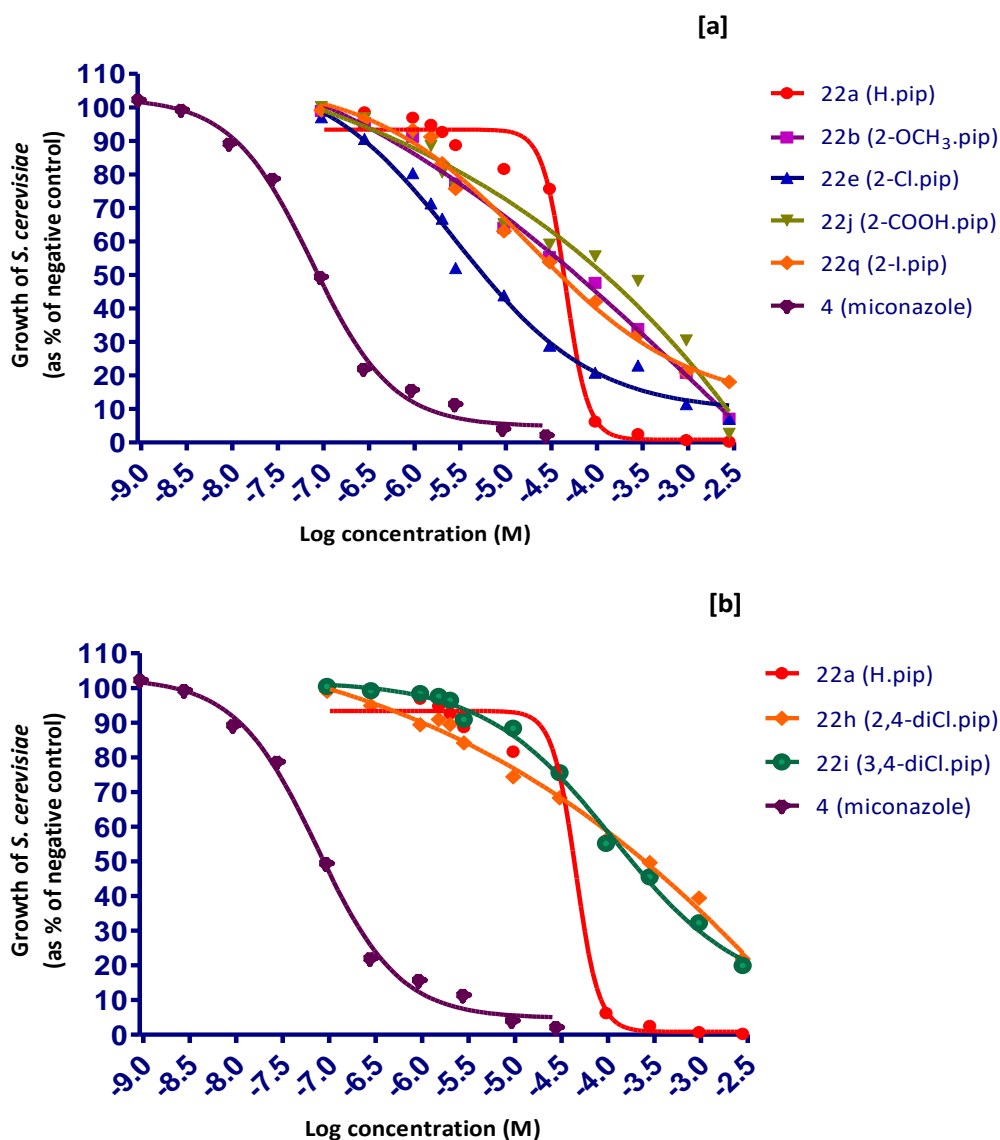


Figure 3. 7. Dose-response curves of the ortho-substituted [a] and dichloro substituted [b] bis-benzylidene derivatives of N-methylpiperidin-4-one against *S. cerevisiae* after 24 hours.

Dose-response curves of the *ortho*-substituted and dichloro substituted bis-benzylidene derivatives of N-methylpiperidin-4-one against *S. cerevisiae*. The *ortho*-substituents were hydrogen, methoxy, chloro, carboxylic acid and iodo [a]; hydrogen, 2,4-dichloro and 3,4-dichloro [b]. The inhibitory activity was determined by comparing the growth of *S. cerevisiae* with and without compound as the percentage of negative control (DMSO 1.5%) after 24 hours. The dose-response curve was fitted using the five-parameter logistic model. Data was recorded as the mean of three individual growth experiments, each assay conducted in duplicate. SD values were omitted for clarity of graphs

Compound **22e** *ortho*-chloro substituted bis-benzylidene derivative of N-methylpiperidin-4-one in Figure 3.7[a] was the most potent inhibitor of *S. cerevisiae* growth compared to other

ortho-substituents with an IC₅₀ of 3.90 μM. However miconazole was 32.5-fold more potent than **22e**. Both compounds **22b** and **22q** (*ortho*-methoxy and *ortho*-iodo substituted bis-benzylidene N-methylpiperidin-4-one) showed moderate inhibitory activity against *S. cerevisiae*, their IC₅₀ values being 53.7 and 21.4 μM respectively. However, the IC₅₀ value of compound **22c** (*meta*-methoxy) was 3.24 μM (Fig 3.6a) whereas the IC₅₀ value of compound **22s** (*para*-methoxy) was 27.9 μM (Fig 3.5a). On the other hand, compound **22r** (*meta*-iodo substituent) showed good potency with its IC₅₀ value of 7.64 μM (Fig 3.6b). This shows a significant difference suggests positional bumping (overlapping of atoms) may be important and not lipophilicity which is similar for *ortho*, *meta* or *para*- substituted compounds. Also this could suggest a large volume group (e.g. iodine or methyl is required at the *meta* position) of the compound for maximum potency. Compound **22j** contains an *ortho*-carboxylic acid group which has been identified as the least active amongst all of the *ortho*-groups tested with IC₅₀ value of 124 μM.

The dose-response curves of 2,4-dichloro and 3,4-dichloro substituted bis-benzylidene N-methylpiperidin-4-one (**22h** and **22i**) were almost identical to each other showing a shallow curve over the range of concentrations (Figure 3.7b). Compounds **22h** and **22i** both displayed poor inhibitory activity showing a maximal response at 3000 μM concentration with 80% inhibition of *S. cerevisiae* growth. The IC₅₀ values of **22h** and **22i** were 153.6 and 153.9 μM respectively, whereas their Hill slopes were 0.22 and 0.64 which indicates these two compounds are not aggregators. In contrast, compounds (**22e**, **22f** and **22g**) with a single chloro group each of the aromatic rings at either *ortho*, *meta* or *para* position gave good potency with IC₅₀ values of 3.90, 1.21 and 5.56 μM (Fig. 3.7a, 3.6b and 3.5b). This suggests that presence of di-chloro groups on the aromatic ring gives about 30-fold decrease. It is more likely that the presence of two chlorine atoms increases the volume of the molecule

sufficiently that although it is able to react, the molecule has less accessibility to the binding site (chlorine being quite large and there being four of them). The potency order of groups in the *ortho*-substituted and di-chloro substituted bis-benzylidene derivatives of N-methylpiperidin-4-one, in terms of their IC₅₀ values, was identified as Cl > I > H > OCH₃ > COOH > 2,4-diCl.

The dose-response curves of bis-pyridylidene derivatives of N-methylpiperidin-4-one is displayed in Figure 3.8.

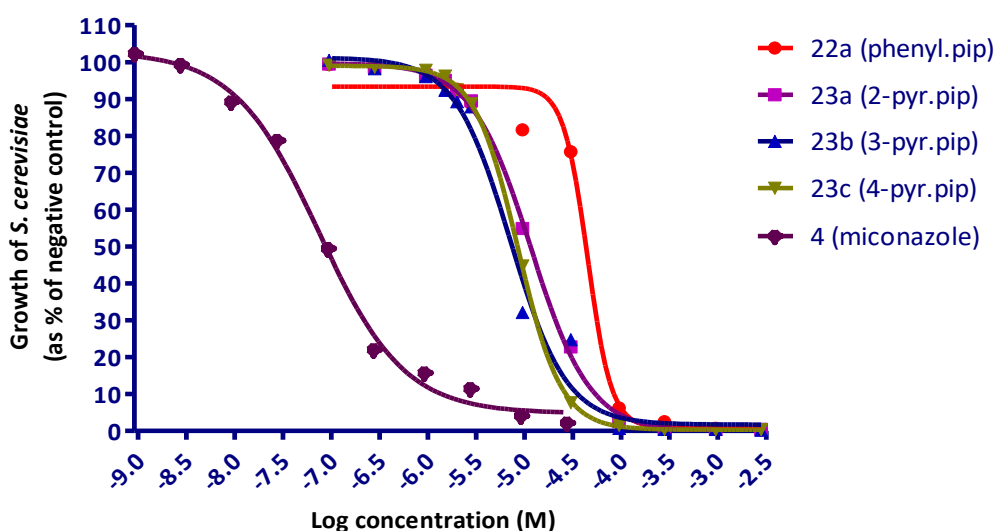


Figure 3. 8. Dose-response curves of the bis-benzylidene and bis-pyridylidene derivatives of N-methylpiperidin-4-one against *S. cerevisiae* after 24 hours.

Dose-response curves of the bis-pyridylidene derivatives of N-methylpiperidin-4-one against *S. cerevisiae* with miconazole as a positive control. The inhibitory activity was determined by comparing the growth of *S. cerevisiae* with and without compound as the percentage of negative control (DMSO 1.5%) after 24 hours. The dose-response curve was fitted using the five-parameter logistic model. Data was determined as the mean of three individual growth experiments each of which conducted in duplicate. SD values were omitted for clarity of graphs.

The position of the nitrogen-atom at either the *ortho*-, *meta*- or *para*- position in the aromatic ring differentiates compounds **23a**, **23b** and **23c** from each other. The dose-response curves of compounds **23a**, **23b** and **23c** showed steep curves between concentrations of 30 and 300

μM with their Hill slope values all being well above 1.5 (see **Table 3.1**, page 105). Similarly, compound **22a** also shows a steep curve between concentrations of 30 and 100 μM . Compounds **23a**, **23b** and **23c** exhibited good inhibitory activity against *S. cerevisiae* with their IC_{50} values being 12.6, 8.84 and 9.45 μM , respectively. The potency order of pyridyl derivatives of N-methylpiperidin-4-one in terms of their IC_{50} values was identified as *meta* > *para* > *ortho*. However the difference in the activity between different isomeric pyridyl rings of compounds is minimal. The major difference is between the pyridine ring and the benzene ring thus suggesting the difference in potency relates to the change in solubility and/or hydrophobicity.

The dose-response curve of bis-pyridylidene derivatives of cyclopentanone is presented in Figure 3.9.

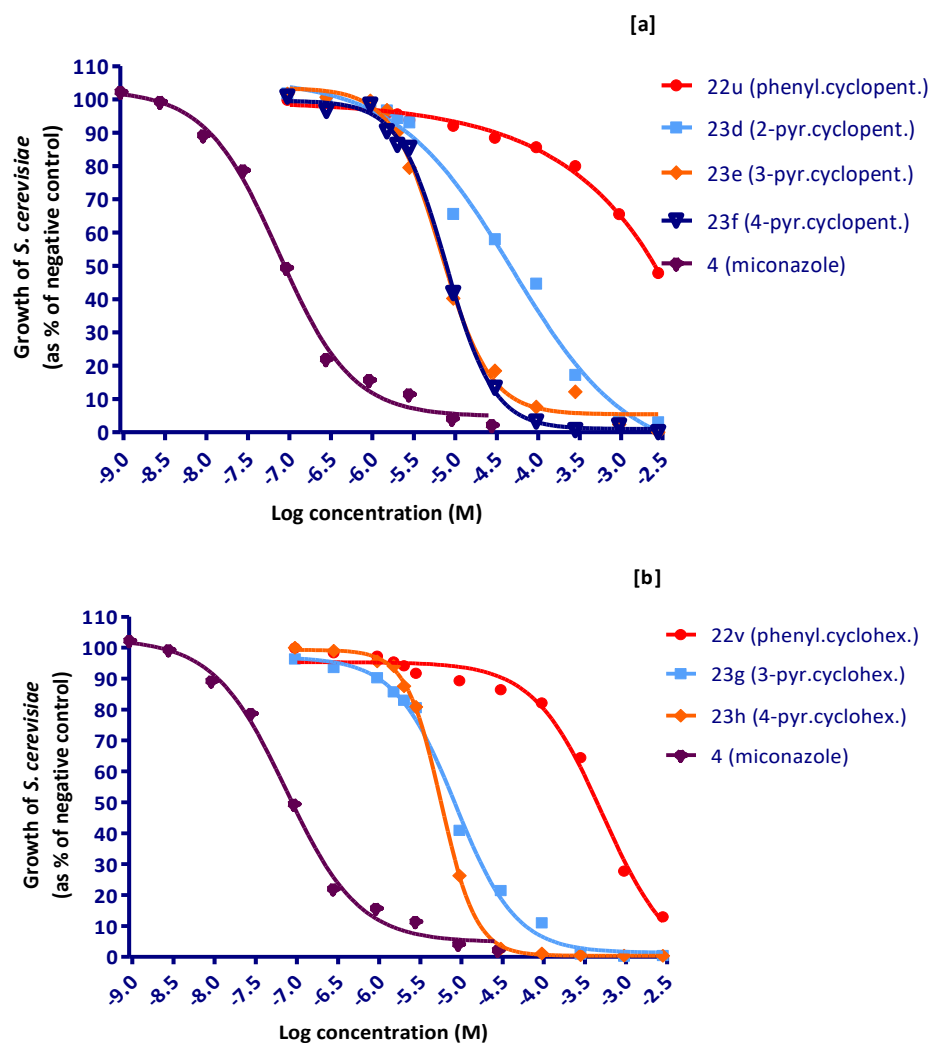


Figure 3. 9. Dose-response curves of the bis-pyridylidene derivatives of cycloalkanones against *S. cerevisiae* after 24 hours.

Dose-response curves of the bis-pyridylidene derivatives of cyclopentanone [a] and cyclohexanone [b] against *S. cerevisiae* with miconazole as a positive control. The inhibitory activity was determined by comparing the growth of *S. cerevisiae* with and without compound as the percentage of negative drug-free control (DMSO 1.5%) after 24 hours. The dose-response curve was fitted using the five-parameter logistic model. Data was displayed as the mean of three individual growth experiment each conducted in duplicate. SD values were omitted for clarity of graphs.

Compound **22u**, the bis-phenylidene derivative of cyclopentanone in Figure 3.9[a] does not contain any nitrogen in the aromatic ring system, whereas compounds **23d**, **23e** and **23f** each contain a single nitrogen atom in the aromatic ring at either *ortho*-, *meta*- or *para*- positions. The inhibition curves of compounds **23e** and **23f** (*meta* and *para*) were very steep and almost

identical to each other whereas compound **23d** (*ortho*) exhibits a shallow curve. Compounds **23e** and **23f** displayed high Hill slopes (1.80 and 1.76 respectively), greater than **23d** (0.94). In addition the IC₅₀ values of compounds **22u**, **23d**, **23e** and **23f** were 1290, 20.33, 9.29 and 8.46 μM respectively. This may be suggestive of compound **23d** having lower levels of aggregation and thus its IC₅₀ being a true representation of the potency compared to compounds **23e** and **23f** which may be aggregating to a greater extent which is suggestive by the high Hill slopes. The above dose-response curves clearly shows that the pyridine containing compounds were more potent than phenyl rings compound suggesting a higher ability to cross the membrane. This information confirms that the introduction of the nitrogen atom in the ring system increases the solubility and it enhances the inhibitory activity of these compounds.

In addition, the clogP values of **22u**, **23d**, **23e** and **23f** were determined to be 4.77, 1.60, 1.91 and 1.90 respectively. This suggests the hydrophobicity of the ring may be related to the potency in the sense that the highly hydrophobic benzene ring would impart a lower aqueous solubility to the potential drug molecule than the equivalent drug with a pyridine ring. Thus the presence of benzene and pyridyl substituted molecules **22u**, **23d**, **23e** and **23f** are consistent with a role for aqueous solubility in defining drug potency.

In Figure 3.9[b] compound **22v**, the bis-phenylidene derivative of cyclohexanone, gave a 10% inhibition of growth at a concentration of 57 μM whereas the bis-pyridylidene derivatives of cyclohexanone, **23g** and **23h**, have shown 10% inhibitory activity at only 0.99 and 2.22 μM. The IC₅₀ value of compound **22v** has been determined to be 309 μM. Compound **23g** represents the pyridyl derivative of cyclohexanone where the nitrogen atom is present at the *meta*-position on the pyridyl ring, whereas compound **23h** represents the *para*-position of N-atom on the pyridyl ring. Compounds **23g** and **23h** both exhibited steep curves between 3.0

and 30 μM with their IC_{50} values being 5.52 and 6.25 μM respectively, thus indicating their good inhibitory activity against *S. cerevisiae* growth.

When comparing the Hill slopes of these compounds it has been identified that **22v**, **23g** and **23h** have a higher Hill slopes (2.50, 2.83 and 2.97) than compounds **22u**, **23e** and **23f** (0.63, 1.80 and 1.76). A high Hill slope is associated with the aggregation status of the drug molecules and a consequent artifactual lowering of the IC_{50} values. When comparing the inhibitory activity in terms of the IC_{50} values of phenylidene or pyridylidene derivatives of cyclopentanone (**22u**, **23d**, **23e** and **23f**) with cyclohexanone (**22v**, **23g** and **23h**), it was determined that compounds containing a cyclohexanone moiety were more potent than their cyclopentanone analogue. This is most likely due to the structural consequence of five carbons in the ring compared to a six-carbon ring. The central ring with five carbon atoms is flatter whereas six carbon ring adopts more a chair like conformation which may increase the effect on the reactivity of the 1,4-diene-3-one with the target enzyme. Therefore, the potency order of bis-pyridylidene derivatives of cyclopentanone and cyclohexanone based on their IC_{50} values can be described as *para* > *meta* > *ortho*-position of nitrogen atom in the ring.

The dose-response curve of bis-thienylidene derivatives of N-methyl-piperidin-4-one, cyclopentanone and cyclohexanone is displayed in Figure 3.10.

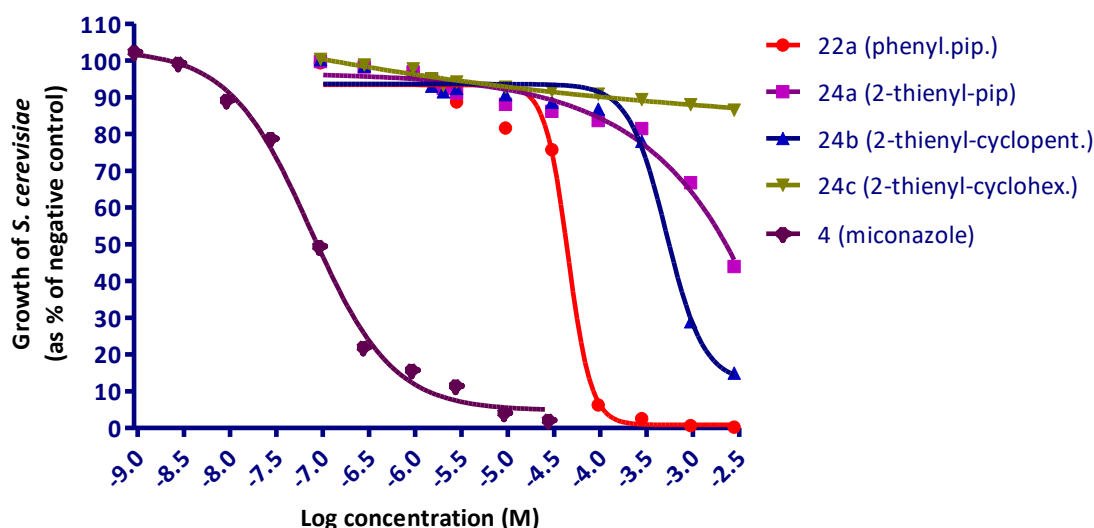


Figure 3. 10. Dose-response curves of the bis-thienylidene derivatives of N-methylpiperidin-4-one and cycloalkanones against *S. cerevisiae* after 24 hours.

Dose-response curves of the bis-thienylidene derivatives of N-methylpiperidin-4-one, cyclopentanone and cyclohexanone against *S. cerevisiae*. Positive control: miconazole. The inhibitory activity was determined by comparing the growth of *S. cerevisiae* with and without compound as the percentage of negative drug-free control (DMSO 1.5%) after 24 hours. The dose-response curve was fitted using a five-parameter logistic model. Data was determined as the mean of three individual growth experiment each of which was conducted in duplicate. SD values were omitted for clarity of graphs.

Compounds **24a** and **24b** both exhibited some activity and capable of inhibiting the growth of *S. cerevisiae* with the IC_{50} values of 2233 and 619 μM , respectively. However, **24c** does not reach even 50% inhibition. In contrast, **22a** (3,5-bis-[(*E*)-benzylidene]-1-methylpiperidin-4-one) gave an IC_{50} value of 41 μM . The curve of **24b** was very steep between the concentration range 300 to 1000 μM , yielding a high Hill slope of 2.29 suggestive of possible compound aggregation whereas **24a** showed a Hill slope of 0.46. In comparison with miconazole, compounds **22a**, **24a**, **24b** and **24c** were far less potent.

The thienyl group is near isosteric with benzene or pyridine due to the size of the sulphur atom being considered isosteric against $\text{CH}=\text{CH}$ and sulphur also containing lone pairs of electrons and being a potential isostere of the N-atom in pyridine. Thienyl derivatives were

identified as the least active amongst the whole 1,4-diene-3-one library against *S. cerevisiae* and they were classified as poor anti-fungal compounds.

When considering the different potencies of **24a** with **24c** it is interesting to note that although these compounds contain the thiophene ring the difference is associated with the central ring structure; **24c** has a cyclohexyl ring whilst **24a** has a piperidine ring. Thus, **24a** may be able to form a hydrogen bond between the lone pair of >N-Me of piperidine ring and a hydrogen atom associated with the target. The cyclohexyl group of **24c** would be unable to form such an interaction.

When comparing compound **24b** (with **24a** and **24c**) which had the highest potency in this group of compounds it is worth considering the fact that a cyclopentyl (five membered) ring is somewhat flatter than the six membered cyclohexyl or piperidine rings (both of which would adopt a near chair conformation). In addition a cyclopentyl ring has smaller bond angle than cyclohexyl or piperidine rings (Schaad & Hess, 1974). Therefore, one potential consequence of this ring flattening could be an increase in the electrophilicity of the β -carbon atom of the dienone structure thus making the compound **24b** more reactive. The five membered ring will be flatter and thus four different sp^2 orbitals of C/C/C/O are more likely to be able to facilitate the keto-enol tautomerism and thus increases the electrophilicity of the β -carbon attached to the five membered ring.

It is a challenge to characterise the inhibitory potency of a compound in terms of a single parameter. The end point of any test to identify the inhibitory potency of 1,4-diene-3-ones is somewhat arbitrary due to the partial inhibition of fungal growth sometimes shown at high inhibitor concentrations. It is, therefore necessary to include other parameters and compare them. Commonly these include the Hill slope, the area under the curve (AUC), IC_{10} , IC_{25} , IC_{50} ,

IC₉₀ and MIC as mentioned in the section 3.2.1.7, their values were obtained from application of five-parameter logistic equation and values were shown in **Table 3.1**, page 105.

The most potent compound identified from the library of 1,4-diene-3-ones was 3,5-bis(4-trifluoromethylbenzylidene)-1-methylpiperidin-4-one (**22n**), having the lowest IC₁₀, IC₂₅, IC₅₀ and AUC values. In contrast, 2,6-bis(thiophen-2ylmethylene)cyclohexan-1-one (**24c**) was identified as the least active compound because this compound was unable to inhibit even 10% growth of *S. cerevisiae*. Most of the 1,4-diene-3-ones exhibited good inhibitory activity against *S. cerevisiae* with their IC₅₀ values usually being less than 100 µM these being **22a-g**, **22m-t** and **23a-h**, respectively. Out of which compounds **22a**, **22c-g**, **22m-t** and **23a-h** exhibited IC₅₀ values <50 µM, whilst compounds **22c-g**, **22m-t** and **23a-h** gave IC₅₀ values <30 µM and compounds **22c**, **22e-g**, **22m-o**, **22r-t**, **23b-c** and **23e-g** gave IC₅₀ values <10 µM. However all continue to be higher than the IC₅₀ of the clinically relevant reference control compound miconazole which was determined to be 0.12 µM.

Moreover only 23 compounds from the library have shown inhibitory activity >90%, these being **22a-g**, **22j-k**, **22m-p**, **22s-t** and **23a-h**, respectively. Comparatively, the IC₉₀ value of miconazole was 1.29 µM. In terms of the Hill slope values of compounds; **22b**, **22d**, **22e**, **22g-r**, **22t**, **22u** and **23d** gave Hill slopes <1 whereas compounds **22c**, **22f**, **23a**, **23e** and **23f**, as well as miconazole, exhibited Hill slopes between 1 and 2. Some compounds gave Hill slope values >2 these being **22a**, **22s**, **23b**, **23c**, **23g**, **23h**, **24b** and **24c**, respectively. The AUCs of all compounds were between 97 and 328 whereas miconazole showed much lower AUC value and this being 43.

Table 3. 1. The antifungal activity of various 1,4-diene-3-ones against *S. cerevisiae*.

Compound	IC ₁₀ ± SD (μM)	IC ₂₅ ± SD (μM)	IC ₅₀ ± SD (μM)	Asymptotic I ₅₀ ± SD (μM)	IC ₉₀ ± SD (μM)	Hill slope ± SD	AUC ± SD
22a	16.17 ± 3.17	25.2 ± 2.90	40.7 ± 0.94	40.4 ± 1.36	101.4 ± 28.04	2.80 ± 1.10	248 ± 1.67
22b	0.76 ± 0.44	6.04 ± 2.99	53.7 ± 11.5	54.1 ± 14.8	2463.4 ± 264	0.49 ± 0.06	249 ± 10.9
22c	0.60 ± 0.37	1.20 ± 0.44	3.24 ± 0.47	3.89 ± 1.43	11.8 ± 4.30	1.65 ± 0.30	144 ± 12.4
22d	0.50 ± 0.30	3.87 ± 2.39	27.9 ± 18.4	29.2 ± 18.9	1024 ± 232.3	0.56 ± 0.01	230 ± 16.1
22e	0.62 ± 0.35	1.50 ± 0.80	3.90 ± 2.81	2.71 ± 1.62	1209 ± 1233	0.62 ± 0.41	188 ± 37.9
22f	0.11 ± 0.06	0.34 ± 0.79	1.21 ± 1.29	1.15 ± 1.16	4.16 ± 3.97	1.73 ± 0.34	97.3 ± 52.5
22g	1.05 ± 0.27	2.90 ± 0.39	5.56 ± 8.01	2.20 ± 1.63	458 ± 406.4	0.25 ± 0.03	160 ± 49.14
22h	1.30 ± 1.26	15.0 ± 13.3	154 ± 33.6	1178 ± 1358	N/R	0.22 ± 0.14	269 ± 15.9
22i	5.11 ± 1.73	27.6 ± 2.54	153 ± 10.9	149 ± 6.58	N/R	0.64 ± 0.01	289 ± 3.42
22j	0.68 ± 0.19	7.35 ± 1.04	124 ± 20.3	383 ± 40.3	2533 ± 389.5	0.13 ± 0.00	258 ± 3.15
22k	21.8 ± 18.9	73.8 ± 37.9	218 ± 26.4	359 ± 123	1077 ± 133	0.97 ± 0.35	299 ± 14.4
22l	17.7 ± 16.9	398 ± 311.6	N/R	4027 ± 551	N/R	0.19 ± 0.12	314 ± 10.5
22m	0.43 ± 0.42	0.65 ± 0.72	2.22 ± 1.71	7.78 ± 11.4	346 ± 155.8	0.43 ± 0.37	138 ± 29.5
22n	0.10 ± 0.04	0.22 ± 0.10	0.62 ± 0.26	0.48 ± 0.28	27.3 ± 17.9	0.63 ± 0.44	104 ± 6.73
22o	0.25 ± 0.27	0.79 ± 0.70	2.83 ± 0.96	3.50 ± 2.71	262 ± 47.6	0.85 ± 0.45	176 ± 31.7
22p	0.25 ± 0.29	1.35 ± 1.58	12.9 ± 0.91	12.5 ± 10.1	142 ± 53.6	0.71 ± 0.09	180 ± 44.8
22q	0.57 ± 0.30	3.34 ± 0.54	21.4 ± 0.99	19.3 ± 7.37	N/R	0.61 ± 0.12	221 ± 17.6
22r	0.29 ± 0.22	1.56 ± 0.33	7.64 ± 0.27	6.69 ± 2.49	N/R	0.65 ± 0.20	196 ± 10.6
22s	0.39 ± 0.49	0.67 ± 0.71	1.87 ± 0.60	1.95 ± 0.56	4.79 ± 1.79	2.90 ± 1.38	125 ± 16.9
22t	0.61 ± 0.52	1.35 ± 1.15	3.37 ± 2.01	3.43 ± 1.92	19.9 ± 15.1	0.56 ± 1.29	146 ± 48.5
22u	69.4 ± 10.7	249 ± 39.8	1290 ± 89.0	1358 ± 125.8	N/R	0.63 ± 0.16	321 ± 12.3
22v	56.9 ± 11.9	167 ± 83.6	309 ± 48.5	306 ± 47.5	N/R	2.50 ± 2.03	314 ± 5.51
23a	2.77 ± 0.56	5.64 ± 0.52	12.60 ± 1.87	12.5 ± 1.33	53.9 ± 25.3	1.62 ± 0.47	208 ± 7.62
23b	2.27 ± 1.18	4.00 ± 0.52	8.84 ± 2.11	8.58 ± 1.93	45.6 ± 30.8	2.22 ± 1.90	194 ± 12.7
23c	3.15 ± 0.72	5.51 ± 0.45	9.45 ± 1.94	9.66 ± 2.15	26.2 ± 11.8	2.52 ± 1.09	194 ± 11.4
23d	2.57 ± 0.63	6.34 ± 0.82	20.3 ± 1.80	18.6 ± 2.18	309 ± 245	0.94 ± 0.26	231 ± 8.80
23e	2.50 ± 1.06	4.50 ± 0.65	9.29 ± 1.75	8.35 ± 0.91	31.7 ± 6.91	1.80 ± 0.68	207 ± 17.0
23f	2.20 ± 0.91	4.29 ± 1.04	8.46 ± 0.68	8.42 ± 0.80	38.4 ± 24.5	1.76 ± 0.65	194 ± 6.52
23g	0.99 ± 0.78	2.80 ± 1.31	5.52 ± 2.47	5.76 ± 2.31	13.9 ± 5.26	2.83 ± 1.83	164 ± 22.7
23h	2.22 ± 0.76	3.65 ± 0.74	6.25 ± 1.49	6.25 ± 1.33	20.5 ± 17.8	2.97 ± 1.71	178 ± 10.3
24a	77.9 ± 126	467 ± 460	2233 ± 292	3934 ± 2602	N/R	0.46 ± 0.27	315 ± 15.4
24b	132 ± 215	281 ± 201	619 ± 158	539 ± 110.7	N/R	2.29 ± 2.16	319 ± 19.0
24c	N/R	N/R	N/R	N/R	N/R	2.40 ± 3.34	328 ± 14.1
4	0.03 ± 0.01	0.05 ± 0.02	0.12 ± 0.01	0.10 ± 0.01	1.29 ± 0.41	1.40 ± 0.19	43.0 ± 5.73

Note: N/R = Compounds not reached specified level of inhibition (e.g. 10%, 25%, 50% or 90%). Data was expressed in terms of the mean ± SD of the three individual experiment conducted in duplicates, therefore n=6.

3.2.2.2 Susceptibility of *C. albicans* to 1,4-diene-3-ones

The area under the curve (AUC) of each compound was measured by selecting two concentrations, C_1 and C_2 these being 0.1 and 1400 μM respectively i.e. log values of -7.02 and -2.85 (Odds & Abbott, 1984). These latter values specify the lower and upper limits of the test range and are based on the individual ranges associated with the compound library. The reason for selecting C_2 at 1400 μM concentration was that most of the compounds showed low inhibitory activity against *C. albicans*. In addition, all compounds displayed turbidity in the cell suspension at concentrations $>1400 \mu\text{M}$. The AUC for each test compound was determined from the dose-response curves of two individual experiments each assayed in duplicate. The standard deviation was calculated from the AUC obtained from the dose-response curves of these two individual experiments. The relevant IC_{10} , IC_{25} , IC_{50} and IC_{90} values were obtained manually from the percentage inhibition against compound concentration dose-response graphs (Figure 3.11 to 3.16).

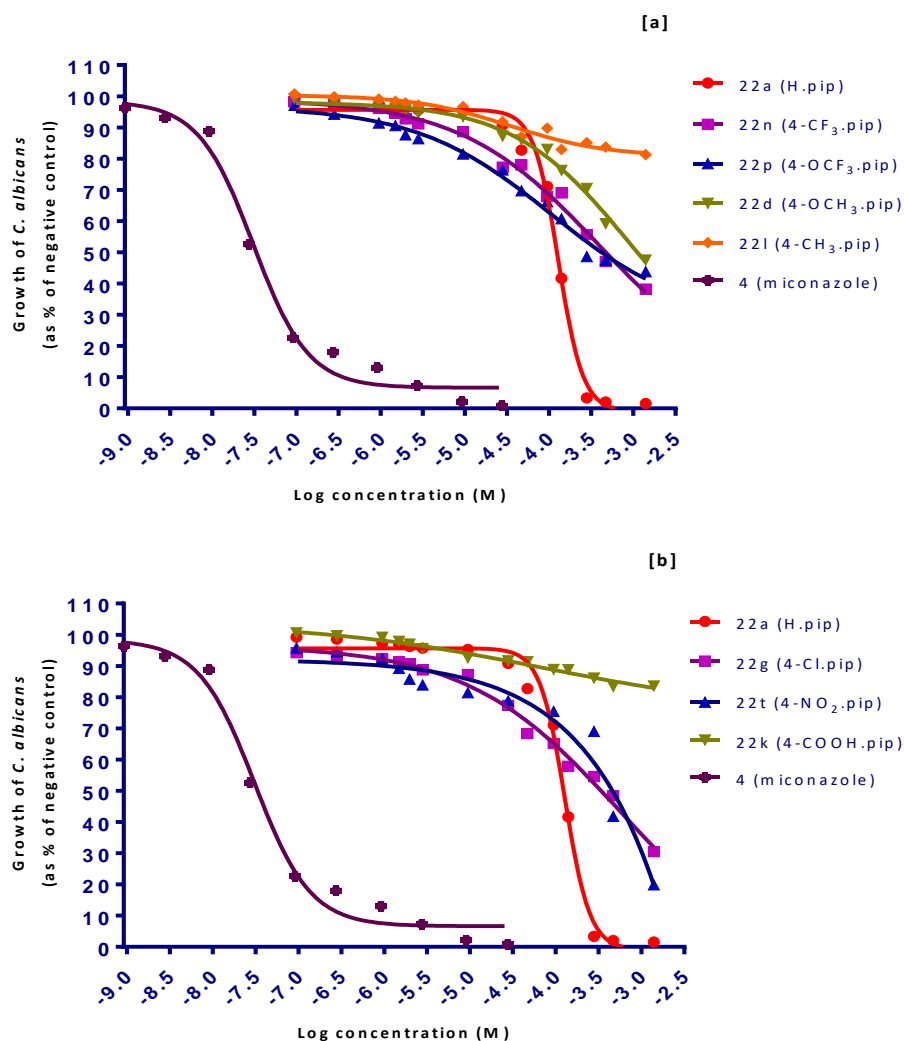


Figure 3. 11. Dose-response curves of the *para*-substituted bis-benzylidene derivatives of *N*-methylpiperidin-4-one against *C. albicans*.

The inhibitory activity was determined by comparing the growth of *C. albicans* with or without the test compound as the percentage of negative drug-free control (DMSO 1.5%) after 24 hours. Internal control: miconazole. The *para*-substituent groups were hydrogen, trifluoromethyl, trifluoromethoxy, methoxy, methyl [a]; hydrogen, chloro, nitro and carboxylic acid [b]. The dose-response curve was fitted using the five-parameter logistic model on GraphPad, Prism 5. Data were presented as the mean of two individual growth experiment each conducted in duplicate. SD values were omitted for clarity of graphs.

Compound **22a** in Figure 3.11[a] exhibited >95% inhibition at concentrations above 300 μ M, but the curve was very steep between 100 to 300 μ M with a Hill slope of 2.13. Compound **22a** gave an IC₅₀ of 128 μ M and AUC of 294. Compound **22a** also displayed a high Hill slope (2.80) for the *S. cerevisiae* dose-response curve. This suggests that compound **22a** aggregates in

both experiments. Compounds **22n** and **22p** demonstrated their inhibitory activity in a concentration-dependent manner against *C. albicans* (Figure 3.11a). Both of these compounds exhibited moderate IC₅₀ values, these being 409.5 and 473.5 μM respectively. In addition compounds **22n** and **22p** gave shallow curves with Hill slopes of 0.46 and 0.63 suggestive of no aggregation. Moreover compound **22d** in Fig 3.11[a] displayed little inhibitory activity with high AUC (356) and IC₅₀ (1112 μM) values, but the shallow curve representing low Hill slope (0.60), which suggests **22d** does not show aggregating issue.

In Figure 3.11[b], compounds **22g** and **22t** displayed reasonable although not high inhibitory activity against *C. albicans* with IC₅₀ values of 309 and 353 μM and their AUCs were 316 and 319, respectively. In addition, **22g** and **22t** displayed low Hill slope these being 0.57 and 0.50, respectively and thus suggesting no inhibitor aggregation occurs. On the other hand, compounds **22k** and **22l** revealed poor activity against *C. albicans*, capable of inhibiting only 16 and 19% of *C. albicans* growth at the highest concentrations tested. Compounds **22k** and **22l** depicted very high AUC, being 387 and 389 respectively. However **22k** and **22l** exhibited low slope factor, being 0.29 and 0.62 respectively.

The order of potency in terms of IC₅₀ values of groups in the *para*-substituted compounds was H>Cl>NO₂>OCF₃>CF₃>OCH₃>CH₃>COOH. The presence of electron-withdrawing groups (e.g. CF₃, OCF₃, NO₂ and Cl) at the *para*-position of the aromatic ring showed an increase in the activity of the bis-benzylidene derivatives of N-methylpiperidin-4-one but the most potent of this set appears to be unsubstituted.

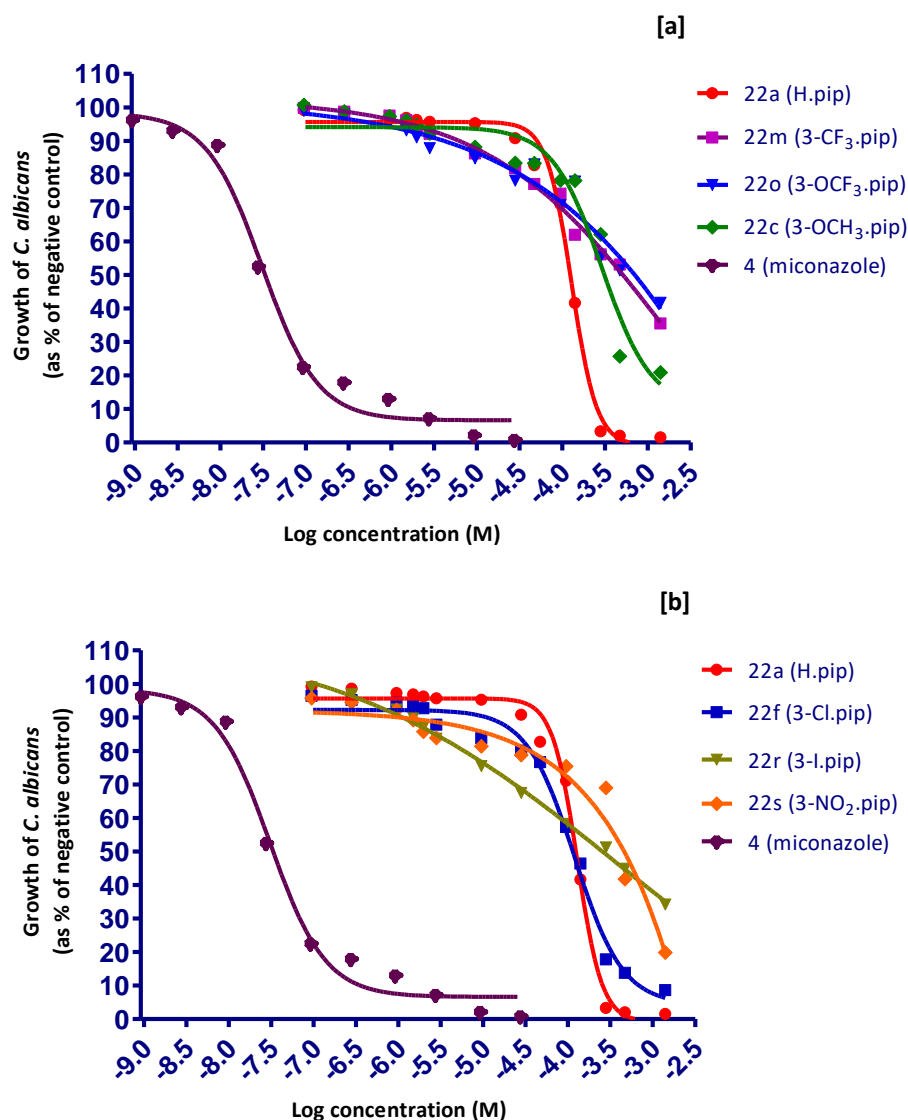


Figure 3.12. Dose-response curves of the meta-substituted bis-benzylidene derivatives of N-methylpiperidin-4-one against *C. albicans*.

Inhibition was determined by comparing the growth of *C. albicans* with and without the test compound as the percentage of negative drug-free control (DMSO 1.5%) after 24 hours. Positive control: miconazole. The *meta*-substituent groups were hydrogen, trifluoromethyl, trifluoromethoxy, methoxy [a]; hydrogen, chloro, iodo and nitro [b]. The dose-response curve was fitted using the five-parameter logistic model (GraphPad, Prism 5). Data were presented as the mean of two individual growth experiments each conducted in duplicate. SD values were omitted for clarity of graphs.

The dose-response curves in Figure 3.12 represent the *meta*-substituted bis-benzylidene derivatives of N-methylpiperidin-4-one against *C. albicans* after 24 hours growth. Compounds **22c**, **22m** and **22o** demonstrated their inhibitory activity in a concentration-dependent

manner over the range of concentrations studied (Figure 3.12a). The IC_{50} values of compounds **22c**, **22m** and **22o** were 313, 525 and 549 μ M whereas their AUC being identified as 329, 335 and 329, respectively. Thus IC_{50} values suggest **22m** and **22o** were less potent than compound **22c** whilst AUC does not support this all because AUV values were very close. Compounds **22m** and **22o** displayed shallow curves with Hill slope of 0.39 and 0.60 whereas **22c** gave a steep curve between the concentrations 100 and 300 μ M and high Hill slope (1.27). Thus suggesting higher potency of **22c** in terms of IC_{50} is a reflection of aggregation status.

Among all *meta*-substituents (**22c**, **22m**, **22o**, **22r** and **22s**), compound **22f** exhibited higher degree of inhibition of *C. albicans* growth with the IC_{50} and IC_{90} values of 114 and 677 μ M, respectively. The AUC of compound **22f** was 288 however the Hill slope of 1.21 demonstrating a steep curve. In contrast, compound **22r** displayed moderate inhibitory activity with moderate IC_{50} (243 μ M) and low Hill slope (0.26) values. Thus a significant component of the inhibition in compound **22f** was due to non-aggregation. Similarly, compound **22s** showed low to moderate inhibitory activity with the IC_{50} value of 666 μ M and AUC of 316 but low Hill slope, this being 0.33. The order of potency of groups in the *meta*-substituted compounds in terms of the IC_{50} values was Cl > H > I > OCH₃ > CF₃ > OCF₃ > NO₂. Iodine containing 1,4-diene-3-one compound has a lower electronegativity, lower electron affinity, lower ionisation energy and lower reactivity than chlorine. Hence the lower AUC and IC_{50} values of compound **22f** than **22r** proves that compound containing chlorine group at *meta*-position of the aromatic ring is more potent than iodine group.

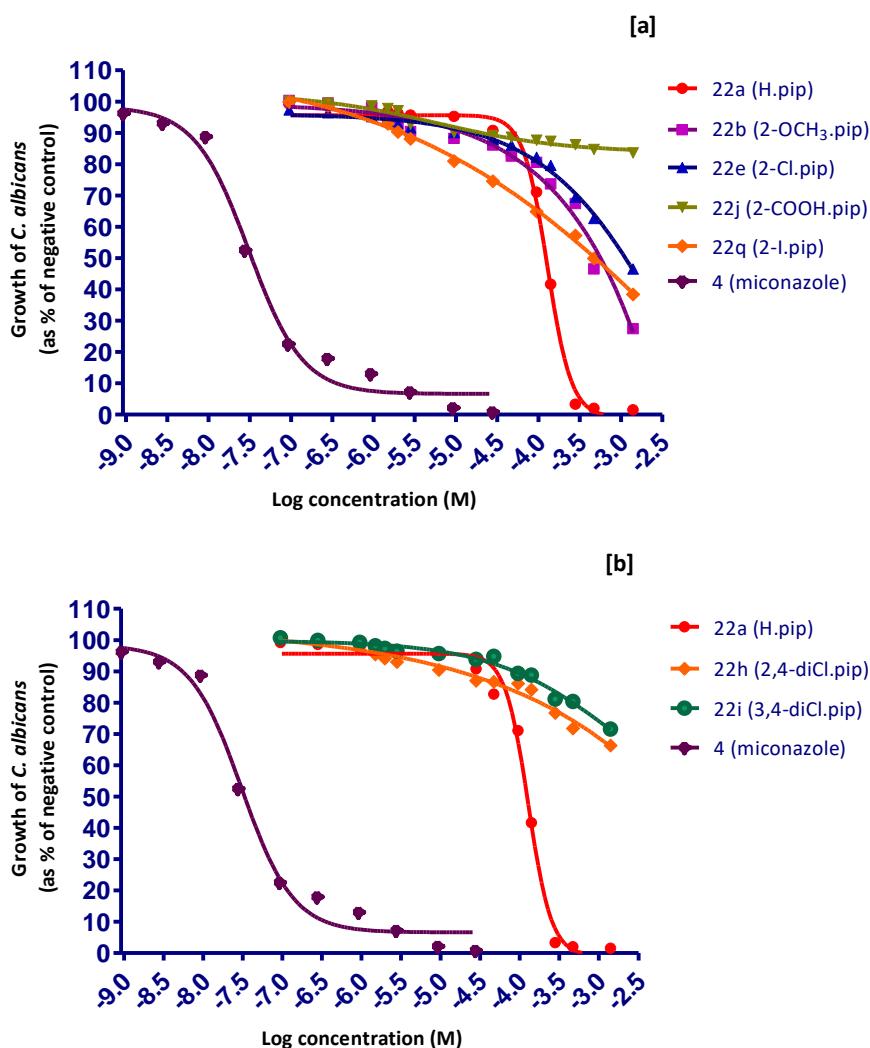


Figure 3.13. Dose-response curves of the ortho-substituted [a] and dichloro substituted [b] bis-benzylidene derivatives of *N*-methylpiperidin-4-one against *C. albicans*.

The inhibitory activity was determined by comparing the growth of *C. albicans* with and without compound as the percentage of negative control (DMSO 1.5%) after 24 hours. Positive control: miconazole. The *ortho*-substituents were hydrogen, methoxy, chloro, carboxylic acid and iodo [a]; hydrogen, 2,4-dichloro and 3,4-dichloro [b]. The dose-response curve was fitted using the five-parameter logistic model (GraphPad, Prism 5). Data were presented as the mean of two individual growth experiment each conducted in duplicate. SD values were omitted for clarity of graphs.

C. albicans was, to some extent, susceptible to compounds **22b**, **22e** and **22q** (Figure 3.13).

Compounds **22b**, **22e** and **22q** all exhibited shallow dose-response curves with low Hill slopes of 0.49, 0.62 and 0.61 respectively. Compounds, **22b** and **22q** exhibited higher degree of potency with IC₅₀ values being 531.5 and 454.3 μM respectively. In contrast **22e** gave an IC₅₀

of 1101 μM and **22j** capable of inhibiting only 16% of *C. albicans* growth at highest concentration.

On the other hand in Figure 3.13[b], both compounds **22h** and **22i** (2,4-dichloro and 3,4-dichloro-substituted bis-benzylidene derivatives of *N*-methylpiperidin-4-one) showed identical dose-response curves which may be because the clogP values for both **22h** and **22i** are the same (6.51). Low activity of **22h** and **22i** is possibly related to their high clogP values, which makes these compounds more lipophilic therefore making it difficult to exit the membrane. Compounds **22h** and **22i** both gave their maximum response inhibiting only 30% growth of *C. albicans*. Based on the IC_{50} values of *ortho*-substituted compounds, the potency order of this group of compounds can be described as $\text{H} > \text{I} > \text{OCH}_3 > \text{Cl} > \text{COOH}$.

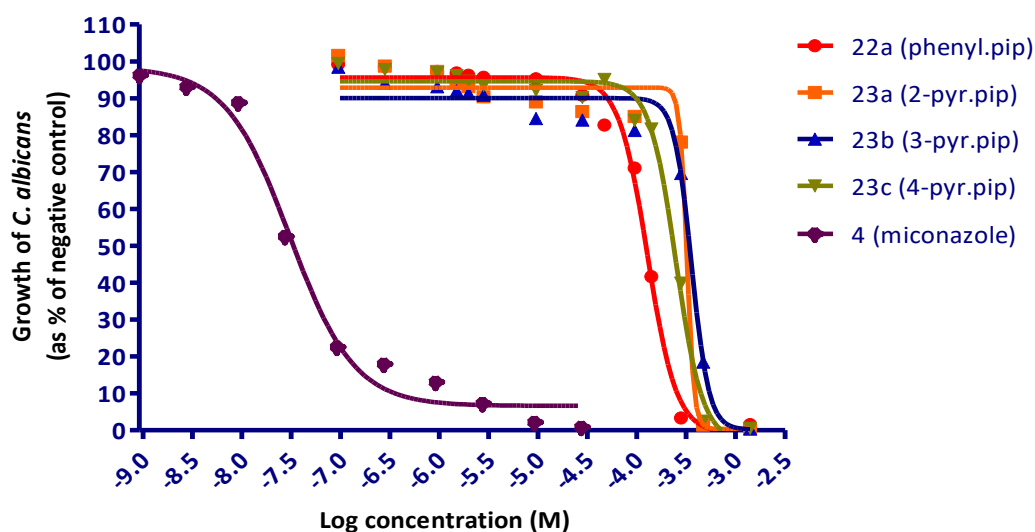


Figure 3. 14. Dose-response curves of the bis-pyridylidene derivatives of *N*-methylpiperidin-4-one against *C. albicans* after 24 hours.

The inhibitory activity was determined by comparing the growth of *C. albicans* with and without the test compound as the percentage of negative drug-free control (DMSO 1.5%). Positive control: miconazole. A dose-response curve was fitted using the five-parameter logistic model (GraphPad, Prism 5). Data were presented as the mean of two individual growth experiment each conducted in duplicate. SD values were omitted for clarity of graphs.

Compounds **23a**, **23b** and **23c** differ from each other by the *ortho*-, *meta*- or *para*- position of the nitrogen atom in the aromatic ring (Figure 3.14). A heteroatom, such as a nitrogen atom, in the aromatic system is likely to facilitate an increase in the aqueous solubility of the compound compared to the phenyl equivalent. It was anticipated that the clogP values of N-containing ring compounds would be lower than the non-N-containing ring compound. The clogP of compounds **22a**, **23a**, **23b** and **23c** were calculated to be as 4.07, 1.53, 1.83 and 1.61 respectively thus confirming our hypothesis.

The IC₅₀ values of compounds **22a**, **23a**, **23b** and **23c** were good being 128, 367, 238 and 248.5 μM compared to their AUC values which were 294, 329, 320 and 314 respectively. Compound **22a** gave the highest potency whereas **23a** exhibited lowest potency based on their ability to inhibit the growth of *C. albicans*. However, **23b** and **23c** were similar in their activities in terms of both the AUC and IC₅₀ values. The dose-response curves of all of these compounds displayed steep curve between 100 and 470 μM. Consequently their Hill slopes were high, these being 2.13, 3.27, 1.36 and 2.57 respectively. Compounds **22a**, **23a**, **23b** and **23c** were all significantly less potent than miconazole. The order of potency of the bis-pyridylidene derivatives of N-methylpiperidin-4-one in terms of their IC₅₀ values can be described as *meta* > *para* > *ortho*-position of N-atom on the ring. However, when comparing the AUC values, their order of potency has changed to *para* > *meta* > *ortho*-position of N-atom on the ring.

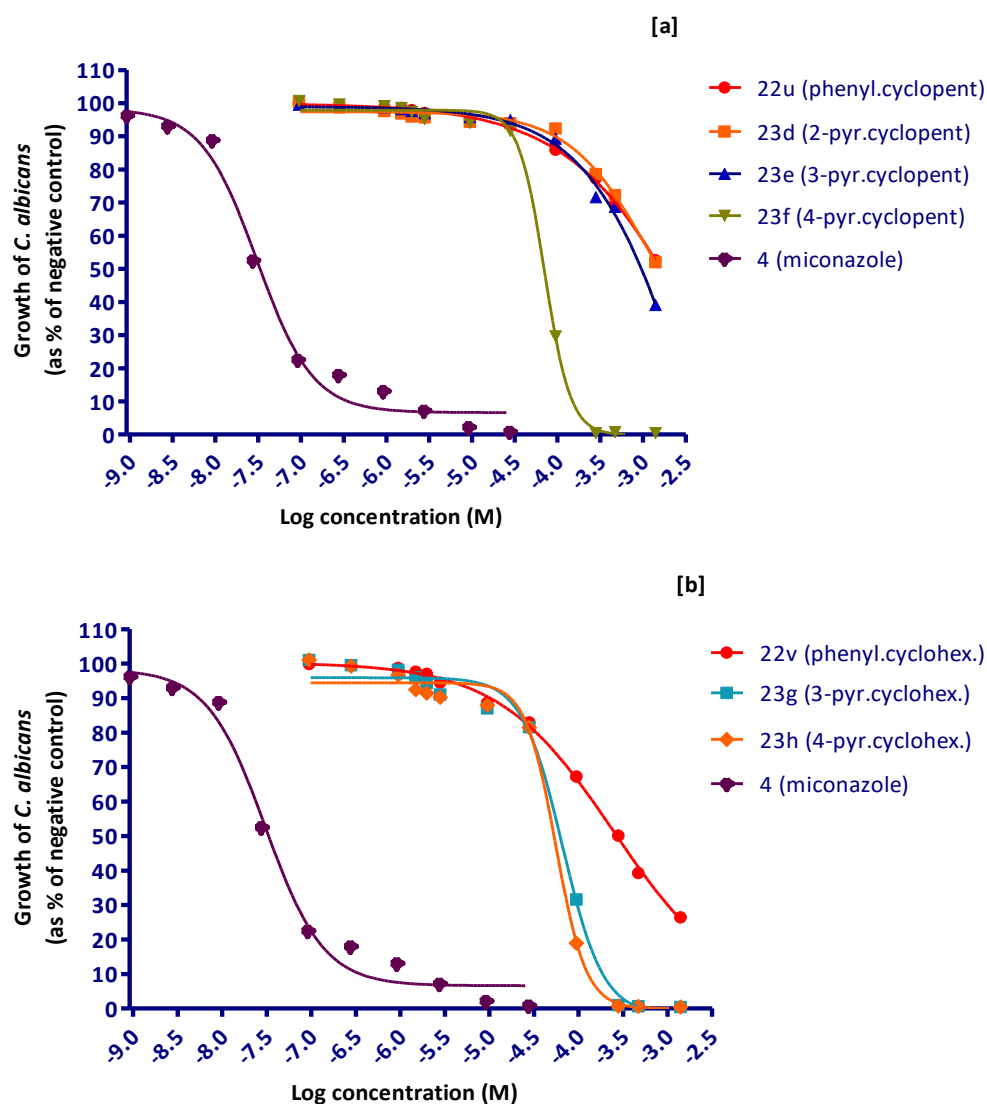


Figure 3. 15. Dose-response curves of bis-benzylidene and bis-pyridylidene derivatives of cycloalkanones against *C. albicans* after 24 hours.

Dose-response curves of the bis-pyridylidene derivatives of cyclopentanone [a] and cyclohexanone [b] against *C. albicans*. The inhibitory activity was determined by comparing the growth of *C. albicans* with and without compound as the percentage of negative control (DMSO 1.5%) after 24 hours. Positive control: miconazole. A dose-response curve was fitted using the five-parameter logistic model (GraphPad, Prism 5). Data was determined as the mean of two individual growth experiment each conducted in duplicate. SD values were omitted for clarity of graphs.

Compound **22u** in Figure 3.15[a] represents the bis-benzylidene derivative of cyclopentanone, while compounds **23d**, **23e** and **23f** are analogues containing a nitrogen atom in the aromatic ring at either the *ortho*-, *meta*- or *para*-positions. Compounds **22u**, **23d** and **23e** all exhibited

very low potencies, with IC_{50} values of 1604, 2196 and 1493 μM respectively. The dose-response curves of **22u**, **23d** and **23e** were shallow and had Hill slope values were 0.55, 0.99 and 0.90 respectively. Compound **23f** exhibited good potency against *C. albicans* growth with an IC_{50} value of 68.5 μM but a high Hill slope (2.33).

In Figure 3.15[b], bis-benzylidene derivative of cyclohexanone (**22v**) exhibited modest inhibitory activity with an IC_{50} value of 263 μM and a maximum of 70% inhibition of *C. albicans* growth at the highest concentration tested. Compound **22v** gave a shallow dose-response curve with a Hill slope of 0.67. Compounds **23g** and **23h** both exhibited the highest potency against *C. albicans* with IC_{50} values of 57.6 and 50.7 μM and AUCs of 273 and 261 respectively. However **23g** and **23h** displayed steep dose-response curves between the concentration ranges of 100 and 300 μM and high Hill slope values (1.45 and 2.21 respectively).

Considering the IC_{50} values, the order of potency of pyridyl derivatives of cyclopentanone was identified as *para* > *meta* > *ortho* > non-nitrogen whilst the pyridyl derivatives of cyclohexanone can be classified as *para* > *meta* > non-nitrogen.

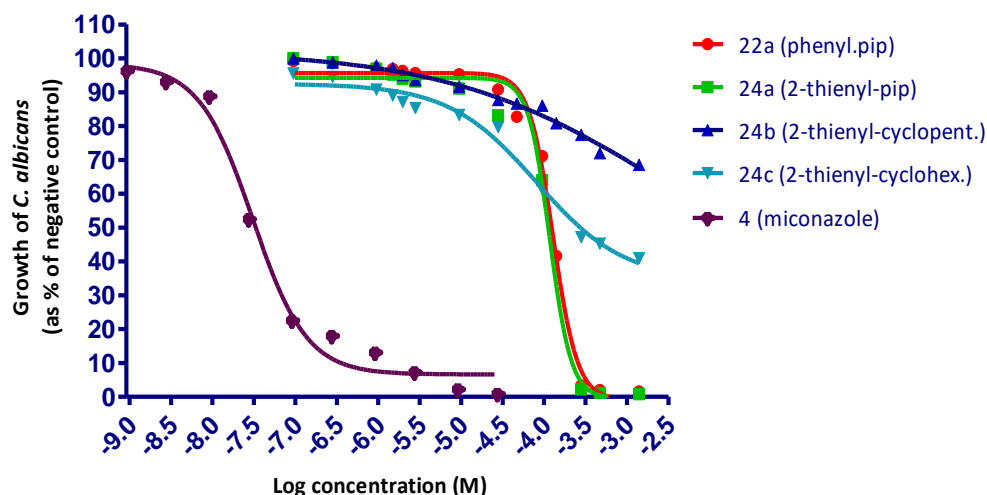


Figure 3. 16. Dose-response curves of the bis-benzylidene and bis-thienylidene derivatives of N-methylpiperidin-4-one and cycloalkanones against *C. albicans* after 24 hours.

The inhibitory activity was determined by comparing the growth of *C. albicans* with and without the test compound as the percentage of negative control (DMSO 1.5%). Positive control: miconazole. The dose-response curve was fitted using a five-parameter logistic model (GraphPad, Prism 5). Data were presented as the mean of two individual growth experiments, each performed in duplicate. SD values were omitted for clarity of graphs.

The dose-response curves of the bis-benzylidene and bis-thienylidene derivatives of N-methylpiperidin-4-one, cyclopentanone and cyclohexanone along with the reference control miconazole are shown in Figure 3.16. Compounds **22a** and **24a** both exhibited good inhibitory activity against *C. albicans*, with IC_{50} values of 128 and 138 μ M and AUCs of 298 and 288.5 respectively. Both of these compounds showed steep dose-response curves and therefore their Hill slopes were high (2.13 and 2.22) thus possibly showing aggregation. Compounds **22a** and **24a** both contain a central piperidine ring therefore giving an increase in their solubility compared to central cyclohexyl or cyclopentyl ring. Also the presence of N-methyl in the central ring may lead to the formation of a hydrogen bond using the nitrogen lone pair.

Compound **24c** showed moderate activity with an IC_{50} of 334 μ M and AUC of 312. The shallow curve of **24c** thus gave a low Hill slope value (0.40). In contrast, 2,5-bis[(*E*)-(2-thienylidene)cyclopentanone (**24b**) displayed poor activity against *C. albicans* and was capable of inhibiting only a maximum 31% of growth. IC_{25} value of **24b** was calculated as being 437.9 μ M. Although **24a**, **24b** and **24c** all contain the thiophene rings, the only difference between them is the structure of the central ring; **24a** has a piperidine ring **24b** has a cyclopentyl ring and **24c** has a cyclohexyl ring. As mentioned previously that cyclohexyl or piperidine rings can adopt more chair like conformation which facilitates the increase reactivity of molecule to the target enzyme whereas cyclopentyl ring are flatter and can't form chair conformation. Thus **24b** depicted lower activity than **24a** and **24c**.

The antifungal activity of thirty-three symmetrical 1,4-diene-3-ones against *C. albicans* is presented in **Table 3.2**, page 119. The inhibitory activity values were expressed in terms of their Hill slope, AUC, IC_{10} , IC_{25} , IC_{50} and IC_{90} . The most potent compound identified from the library of 1,4-diene-3-ones was bis-(pyridin-4-ylmethylene)cyclohexan-1-one (**23h**), based on its AUC (261 arbitrary unit), IC_{10} , IC_{25} , IC_{50} and IC_{90} (10.4, 32.9, 50.7 and 138 μ M) values against *C. albicans*. In addition, both bis-(pyridin-4-ylmethylene)cyclopentan-1-one (**23f**) and bis-(pyridin-3-ylmethylene)cyclohexan-1-one (**23g**) displayed good potency with low IC_{50} values, this being 68.5 and 57.6 μ M. However, the Hill slopes of **23f-h** were relatively high which suggests promiscuous aggregation at higher concentrations. Compounds **23a**, **23b** and **23c** exhibited moderate activity against *C. albicans*. High Hill slope of compounds **23a**, **23b** and **23c** were due to steep curves and this may give rise to aggregation artefacts.

Compounds which demonstrated >90% inhibitory action were determined to be **22a**, **22f**, **23a-c**, **23f-h** and **24a**. Most of the other compounds from the library of 1,4-diene-3-ones did

not achieve 90% growth inhibition of *C. albicans*. Compounds **22a** and **22f** both gave moderate inhibitory activity against *C. albicans* with IC₅₀ values of 128 and 114 μM. However, both **22a** and **22f** displayed high Hill slopes these being 2.13 and 1.21 respectively. Compound **22f** being potent may be due to the presence of weak EWG (-Cl) at the *meta*-position of the aromatic ring which makes the β-carbon slightly more electrophilic so that nucleophiles (such as the cysteine -SH) can easily attack and form a C-S bond potentially inhibiting the H⁺-ATPase. However the *meta*-position for substitution would not give rise to a resonance structure facilitating enhanced electrophilicity at the β-carbon so any effect would be due to the aggregate change in electron withdrawing power of the *meta*-chloro benzene ring. However, good potency of compounds **22a** could possibly be due to aggregation of the molecule as suggested by the high Hill slope (2.13).

Certain compounds from the library did not reach 50% inhibition of the growth of *C. albicans*, these being **22h**, **22i**, **22j**, **22k**, **22l** and **24b**. Out of these compounds, **22j** and **22k** did not even reach 25% inhibition. All the synthesized 1,4-diene-3-ones exhibited wide range of AUC (261 to 388 arbitrary units) between the concentrations of 0.1 and 1400 μM but miconazole gave an AUC of only 25.3 arbitrary unit. This shows that miconazole is a very potent inhibitor of *C. albicans* growth compared to all tested 1,4-diene-3-ones.

Table 3. 2. The antifungal activity of various 1,4-diene-3-ones against *C. albicans*.

Compound	IC ₁₀ ± SD (µM)	IC ₂₅ ± SD (µM)	IC ₅₀ ± SD (µM)	Asymptotic I ₅₀ ± SD (µM)	IC ₉₀ ± SD (µM)	Hill slope ± SD	AUC ± SD
22a	41.1 ± 9.14	85.4 ± 27.3	128 ± 28.3	125 ± 37.2	272 ± 4.24	2.13 ± 0.31	294 ± 16.26
22b	15.78 ± 12.5	112 ± 36.0	532 ± 43.1	630 ± 453	N/R	0.70 ± 0.02	341 ± 9.55
22c	9.96 ± 6.83	104 ± 52.1	313 ± 25.5	696 ± 590	N/R	1.27 ± 0.99	329 ± 1.98
22d	24.2 ± 6.61	161 ± 13.1	1112 ± 126.4	375 ± 55.2	N/R	0.60 ± 0.24	356 ± 0.78
22e	14.9 ± 1.92	192 ± 67.4	1148 ± 241	567 ± 208	N/R	0.68 ± 0.36	353 ± 1.84
22f	22.1 ± 27.5	71.0 ± 22.7	114 ± 9.35	119 ± 10.7	677 ± 21.9	1.21 ± 0.21	288 ± 1.77
22g	5.57 ± 4.07	37.7 ± 20.9	309 ± 99.8	133 ± 57.5	N/R	0.57 ± 0.09	316 ± 7.00
22h	15.1 ± 5.05	407 ± 96.3	N/R	233 ± 290	N/R	0.20 ± 0.03	368 ± 3.61
22i	73.8 ± 42.7	861 ± 14.0	N/R	636 ± 261	N/R	0.53 ± 0.37	385 ± 4.88
22j	16.3 ± 10.9	N/R	N/R	49.5 ± 4.45	N/R	0.84 ± 0.61	383 ± 0.71
22k	45.4 ± 11.7	N/R	N/R	49.6 ± 27.5	N/R	0.29 ± 0.37	387 ± 1.41
22l	152 ± 173.6	3094 ± 825	N/R	2099 ± 2927	N/R	0.62 ± 0.31	389 ± 10.5
22m	6.55 ± 0.74	59.6 ± 2.91	525 ± 33.9	3816 ± 1752	N/R	0.39 ± 0.00	335 ± 1.98
22n	6.18 ± 1.98	49.9 ± 24.9	474 ± 7.78	149 ± 130	N/R	0.63 ± 0.21	327 ± 3.96
22o	10.5 ± 12.8	59.6 ± 63.8	549 ± 115	229 ± 290	N/R	0.60 ± 0.28	329 ± 20.9
22p	1.86 ± 0.12	20.0 ± 6.41	409 ± 10.6	62.0 ± 60.8	N/R	0.46 ± 0.10	314 ± 0.99
22q	2.87 ± 1.97	26.4 ± 12.8	454 ± 66.3	476 ± 88.4	N/R	0.25 ± 0.18	321 ± 11.2
22r	1.03 ± 0.36	11.15 ± 1.63	243 ± 11.9	386 ± 174	N/R	0.26 ± 0.02	302 ± 5.59
22s	1.14 ± 1.21	29.9 ± 25.3	666 ± 70.7	682 ± 89.8	N/R	0.33 ± 0.08	316 ± 10.4
22t	1.88 ± 0.09	59.4 ± 14.7	354 ± 361	361 ± 62.2	N/R	0.50 ± 0.11	319 ± 11.4
22u	51.4 ± 5.01	320 ± 15.6	1604 ± 78	3336 ± 2062	N/R	0.55 ± 0.03	372 ± 1.27
22v	5.65 ± 2.74	36.9 ± 12.4	263 ± 17.1	256 ± 88.8	N/R	0.67 ± 0.04	327 ± 3.18
23a	257 ± 25.5	305 ± 59.2	367 ± 82.0	323 ± 18.4	820 ± 287.1	3.27 ± 0.04	329 ± 34.4
23b	58.4 ± 78.6	158 ± 166.60	238 ± 177	928 ± 884	533 ± 202.9	1.36 ± 9.05	320 ± 49.9
23c	76.8 ± 49.7	172 ± 3.25	249 ± 20.5	256 ± 29.7	557 ± 125.2	2.57 ± 4.01	314 ± 27.7
23d	113 ± 69.9	524 ± 283	2196 ± 59.1	499 ± 453	N/R	0.99 ± 0.24	386 ± 15.4
23e	70.4 ± 41.9	356 ± 239	1493 ± 881	3371 ± 3150	N/R	0.90 ± 0.14	379 ± 22.8
23f	31.6 ± 1.03	46.3 ± 3.77	68.5 ± 3.27	70.7 ± 0.27	145 ± 19.1	2.33 ± 0.68	279 ± 4.45
23g	19.8 ± 5.11	34.1 ± 9.33	57.6 ± 5.78	66.7 ± 1.34	215 ± 67.9	1.45 ± 0.51	273 ± 13.4
23h	10.4 ± 1.19	32.9 ± 4.81	50.7 ± 3.50	56.0 ± 5.11	138 ± 9.19	2.21 ± 0.02	261 ± 0.42
24a	43.3 ± 24.0	100 ± 82.6	138 ± 24.0	117 ± 4.95	276 ± 66.5	2.22 ± 0.28	288 ± 9.76
24b	18.3 ± 12.1	438 ± 140.1	N/R	425 ± 289	N/R	0.36 ± 0.29	369 ± 3.46
24c	1.66 ± 1.37	33.6 ± 3.83	334 ± 65.1	356 ± 64.4	N/R	0.40 ± 0.06	312 ± 12.2
4	0.01 ± 0.01	0.01 ± 0.00	0.04 ± 0.02	0.03 ± 0.02	0.86 ± 1.08	0.95 ± 0.17	25.3 ± 9.64

Note: N/R = Compounds not reached specified level of inhibition (10%, 25%, 50% or 90%). Data were presented as the mean ± SD of two individual experiment conducted in duplicates, n=4.

3.4 Discussion of macro-broth susceptibility assay

The goal of the macro-broth susceptibility assay was to investigate the potential antifungal activity of 1,4-diene-3-one compounds (**22a-v**, **23a-h** and **24a-c**) against *S. cerevisiae* and *C. albicans*. Time based endpoint tests to identify the inhibitory potency of 1,4-diene-3-ones can sometimes give arbitrary results due to partial inhibition of fungal growth over the range of concentrations. For example, in the current set of experiments, some compounds showed an increase in inhibitory activity with a gradual increase in concentration represented by a shallow curve whereas some compounds showed a sudden rise in inhibitory activity with a steep curve at higher concentrations. Such results, associated with high Hill factors may be due to the concentration at which molecular aggregation becomes significant.

The dose-response curves of 1,4-diene-3-ones varied extensively making it very easy to rank them into activity order over the range of concentrations. However the shape of the dose-response curve varies significantly. Therefore, it is necessary to include and compare various inhibitory parameters. Hence the AUC, Hill coefficient, IC_{10} , IC_{25} , IC_{50} , asymptotic I_{50} and IC_{90} values were calculated and analysed. These values were presented in Table 3.1 and 3.2. The potency of the various compounds relates to the AUC enclosed within the rectangular portion between two concentrations (Odds & Abbott, 1984). The Hill slope is the reflection of the steepness of the curve. Differences in the Hill slope reflects potential interactions such as inhibitor aggregation or changes in cell structure or morphology (Rautenbach *et al.*, 2006).

3.4.1 Discussion of susceptibility assay of *S. cerevisiae*

A library of 1,4-diene-3-ones demonstrated significant level of growth inhibition of *S. cerevisiae* (0.2 - 99% inhibition) over the concentration range between 0.10 to 3000 μ M. In terms of the IC_{50} , certain compounds (**22c**, **22e**, **22f**, **22g**, **22m**, **22n**, **22o**, **22r**, **22s**, **22t**, **23b**,

23c and **23e-h**) displayed good potency against *S. cerevisiae* and their IC₅₀ values were between 0.62 and 9.45 μM. While some compounds (**22a**, **22b**, **22d**, **22p**, **22q**, **23a** and **23d**) were considered to be moderate inhibitors based on their IC₅₀ values ranged between 10 and 100 μM. In contrast, compounds with IC₅₀ values >100 μM were classified as moderate to poor inhibitor of *S. cerevisiae* and these being compounds **22h-l**, **22u-v** and **24a-c**.

The compound which exhibited the highest ability to inhibit the growth of *S. cerevisiae* was 3,5-bis(4-trifluoromethylbenzylidene)-1-methylpiperidin-4-one (**22n**) having the lowest IC₁₀, IC₂₅, IC₅₀ values as shown in **Table 3.1**, page 105. Additionally, 3,5-bis(3-chlorobenzylidene)-1-methylpiperidin-4-one (**22f**), 3,5-bis(3-nitrobenzylidene)-1-methylpiperidin-4-one (**22s**) and 3,5-bis(3-trifluoromethylbenzylidene)-1-methylpiperidin-4-one (**22m**) have been identified as the second, third and fourth most potent inhibitors of *S. cerevisiae* growth based on their low AUC (97.4, 125 and 138) and IC₅₀ (1.21, 1.87 and 2.22 μM) values.

Although compound **22n** depicted higher degree of potency (IC₅₀ = 0.62 μM) and inhibited the growth of *S. cerevisiae*, it was 5-fold less potent than the clinically used miconazole nitrate (IC₅₀ = 0.12 μM). Interestingly in this study, the IC₅₀ of miconazole was 0.12 μM whereas in literature it was reported 3 μM (Ottillie *et al.*, 2018), suggesting 25-fold difference between the two sets of experiments. The reason for this difference in susceptibility is not clear. Although variations between methodologies for determining antimicrobial potency are uncommon. The susceptibilities of microbes to anti-microbial agents is known to vary with the growth medium used for their assay (Ottillie *et al.*, 2018) who performed their assay using YPD medium. They incubated *S. cerevisiae* at 30 °C until mid-log phase (absorbance at 600 nm; 0.1 and 0.5), then the diluted cell suspension (absorbance at 600 nm; 0.01) and incubated with miconazole into a 96-well plate at 30 °C for 18 hours, followed by the absorbance

measurement. Thus this variation may also be due to the different growth procedure (i.e. Bijou in this study vs microtitre plate in the literature).

The high activity of **22n** is possibly suggesting the importance of the strong electron-withdrawing group (EWG), trifluoromethyl attached at the *para*-position on the aromatic ring of this compound. Strong EWGs facilitate other atoms becoming more electrophilic in nature whereas strong electron-donating groups (EDG) facilitate other atoms becoming more nucleophilic in nature (Sivakumar, Muthu Kumar, & Doble, 2009). The presence of EWG (such as CF₃, NO₂, CCl₃, halides) on the aromatic ring will increase the electrophilicity of the β -carbon of the 1,4-diene-3-ones, a representative example of compound **22n** shown in Figure 3.17.

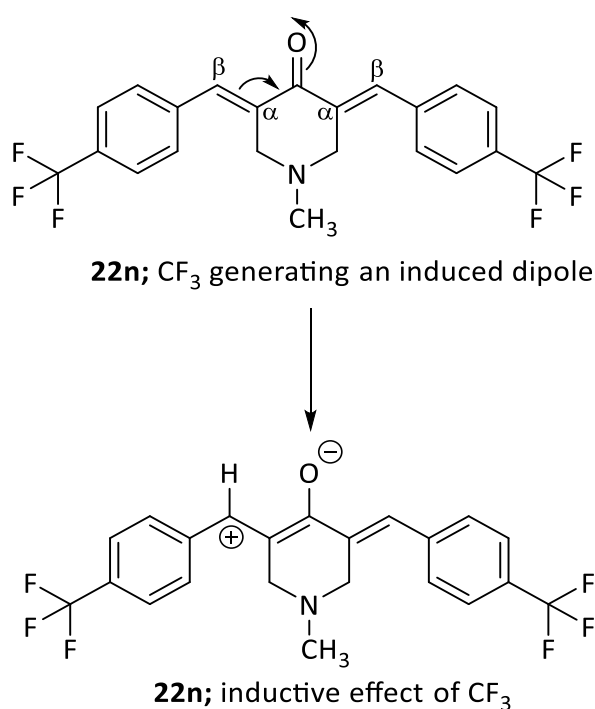


Figure 3. 17. A representative example of a compound which shows an increase in the electrophilicity of β -carbon of the bis-benzylidene derivative of N-methylpiperidin-4-one.

This suggests a possible mechanism of action, that the nucleophilic sulfhydryl (-SH) of a cysteine present in the fungal PM H⁺-ATPase could attack one of the electrophilic β -carbons present in the 1,4-diene-3-ones via a Michael addition reaction (Dao *et al.*, 2016). The

presence of EDG (-H, -CH₃, OCH₃, -OH) on the aromatic rings will cause the β -carbons of dienone to become less electrophilic due to a higher electron density on the β -carbons, hence this would possibly result in a decrease in the reactivity of the compounds if it follows the above mention mechanism (Sivakumar *et al.*, 2009).

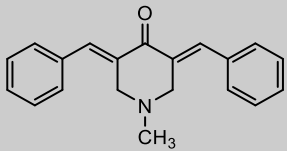
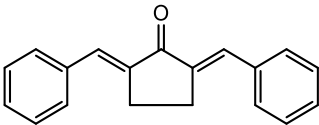
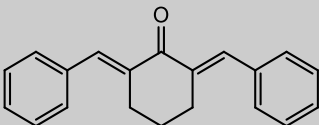
The second most potent inhibitor of *S. cerevisiae* growth was identified to be compound **22f** (IC₅₀ = 1.21 μ M), which contain chloro-group at the *meta*-position on the aromatic rings. Likewise, the *ortho*-chloro substituted (**22e**) and *para*-chloro substituted (**22g**) bis-benzylidene-piperidin-4-one also exhibited good potency with low IC₅₀ values (3.90 and 5.56 μ M). However, compounds containing two chlorine atoms on the aromatic rings (**22h**; 2,4-dichloro and **22i**; 3,4-di-chloro) gave moderate inhibitory activity against *S. cerevisiae* with IC₅₀ values of 153.6 and 153.9 μ M (Figure 3.7b). This suggests that presence of di-chloro groups (**22h** and **22i**) on the aromatic ring gives about 30-fold decrease in the activity compared to **22e**, **22f** and **22g**. It is more likely that the presence of two chlorine atoms increases the volume of the molecule sufficiently that although it is able to react, the molecule has less accessibility to the binding site (chlorine being quite large and there being four of them). In addition due to the di-chloro substitution there has been an increase in the molecular weight, clogP values, larger volume and increased surface area of the molecule than when a single chlorine atom is present on the aromatic rings. Compounds **22h** and **22i** both have the same clogP values (6.51), which is slightly greater than clogP values of **22e**, **22f** and **22g** (5.25, 5.33 and 5.25 respectively). In addition **22h** and **22i** have higher molecular mass (427.2 g/mole) than **22e**, **22f** and **22g** (358.3 g/mole). Hence **22h** and **22i** exhibited less potency than **22e**, **22f** and **22g**.

On the other hand, both compounds **(24c)** and **(22l)**; 2,6-bis(thiophen-2ylmethylene)cyclohexan-1-one and 3,5-bis(4-methylbenzylidene)-1-methylpiperidin-4-one failed to reach an IC₅₀ value in the assay, possibly due to self-aggregation of the compounds (Giannetti *et al.*, 2008). Giannetti *et al.*, (2008) have mentioned that promiscuously binding compounds often form soluble or colloidal aggregates in solution. These aggregates can bind to proteins with high affinity and preventing the substrate accessing and thus binding to the target protein hence inhibiting the protein function.

From the dose-response curves of bis-benzylidene derivative of N-methylpiperidin-4-one **(22a)**, bis-pyridylidene derivatives of cyclopentanone **(22u)** or cyclohexanone **(22v)**, it was identified that **22a** was a more potent inhibitor than **22u** or **22v**. The IC₅₀ values of **22a**, **22u** and **22v** were 40.7, 1290 and 309 μM whereas their AUCs were 248, 320 and 313 respectively thus although the difference in the AUC are smaller than the differences between the IC₅₀ values the order was the same (**Table 3.3**, page 125). Thus in both measurements, compound **22a** displayed a higher degree of potency while **22v** showed intermediate activity and **22u** being the least active inhibitor of *S. cerevisiae* growth. As with the inhibitory effects of **22a** and **22v**, the high Hill slopes may indicate promiscuous aggregation of the molecule which may also contribute to the enhanced inhibitory activity commonly associated with such aggregations (Giannetti *et al.*, 2008; Baell & Holloway, 2010; Ingólfsson *et al.*, 2014).

The difference in the activity of these compounds is related to the central ring structure. Compound **22a** has a piperidone ring whereas **22u** has a cyclopentyl ring and **22v** has a cyclohexyl ring. Consequently they have different clogP values, these being 4.07, 4.77 and 5.33 respectively. The lower clogP of **22a** indicated a slightly better aqueous solubility and it is this which is believed to give contribute to the higher potency.

Table 3. 3. Ranking of bis-benzylidene derivatives of N-methylpiperidin-4-one, cyclopentanone and cyclohexanone based on their inhibitory activity against *S. cerevisiae*.

Compounds	Compound structures	IC ₅₀ ± SD (μM)	AUC ± SD	ClogP
22a		40.7 ± 0.94	248 ± 1.67	4.07
22u		1290 ± 89.0	321 ± 12.3	4.77
22v		309 ± 48.5	314 ± 5.51	5.33

Therefore the potency order of the central ring of the bis-benzylidene derivatives can be classified as N-methylpiperidin-4-one >cyclohexanone >cyclopentanone. When IC₅₀ and AUC of **22a**, **22u** and **22v** were compared with *C. albicans*, the rank order remains the same although specific values were different. Compounds **22a**, **22u** and **22v** gave IC₅₀ of 128, 1604 and 263 μM against *C. albicans* whereas their AUCs were determined to be 294, 372 and 327, respectively (**Table 3.2**, page 119). Thus these compounds have same activity order against both *S. cerevisiae* and *C. albicans*.

In addition to comparing the isosteric nitrogen-atom replacements in the aromatic ring of bis-pyridylidene derivatives of N-methylpiperidin-4-one, cyclopentanone or cyclohexanone with the parent compound having an unsubstituted phenyl ring, it was identified that *meta*-N >*para*-N >*ortho*-N >phenyl ring for compounds with a central cyclohexyl ring and a piperidone ring however compounds with a cyclopentyl ring showed potency order of *para*-N >*meta*-N >*ortho*-N >phenyl ring. The six-membered ring structures of cyclohexyl and piperidine rings adapt a near chair conformation and larger bond angle whilst cyclopentyl ring is slightly flatter and has smaller bond angles in the ring. Therefore, it is possible that the chair conformation

might show an increase in the electrophilicity of the β -carbon and makes these compounds more reactive to the target site.

The IC_{50} values of bis-pyridylidene derivative of compounds; **22a**, **23a**, **23b**, **23c**, **23d**, **23e**, **23f**, **23g** and **23h** were 40.7, 12.6, 8.84, 9.45, 20.3, 9.29, 8.46, 5.52 and 6.25 μ M whereas their AUCs were 248, 207, 194, 194, 231, 206, 193, 164 and 177 respectively. Again the rank order is maintained irrespective of the method used to determine the potency. The $clogP$ values of **22a**, **23a**, **23b**, **23c**, **23d**, **23e**, **23f**, **23g** and **23h** were 4.07, 1.53, 1.83, 1.61, 1.90, 1.91, 1.60, 2.34 and 1.60 respectively. Due to the presence of a nitrogen atom in the aromatic ring of compounds **23a-h** their $clogP$ values were significantly lower than **22a**. However, the difference between the $clogP$ of **23a-h** is due to resonance effects. The lower degree of inhibitory action of compounds **22a**, **22u** and **22v** than **23a-h** is highly suggestive that the potency of these compounds is partly associated with their increased solubility. The N-analogue of benzene (pyridine) is miscible with water whereas benzene is immiscible (Zafar *et al.*, 2018). Because the pyridyl ring is amphipathic, the presence of the two-pyridine rings should increase both the solubility and permeability across membranes. This suggests that the introduction of a nitrogen atom on the aromatic ring has shown an increase in the solubility, and probably the permeability of compounds (**23a-h**) across the yeast (*S. cerevisiae*) plasma membrane.

Most of the compounds from the library of 1,4-diene-3-ones exhibited Hill slopes <1 , with the exception of certain compounds (**22c**, **22f**, **23a**, **23e** and **23f**) being between 1 and 2, and compounds **22a**, **22s**, **22t**, **22v**, **23b**, **23c**, **23g**, **23h**, **24b** and **24c** having Hill slopes >2 . The highest Hill slope (2.97) was observed for (2*E*,6*E*)-2,6-bis(pyridine-4-ylmethylene)cyclohexan-1-one (**23h**). Compounds with a Hill slope <2 reflects that they are active even at low

concentrations. In contrast, compounds with Hill slope >2 represents their activity is dependent on higher concentrations (Rautenbach *et al.*, 2006). Interpretation of Hill coefficients is complex, Rautenbach *et al.*, (2006) mentioned that self-association of peptide inhibitors may result in a lower than expected levels of inhibition. However other authors (Baell & Holloway, 2010; McGovern, Caselli, Grigorieff, & Shoichet, 2002; Pouliot & Jeanmart, 2016; Seidler *et al.*, 2003) argues that self-association/aggregation may lead to non-competitive inhibition and higher than expected inhibition. Thus the situation regarding the Hill slope is both complex and confusing and incompletely understood.

3.4.2 Discussion of susceptibility assay of *C. albicans*

Compounds **22a-v**, **23a-h** and **24a-c** have shown wide range of inhibition against *C. albicans* (0 - 99% inhibition) over the concentration range 0.1 to 1400 μM . Most of the test compounds from the library did not cause 90% inhibition of growth of *C. albicans*, except compounds **22a**, **22f**, **23a-c**, **23f-h** and **24a**. Compound **23h** (*2E,6E*)-2,6-bis(pyridine-4-ylmethylene)cyclohexan-1-one has been identified as the most potent inhibitor of *C. albicans* based on the lower IC_{10} , IC_{25} , IC_{50} , IC_{90} and AUC values (**Table 3.2**, page 119). Compounds **23f** and **23g** have also shown good inhibitory activity against *C. albicans* with their low AUC (279 and 273) and IC_{50} (68.5 and 57.6 μM) values.

The least active compounds against *C. albicans* were determined to be **22j**, **22k** and **22l**, which exhibited a maximum of 16% inhibition of *C. albicans* growth at the highest concentration tested (1400 μM). Sivakumar *et al.*, (2009) have mentioned in their QSAR studies on chalcones that usually the EWG at *ortho*, *meta* or *para*-position shows an increase in the electrophilicity of the β -carbon however, in this our research work, compounds **22j** and **22k** which contains COOH group at either *ortho* or *para*-position showed decrease in their activity. This could

possibly due to the presence of carboxylic acid groups either interacting with other target enzymes or there being a negative charge able to interact with the carboxyl group close to the potential drug-binding site on the target enzyme, which could thus act in a repulsive manner (Das *et al.*, 2008). Compound **22i** contains an EDG (CH₃) at the *para*-position of the aromatic ring, which makes the compound less electrophilic so that the nucleophiles (-SH) can attack at the β -carbon but the rate of reaction will be slower due to the EDG (Sivakumar *et al.*, 2009). Compound **22i** has shown a similar effect against *S. cerevisiae* in this study.

Compounds **22e**, **22f** and **22g** (containing mono-chloro group) exhibited some activity against *C. albicans* with IC₅₀ of 1148, 114 and 309 μ M. In addition, **22f** exhibited higher potency than **22e**, **22g**, **22h** and **22i** in *S. cerevisiae* study. However compounds **22h** and **22i** showed poor activity, which is possibly due to the presence of two halo atoms (e.g. dichloro) as EWGs on the aromatic ring of benzylidene derivatives of N-methylpiperidin-4-one. Halogens (F, Cl, Br and I) vary in their electronegativity from 9 to 53 (arbitrary units), which cause the withdrawal of electrons from the benzene rings causing ring deactivation. In addition, clogP for both **22h** and **22i** is 6.51 which makes these compounds very lipophilic. As mentioned previously in the *S. cerevisiae* study (in **section 3.4.1**, page 123) that due to the high molecular weight, large size and surface area of the molecule these compounds (**22h** and **22i**) have less accessibility to the binding site of the target enzyme.

From the dose-response curves it was identified that bis-benzylidene derivative of N-methylpiperidin-4-one (**22a**) was more potent inhibitor of *C. albicans* growth than bis-pyridylidene derivatives of cyclopentanone (**22u**) or cyclohexanone (**22v**). The IC₅₀ values of **22a**, **22u** and **22v** were 128, 1604 and 263 μ M whereas their AUCs were 294, 372 and 327 respectively (**Table 3.2**, page 119). Again, the rank order is independent of the method of

analysis for both *S. cerevisiae* and *C. albicans* study. Compound **22a** is capable of forming a hydrogen bond between the N-me lone pair of a piperidine ring and a hydrogen atom of the target enzyme whereas a cyclopentyl group of **22u** or a cyclohexyl group of **22v** cannot form such an interaction. As previously mentioned in the *S. cerevisiae* study, piperidine and cyclohexyl rings would adopt a near chair conformation, which facilitate the reactivity of molecule towards the target enzyme whilst the cyclopentyl ring is slightly flatter which facilitate sp² delocalisation of the ring. Additionally, the N-methyl being both fairly polar and basic should increase the solubility possibly due to nitrogen forming a hydrogen bond using its lone pair of electrons.

As mentioned earlier that the nitrogen-containing aromatic rings increases compound solubility when compared to their phenyl analogs. Therefore the potencies of bis-pyridylidene derivatives (**23a-h**) were compared to each other based on their IC₅₀ and AUCs. Although **23d**, **23e** and **23f** were similar in structures the difference in the position of nitrogen atom in the aromatic ring will cause variability in activity and this ultimately depends on the interaction of the nitrogen atom with the target protein(s). It was identified that the bis-pyridylidene derivatives of cyclohexanones were more potent than bis-pyridylidene derivatives of cyclopentanone or N-methylpiperidin-4-one. The reason for better potency of compounds (**23g-h**) with a central cyclohexyl ring is possibly due to the steep curve and associated high Hill slopes, which suggests, and is consistent with, the increase in inhibition being due to promiscuous aggregation.

When comparing the inhibitory activities of **23a-h** between *C. albicans* and *S. cerevisiae* study, it has been identified that these compounds exhibited a higher level of potency against *S. cerevisiae* than *C. albicans*. This is probably due to differences in the genetic and

morphological profiles of *S. cerevisiae* compared to *C. albicans*. Dimorphic nature of *C. albicans* can change its structure from mycelium to hyphae growth and might form a biofilm. On the other hand *S. cerevisiae* can change its ploidy state from haploid to diploid and vice versa whereas *C. albicans* is obligate diploid.

Moreover, all of the synthesized compounds (**22a-v**, **23a-h** and **24a-c**) demonstrated their inhibitory activities were significantly less potent than miconazole nitrate ($IC_{50} = 0.04 \mu\text{M}$) against *C. albicans* and in literature, Isham & Ghannoum, (2010) have reported the IC_{50} of miconazole was $0.016 \mu\text{g/ml}$ which is equivalent to $0.04 \mu\text{M}$.

3.5 Conclusions

From the library of 1,4-diene-3-ones, the four most potent compounds capable of inhibiting the growth of *S. cerevisiae* were the 4-trifluoromethyl (**22n**, $IC_{50} = 0.62 \mu\text{M}$), 3-chloro (**22f**, $IC_{50} = 1.21 \mu\text{M}$), 3-nitro (**22s**, $IC_{50} = 1.87 \mu\text{M}$) and 3-trifluoromethyl (**22m**, $IC_{50} = 2.22 \mu\text{M}$) substituted bis-benzylidene derivatives of N-methylpiperidin-4-one. All of these compounds contain an electron-withdrawing group present at either the *meta*- or *para*-position of the aromatic ring. The presence of EWGs will increase the electrophilicity of the β -carbon of these compounds. However, **22n** exhibited a 5-fold less potency than miconazole nitrate ($IC_{50} = 0.12 \mu\text{M}$), while **22f**, **22s** and **22m** exhibited 10 to 19-fold lower potency than miconazole nitrate against *S. cerevisiae*.

Overall, the bis-benzylidene and bis-pyridylidene derivatives of N-methylpiperidin-4-one, cyclopentanone and cyclohexanone exhibited good potency against *S. cerevisiae* with IC_{50} values between 0.62 to 23 μM . However, the thienyl derivatives of N-methylpiperidin-4-one, cyclopentanone or cyclohexanone (**24a**, **24b** and **24c**) were not effective inhibitors of *S. cerevisiae* growth.

In terms of the 1,4-diene-3-ones activity against *C. albicans*, the most potent compounds identified were 4-pyridylidene cyclohexanone (**23h**, $IC_{50} = 50.7 \mu\text{M}$), 3-pyridylidene cyclohexanone (**23g**, $IC_{50} = 57.6 \mu\text{M}$), 4-pyridylidene cyclopentanone (**23f**, $IC_{50} = 68.5 \mu\text{M}$) and 3,5-bis(3-chlorobenzylidene)-1-methylpiperidin-4-one (**22f**, $IC_{50} = 114 \mu\text{M}$). Compounds **23f**, **23g** and **23h** depicted 8, 10 and 8-fold more potent against *S. cerevisiae* than *C. albicans*, whereas **22f** exhibited 94-fold higher potency against *S. cerevisiae* than *C. albicans*. However, all of these compounds were significantly less potent than the clinically used drug miconazole nitrate ($IC_{50} = 0.04 \mu\text{M}$) against *C. albicans*.

The thienyl derivatives of N-methylpiperidin-4-one, cyclopentanone or cyclohexanone (**24a**, **24b** and **24c**) gave low to poor inhibitory activity against *C. albicans*. Moreover, compounds **22j** and **22k** (carboxylic acid substituted bis-benzylidene derivatives of N-methylpiperidin-4-one) have been identified as the least active inhibitors of *C. albicans* growth.

CHAPTER FOUR

PROTON EXTRUSION ASSAY

4 Proton extrusion assay

4.1 Introduction

The plasma membrane (PM) H⁺-ATPase is an essential enzyme for the growth of fungi (Portillo, 2000; Kjellerup *et al.*, 2017). The presence of an electrogenic proton pump (H⁺-ATPase) in fungal and plant plasma membranes had been hypothesized based on the measurements of the membrane potentials using a micro pH electrode (Serrano, 1980 & 1983; Perlin, Brown, & Habern, 1988; Ben-Josef, Manavathu, Platt, & Sobel, 2000). According to Petrov & Slayman, (1995), the PM H⁺-ATPase of fungi contains three cysteine residues in the transmembrane segment and six cysteine residues in the cytoplasmic domains. The PM H⁺-ATPase pumps protons from the cytosol to the exterior of the cell by hydrolysing ATP. This results in an increase in the cytoplasmic pH (pH_i) causing alkalization of the cytoplasm which results in stimulation of cell growth (Serrano, 1993). The proton (H⁺) gradient generated by the PM H⁺-ATPase facilitates secondary uptake of nutrients into cells (Portillo, 2000).

Given both the essential and unique nature of the H⁺-ATPase, this enzyme represents a potential novel antifungal target for novel classes of the therapeutic agent (Monk & Perlin, 1994; Monk *et al.*, 1995). It has been reported that NEM, a sulfhydryl reactant binds to cysteine-532 in the cytoplasmic region causing inhibition of the PM H⁺-ATPase as shown in Figure 1.14 (Petrov & Slayman, 1995). An interesting study conducted by Portillo & Gancedo, (1984) demonstrated that miconazole inhibits the mitochondrial (F_oF₁) ATPase of *S. cerevisiae*. They demonstrated that miconazole inhibits ATP synthesis without affecting the oxidation of NADH. This suggests that miconazole may have some membrane disrupting or uncoupling activity as well as inhibiting F_oF₁-ATP(synth)ase activity. Miconazole blocks ATP synthesis via mitochondrial oxidative phosphorylation, which could result in a decrease of proton pumping

from the *S. cerevisiae* cell due to cytoplasmic depletion of substrate ATP concentration (Portillo & Gancedo, 1984). Other H⁺-ATPase inhibitors which have been shown to inhibit the P-type H⁺-ATPase include dicyclohexyl carbodiimide, omeprazole, ebselen and diethylstilbestrol (Serrano, 1980).

It has also been reported that curcumin (**11**) a natural product which contains α,β -unsaturated enone structures, inhibited the Ca²⁺-ATPase of skeletal muscle sarcoplasmic reticulum (Logan-Smith *et al.*, 2001). The logP of curcumin is 2.92, which is within the limit set by Lipinski, Lombardo, Dominy, & Feeney, (1997) and the logP of the molecule should be <5 for drug-likeness. However curcumin has some drawback like low solubility and rapid metabolism (Sharma, Manoharlal, Puri and Prasad, 2010). Curcumin is also not considered as a potential drug candidate due to its poor bioavailability as mentioned in the chapter 1. However due to some structural similarities of curcumin to 1,4-diene-3-ones it was considered worthwhile to investigate the ability of curcuminoids to inhibit proton pumping by *S. cerevisiae*.

Having synthesized various 1,4-diene-3-ones (detailed in Chapter-2) and identified their antifungal activity (described in Chapter-3) there is a need to identify the possible mechanism(s) of action of these compounds. Therefore, a library of 1,4-diene-3-ones (**22a-v**, **23a-h** and **24a-c**) have been screened against *S. cerevisiae* with the aim of determining if they inhibit proton pumping. Compounds containing the 1,4-diene-3-one pharmacophore have the potential to react with cysteine(s) found in transmembrane loops M₁ and M₂ (Monk *et al.*, 1995) and/or the cysteine residue found in the nucleotide binding site of the H⁺-ATPase (Brooker & Slayman, 1982; Katz & Sussman, 1987). The β -carbon of the 1,4-diene-3-one is electrophilic in nature which can be attacked by the nucleophilic sulfhydryl-containing amino

acid, cysteine, located in the membrane segment of the ATPase (Manavathu *et al.*, 1999). This approach has been used by other workers in studying proton transport across the plasma membrane of *S. cerevisiae* (Dao *et al.*, 2016; Kjellerup *et al.*, 2017; Tung *et al.*, (2017).

Glucose-induced medium acidification allows comparison of H⁺ pumping by the H⁺-ATPase of *S. cerevisiae* under different conditions (Perlin, Brown & Habern, 1988). The acidification of the medium was studied by measuring the pH of the external medium of carbon-starved *S. cerevisiae* by activating the H⁺ pump with glucose (Manavathu *et al.*, 1999; Ben-Josef *et al.*, 2000). Glucose induces a high rate of H⁺ efflux from yeast cells, about 20 nmol H⁺/min/mg fresh weight. The first few minutes of acidification are almost solely due to the activity of the plasma membrane ATPase and not with other aspects of acid generating metabolism (Serrano, 1983). This H⁺ transport has been shown to be sensitive to arsenate which acts as a phosphate analogue and which depletes the cell of ATP. Brooker & Slayman, (1982) demonstrated that addition of glucose to carbon-starved yeast cells led to a five to ten-fold increase in ATPase activity within minutes. This activation is associated with a glucose activated protein kinase cascade which results in a several fold decrease in K_m for MgATP²⁻ and an alkaline shift in the pH optimum of the ATPase (Brooker & Slayman, 1982).

4.2 Materials and Methods

4.2.1 Materials, growth medium and growth condition for proton extrusion assay

YPD (bacteriological peptone 20%, yeast extract 10% and glucose 20%) broth (Sigma-Life Science, Y1375, Lot: SLBS2093V) was used to grow *S. cerevisiae* in the planktonic form. YPD powder (50 g) was dissolved in distilled water to a final volume of 1 litre. Aliquots of 100 ml of YPD broth was prepared into 250 ml conical flasks, autoclaved at 121 °C/15 psi for 15 minutes and subsequently stored at 4 °C until used. Potassium chloride powder (for molecular biology ≥ 99%, Sigma Life Science, P9541, Lot: BCBQ0895V) was prepared at 50 mM by dissolving in distilled water and autoclaved as mentioned earlier. D-glucose powder (Fisher Scientific UK Limited, G/0500/61, Lot: 1156267) was dissolved in sterile distilled water to prepare a 40 % solution which was filter sterilised using a 0.2-micron membrane filter. D-glucose solution was prepared fresh daily and stored at 4 °C until required.

A few colonies of *S. cerevisiae* from a working culture were inoculated into 100 ml YPD broth and the yeast was grown to late log phase at 30 °C, 120 rpm for 16 hours (Monk *et al.*, 1995). The late log phase cells were collected by centrifugation at 3500 x g for 10 minutes at 4 °C and washed with 100 ml each of sterile distilled water and 50 mM KCl. The pellet was re-suspended into 50 mM KCl (100 ml), followed by incubation at room temperature overnight (approximately 16 hours) by supplying filtered air (via a 0.2 µm filter) using an aquarium pump at a flow rate of 2 ml air pumped per minute to deplete the cells carbon reserves. Cell counts were performed to identify the number of viable cells present in the carbon starved cell suspension using methylene blue dye and a Naubauer haemocytometer (identical to the methodology described in **section 3.2.1.6**). The carbon-starved cells were harvested by

centrifugation at 3500 x g for 10 mins at 4 °C after which the pellet was re-suspended in 50 mM KCl to a final cell density of 1×10^8 cells/ml.

4.2.2 Stock solution of test compounds and controls

N-ethyl maleimide (NEM) powder (ThermoFisher Scientific, Pierce™, 23030) was used as a positive control inhibitor. In addition, miconazole nitrate powder (azole antifungal) and curcumin powder (Sigma-Aldrich, C1386) were tested to determine their effect on the proton pumping activity of *S. cerevisiae*. Stock solutions of NEM, miconazole and curcumin were prepared in DMSO (Hybri-Max; D2650) at 12.5 mM. Stock solutions were diluted with DMSO to obtain the standard concentrations of 3.13 mM, 6.25 mM and 10 mM, respectively. From the library of 1,4-diene-3-ones, compound **23b** was selected to test a range of concentrations because of its increased solubility and probable enhanced membrane permeability profile with optimal clogP value (1.827), and an IC₅₀ value (8.84 μM) against *S. cerevisiae*. A stock solution of compound **23b** (12.5 mM) was prepared in DMSO. The stock solution was serially diluted by 2 and 2x2-fold and 1.25fold to achieve 6.25, 3.13 and 10 mM. The 10 mM was subsequently diluted to achieve 5 and 2.5 mM. The test compounds were all freshly prepared on the day of the experiment.

Stock solutions of all the 1,4-diene-3-ones (**22a-v**, **23a-h** and **24a-c**) were prepared in DMSO at 12 mM followed by diluting 1:1 with DMSO to obtain a working stock concentration of 6 mM. For each experiment, 15 μl of appropriate concentration of 1,4-diene-3-one was added to cell suspension (1.5 ml) giving a final concentration of 60 μM. DMSO (15 μl) was used as a negative control (1%) when treating yeast cells with a solution of the test compounds. Similarly, NEM (15 μl, 60 μM) was used as a positive control.

Method optimisation was implemented using various concentrations of N-ethyl maleimide (31.3, 62.5, 100 and 125 μM) for various pre-incubation times. A carbon starved cell suspension (1.5 ml at a cell density of 1×10^8 cells/ml) of *S. cerevisiae* was loaded into a water-jacketed glass chamber maintained at 30 °C. Subsequently, 15 μl of the NEM solution was added and incubated at 30 °C with gentle stirring using a glass-covered metal flea (made in house from glass pipettes and metal wire from a paper clip) for various periods of time (10, 30, 45, 60, 75, 90 and 120 minutes). After appropriate preincubation with NEM, the H^+ pump was activated by adding D-glucose solution (150 μl , 4% final concentration) with continuous stirring. A micro pH electrode was immediately placed into the cell suspension and the pH of the external medium was monitored for 30 minutes with automated recording every 3 seconds.

Control experiments were performed using 1.5 ml of cell suspension and 15 μl of 50 mM KCl (no-drug) or 15 μl of DMSO (solvent control) to measure the effect of DMSO on the acidification of the external medium. The positive control was included to determine the extent if any of inter-day variability using NEM as an internal standard -SH reagent to inhibit the H^+ pumping by *S. cerevisiae*. NEM (62.5 μM) pre-incubated with carbon starved *S. cerevisiae* cells for 60 mins showed optimum response by inhibiting the H^+ pumping ability of *S. cerevisiae*.

The method was further optimised and validated using NEM (60 μM), where the cells were pre-incubated with NEM at 30 °C for 60 mins. The NEM validated method was applied to all further experiments using the 1,4-diene-3-one compound library. All compounds (**22a-v**, **23a-h** and **24a-c**) were tested at a single concentration of 60 μM . Each compound was tested independently at least three times to compare the time of day and inter-day variability.

4.3 Results of proton extrusion assay

4.3.1 Effect of N-ethyl maleimide on the proton pumping activity by *S. cerevisiae*

The carbon starved *S. cerevisiae* cells were tested for their ability to pump protons to the external medium in the presence of variable concentrations of NEM (31.3, 62.5, 100 and 125 μM). The ability of *S. cerevisiae* to extrude protons in the presence of NEM (**9a**) is shown in Figure 4.2 and is expressed as the pH of the external medium varying with time.

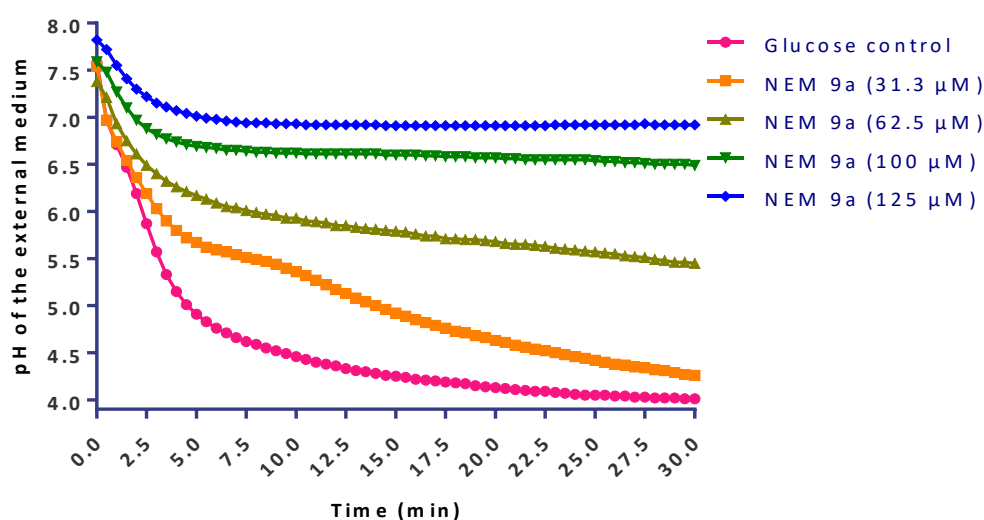


Figure 4. 2. Effect of N-ethyl maleimide on the H^+ pumping ability of *S. cerevisiae*.

Effect of N-ethyl maleimide on glucose-induced medium acidification of carbon starved *S. cerevisiae* cells. Each data point represents the mean of three individual experiments.

A decrease in the pH of the external medium of concentrated cell suspension was observed (Figure 4.2). N-ethyl maleimide inhibited proton pumping by *S. cerevisiae* in a concentration-dependent manner. NEM at 125 μM gave maximum response by inhibiting the initial rate of proton pumping compared to the glucose control. In addition, NEM at 62.5 and 100 μM showed near complete inhibition of both rate proton pumping and extent of acidification of the medium. At 100 and 125 μM , steady state of proton flux was seen within 5 mins of

medium acidification. NEM at 62.5 μM was selected as optimal concentration as it exhibited good response by inhibiting both the initial rate of proton pumping and the extent H^+ pump after 10 mins. NEM at 31.3 μM depicted limited inhibitory activity against proton pumping by *S. cerevisiae*.

The inhibitory activity of NEM was calculated by comparing the difference in the pH (ΔpH) of the NEM with control (carbon-starved cells in 1% DMSO) using **Equation 5**.

$$\Delta\text{pH (initial rate) of the external medium} = \text{pH}(t_0) - \text{pH}(t_n) \quad (\text{Eq.5})$$

Where, t_0 = time (min) at glucose added and

t_n = time (min) after addition of glucose.

Besides this, the initial rates of H^+ pumping by *S. cerevisiae* was also calculated which include; $\Delta\text{pH}/0.5$ min, $\Delta\text{pH}/1$ min, $\Delta\text{pH}/1.5$ min and $\Delta\text{pH}/2$ min, respectively [Data not shown].

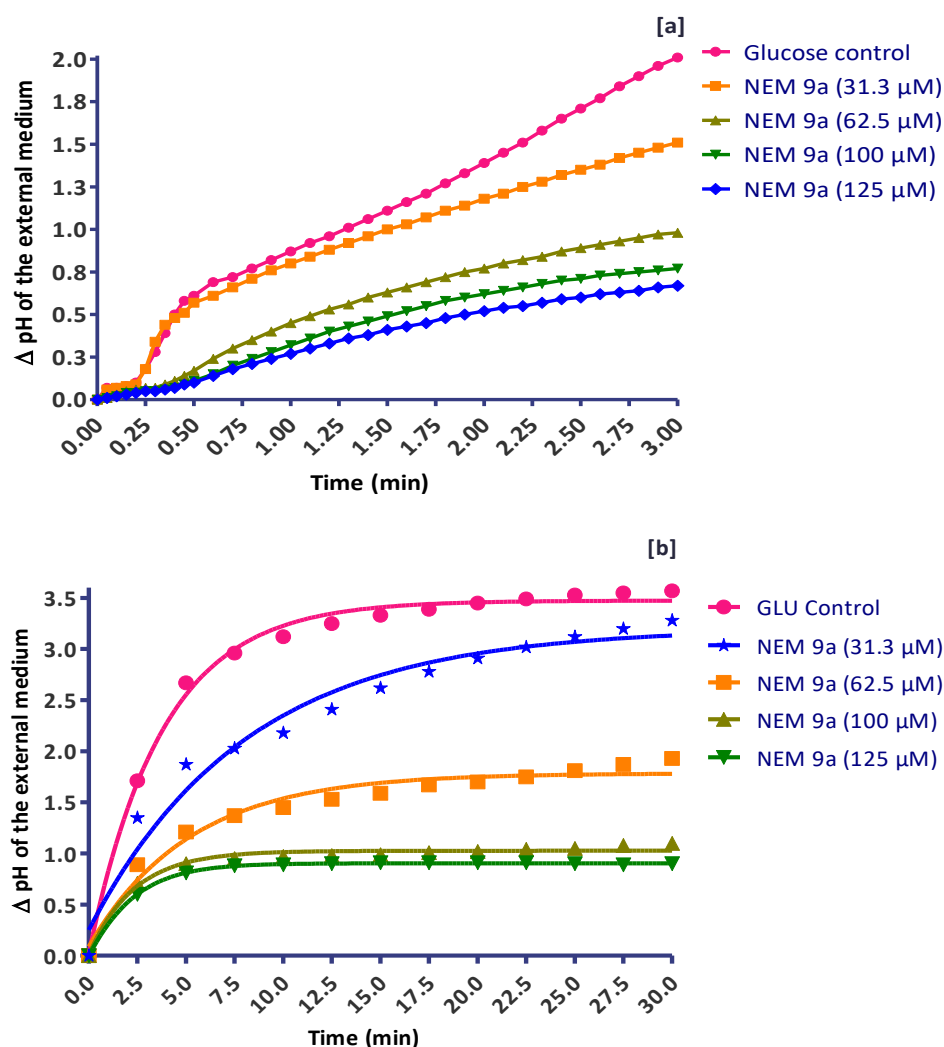


Figure 4. 3. Effect of N-ethyl maleimide on proton pumping of *S. cerevisiae*.

N-ethyl maleimide induced inhibition of glucose-dependent H^+ pumping by *S. cerevisiae*. The difference in the pH of the external medium of cell suspension containing NEM was compared with glucose control (no drug). The initial rate of H^+ pumping measured as ΔpH for first 3 mins [a] and the $\Delta \text{pH}_{\text{min to max}}$ [b]. Each data point represents the mean of the three experiments.

NEM at 62.5, 100 and 125 μM exhibited effective inhibition of the proton pumping activity by *S. cerevisiae* both in terms of the initial rate after 3 mins (46%, 69% and 75% inhibition, Fig. 4.3a) and the total extent of the change in the pH ($\Delta \text{pH}_{\text{max}}$) after 30 mins (51%, 62% and 67% inhibition, Fig. 4.3b). In addition, NEM at 100 and 125 μM inhibited the proton pump after 5 mins of medium acidification while 62.5 μM displayed inhibition after 10 minutes of pump activation, no further change in the pH was observed due to a steady state of proton flux (H^+

in = H⁺ out). In contrast at 31.3 μM, NEM only exhibited 25% inhibition of the proton pump in terms of the initial rate (after 3 mins) and only 8% inhibition after 30 mins when compared to the glucose control. This demonstrates NEM (>62.5 μM) is a potent inhibitor of the H⁺ efflux from *S. cerevisiae*. Therefore, NEM 62.5 μM was rounded to 60 μM for simplicity when used as a control in further experiments.

4.3.2 Investigation of the effect of curcumin and miconazole on the H⁺ pumping activity by *S. cerevisiae*

Curcumin (**11**) and miconazole (**4**) were also investigated for their ability to inhibit the H⁺ pumping by *S. cerevisiae* using range of concentrations (31.3, 62.5, 100 and 125 μM, respectively). The ΔpH of the external medium was obtained by using **Eq. 5** mentioned in **section 4.3.1**. In addition, the initial rate of proton pumping by *S. cerevisiae* was calculated as ΔpH/min for the 2.5 mins after pump activation. Both miconazole (**4**) and curcumin (**11**) exhibited good inhibition of proton pumping from *S. cerevisiae* in a concentration-dependent manner (Fig. 4.4a, b).

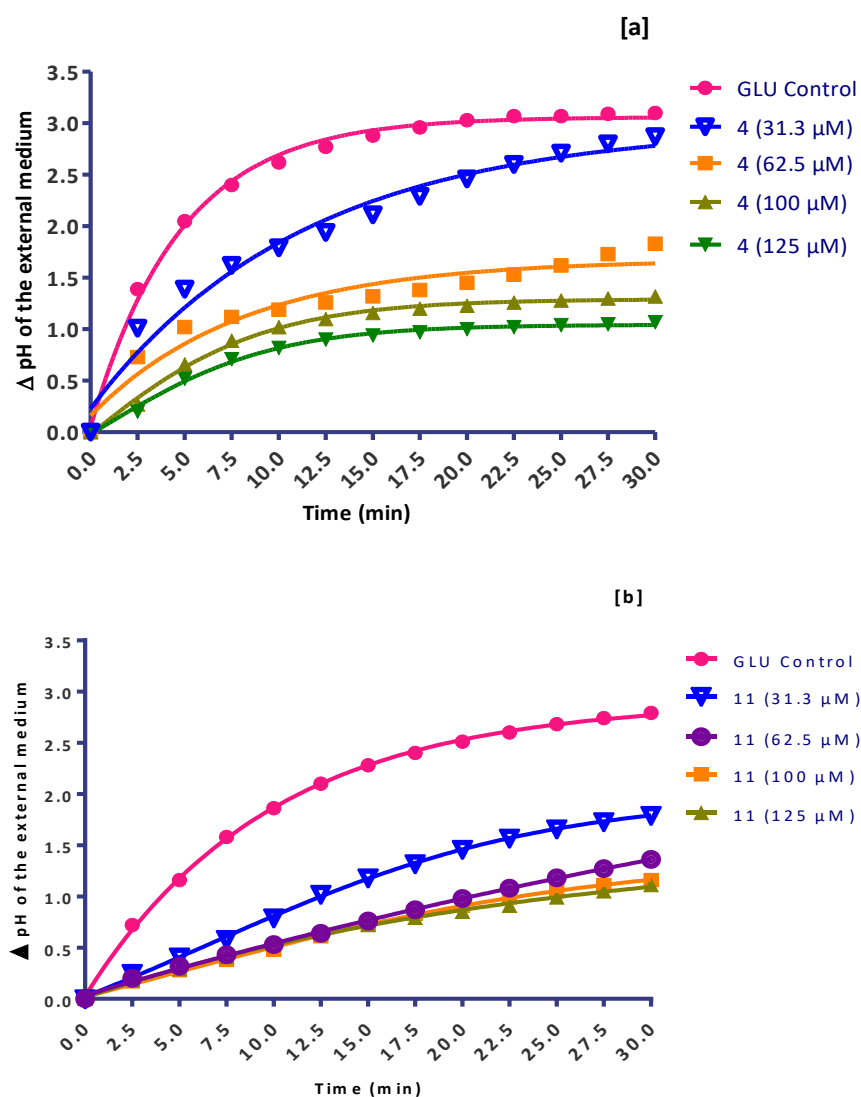


Figure 4. 4. Analysis of miconazole [a] and curcumin [b] susceptibility of the H^+ pumping in *S. cerevisiae*.

Effect of miconazole and curcumin on medium acidification by carbon starved *S. cerevisiae* cells. The difference in the pH measured for 30 mins after proton pump activation. The Δ pH of miconazole and curcumin was calculated every 2.5 mins and presented in the above figures. Each data point represents the mean of the three individual experiments, glucose control (without compounds).

Miconazole at 31.3 μ M displayed the lowest level of inhibition (7%) after 30 mins, whilst at 62.5, 100 and 125 μ M miconazole gave 44%, 57% and 65% inhibition of H^+ pumping after 30 mins of medium acidification (Figure 4.4a). However, it should be noted that in growth inhibition study in chapter-3, miconazole (0.12 μ M) gave 50% inhibition of *S. cerevisiae*

growth. This shows that miconazole requires 1000-fold higher concentration to inhibit the H⁺ pump compared to inhibiting the 4 α and 14 α demethylase enzymes. In addition, miconazole exhibited inhibition of the H⁺ pumping ability by *S. cerevisiae* within 7.5 minutes of glucose-induced pump activation at 62.5, 100 and 125 μ M respectively. Further acidification of the medium ceased after 7.5 mins and a steady state of proton flux was achieved.

Curcumin showed poor solubility over the concentration range tested, which is also reported in the literature. Considering this fact and the structural similarity of curcumin with 1,4-diene-3-ones, we have decided to investigate its activity to inhibit the proton pump. Curcumin exhibited effective potency by inhibiting proton export (36%, 51%, 58% and 60% inhibition) at 31.3, 62.5, 100 and 125 μ M respectively in Figure 4.4[b]. The Δ pH_{max} (change in pH in terms of the total extent after 30 mins) values of curcumin were 1.79, 1.36, 1.16 and 1.11 respectively at 31.3, 62.5, 100 and 125 μ M compared to glucose control (Δ pH_{max} = 2.79).

4.3.3 Effect of 1,4-diene-3-ones on the H⁺ pumping activity by *S. cerevisiae*

It has been identified from the results of NEM optimisation experiments that 62.5 μ M gives good level of inhibition of proton pumping by *S. cerevisiae*. Therefore the library of thirty-three symmetrical 1,4-diene-3-ones (**22a-v**, **23a-h** and **24a-c**) was tested at a single concentration of 60 μ M against late log phase carbon starved cells of *S. cerevisiae*. This is also a concentration commonly used in single concentration high throughput screening systems (McGovern *et al.*, 2002; Odds, 1992). The inhibitory activity of each compound was obtained by comparing their Δ pH with control (carbon-starved cells in 1% DMSO and 4% glucose solution). The initial rate of proton pumping of *S. cerevisiae* was calculated as Δ pH/min for the first 2.5 minutes. Similarly, the Δ pH_{max} of each 1,4-diene-3-one was measured after 30 minutes of medium acidification.

The statistical significance for each compound compared to the control was determined by comparing the 't' ratio with the 't' distribution for the number of differences shown using a two-way ANOVA using the Bonferroni correction (which lowers the P value that is considered to be significant to 0.05, divided by the number of comparisons). The Bonferroni correction ensures that the 5% probability applies to the entire data of comparisons and not separately to each individual comparison (Dao *et al.*, 2016). The activity of bis-benzylidene derivatives of N-methylpiperidin-4-one on the inhibition of proton efflux from *S. cerevisiae* is shown in Figure 4.5.

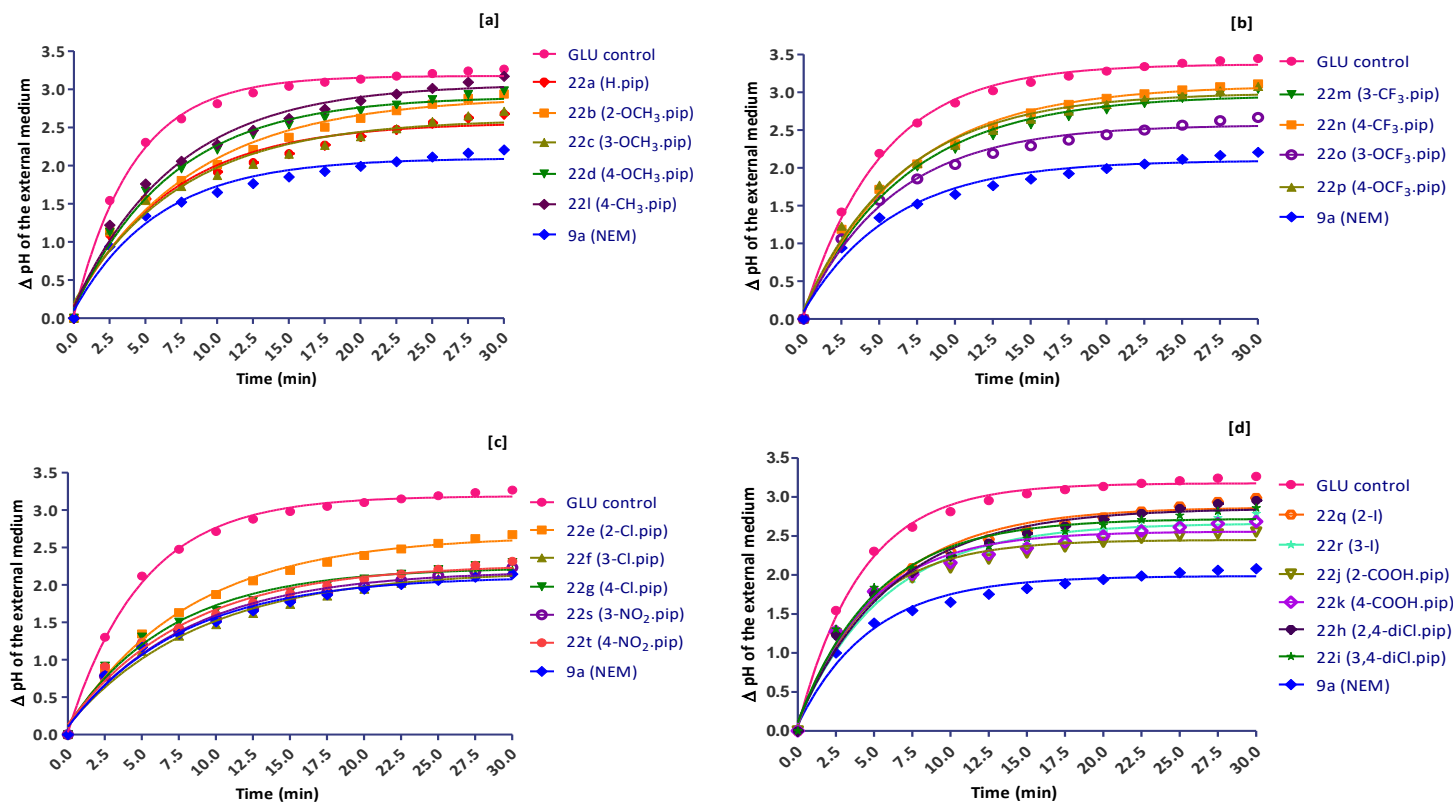


Figure 4.5. Effect of bis-benzylidene derivatives of N-methylpiperidin-4-one on the H⁺ pumping by *S. cerevisiae*.

Data were displayed as ΔpH of the external medium measured after the H⁺ pump activation. The R-substituents attached to the aromatic ring on bis-benzylidene derivatives of N-methylpiperidin-4-one includes: Hydrogen, 2-methoxy, 3-methoxy, 4-methoxy and 4-methyl [a]; 3-trifluoromethyl, 4-trifluoromethyl, 3-trifluoromethoxy and 4-trifluoromethoxy [b]; 2-chloro, 3-chloro, 4-chloro, 3-nitro and 4-nitro [c]; 2-iodo, 3-iodo, 2-carboxylic acid, 4-carboxylic acid, 2,4-di-chloro, 3,4-di-chloro [d]. NEM was used as a positive control and DMSO was used as negative control in all experiments. Each data point represents the mean of three individual experiments. Two-way repeated measures ANOVA (Bonferroni correction): *, p<0.05; **, p<0.01; ***, p<0.001 relative to glucose control (without compounds).

Compounds **22a-t** (at 60 μM) in Figure 4.5 exhibited a wide range of inhibitions (8.7% to 52%) in terms of the initial rate of proton pumping by *S. cerevisiae*. Measurement of pH changes of **22a-t** in terms of the initial rate of H^+ pumping after 1 min ($\Delta\text{pH}_{\text{ir}}$) ranged from 0.33 to 0.66 pH units, while the glucose control gave the $\Delta\text{pH}_{\text{ir}}$ of 0.69 arbitrary pH units. Additionally, compounds **22a-t** inhibited between 4.6% and 32% in terms of the total pH change ($\Delta\text{pH}_{\text{max}}$) after 30 mins. The $\Delta\text{pH}_{\text{max}}$ values of **22a-t** ranged from 2.23 to 3.23 pH units whilst NEM (60 μM) gave a $\Delta\text{pH}_{\text{max}}$ of 2.23 and glucose control gave 3.26. The most potent compounds in terms of the inhibition of the total extent of the change in pH were compounds **22f**, **22s**, **22g** and **22t**, which showed 29% to 33% inhibition of the H^+ efflux from *S. cerevisiae*. Moreover, compounds **22f**, **22g**, **22s**, **22t** showed similar activity as the NEM control (32% inhibition) and they were significantly different from the glucose control ($P < 0.05$ and $P < 0.01$). Compounds **22f**, **22g**, **22s** and **22t** all have EWGs (either chloro or nitro) attached to the aromatic ring at *meta* or *para* position. The higher potency of these compounds suggesting the importance of the electronic property associated with the β -carbon atoms. This suggests that the inhibition of H^+ -ATPase is responsible for the inhibition of proton efflux via the Michael reaction between the compounds and PMA1.

On the other hand, compounds **22o**, **22e**, **22a**, **22j**, **22k**, **22c**, **22r**, **22i**, and **22b** exhibited low to moderate activity by inhibiting 10% to 18% of the proton efflux from *S. cerevisiae* after 30 mins of medium acidification. The $\Delta\text{pH}_{\text{max}}$ values after 30 mins of these compounds ranged from 2.67 to 2.93. However, these compounds showed slightly better activity in terms of inhibiting the initial rate of proton efflux after 1 min, these being 10-32% inhibition. Compounds **22h**, **22q**, **22d**, **22m**, **22p**, **22n** and **22l** exhibited poor activity (<10% inhibition)

against proton pumping by *S. cerevisiae* and their $\Delta\text{pH}_{\text{max}}$ values ranged between 2.95 and 3.17 arbitrary units, which was very close to the glucose control ($\Delta\text{pH}_{\text{max}} = 3.26$).

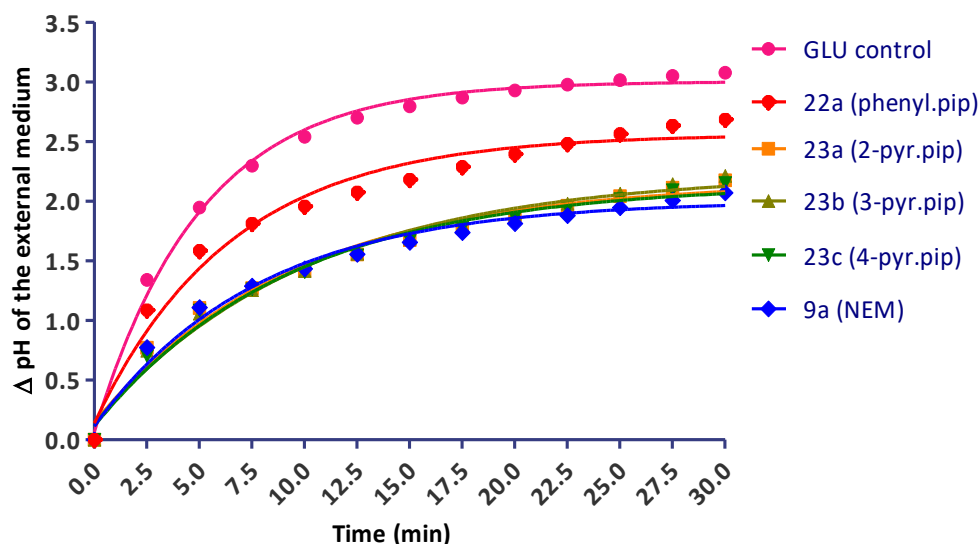


Figure 4. 6. Effect of bis-pyridylidene derivatives of N-methylpiperidin-4-one on the H⁺ pumping by *S. cerevisiae*.

Data were presented as the ΔpH of the external medium measured after the activation of proton pump. Each data point represents the mean of three individual experiments. SD values were omitted for clarity of graphs. Two-way repeated measures ANOVA (Bonferroni correction): *, $p < 0.05$; **, $p < 0.01$; ***, $p < 0.001$ relative to glucose control (without compounds).

The effect of bis-benzylidene and bis-pyridylidene derivatives of N-methylpiperidin-4-one on inhibition of proton efflux from *S. cerevisiae* is shown in Figure 4.6. After 30 minutes of medium acidification, the $\Delta\text{pH}_{\text{max}}$ of **22a**, **23a**, **23b** and **23c** were 2.56, 2.07, 2.09 and 2.08 whilst NEM and the glucose control were 2.07 and 3.26 respectively. Compounds **23a**, **23b** and **23c** at 60 μM exhibited good activity in terms of inhibiting the initial rate (48%, 46% and 49% inhibition) and the total extent (33%, 32% and 34% inhibition) of proton efflux by *S. cerevisiae*. This is comparable to NEM control at the same concentration exhibited 49% and 33% inhibition of the initial rate and the total extent of proton pumping by *S. cerevisiae*. Compounds **23a**, **23b** and **23c** exhibited inhibition of H⁺ pumping ability by *S. cerevisiae* within

10 minutes of glucose-induced medium acidification and no further change in the pH representing a steady state of proton flux was achieved ($J_{H^+in} = J_{H^+out}$). This possibly suggests that compounds **23a-c** work by a similar mechanism to NEM, by interacting with either the nucleotide-binding site in the cytoplasmic region or at the omeprazole binding site in the membrane segment of the H^+ -ATPase enzyme (Brooker & Slayman, 1982).

However the bis-benzylidene (**22a**) derivative exhibited slightly lower activity in decreasing the proton efflux from *S. cerevisiae*, showing 32% inhibition of initial rate and only 18% inhibition of the total extent of proton efflux. Following statistical analysis it has been identified that there was no significant difference ($p > 0.05$) between **23a-c**, NEM and control (no drug) for initial 2.5 mins of medium acidification. This is due to the Bonferroni correction because this equation lowers the P value that is considered significant to 0.05 divide by the number of comparisons. However, between 5 and 30 mins of medium acidification, compounds **23a-c** and NEM displayed significant difference from the glucose control with $p < 0.05$, $p < 0.01$ and $p < 0.001$ respectively.

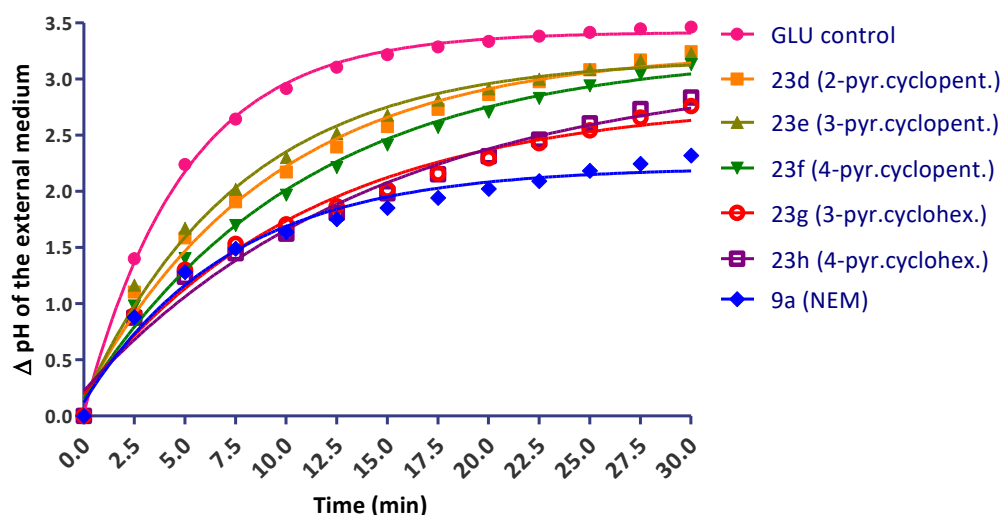


Figure 4. 7. Effect of bis-pyridylidene derivatives of cyclopentanone and cyclohexanone on the H^+ pumping by *S. cerevisiae*.

Data were shown as the ΔpH of the external medium measured after activation of proton pumping with 4% glucose. Each data point represents the mean of three individual experiments. SD values were omitted for clarity of graphs. Two-way repeated measures ANOVA (Bonferroni correction): *, $p < 0.05$; **, $p < 0.01$; ***, $p < 0.001$ relative to glucose control (without compounds).

The ΔpH_{max} (after 30 mins) of NEM, **23d**, **23e**, **23f**, **23g** and **23h** were 3.24, 3.23, 3.13, 2.76, and 2.84 respectively while glucose control has 3.46 (Figure 4.7). When comparing the total extent of the change in pH after 30 mins, the bis-pyridylidene derivatives of cyclohexanone (**23g** and **23h**) exhibited better inhibitory potency (20% and 18% inhibition) than the bis-pyridylidene derivatives of cyclopentanone (**23d**, **23e** and **23f**; 6%, 7% and 10% inhibition) although neither class exhibited reasonable to moderate levels of inhibition. NEM, **23g** and **23h** either completely inhibited proton pumping by *S. cerevisiae* within 10 mins of medium acidification or the in/out flux ($J_{H^+in} = J_{H^+out}$) reached a steady state of the proton ($\Delta J_{H^+} = 0$). In addition, compounds **23g** and **23h** both displayed significant difference from the glucose control between 5 and 30 mins of pump activation, their P values were $p < 0.001$, $p < 0.01$ and $p < 0.05$ respectively.

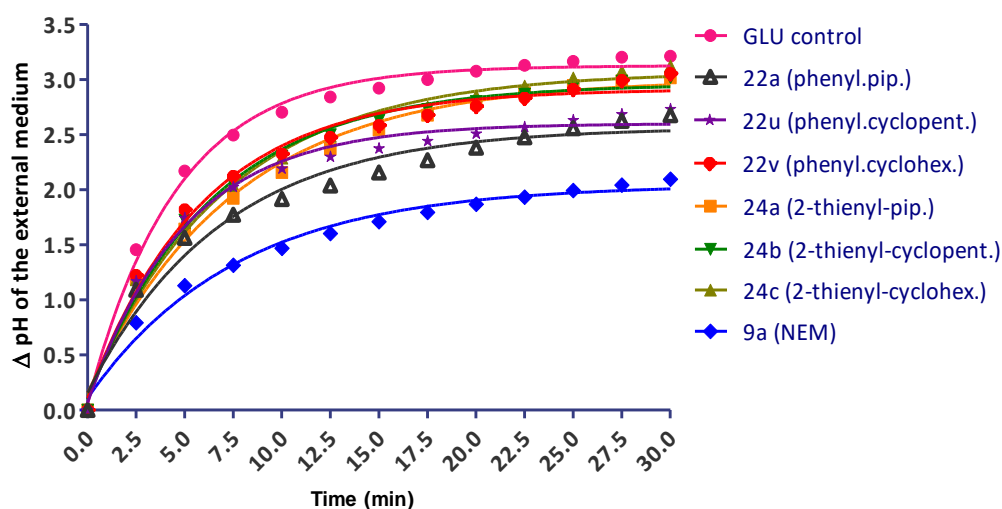


Figure 4. 8. Effect of bis-benzylidene or thienylidene derivatives of *N*-methylpiperidin-4-one, cyclopentanone and cyclohexanone on the H^+ pumping by *S. cerevisiae*.

Data were displayed as the difference in the pH of the external medium measured after activation of proton pumping with 4% glucose. Each data point represents the mean of three individual experiments. SD values were omitted for clarity of graphs. Two-way repeated measures ANOVA (Bonferroni correction): *, $p < 0.05$; **, $p < 0.01$; ***, $p < 0.001$ relative to glucose control (without compounds).

As shown in Figure 4.8, compounds **22a**, **22u**, **22v**, **24a**, **24b** and **24c** have all demonstrated minimal inhibitory activity of H^+ pumping by *S. cerevisiae*. The ΔpH_{max} of **22a**, **22u**, **22v**, **24a**, **24b** and **24c** were 2.67, 2.73, 3.06, 3.02, 3.13 and 3.02 respectively and they were not significantly different from the glucose control ($\Delta pH_{max} = 3.26$) using the Bonferroni correction. After 30 mins of pump activation, compounds **22a**, **22u**, **22v**, **24a**, **24b** and **24c** exhibited only 18%, 15%, 5%, 6%, 3% and 6% inhibition of proton efflux from *S. cerevisiae* respectively although NEM demonstrated a significant difference from the glucose control ($P < 0.001$). On the other hand, compounds **22a**, **22u**, **22v**, **24a**, **24b** and **24c** exhibited significant inhibition after 10 mins of medium acidification ($P < 0.01$).

4.3.4 Effect of (3*E*, 5*E*)-1-methyl-3,5-bis(pyridine-3-ylmethylene)piperidin-4-one on the proton pumping activity by *S. cerevisiae*

From the results of macro-broth susceptibility assay against *S. cerevisiae* in chapter-3, it has been identified that the pyridyl group of compounds exhibited better solubility than the equivalent benzyl group of compounds. This change in solubility associated with the change of benzyl to pyridyl is observed in many classes of compound. Because the pyridyl is amphipathic whereas benzene is hydrophobic. Additionally, pyridyl group of compounds has lower clogP (between 1.60 and 2.34) whereas benzyl group has higher clogP (4.07).

From the pyridyl group of compounds, bis-(pyridine-3-ylmethylene)-1-methylpiperidin-4-one (**23b**) exhibited lower AUC (194) and IC₅₀ (8.84 μM) values against *S. cerevisiae*, which makes this compound a good example to investigate its effect against proton pumping by *S. cerevisiae*. Therefore, **23b** was examined for its effect on proton export using range of concentrations such as 25, 31.3, 50, 62.5, 100 and 125 μM respectively. The bis-(pyridine-3-ylmethylene)-1-methylpiperidin-4-one (**23b**) inhibited H⁺ pumping by *S. cerevisiae* in a concentration-dependent fashion (Figure 4.9).

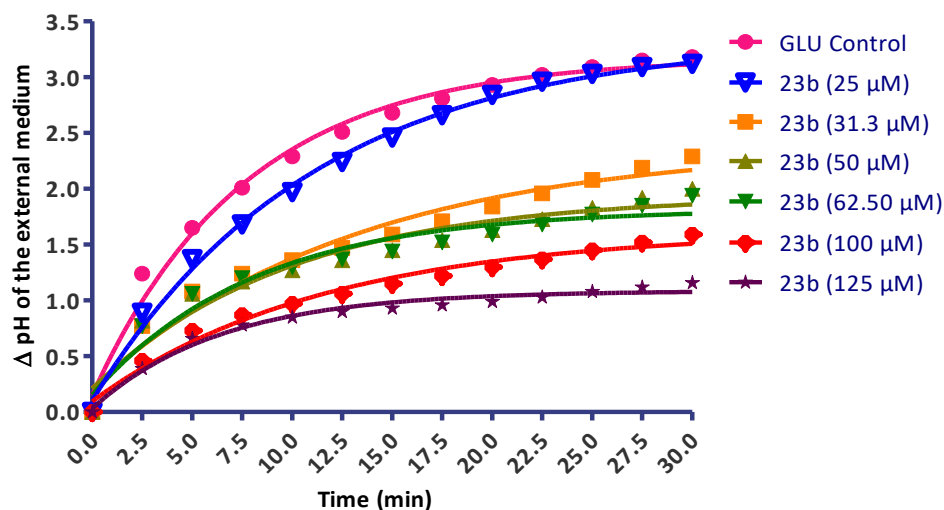


Figure 4. 9. Effect of Bis-(pyridine-3ylmethylene)-1-methylpiperidin-4-one on the H^+ pumping by *S. cerevisiae*.

Each data point represents the mean of the three individual experiments, displaying the ΔpH measured every 2.5 mins after activation of the proton pumping with glucose (4%) against time.

Compound **23b** at 25 μM gave only 2% inhibition both in terms of the initial rate and the ΔpH_{max} (30 mins). However at 31.3, 50 and 62.5 μM , the ΔpH_{max} values of **23b** were 2.29, 2.00 and 1.94 respectively whilst the glucose control was 3.18: thus exhibiting 28%, 37% and 39% inhibition of proton efflux from *S. cerevisiae* after 30 mins of medium acidification. At higher concentrations (100 and 125 μM), **23b** exhibited 50% and 64% inhibition of proton efflux from *S. cerevisiae* exhibiting low final ΔpH_{max} values 1.59 and 1.16, respectively. This suggests that **23b** is a good inhibitor of proton pumping by *S. cerevisiae*.

The effect of N-ethyl maleimide, miconazole, curcumin and various synthesized 1,4-diene-3-ones on proton pumping ability by *S. cerevisiae* is shown in **Table 4.1**, page 158. After glucose-induced acidification of external medium, the difference in the pH due to proton pumping by *S. cerevisiae* is expressed as ΔpH after 1 and 2.5 mins (initial rate), 5 mins (degree of pH change), and at 30 mins (total extent of the pH change represented as the ΔpH_{max}). The most

potent compounds identified from the library of 1,4-diene-3-ones were **22e**, **22f**, **22g**, **22s**, **22t**, **22u**, **23a**, **23b** and **23c**, which exhibited 40-52% inhibition of the initial rate of proton efflux from *S. cerevisiae*. Conversely, in terms of inhibition of the total extent of the change in pH ($\Delta\text{pH}_{\text{max}}$ after 30 mins), the most potent compounds identified were **22f**, **22g**, **22s**, **22t**, **23a**, **23b** and **23c** exhibiting 29-34% inhibition of proton efflux. In contrast, the least active inhibitors (<20% inhibition) in terms of initial rate of H^+ pumping by *S. cerevisiae* were **22b**, **22c**, **22h**, **22i**, **22k**, **22l**, **22n**, **22p**, **22q**, **22r**, **23d**, **23e** and **24a-c**. Subsequently, the least active inhibitors (<10% inhibition) based on $\Delta\text{pH}_{\text{max}}$ values after 30 mins were **22d**, **22h**, **22l**, **22m**, **22n**, **22p**, **22q**, **22v**, **23d-f** and **24a-c**.

Overall, **22s** [3,5-bis(3-nitrobenzylidene)-1-methylpiperidin-4-one] and **23c** [bis-pyridin-4-ylmethylene)-1-methylpiperidin-4-one] have been identified as the two most potent inhibitors of H^+ efflux with its lowest initial rate ΔpH over the first minute (0.33 and 0.35) and $\Delta\text{pH}_{\text{max}}$ after 30mins (2.15 and 2.23). It is believed that the increased potency of compounds **23a-c** is due to their increased permeability and amphipathic nature as suggested by their low clogP values (1.53, 1.83 and 1.61 respectively) and which are within the logP range suggested by Lipinski *et al.*, (1997). Thus compounds **23a-c** appears to be very effective at inhibiting H^+ pumping by *S. cerevisiae*.

In addition the good inhibitory activity of compounds **22f**, **22g**, **22s** and **22t** due to low $\Delta\text{pH}_{\text{max}}$ suggests the importance of an electron-withdrawing group attached at either the *meta*- or *para*-position on the aromatic ring of bis-benzylidene derivatives of N-methylpiperidin-4-one. In comparison and from the $\Delta\text{pH}_{\text{max}}$ perspective, compound **22a** (un-substituted bis-benzylidene-N-methyl-piperidin-4-one) exhibited poor activity by inhibiting only 18% of the

proton efflux from *S. cerevisiae* with $\Delta\text{pH}_{\text{max}}$ value of 2.67 as compared to the glucose control $\Delta\text{pH}_{\text{max}}$ value of 3.26.

Compound **22f** contains a *meta*-chloro group, whereas compound **22g** contains a *para*-chloro group. Similarly compound **22s** contains a *meta*-nitro group and compound **22t** contains a *para*-nitro group on the aromatic ring of the bis-benzylidene derivatives of N-methylpiperidin-4-one. When comparing the difference between compounds **22f** and **22g**, it has been identified that the **22f** was more potent than **22g** possibly due to resonance effects induced by the electron-withdrawing group (refer to figure 3.17 for representative example of trifluoromethyl group at *para*-position).

Similar effects were seen for compounds **22s** and **22t**. The presence of a EWG at the *meta*-position of the aromatic ring increases the electrophilicity of the β -carbon compared to the *para*-position. This observation is consistent with the lower AUCs and IC_{50} values of **22f**, **22g**, **22s** and **22t** against *S. cerevisiae* shown in the 24 hour growth inhibition experiments (chapter 3). Compounds containing EWG at *meta*-position (**22f** and **22s**) exhibited higher potency than compounds with EWG at *para*-position (**22g** and **22t**). This is because compound **22g** and **22t** has electronegative atom adjacent to the π system, which deactivate the aromatic ring by decreasing the electron density on the ring through resonance withdrawing effect. In addition, some property of the enzyme which may interfere with compounds binding effectively when *para*-substituted EWG is present. Overall this suggests the presence of an electron-withdrawing group on an aromatic ring increases the electrophilicity of the β -carbon of this molecule and therefore their reactivity towards system involved in the H^+ pumping.

Table 4. 1. Effect of NEM and various 1,4-diene-3-ones on the H⁺ pumping by *S. cerevisiae*.

Compounds	ΔpH at 1 min	% inhibition after 1 min	ΔpH at 2.5 mins	% inhibition after 2.5 mins	ΔpH at 5 mins	% inhibition after 5 mins	$\Delta\text{pH}_{\text{max}}$ at 30 mins	% inhibition after 30 mins
Glucose control	0.69 ± 0.06	0.00	1.47 ± 0.36	0.00	2.19 ± 0.54	0.00	3.26 ± 0.31	0.00
4 (MIC)	0.33 ± 0.16	52.17	0.73 ± 0.14	50.34	1.02 ± 0.22	53.42	1.83 ± 0.15	43.87
9a (NEM)	0.35 ± 0.11	49.28	0.87 ± 0.18	40.82	1.24 ± 0.25	43.38	2.23 ± 0.50	31.60
11 (CUR)	0.11 ± 0.13	84.06	0.20 ± 0.31	86.39	0.32 ± 0.26	85.39	1.36 ± 0.59	58.28
22a	0.47 ± 0.26	31.88	1.09 ± 0.20	25.85	1.56 ± 0.20	28.77	2.67 ± 0.39	18.10
22b	0.60 ± 0.05	13.04	1.13 ± 0.11	23.13	1.54 ± 0.19	29.68	2.93 ± 0.15	10.12
22c	0.57 ± 0.11	17.39	1.15 ± 0.08	21.77	1.55 ± 0.11	29.22	2.71 ± 0.34	16.87
22d	0.49 ± 0.18	28.99	1.12 ± 0.20	23.81	1.66 ± 0.20	24.20	2.98 ± 0.14	8.59
22e	0.40 ± 0.25	42.03	0.88 ± 0.35	40.14	1.34 ± 0.38	38.81	2.67 ± 0.70	18.10
22f	0.38 ± 0.24	44.93	0.77 ± 0.36	47.62	1.11 ± 0.37	49.32	2.19 ± 0.66	32.82
22g	0.40 ± 0.28	42.03	0.91 ± 0.50	38.10	1.30 ± 0.58	40.64	2.30 ± 0.64	29.45
22h	0.57 ± 0.11	17.39	1.23 ± 0.35	16.33	1.75 ± 0.49	20.09	2.95 ± 0.16	9.51
22i	0.61 ± 0.17	11.59	1.30 ± 0.28	11.56	1.84 ± 0.37	15.98	2.86 ± 0.16	12.27
22j	0.55 ± 0.12	20.29	1.25 ± 0.29	14.97	1.75 ± 0.30	20.09	2.68 ± 0.28	17.79
22k	0.57 ± 0.09	17.39	1.27 ± 0.13	13.61	1.78 ± 0.13	18.72	2.68 ± 0.30	17.79
22l	0.61 ± 0.04	11.59	1.22 ± 0.13	17.01	1.76 ± 0.26	19.63	3.17 ± 0.18	2.76
22m	0.54 ± 0.07	21.74	1.13 ± 0.26	23.13	1.69 ± 0.50	22.83	3.04 ± 0.33	6.75
22n	0.63 ± 0.07	8.70	1.18 ± 0.24	19.73	1.71 ± 0.37	21.92	3.11 ± 0.15	4.60
22o	0.52 ± 0.12	24.64	1.06 ± 0.32	27.89	1.57 ± 0.55	28.31	2.66 ± 0.81	18.40
22p	0.61 ± 0.08	11.59	1.23 ± 0.30	16.33	1.77 ± 0.50	19.18	3.07 ± 0.33	5.83
22q	0.62 ± 0.06	10.14	1.26 ± 0.14	14.29	1.79 ± 0.33	18.26	2.98 ± 0.58	8.59
22r	0.62 ± 0.19	10.14	1.22 ± 0.18	17.01	1.69 ± 0.26	22.83	2.78 ± 0.56	14.72
22s	0.33 ± 0.23	52.17	0.78 ± 0.41	46.94	1.19 ± 0.55	45.66	2.23 ± 0.73	31.60
22t	0.38 ± 0.18	44.93	0.90 ± 0.16	38.78	1.23 ± 0.24	43.84	2.31 ± 0.33	29.14
22u	0.41 ± 0.19	40.58	1.17 ± 0.30	20.41	1.74 ± 0.43	20.55	2.73 ± 0.72	16.26
22v	0.46 ± 0.19	33.33	1.22 ± 0.20	17.01	1.82 ± 0.35	16.89	3.05 ± 0.32	6.44
23a	0.36 ± 0.22	47.83	0.77 ± 0.25	47.62	1.10 ± 0.22	49.77	2.17 ± 0.58	33.44
23b	0.37 ± 0.21	46.38	0.74 ± 0.38	49.66	1.05 ± 0.45	52.05	2.21 ± 0.60	32.21
23c	0.35 ± 0.24	49.28	0.70 ± 0.34	52.38	1.09 ± 0.30	50.23	2.15 ± 0.55	34.05
23d	0.58 ± 0.06	15.94	1.10 ± 0.12	25.17	1.58 ± 0.13	27.85	3.24 ± 0.10	0.61
23e	0.61 ± 0.07	11.59	1.16 ± 0.13	21.09	1.67 ± 0.11	23.74	3.23 ± 0.17	0.92
23f	0.53 ± 0.08	23.19	0.98 ± 0.15	33.33	1.40 ± 0.19	36.07	3.13 ± 0.13	3.99
23g	0.47 ± 0.11	31.88	0.89 ± 0.17	39.46	1.30 ± 0.21	40.64	2.76 ± 0.31	15.34
23h	0.48 ± 0.09	30.43	0.87 ± 0.12	40.82	1.24 ± 0.16	43.38	2.83 ± 0.17	13.19
24a	0.63 ± 0.06	8.70	1.19 ± 0.13	19.05	1.64 ± 0.26	25.11	3.01 ± 0.04	7.67
24b	0.62 ± 0.09	10.14	1.18 ± 0.13	19.73	1.70 ± 0.19	22.37	3.12 ± 0.26	4.29
24c	0.62 ± 0.10	10.14	1.18 ± 0.11	19.73	1.72 ± 0.21	21.46	3.02 ± 0.32	7.36

Note: The difference in the pH (ΔpH) of the external medium was expressed as an initial rate (1 and 2.5 mins), ΔpH after 5 mins (degree of pH change) and $\Delta\text{pH}_{\text{max}}$ at 30 mins. MIC: miconazole, CUR: curcumin and NEM: N-ethyl maleimide. Each data point represents the mean ± SD of three individual experiments. Glucose and NEM were used as controls in all experiments. Glucose control stands for *S. cerevisiae* cells (10^8 cells/ml) in DMSO (1%) without any inhibitor.

4.4 Discussion of H⁺ extrusion assay

The 1,4-diene-3-one compounds are tentatively thought to act by forming a C-S (thio-ether) bond with cysteine amino acid in the plasma membrane and inhibiting ATPase, thus changing the membrane structure and integrity (Manavathu *et al.*, 1999; Khan *et al.*, 2012). The effect of thirty-three symmetrical 1,4-diene-3-ones (**22a-v**, **23a-h**, **24a-c**) on inhibiting the initial rate and overall level of H⁺ pumping by *S. cerevisiae* was measured at a single inhibitor concentration of 60 μM. This is also a concentration usually employed in single concentration high throughput screening systems (McGovern *et al.*, 2002; Odds, 1992).

From the library of 1,4-diene-3-ones, it has been identified that bis-pyridylidene derivatives of N-methylpiperidin-4-one (**23a-c**, 60 μM) either completely inhibited H⁺ pumping ability by *S. cerevisiae* within 10 minutes of medium acidification being initiated or the proton in/out flux ($J_{H^+in} = J_{H^+out}$) reached a steady state (net $J_{H^+} = 0$). This indicates that flux out (ATPase pumping) is equal to the flux in possibly due to leakage in the membrane. Moreover, compounds **23a-c** were as potent as NEM at 60 μM, which exhibited 49% inhibition of initial rate of H⁺ efflux and 32% inhibition of the total extent of H⁺ efflux by *S. cerevisiae*. NEM has been shown to inhibit the PM H⁺-ATPase of both *Neurospora crassa* (Brooker & Slayman, 1982) and *Avena sativa* root cells (Katz & Sussman, 1987). For this reason that NEM was investigated for its action against proton export by *S. cerevisiae* and used as a control. When NEM and **23b** were compared at various concentrations (62.5, 100 and 125 μM), NEM inhibited 46%, 69% and 75% of proton export (in terms of ΔpH_{max} at 30 mins) from *S. cerevisiae* while **23b** exhibited 39%, 50% and 64% inhibition.

From the bis-benzylidene derivatives of N-methylpiperidin-4-one, the most potent compounds identified were **22f**, **22g**, **22s** and **22t**; based on their low ΔpH_{ir} values (0.38, 0.40,

0.33 and 0.38) and $\Delta\text{pH}_{\text{max}}$ values (2.19, 2.30, 2.23 and 2.31). NEM control also depicted similar $\Delta\text{pH}_{\text{ir}}$ and $\Delta\text{pH}_{\text{max}}$ values and these being 0.35 and 2.23, respectively whereas glucose control values for $\Delta\text{pH}_{\text{ir}}$ and $\Delta\text{pH}_{\text{max}}$ were 0.69 and 3.26 respectively. Compounds **22f**, **22g**, **22s** and **22t** exhibited 44.9%, 42%, 52.2% and 44.9% inhibition of the initial rate of proton efflux after 1 min, which was fairly close to the activity of NEM (49.3% inhibition). Subsequently, in terms of inhibition of the total extent $\Delta\text{pH}_{\text{max}}$, **22f**, **22g**, **22s** and **22t** exhibited 32.8%, 29.5%, 31.6% and 29.1% inhibition, again their activity is fairly similar compared to NEM (32% inhibition).

It seems probable that high potency of compounds **22f**, **22g**, **22s** and **22t** compared to the other compounds from the library is due to the presence of EWGs (e.g. Cl or NO_2) at either the *meta*- or *para*-position of the aromatic rings. As mentioned previously in chapter 2, such EWGs enhance the electrophilicity of the β -carbon atom so that the nucleophilic S^- (cysteine thiolate) anion of the plasma membrane H^+ -ATPase can easily attack and form a C-S thio-ether bond and inhibit the H^+ -ATPase (Sivakumar *et al.*, 2009; Jackson *et al.*, 2017). The inhibition of the H^+ pump will thus cause an internal acidification of the cell which will eventually lead to cell death. Other benzene ring substituted benzylidene derivatives of N-methylpiperidin-4-one exhibited a lower degree of potency against H^+ pumping by *S. cerevisiae* in terms of both the initial rate after 1 min (8.7-40.6% inhibition) and the total extent over 30 mins (0.61-18.4% inhibition).

It has been reported by Fonyo, (1979) that H^+/Pi^- carrier and cytochrome oxidase are very sensitive to enones such as NEM, therefore it is possible that 1-3-diene-2-ones have some effect on mitochondrial function by either inhibiting the H^+/Pi^- carrier or cytochrome oxidase activities. This would need to be tested using either a mitochondrial swelling technique to

measure the activity of the phosphate or other organic acid carriers (Fonyo, 1979) or to measure electron transport activities using an oxygen electrode (Casey, Thelen, & Azzi, 1980; Helmerhorst, Murphy, Troxler, & Oppenheim, 2002). In addition, it will be necessary to purify the PM H⁺-ATPase enzyme and assay the potency of these compounds. This should also provide some indication of any polypharmacological effect of the enone compounds i.e. to what extent is compound potency and antifungal activity associated with a particular set of assays (Ma, Lv, & Zhang, 2018).

It is known that the ADP/ATP nucleotide transporter, cytochrome c oxidase and the proton/phosphate transporter are all susceptible to sulfhydryl reagents such as NEM, omeprazole, curcumin, etc (Fonyo, 1979; Monk *et al.*, 1995; Schultz *et al.*, 2007; Dao *et al.*, 2016). The sulphenamide of omeprazole affects growth of *S. cerevisiae* in a pH dependent manner (Monk *et al.*, 1995). Monk *et al.*, (1995) have mentioned that acid-activated omeprazole inhibits the H⁺ efflux by *S. cerevisiae* by forming a di-sulphide bond with cysteine present on the transmembrane segment of the H⁺-ATPase.

Many researchers have reported that miconazole has multiple activities besides inhibiting the enzymes involved in ergosterol biosynthesis, alteration of membrane permeability and interaction with the cell wall (Portillo & Gancedo, 1984; Abbott & Odds, 1989). Miconazole **(4)** targets mainly 4 α -demethylase but also 14 α -demethylase and thus inhibits ergosterol synthesis in fungal cells. The literature IC₅₀ value for miconazole (3 μ M) was based on the growth inhibitory assay against *S. cerevisiae* (Ottillie *et al.*, 2018). However, Portillo & Gancedo, (1984) have demonstrated that miconazole required 50 μ M to inhibit the mitochondrial ATPase by interfering with the F_o component but had no effect on F₁-ATPase activity. Thus the inhibition of F_oF₁-ATPase by miconazole is unlikely to be of any therapeutic

or clinical relevance since a 20 fold excess is needed to inhibit F_0F_1 -ATPase compared to the IC_{50} for growth.

Miconazole may have a more complex effect since in the 50 μ M range it inhibits (F_0F_1) ATPase which is significantly higher than the concentration required to inhibit ergosterol synthesis. Inhibition of the F_0F_1 -ATPase synthase will result in a decrease in both mitochondrial and cytoplasmic ATP concentrations. The build-up of mitochondrial Δ pH will also result in protonic such pressure in the electron transport system and a subsequent decrease in electron transport chain activity. This will result in decrease cytoplasmic ATP and thus lower PM H^+ -ATPase activity due to substrate depletion. Additionally lack of ergosterol in the plasma membrane will result in this membrane becoming leakier to H^+ and the extent and ratio of back-flux of H^+ into the cell will increase. This will result in the pH vs time graph being both shallower and lower in extent. In this study, miconazole exhibited good activity by inhibiting the initial rate and the total extent (Δ pH_{max}) of H^+ efflux from *S. cerevisiae*. Miconazole exhibited 44%, 57% and 65% inhibition of the Δ pH_{max} at 62.5, 100 and 125 μ M, respectively.

In this study, curcumin (**11**) activity was also investigated to determine its effect on H^+ efflux from *S. cerevisiae* because of its structural similarities with dienones. It has been reported that curcumin inhibits the P-type Ca^{2+} -ATPase of skeletal muscle sarcoplasmic reticulum (Logan-Smith *et al.*, 2001). In many studies it has been reported that curcumin exhibits poor bioavailability (Nelson *et al.*, 2017). Curcumin is also known for its stability issue in solution form but Dao *et al.*, (2016) have shown in their experiments that lack of methoxy group in demethoxycurcumin makes this compound more stable. Dao *et al.*, (2016) have reported that demethoxycurcumin is a potent inhibitor of AHA2, Ca^{2+} -ATPase and Pma1p PM H^+ -ATPase. The activity of the H^+ -ATPase AHA2 was reduced by demethoxycurcumin with an IC_{50} of 18.7

μM , Pma1p with IC_{50} of $28.9 \mu\text{M}$ and Ca^{2+} -ATPase with IC_{50} of $2.6 \mu\text{M}$. A study conducted by Khan *et al.*, (2012) have shown that curcumin (MIC_{90} ranging from $250 - 650 \mu\text{g/ml}$) exhibited 38%, 48% and 50% inhibition of H^+ efflux from three different *C. albicans* isolates; standard, clinical and fluconazole-resistant.

To gain insight into mechanism of action of curcumin and its effect on proton extrusion by PM H^+ -ATPase has been investigated in this study against carbon-starved cells of *S. cerevisiae*. Curcumin exhibited good activity and revealed 36%, 43%, 51%, 58% and 60% inhibition of H^+ efflux from *S. cerevisiae* (in terms of its $\Delta\text{pH}_{\text{max}}$) over the range of concentrations ($31.3, 50, 62.5, 100$ and $125 \mu\text{M}$). However, curcumin routinely displayed turbidity in the aqueous medium at all tested concentrations. The true nature of its activity remain suspect due to turbidity or aggregation of molecule when added to the cell suspension.

The bis-pyridylidene derivatives of cyclohexanone (**23g** and **23h**) exhibited poor to moderate activity, inhibiting only 32% and 30% of the initial rate (after 1 min) of H^+ efflux with their $\Delta\text{pH}_{\text{ir}}$ values of 0.47 and 0.48 respectively. In terms of inhibiting the total extent of change in the pH after 30 mins, **23g** and **23h** exhibited only 15 and 13% inhibition of H^+ pumping by *S. cerevisiae* and their $\Delta\text{pH}_{\text{max}}$ were measured as 2.76 and 2.83 pH units respectively compared to glucose control (3.26 pH units). In contrast the bis-pyridylidene derivatives of cyclopentanone (**23d-f**) exhibited even lower potency (15.9%, 11.6% and 23% inhibition) than **23g** and **23h** in terms of the initial rate of H^+ pumping by *S. cerevisiae*. In addition **23d**, **23e** and **23f** exhibited poor activity in terms of inhibiting the total extent of $\Delta\text{pH}_{\text{max}}$ over 30 mins (0.61%, 0.92% and 4% inhibition).

The difference in the activity of **23a-c**, **23d-f** and **23g-h** is therefore apparently linked to the structure of the central ring. Compounds **23a-c** have a piperidine ring whilst **23d-f** have a

cyclopentyl ring, and **23g-h** have a cyclohexyl ring. The presence of the piperidine structure influences the inhibitory action possibly by increasing the aqueous solubility of the compound at least as measured by clogP values. As mentioned in previous chapters that piperidine ring structure are able to form a hydrogen bond between the N-methyl lone pair and a hydrogen atom associated with the target site whereas a cyclopentyl or cyclohexyl ring structure are unable to form such an interaction. Therefore, compounds **23a-c** (central piperidine ring) were more effective at inhibiting the proton efflux from *S. cerevisiae* than **23d-f** (central cyclopentyl ring) or **23g-h** (central cyclohexyl ring). This is consistent with the results exhibited by the bis-benzylidene derivatives such as compounds **22a** (a piperidine ring) **22u** (a cyclopentyl ring) and **22v** (a cyclohexyl ring). In terms of total extent of the change in pH after 30 mins, compound **22a** exhibited better potency by inhibiting 18.1% of proton efflux whereas **22u** showed 16.3% inhibition and **22v** revealed only 6.44% inhibition.

The bis-thienylidene derivatives of N-methylpiperidin-4-one and cycloalkanones (**24a**, **24b** and **24c**) exhibited little inhibition in terms of either the initial rate (8.70, 10.1 and 10.1% inhibition) or the $\Delta\text{pH}_{\text{max}}$ (7.67, 4.29 and 7.36% inhibition) of H^+ pumping by *S. cerevisiae* cells. The result of the proton extrusion assay using the bis-thienyl derivatives against *S. cerevisiae* is in agreement with their higher IC_{50} values and AUCs obtained from the general growth susceptibility assay. These collective results are all consistent with this group of compounds being less effective at inhibiting H^+ pumping by *S. cerevisiae*.

The decrease in inhibitory potency of most of the compounds from the library in proton extrusion assay compared to the broth susceptibility assay is possibly due to the difference in the timing of the assay. In the growth inhibitory assay, compounds have more time to interact with other components of the cells because it was performed over a 24 hour period whereas

in the proton extrusion assay, compounds have only 90 minutes to interact with cells. Therefore, it is possible that the decrease in the activity of some compounds when comparing the two assay formats may be due to an increase in the number of interacting components or the time required to access the cytoplasmic side of the ATPase.

4.5 Conclusions

The bis-pyridylidene derivatives of N-methylpiperidin-4-one (**23a**, **23b** and **23c**, 60 μM) exhibited higher levels of inhibition of H^+ efflux from *S. cerevisiae*, in terms of inhibiting the initial rate (48, 46 and 49% inhibition) and the $\Delta\text{pH}_{\text{max}}$ (33, 32 and 34 % inhibition). In addition, **23a-c** showed similar activity as the control inhibitor NEM (initial rate; 49% inhibition and $\Delta\text{pH}_{\text{max}}$; 32% inhibition). Furthermore this is consistent with **23a-c** exhibiting good potency in the macro-broth susceptibility assay against *S. cerevisiae* with their IC_{50} values being 12.6, 8.84 and 9.45 μM .

Moreover, the most effective compounds from the bis-benzylidene derivatives of N-methylpiperidin-4-one were **22f**, **22g**, **22s** and **22t**, all of which exhibited good potency in terms of inhibiting both the initial rate and $\Delta\text{pH}_{\text{max}}$ of H^+ pumping by *S. cerevisiae*. Additionally, **22f**, **22g**, **22s** and **22t** also exhibited good potency in macro-broth susceptibility assay with their IC_{50} values being 1.21, 5.56, 1.87 and 3.37 μM . In contrast, the bis-pyridylidene derivatives of cycloalkanones (**23d-h**) exhibited poor activity against proton pumping by *S. cerevisiae*.

The bis-thienylidene derivatives of N-methylpiperidin-4-one and the cycloalkanones (**24a**, **24b** and **24c**) did not inhibit H^+ pumping by *S. cerevisiae*. These results were consistent with their higher AUCs and IC_{50} values against *S. cerevisiae* shown in the 24 hour growth inhibition experiments (chapter 3). This confirms that compounds containing thienyl group (**24a-c**) were not effective inhibitors of *S. cerevisiae* cells and no further derivative with this ring structure should probably be synthesized.

In conclusion, the antifungal activity of **22f**, **22g**, **22s**, **22t**, **23a**, **23b** and **23c** may be originating from the inhibition of the plasma membrane H⁺-ATPase of *S. cerevisiae* and drop of internal pH leading to membrane damage.

CHAPTER FIVE

STRUCTURE-ACTIVITY RELATIONSHIPS

5 Structure-activity relationship

5.1 Introduction - Structure-activity relationship

As stated in chapter-1 section 1.3.2, the frequency of invasive fungal infections has increased significantly in recent decades and the treatments for invasive fungal infections are limited despite the increase in our understanding of the molecular basis of antifungal drug therapy (Giraud *et al.*, 2009).

Over past decades, quantitative structure-based drug discovery and design has become increasingly important. Such advances are linked to an increased knowledge of structural biology and protein structure (De Cesco *et al.*, 2017). This approach indicates possible structural modifications which may be made to a lead molecule in order to optimise ligand interactions with the target enzyme.

In 1997 Lipinski *et al.*, (1997) reviewed the literature related to computational approaches for evaluating the permeability and solubility of molecules in the process of drug discovery and development. They developed four rules and discussed how they could be applied to evaluate drug-likeness in the discovery process. These being: a molecular mass <500 Daltons, log P (octanol/water partition coefficient) <5, the number of hydrogen bond donors being fewer than five and the number of hydrogen bond acceptors being fewer than ten.

Based on what is known about inhibitors of the fungal H⁺-ATPase, a library of 1,4-diene-3-one compounds have been synthesized where both the nature and substituent groups of aromatic rings, and the size and nature of the core ring carbonyl structure have been varied. The synthesized compounds will act in the same fashion and be consistent with Lipinski's rule. A library consist of the bis-benzylidene derivatives of N-methylpiperidin-4-ones with various

substituents attached to the aromatic rings (**22a-t**), bis-benzylidene derivative of cyclopentanone (**22u**), bis-benzylidene derivative of cyclohexanone (**22v**), bis-pyridylidene derivatives of N-methylpiperidin-4-one and cycloalkanones (**23a-h**) and bis-thienylidene derivatives of N-methylpiperidin-4-one and cycloalkanones (**24a-c**). The compounds in this library were tested for their antifungal activities (details and results of which are given in **Chapters 3** and **4**). This class of compounds are synthetic α' -dimethylene ketone homologues of curcumin where aromatic rings such as pyridine or benzene or pseudo-aromatic structures, such as thiophene are attached to a methylene group α or α' to the carbonyl group such as N-methylpiperidin-4-one, cyclopentanone or cyclohexanone. In the library developed for this project, various heterocycles were introduced in order to increase both the solubility and bioavailability.

Enones or dienones are both able to undergo a Michael addition reaction with intracellular thiol containing compounds (e.g. glutathione, protein cysteines) with the olefinic C=C double bond of the enone. Chemically it was expected that conjugated enones/dienones could inhibit glutathione-S-transferase which could improve the general cytotoxicity of 3,5-bis(benzylidene)-4-piperidone compounds along with other proteins containing essential cysteine residue (Lagisetty, Vilekar, Sahoo, Anant, & Awasthi, 2010).

The evidence from this study suggest that 1,4-diene-3-ones (**22a-v** and **23a-h**) possess a good level of antifungal activity against *S. cerevisiae* but are only poor to moderately active against *C. albicans*. This was established using *in vitro* macro-broth susceptibility assay against both *S. cerevisiae* and *C. albicans* (**Chapter-3**) and proton extrusion assays on *S. cerevisiae* (**Chapter-4**). It was identified that compounds **24a-c** were not effective inhibitors of either *S. cerevisiae* or *C. albicans*.

The magnitude of their hydrophobic, electrophilic, volumetric and steric properties has been altered and tested for potential SAR. SAR attempts to investigate the influence of various physicochemical properties of the molecule such as the nature and pattern of ring substitution on the electrophilicity of the β -carbon, or the presence of pyridine rings having a direct relationship with the solubility and lipophilicity of a molecule. The benzene ring will be more lipophilic whereas a pyridine ring will be more amphipathic in nature.

Initial analysis of the relationships between the structure and biological activity of the synthesized 1,4-diene-3-ones was performed in order to identify physicochemical features of the 1,4-diene-3-ones which could lead to improved antifungal properties of this class of compounds or alternatively be incorporated into other potentially more targeted compounds. Information obtained from the SAR analysis offers a useful starting point for further chemical modification of the pharmacophore structure (1,4-diene-3-one), which hopefully would result in compounds having higher bioavailability and target specificity thus hopefully leading to more potent compounds.

5.2 Methods – Structure activity-relationship

5.2.1 Structure-activity relationships of 1,4-diene-3-ones

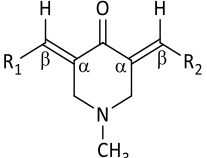
Structure-activity relationship (SAR) studies were performed by selecting two parameters namely; the lipophilic and electronic properties of various sub-libraries of the 1,4-diene-3-one compounds. Correlation plots were constructed to determine whether any correlations existed between either the activity (e.g. compound which inhibited 50% of *S. cerevisiae* growth; IC_{50}) or its derivative parameter ($\log 1/IC_{50}$), clogP or $^1\text{H-NMR}$ δ -values of olefinic protons present on the β -carbon of the 1,4-diene-3-ones. This latter property was chosen as a good descriptor for both electron density and shielding of the β -carbon. Individual clogP values were calculated for each compound using the software programme Molecular Orbital Environment 2014.09 Software (MOE). For the purpose of this study, calculated $\log P$ (clogP) was used as a lipophilic parameter.

The clogP of various 1,4-diene-3-ones ranged between 1.53 and 6.94 (**Table 5.1 and 5.2**, page 174 and 176). Pyridine-containing compounds (**23a-h**) have lower clogP values (between 1.53 and 2.34). Compounds (**23a** and **23d**) containing nitrogen atom at the *ortho*-position of aromatic ring have clogP values of 1.53 (N-methylpiperidin-4-one derivative) and 1.90 (cyclopentanone derivative). While compounds (**23b**, **23e** and **23g**) with a nitrogen-atom at the *meta*-position of the aromatic ring have clogP values of 1.83 (N-methylpiperidin-4-one derivative), 1.91 (cyclopentanone derivative) and 2.34 (cyclohexanone derivative). In addition compounds (**23c**, **23f** and **23h**) with a N-atom at the *para*-position of aromatic ring have the same clogP values of 1.60 for N-methylpiperidin-4-one, cyclopentanone and cyclohexanone derivatives.

The $^1\text{H-NMR}$ δ -value of proton on the β -carbon of 1,4-diene-3-ones was selected as an indicator of electron density and thus electrophilicity. The δ -values of proton of 1,4-diene-3-ones was obtained from individual $^1\text{H-NMR}$ spectra and ranged from 7.47 to 7.98 ppm. Out of which, the δ -values of proton on the β -carbon of bis-benzylidene, bis-pyridylidene and bis-thienylidene derivatives of N-methylpiperidin-4-one varied from 7.65 to 7.98 ppm (**Table 5.1**, Page 174). Similarly the δ -value of the carbon atom from the carbonyl (C=O) group of each compound was obtained from the $^{13}\text{C-NMR}$ spectra. The δ -value of the ^{13}C carbon C=O groups for the bis-benzylidene, bis-pyridylidene and bis-thienylidene derivatives of N-methylpiperidin-4-one ranged from 167.3 to 187.1 ppm (**Table 5.1**, Page 174).

The inhibitory activities of the 1,4-diene-3-ones compounds described as either IC_{50}s or AUCs against *S. cerevisiae* (data taken from **Table 3.1**, Page 105) were converted to $\log(1/\text{IC}_{50})$ and $\log(1/\text{AUC})$. Transformations of the data to a logarithmic scale were implemented to linearize the relationships. The values of clogP , $^1\text{H-NMR}$ δ -values of proton on the β -carbon, $^{13}\text{C-NMR}$ δ -value of C=O, $\log(1/\text{IC}_{50})$ and $\log(1/\text{AUC})$ with various substituent groups attached to the aromatic rings or the position of nitrogen in the pyridine rings are shown in **Table 5.1**, page 174. The $\log(1/\text{IC}_{50})$ of the bis-benzylidene, bis-pyridylidene and bis-thienylidene derivatives of N-methylpiperidin-4-ones varied between 2.65 and 6.21. Similar calculations for the $\log(1/\text{AUC})$ gave values ranging from 1.99 to 2.50. Compounds containing the pyridine functionality were lowest in terms of their clogP values and were within the Lipinski range (1-5).

Table 5. 1. Electronic and lipophilic properties of bis-benzylidene, bis-pyridylidene and bis-thienylidene derivatives of N-methylpiperidin-4-ones and their anti-fungal activity against *S. cerevisiae*.

Compounds	Groups attached at R ₁ and R ₂	ClogP	¹ H-NMR, δ value of protons on the β-carbon (ppm)	¹³ C-NMR, δ value of C=O (ppm)	log (1/IC ₅₀)	log (1/AUC)
						
22a	H-Ar	4.07	7.88	186.7	4.39	2.39
22b	2-OCH ₃ -Ar	3.71	7.82	187.1	4.64	2.41
22c	3-OCH ₃ -Ar	4.06	7.76	187.0	5.49	2.16
22d	4-OCH ₃ -Ar	3.98	7.54	186.7	4.65	2.36
22e	2-Cl-Ar	5.25	7.75	186.7	5.41	2.27
22f	3-Cl-Ar	5.33	7.56	186.7	5.92	1.99
22g	4-Cl-Ar	5.25	7.57	186.4	5.26	2.20
22h	2, 4-diCl	6.51	7.90	185.9	3.81	2.43
22i	3, 4-diCl	6.51	7.65	186.1	3.81	2.46
22j	2-COOH	3.42	7.85	170.1	3.90	2.41
22k	4-COOH	3.42	7.91	167.3	3.65	2.47
22l	4-CH ₃ -Ar	4.67	7.79	187.0	N/R	2.50
22m	3-CF ₃ -Ar	6.01	7.76	186.2	5.82	2.14
22n	4-CF ₃ -Ar	5.94	7.81	186.4	6.21	2.02
22o	3-OCF ₃ -Ar	6.94	7.75	186.5	5.55	2.24
22p	4-OCF ₃ -Ar	6.87	7.81	186.1	4.89	2.25
22q	2-I-Ar	6.45	7.81	185.9	4.72	2.34
22r	3-I-Ar	6.52	7.71	186.5	5.18	2.29
22s	3-NO ₂ -Ar	4.01	7.60	186.0	5.73	2.10
22t	4-NO ₂ -Ar	3.94	7.80	186.2	5.47	2.16
23a	2-pyridine	1.53	7.72	186.0	4.90	2.32
23b	3-pyridine	1.83	7.68	185.9	5.05	2.29
23c	4-pyridine	1.61	7.70	186.0	5.03	2.29
24a	2-thiophene	3.13	7.98	185.9	2.65	2.50

Note: Ar= Six membered aromatic ring. N/R means compound did not give 50% inhibition of *S. cerevisiae* growth and therefore log (1/IC₅₀) was not calculated.

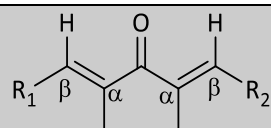
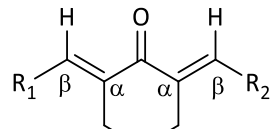
The electronic and lipophilic properties of the bis-benzylidene, bis-pyridylidene and bis-thienylidene derivatives of cyclopentanone and cyclohexanone, together with their antifungal activity against *S. cerevisiae*, expressed as either log (1/IC₅₀) or log (1/AUC), are given in **Table 5.2**, page 176. For the bis-benzylidene, bis-pyridylidene and bis-thienylidene derivatives of

cyclopentanone, compounds containing pyridine rings with the varying position of nitrogen-atom (*ortho*, *meta* or *para*) have low clogP values (1.60 to 1.91) whilst thiophene rings (3.43) or benzene rings (4.77) have higher clogP values. The bis-benzylidene, bis-pyridylidene and bis-thienylidene derivatives of cyclohexanone also effect the clogP values, such as displayed in compounds with pyridine rings having clogP values of 1.60 and 2.34 compared to thiophene rings (3.87) or benzene rings (5.33). Compound 2-pyridylcyclohexan-1-one was not included in the entire study as the final “purified” product contained impurities such as a putative dimeric form and the presence of hydrochloride salts in the mixture (Data not shown in chapter 2).

The $^1\text{H-NMR}$ δ -value of proton on the β -carbon of the bis-benzylidene, bis-pyridylidene and bis-thienylidene derivatives of cyclopentanone ranged from 7.47 to 7.79 ppm whereas the bis-benzylidene, bis-pyridylidene and bis-thienylidene derivatives of cyclohexanone ranged from 7.65 to 7.97 ppm. Compounds containing a central cyclohexyl ring gave slightly higher ^1H δ -values compared to the compounds with a cyclopentyl ring.

The bis-benzylidene, bis-pyridylidene and bis-thienylidene derivatives of cyclopentanone gave their $^{13}\text{C-NMR}$ δ -value of the ^{13}C carbon C=O groups ranged between 195.1 and 197.8 ppm and inhibitory potencies of 2.89-5.08 ($\log(1/\text{IC}_{50})$) and 2.29-2.51($\log(1/\text{AUC})$). Subsequently the bis-benzylidene, bis-pyridylidene and bis-thienylidene derivatives of cyclohexanone gave their $^{13}\text{C-NMR}$ δ -value of the ^{13}C carbon C=O groups varied from 189.1 to 190.4 ppm, while their $\log(1/\text{IC}_{50})$ values were between 3.51 to 5.25 and $\log(1/\text{AUC})$ values were 2.22 to 2.52 respectively.

Table 5. 2. Electronic and lipophilic properties of bis-benzylidene, bis-pyridylidene and bis-thienylidene derivatives of cyclopentanone and cyclohexanone and their anti-fungal activity against *S. cerevisiae*.

	Groups attached at R ₁ and R ₂	Compounds	ClogP	¹ H-NMR, δ values of proton on the β-carbon (ppm)	¹³ C-NMR, δ value of C=O (ppm)	log (1/IC ₅₀)	log (1/AUC)
	H-Ar	22u	4.77	7.62	196.6	2.89	2.51
	2-pyridine	23d	1.90	7.53	195.3	4.69	2.36
	3-pyridine	23e	1.91	7.53	197.8	5.08	2.32
	4-pyridine	23f	1.60	7.47	195.4	5.07	2.29
	2-thiophene	24b	3.43	7.79	195.1	3.21	2.50
	H-Ar	22v	5.33	7.80	190.4	3.51	2.50
	3-pyridine	23g	2.34	7.73	189.1	5.25	2.22
	4-pyridine	23h	1.60	7.65	189.2	5.07	2.25
	2-thiophene	24c	3.87	7.97	189.1	N/R	2.52

Note: Ar= six membered aromatic ring. N/R represents that compound did not give 50% inhibition of *S. cerevisiae* growth and therefore log (1/IC₅₀) was not calculated.

Only 31 compounds were analysed for SAR since only these compounds have exhibited inhibitory activity greater than 50% against *S. cerevisiae*. Compounds **22i** (3,5-bis(4-methylbenzylidene)-1-methylpiperidin-4-one) and **24c** (2,6-bis-(thiophene-2-ylmethylene)cyclohexan-1-one) were excluded from the data set due to a lack of potency. The inhibitory activities against *S. cerevisiae* by 1,4-diene-3-ones were expressed as either log (1/IC₅₀) or log (1/AUC) and compared with both the clogP and the δ -values of proton on the β -carbon of 1,4-diene-3-ones.

Certain compounds in the library contain electron withdrawing groups e.g. I, Cl or COOH whereas some compounds contain electron donating groups such as CH₃ or OCH₃ attached to the aromatic ring while few other compounds consist of either aromatic pyridine rings or a pseudo aromatic sulphur containing five membered ring. SAR analyses were conducted by dividing compounds into several groups based on the different substituents and rings, such as a full data set (containing 31 compounds), bis-benzylidene derivatives of N-methylpiperidin-4-ones (18 compounds) and bis-pyridylidene derivatives of N-methylpiperidin-4-one and cycloalkanones (pyridine ring containing 8 compounds).

The Hammett equation sometimes fails when substituents and other functionalities or reaction centres have the potential to interact with each other (e.g. substituents that are *ortho* to each other). For example in some cases the electronic effect of a substituent *ortho* to the first substituent increases or decreases the substituent effect (Hansch & Leo, 1979). In some SAR analyses, the *ortho*-substituted group of compounds were removed because of the potential for interactions (Figure 5.1). For example, some *ortho*-substituents (e.g. COOH, OH) can interact with the olefinic hydrogen atom present at the β -carbon or hydrogen atom of central piperidine structure and cause either volumetric or steric clashes between hydrogen atoms.

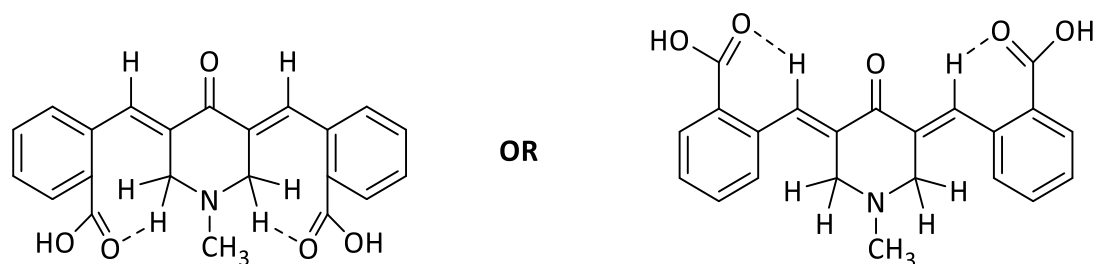


Figure 5. 1. A representative example of potential interaction of *ortho*-substituent with either olefinic proton or protons of central pyridyl ring.

SAR was performed after grouping compounds based on their chemical structures:

- 1) SAR of 31 compounds (**22a-k**, **22m-v**, **23a-h** and **24a-b**),
- 2) SAR of reduced data set excluding *ortho*-substituents compounds – 19 compounds analysed (**22a**, **22c-d**, **22f-g**, **22k**, **22m-p**, **22r-t**, **23b-c** and **23e-h**),
- 3) SAR of bis-benzylidene derivatives of N-methylpiperidin-4-ones – 18 compounds analysed (**22a-k** and **22m-t**).
- 4) SAR of reduced data set of bis-benzylidene derivatives of N-methylpiperidin-4-ones excluding *ortho*-substituents compounds – 13 compounds analysed (**22a**, **22c-d**, **22f-g**, **22k**, **22m-p** and **22r-t**), and
- 5) SAR of bis-pyridylidene derivatives of N-methylpiperidin-4-one and cycloalkanones – 8 compounds analysed (**23a-h**).

Correlation analysis was performed using the following selections:

- (i) $\log (1/IC_{50})$ against clogP of 1,4-diene-3-ones,
- (ii) $\log (1/IC_{50})$ against the δ -values of proton on the β -carbon of 1,4-diene-3-ones,
- (iii) $\log (1/IC_{50})$ against the δ -values of the carbon atom of carbonyl (C=O) group of 1,4-diene-3-ones,
- (iv) $\log (1/AUC)$ against clogP of 1,4-diene-3-ones,
- (v) $\log (1/AUC)$ against the δ -values of proton on the β -carbon of 1,4-diene-3-ones,
- (vi) $\log (1/AUC)$ against the δ -values of the carbon atom of carbonyl (C=O) group of 1,4-diene-3-ones,
- (vii) $\log (1/AUC)$ against $\log (1/IC_{50})$ of 1,4-diene-3-ones,
- (viii) The δ -values of the carbon atom of C=O against δ -values of protons on the β -carbon of 1,4-diene-3-ones and
- (ix) The δ -values of proton on the β -carbon of 1,4-diene-3-ones against their clogP .
- (x) The δ -values of proton on the β -carbon of 1,4-diene-3-ones against clogP and
- (xi) The δ -values of the carbon atom of C=O of 1,4-diene-3-ones against clogP .

5.3 Results – Structure activity-relationship

Structure-activity relationship analysis of full data, the set containing 31 compounds (**22a-k**, **22m-v**, **23a-h** and **24a-b**) were analysed using two possible combinations; $\log(1/IC_{50})$ vs clogP and $\log(1/IC_{50})$ vs the δ -values of proton on the β -carbon of the 1,4-diene-3-ones. Correlation coefficients (R^2 values) derived from the various plots indicates the goodness of fit between the equation of physicochemical parameter and the biological activity of the particular set of compounds. Initial SAR was performed using $\log(1/IC_{50})$ vs clogP and $\log(1/IC_{50})$ vs the δ -values of proton on the β -carbon of the 1,4-diene-3-ones on full data set of 31 compounds by fitting a linear model using the equation (**Eq. 6**). However the R^2 values of the linear correlations of the data set was very low (0.004; clogP plot and 0.135; δ -values of protons).

$$y = bx + c \quad (\text{Eq. 6})$$

Further SAR was conducted using a second order polynomial equation (**Eq. 7**) as this provided a better fit to the data.

$$y = ax^2 + b'x + c \quad (\text{Eq. 7})$$

Polynomial regression is a special case of multiple linear regression (MLR) and it can be used to fit a variety of models such as linear, quadratic, cubic or quartic. In addition polynomial regression is used to fit a nonlinear relationship between independent and dependent variables (e.g. clogP and $\log(1/IC_{50})$). The aim of this study was to correlate the biological properties [$\log(1/IC_{50})$ or $\log(1/AUC)$] with the chemical properties (lipophilic or electronic) of the molecule.

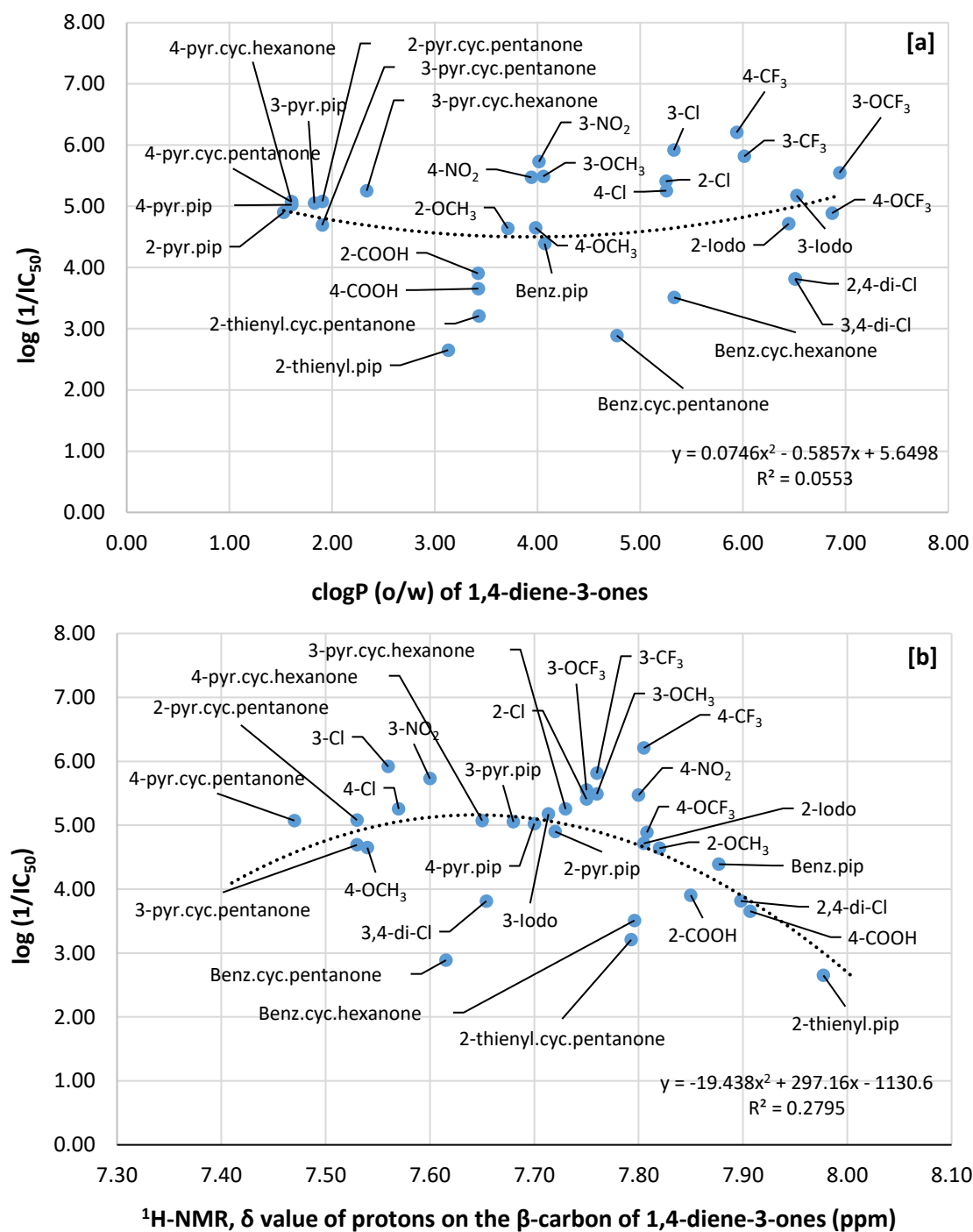


Figure 5. 2. SAR of $\log(1/IC_{50})$ against $clogP$ [a] and $\log(1/IC_{50})$ against the δ -values of the protons on the β -carbon [b] of the 1,4-diene-3-ones.

Correlation analysis of 31 compounds plotting $\log(1/IC_{50})$ against $clogP$ in Fig 5.2[a] shows a parabolic curve with a correlation coefficient (R^2) of 0.0553 whereas the correlation analysis of $\log(1/IC_{50})$ against the δ -values of proton on the β -carbon of the 1,4-diene-3-ones generates a hyperbolic curve with the correlation coefficient of 0.2795 in Fig 5.2[b]. The R^2

values in Fig 5.2[a and b] were very poor, however Fig 5.2[b] show slightly better R^2 value, which possibly suggests better correlation between the electrophilicity and the inhibitory activity. When comparing the coefficient value of 2nd order polynomial ($b'x = -0.5857$) with linear equation ($bx = 0.0327$) it was identified that these two models have a 0.61 fold difference between them in Figure 5.2[a]. Similarly the plot of $\log(1/IC_{50})$ vs the δ -values of protons on the β -carbon in the Figure 5.2[b] showed 299 fold difference between the 2nd order polynomial ($b'x = 297.16$) and linear ($bx = -2.628$). This evidence confirms that second order polynomial provide a better fit of the data compared to the linear equation.

However, low values of R^2 could possibly be the result of three different groups of compounds analysed together in this data set. Additionally, it was clearly observed that the electrophilic parameter (δ -values of proton on the β -carbon of the 1,4-diene-3-ones) correlates reasonably with $\log(1/IC_{50})$ compared to the lipophilic parameter (clogP). Subsequent correlation analysis of $\log(1/AUC)$ against clogP was performed and this gave a correlation coefficient of 0.0208 whereas the plot $\log(1/AUC)$ against δ -values of proton on the β -carbon of the 1,4-diene-3-ones gave a correlation coefficient of 0.1791 (Data not shown).

The full data set was reduced by removing various sub-sets of compounds to determine whether removing a particular property will give a better fit of the data or better correlation coefficient and to see whether this has a beneficial or detrimental effect on the correlation. Therefore SAR analysis was performed by removing the *ortho*-substituted compounds from the library (detailed reasoning for this explained in **section 5.2.1**, page 172-179). The reduced dataset contains 19 compounds from the library. These were compounds **22a**, **22c**, **22d**, **22f**, **22g**, **22k**, **22m-p**, **22r-t**, **23b**, **23c**, and **23e-h**, respectively. The reason for removing the *ortho*-substituted compounds is because *ortho*-substitution is well known to give rise to interactions between groups such as: hydrogen bonding, volumetric or steric clashes (representative

SAR was performed on the remaining 19 compounds excluding the *ortho*-substituted molecules from the library. By removing the *ortho*-substituent groups from the full data set, the R^2 value increase marginally from 0.0553 to 0.1071 (Fig. 5.2a and 5.3a) and 0.2795 to 0.4513 (Fig. 5.2b and 5.3b). This clearly indicates that excluding the *ortho*-substituted group of compounds from the library has generated a slightly better relationship between the activity and physicochemical properties of the compounds. Although some improvement would be expected since the number of compounds included in this data set is lower compared to the Figure 5.2. This suggests that a volumetric 'clash' between the *ortho* group and the proton of the β -carbon may be important in compound potency. So, there is probably some interaction between the *ortho*-substituent and one or more of the hydrogen atoms present on either of the olefinic carbon or methylene group of N-methylpiperidin-4-one or cycloalkanones. In addition, it is obvious that the biological activity of this group of compounds has a better correlation with the electronic term electron density compared to the lipophilicity. This suggests that the electrophilicity of the β -carbon of 1,4-diene-3-ones is important for the inhibitory activity of these compounds.

SAR analysis of the bis-benzylidene derivatives of N-methylpiperidin-4-one was performed to determine which substituent (or position of substituent) is giving rise to correlation between the inhibitory activity and lipophilic or electrophilic parameters. This dataset contains only 18 compounds, these being **22a-k** and **22m-t**, respectively.

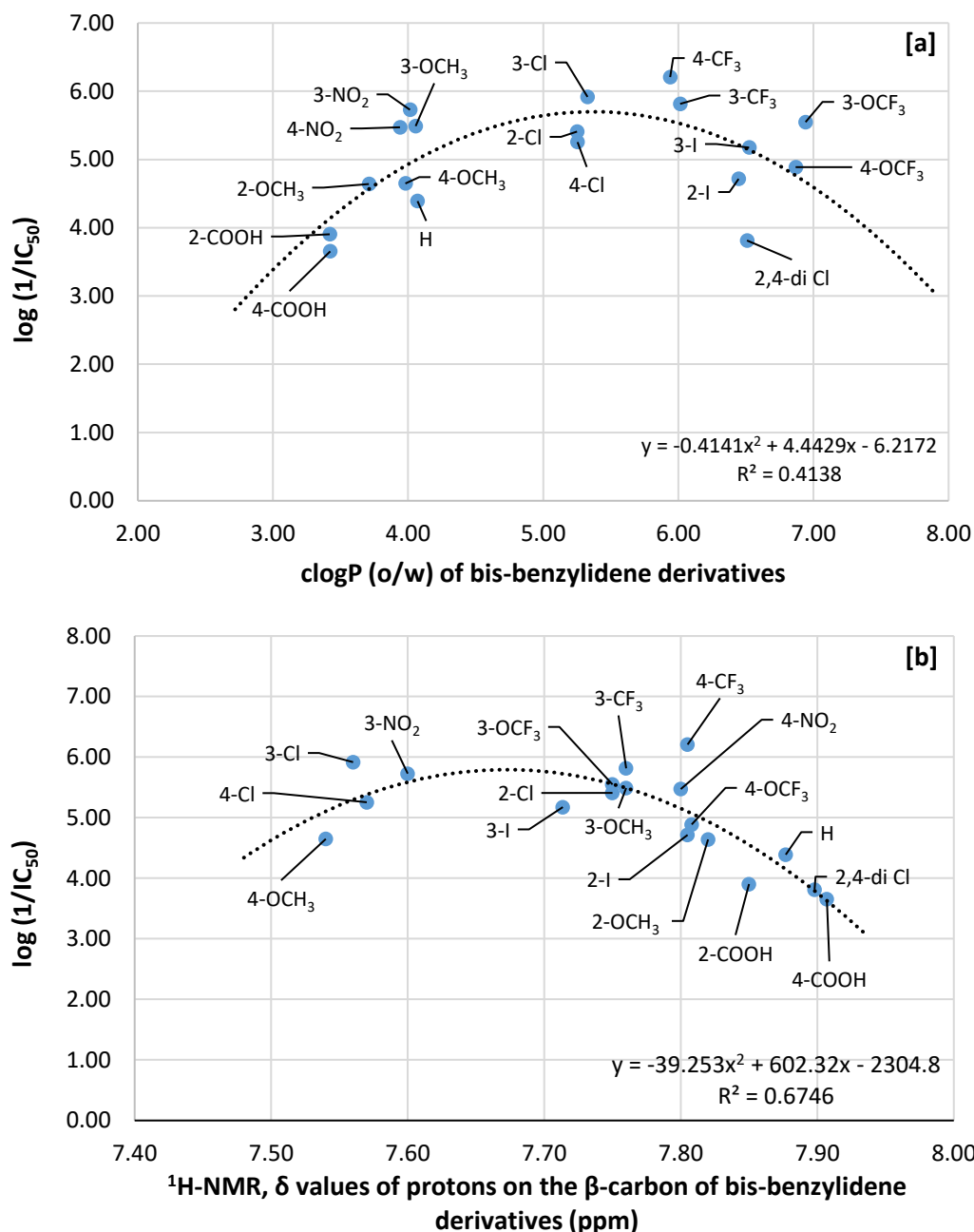


Figure 5. 4. SAR of $\log(1/IC_{50})$ against clogP [a] and $\log(1/IC_{50})$ against the δ -values of protons on the β -carbon [b] of bis-benzylidene derivatives of *N*-methylpiperidin-4-one.

A better fit was obtained when bis-benzylidene derivatives of *N*-methylpiperidin-4-one compounds were analysed for both the lipophilic and electronic properties. Additionally, SAR of $\log(1/IC_{50})$ vs clogP shows a hyperbolic curve with a significant improvement in the correlation coefficient value, these being 0.4138 in Figure 5.4[a] whereas previous two SAR in both the Figure 5.2[a] (full data set) and Figure 5.3[a] (excluding *ortho*-substituents)

presented a parabolic curve. This could be due to compounds with different functionalities have been grouped together in one data set and analysed as shown in Figure 5.2 and 5.3 [a].

On the other hand, the SAR derived from filling $\log(1/IC_{50})$ and δ -values of protons on the β -carbon of bis-benzylidene derivatives of N-methylpiperidin-4-one displayed a substantial increase in the correlation coefficient value, ($R^2 = 0.6746$; Fig 5.4b) which demonstrates a significant relationship between the activity and the electronic property. This suggests that bis-benzylidene derivatives of N-methylpiperidin-4-one were dependent on the electrophilicity of the β -carbon for their activity against *S. cerevisiae*. Lipophilicity has some influence but it does not appear to play a major role in the activity of this class of compounds.

The higher correlation coefficient for this group of compounds is possibly due to the presence of the nitrogen atom in the central ring, which is believed to cause an increase in the solubility of the compound based on clogP values and decrease the likelihood of molecules forming aggregates. If cyclopentanone or cyclohexanone derivatives were included in these data sets then the R^2 values decreases significantly, therefore these compounds were removed for this particular analysis.

Certain isomeric pairs of compounds with substituents such as 3-chloro or 4-chloro, 3-trifluoromethyl or 4-trifluoromethyl, 3-trifluoromethoxy or 4-trifluoromethoxy, 3-nitro or 4-nitro were very close together. These compounds were associated very well with their clogP irrespective of their position, whether is at *meta* or *para* their clogP values were similar. This is consistent with many other studies (Hansch & Leo, 1979). Therefore, if there was a major difference between compounds then it could be due to the structural property of these isomeric sets of compounds. The low differences here are unlikely due to the positioning of those particular groups. However in the correlation plot of $\log(1/IC_{50})$ against the δ -values of

activity and lipophilic/electronic properties of compounds. Figure 5.5[a] shows moderate relationship between the activity $\log(1/IC_{50})$ and clogP with a correlation coefficient of 0.5312, which is slightly better than previous SAR (including *ortho*-substituted compounds). In contrast, SAR of $\log(1/IC_{50})$ and δ -values of proton on the β -carbon of these compounds depict a reasonably good relationship with a correlation coefficient of 0.6286 (Figure 5.5b). It has been observed that removing compounds having an *ortho*-substituent from the data set give rise to a better relationship between activity and lipophilicity. However it should be noted that simply decreasing the number of compounds in a data set will, for fundamental mathematical and statistical reasons give rise to some improvement in the R^2 value. The presence of an *ortho*-substituent potentially twists the aromatic rings out of a 2D plane. However, the relationship between activity and the electrophilic parameter showed a slight deviation in the R^2 values. This could be due to the fact that substituents such as 2-iodo, 2-chloro and 2,4-dichloro were very close to the hyperbolic curve and removal of these has shown some effect on the correlation coefficient.

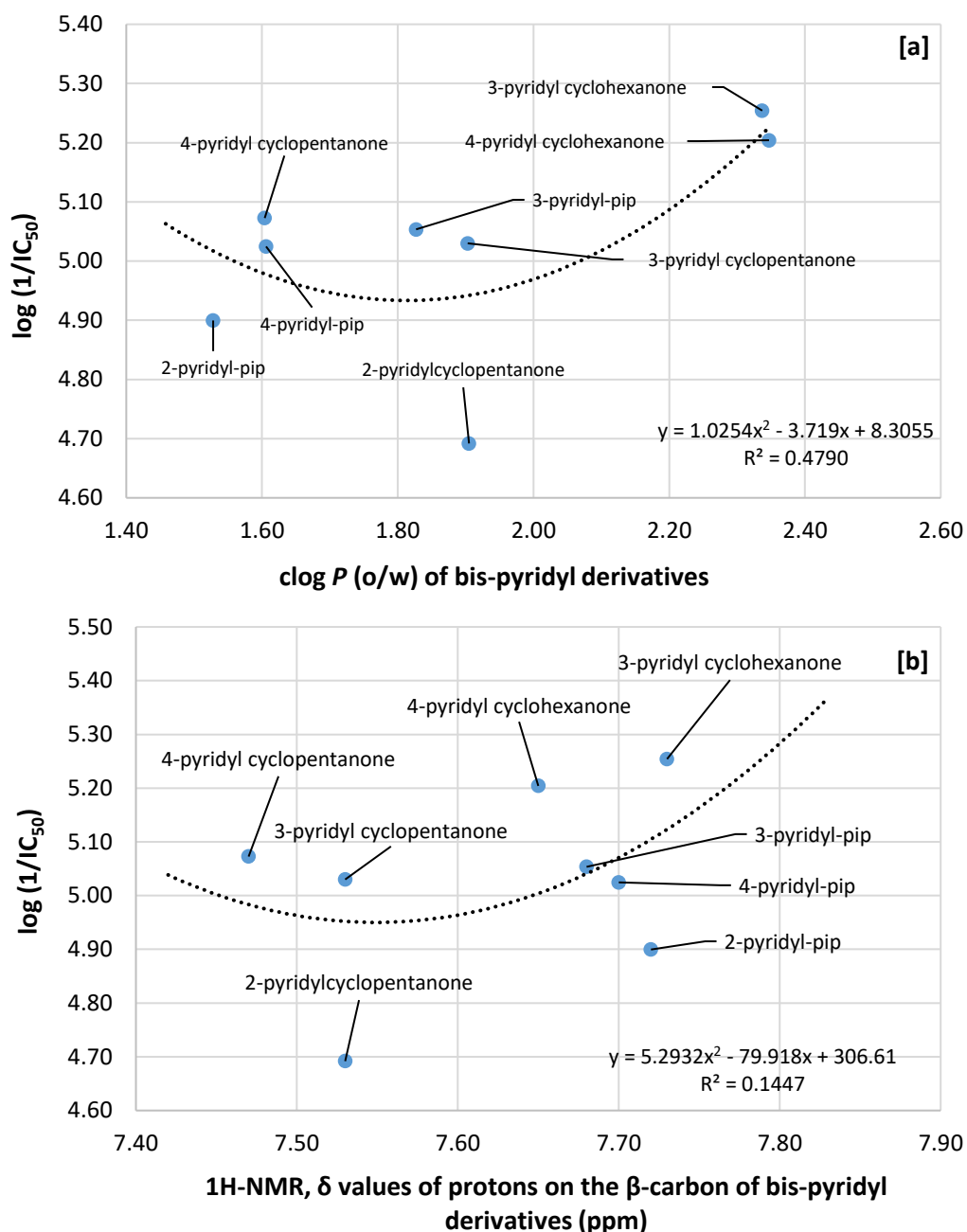


Figure 5. 6. SAR of $\log(1/IC_{50})$ against $\text{clog } P$ [a] and $\log(1/IC_{50})$ against the δ -values of the proton on the β -carbon [b] of bis-pyridylidene derivatives of *N*-methylpiperidin-4-one and cycloalkanones.

SAR of bis-pyridylidene derivatives of *N*-methylpiperidin-4-one and cycloalkanones showed a better relationship between the activity and lipophilic property rather than with electrophilicity (Figure 5.6[a, b]). However, both of these figures shows a hyperbolic curves, with poor to medium fitting even though the number of compounds used was quite small (8

compounds). Compounds containing pyridine rings are known to increase the solubility of the homologs compounds and the clogP values of this group of compounds suggests that the activity of these compounds should correlate better with their lipophilic properties. The correlation coefficient of the $\log(1/IC_{50})$ vs clogP plot ($R^2 = 0.4790$) was greater than $\log(1/IC_{50})$ vs δ -values of proton on the β -carbon ($R^2 = 0.1447$). This is exactly the opposite of what is found in the other plots suggesting that inhibition linked to the extended time period of growth assays possibly involves a complex series of interactions.

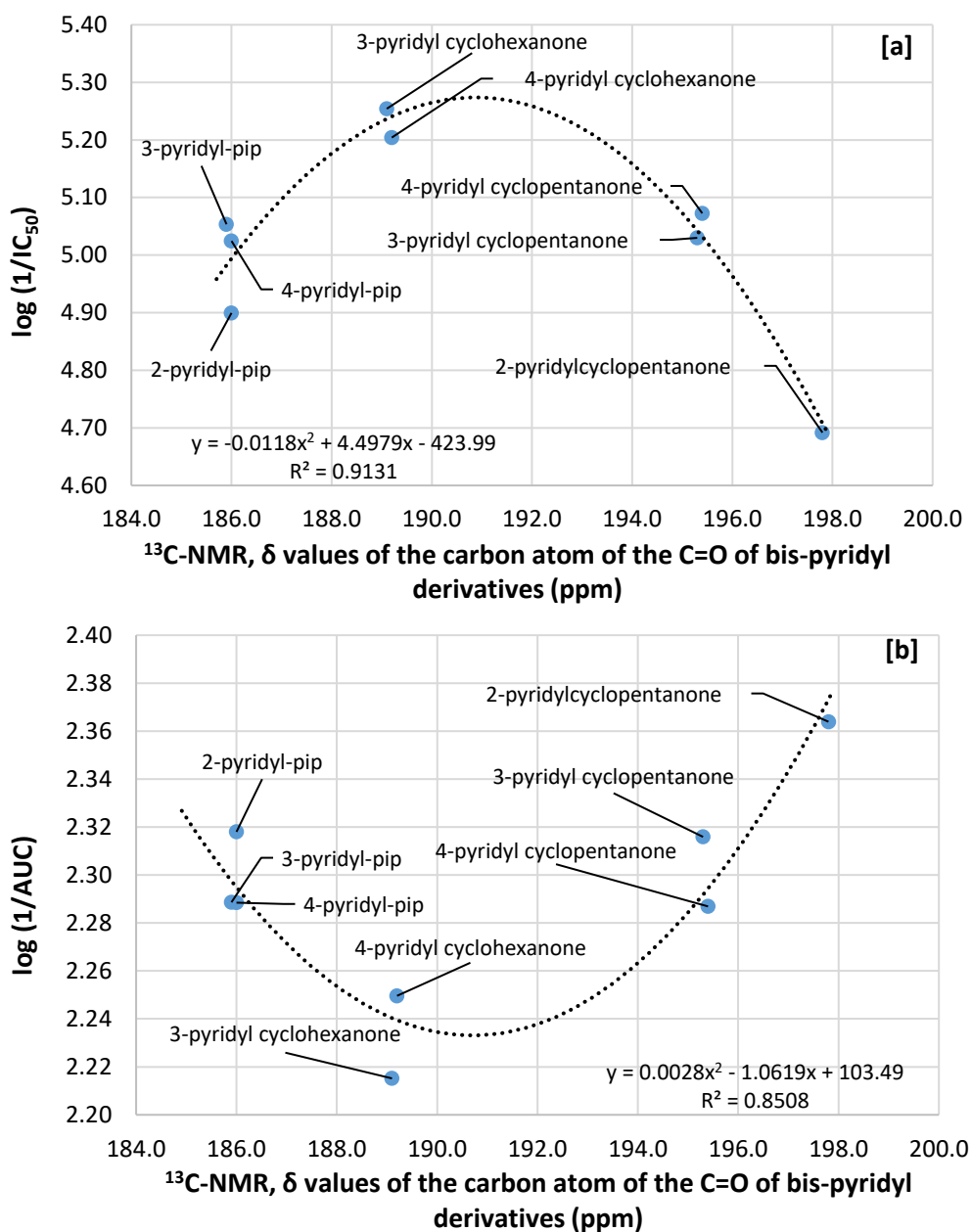


Figure 5. 7. SAR of $\log(1/IC_{50})$ against the δ -values of the carbon atom of the carbonyl [a] and $\log(1/AUC)$ against the δ -values of the carbon atom of the carbonyl [b] of bis-pyridylidene derivatives of *N*-methylpiperidin-4-one and cycloalkanones.

The pyridyl derivatives of compounds showed poor correlation between $\log(1/IC_{50})$ and the δ -values of the proton on the β -carbon atom in Figure 5.6[b] therefore further SAR was conducted using the δ -values of the carbonyl carbon atom as another electronic descriptor. Attempts to model $\log(1/IC_{50})$ and $\log(1/AUC)$ against δ -values of the carbon atom of the carbonyl gave totally different results yielding a parabolic curve in Figure 5.7[a] and an inverse

parabolic curve in Figure 5.7[b]. However SAR in both cases displayed a very good relationship between the activity of compounds and carbonyl group with high R^2 values (0.9131 and 0.8508). This suggests that carbonyl group have some influence on the activity of this set of compounds. In order to attempt to understand the different plots shown in Fig. 5.7, the correlation analysis of two inhibition parameters $\log(1/AUC)$ and $\log(1/IC_{50})$ for the full data set of various 1,4-diene-3-ones containing 31 compounds were plotted (Figure 5.8).

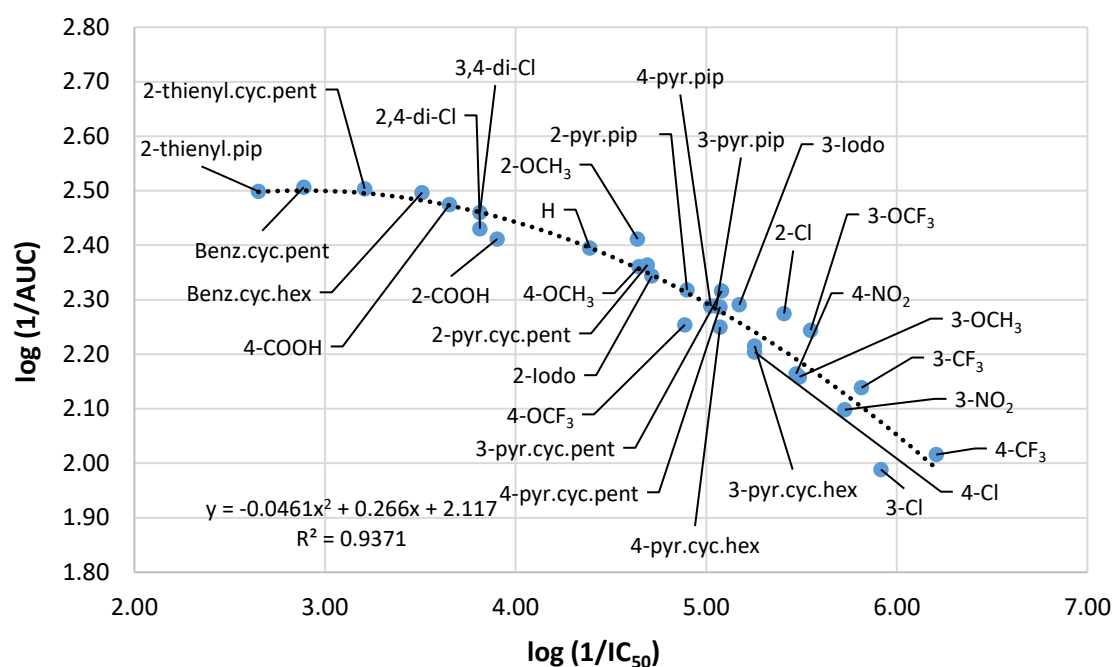


Figure 5. 8. Comparison of $\log(1/AUC)$ with $\log(1/IC_{50})$ of the 1,4-diene-3-ones against *S. cerevisiae* (full data set containing 31 compounds).

The above Fig 5.8 depicts a significant relationship between the two inhibition parameters analysed using either the second order polynomial equation ($R^2 = 0.9371$) or the linear equation ($R^2 = 0.8523$, graph not shown). In addition the bis-benzylidene derivatives of N-methylpiperidin-4-one and bis-benzylidene derivatives of N-methylpiperidin-4-one demonstrated a good relationship between the $\log(1/IC_{50})$ and $\log(1/AUC)$ with an R^2 value of 0.9092 and 0.8989 (Graphs not shown). To gain better understanding regarding the similarities or difference between the inhibitory parameters, AUC and IC_{50} values further

correlation plot was constructed using $1/(\log (1/AUC))$ vs $\log (1/IC_{50})$ and this gave an R^2 of 0.8098 for linear equation and R^2 of 0.9267 for second order polynomial equation. Similarly correlation plot of $\log (1/AUC)$ vs $1/(\log (1/IC_{50}))$ gave an R^2 of 0.6977 for linear equation and R^2 of 0.8986 for second order polynomial equation. In all cases, the second order polynomial equation gave better R^2 values compared to the linear equation. This confirms that data generated in different ways from the susceptibility assays were reliable and robust.

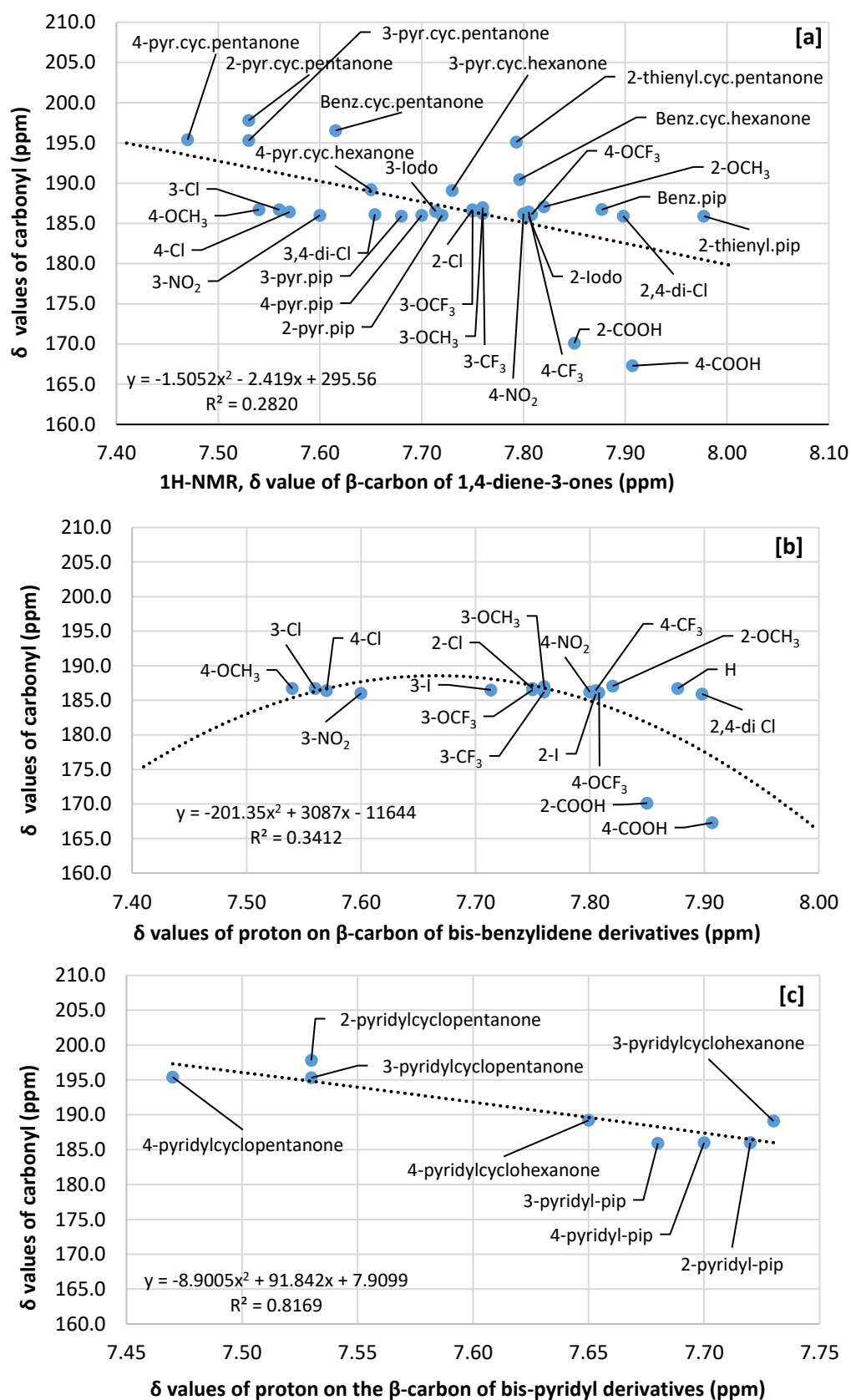


Figure 5. 9. Comparison of the δ -values of the carbon atom of the carbonyl with the δ -values of the proton on the β -carbons; full data [a], bis-pyridylidene derivatives of *N*-methylpiperidin-4-one [b] and bis-pyridylidene derivatives of *N*-methylpiperidin-4-one and cycloalkanones [c].

The correlation plots of the δ -values of proton on the β -carbons with the δ -values of the carbon atom of the carbonyl group was performed to compare the relationship between these two electronic parameters (Figure 5.9). The correlation plot of full data sets includes 31 compounds showed a poor correlation coefficient with R^2 of 0.2820 (Fig. 5.9a). Subsequently correlation plot was constructed again by removing any compounds with Hill slope greater than 2.0 from the data set to decrease the influence of molecular aggregation on the analysis (therefore only 23 compounds were analysed) and this resulted in an increase in the R^2 value (0.3988). However this is still a low level of correlation. The information obtained from the chapter 3 suggest that the inhibitory action of compounds having high Hill slopes is possibly enhanced in a non-specific fashion due to the level of aggregation of the molecules. The above correlation plot indicates that those compounds with high Hill slope showed a 1.5 fold increase in the R^2 value.

The correlation plot of bis-benzylidene derivatives of N-methylpiperidin-4-one (18 compounds) gave an R^2 value of 0.3412. It is expected that the correlation of the δ -values of the proton and the δ -values of the carbon atoms of the carbonyl should be close to linear thus giving a good correlation of data. However in this case such a correlation was not observed. This could be because in the full data set (Fig 5.9a) three different functionalities have been grouped together and analysed which resulted in low R^2 value in figure 5.9[b]. This is probably due to the δ -proton being associated with the point of reaction whereas the ^{13}C of the carbonyl is not associated with the reaction centre.

Interestingly in figure 5.9[c], the bis-pyridylidene derivatives of N-methylpiperidin-4-one and cycloalkanones (only 8 compounds) displayed very good correlation with R^2 value of 0.8169. This could be due to a low numbers of compound being analysed in the data sets. In addition,

compounds analysed in this plot (Fig 5.9c) were aggregators as all of them (**23a-h**) have a Hill slope greater than 1.

SAR analyses of various 1,4-diene-3-ones describing the relationships between the activity with lipophilicity and electrophilicity were shown in **Table 5.3**, page 198. Only two parameters have been used to generate SAR these being clogP and electrophilicity as defined by $^1\text{H-NMR}$ although many more are available in the programme MOE. Bis-benzylidene derivatives of N-methylpiperidin-4-one shown a reasonably good relationship between $\log(1/\text{IC}_{50})$ and the δ -values of proton on the β -carbons ($R^2 = 0.6746$). However SAR of this group of compounds for $\log(1/\text{IC}_{50})$ against clogP generated a correlation coefficient of only 0.4138. This collective information suggests that the inhibitory activity of bis-benzylidene derivatives of N-methylpiperidin-4-one is predominantly dependent on the electronic property of this class of compounds. In addition this group of compounds demonstrated a good relationship between the two selected activity parameters namely $\log(1/\text{IC}_{50})$ and $\log(1/\text{AUC})$ with an R^2 value of 0.9092.

SAR analysis of the δ -values of proton on the β -carbons against the δ -values of carbonyl displayed good relationship for bis-pyridylidene derivatives ($R^2 = 0.8169$) but this was for a very small subset of compounds. SAR of the full data set or bis-benzylidene derivatives gave a poor correlation coefficient ($R^2 = 0.2820$ and 0.3412 respectively). Even when SAR was performed by excluding *ortho*-group of compounds from both the full data set or the bis-benzylidene derivatives the improvement in the correlation coefficient values obtained were limited ($R^2 = 0.4364$ and 0.5558).

SAR of bis-pyridylidene derivatives of N-methylpiperidin-4-one and cycloalkanones for $\log(1/\text{IC}_{50})$ against clogP generated a reasonable relationship with an R^2 of 0.4790 but a very poor

correlation for $\log(1/IC_{50})$ against the δ -values of proton on the β -carbons ($R^2 = 0.1447$). This suggests that the inhibitory activity of bis-pyridylidene derivatives of N-methylpiperidin-4-one and cycloalkanones is highly dependent on its lipophilic property rather than electrophilic. This appear to be contrary to the previous data when electrophilicity appear to be dominant. This difference may be due to the pyridyl derivatives being more soluble (but aggregating an effect confirmed by the high Hill coefficients) than their phenyl equivalents (which showed less aggregating effect confirmed by their lower Hill coefficient values).

Table 5. 3. Comparison of the correlation coefficients of the lipophilic and electronic parameters of various 1,4-diene-3-ones with the inhibitory activities obtained from *S. cerevisiae* study.

List of various correlation analyses	Correlation coefficient (R ²)				
	Full dataset with 31 compounds	Reduced dataset - excluding <i>ortho</i> substituents (19 compounds)	Bis-benzylidene derivatives of N-methylpiperidin-4-one (18 compounds)	Bis-benzylidene derivatives of N-methylpiperidin-4-one (Excluding <i>ortho</i> substituents - 13 compounds)	Bis-pyridylidene derivatives of N-methylpiperidin-4-one and cycloalkanones (8 compounds)
log (1/IC ₅₀) vs clogP	0.0553	0.1071	0.4138	0.5312	0.4790
log (1/IC ₅₀) vs δ -value of olefinic proton	0.2795	0.4513	0.6746	0.6286	0.1447
log (1/IC ₅₀) vs δ -value of ¹³ C of C=O	0.1828	0.2783	0.3777	0.4933	0.9131
log (1/AUC) vs clogP	0.0208	0.1318	0.3809	0.5004	0.6416
log (1/AUC) vs δ -value of olefinic proton	0.1791	0.2363	0.4493	0.4014	0.3034
log (1/AUC) vs δ -value of ¹³ C of C=O	0.1875	0.2906	0.2221	0.3273	0.8508
log (1/AUC) vs log (1/IC ₅₀)	0.9371	0.8906	0.9092	0.9102	0.8989
δ of ¹³ C of C=O vs δ value of olefinic proton	0.2820	0.4364	0.3412	0.5558	0.8169
δ -value of olefinic proton vs clogP	0.1183	0.1230	0.2692	0.2747	0.2749
clogP vs δ -value of olefinic proton	0.1183	0.1230	0.2692	0.2747	0.2749
clogP vs δ -value of ¹³ C of C=O	0.0634	0.1628	0.4730	0.4254	0.2640

5.4 Discussion – Structure-activity relationship

The antifungal properties of the 1,4-diene-3-one compounds were compared using structural and physicochemical features to establish the relative importance of either hydrophobicity, or electron density at the β -carbons. Two parameters namely lipophilic (expressed as clogP) and the electrophilic parameter (expressed as the δ -value of proton on the β -carbon) of 1,4-diene-3-ones were selected to use in the analysis although many other parameters are also available from MOE software. Similarly, the IC_{50} and area under the curve (AUC) for each compound were selected as their biological activity obtained from the macro-broth susceptibility assay against *S. cerevisiae*.

The reason for selecting IC_{50} as one parameter is that most of the compounds gave 50% inhibition of growth of *S. cerevisiae*. However measurement of the IC_{50} alone can often give ambiguous results. As mentioned by Odds & Abbott, (1984) that by measuring the AUC, better reproducibility of the inhibitory potency of compounds can be obtained. Therefore, AUC of each compound was used as a second parameter to possibly identify any differences between compound potency.

For SAR analysis, compounds which shown greater than 50% inhibition of *S. cerevisiae* growth in the macro-broth susceptibility assay were selected. Therefore only 31 compounds (**22a-k**, **22m-v**, **23a-h** and **24a-b**) were analysed. The correlation coefficient (R^2) values from the correlation analysis of $\log(1/\text{IC}_{50})$ vs clogP and $\log(1/\text{IC}_{50})$ vs δ -value of proton on the β -carbon of 1,4-diene-3-ones were poor (0.0553 and 0.2795). However, the difference between lipophilic and electronic properties was very high in terms of their R^2 values. This evidence suggests that the electrophilic property of 1,4-diene-3-ones play a significant role in the inhibitory action of these compounds rather than the lipophilicity. This simply suggests that

the electron density (or lack thereof) at the β -carbon of 1,4-diene-3-ones is important in potency.

The Hammett equation sometimes fails when substituents and reaction centres have the potential to interact with each other such as an *ortho* substituents (Hansch & Leo, 1979). Taking this point into consideration further investigation was performed by arranging the library of compounds into several groups as mentioned in the result **section 5.3** and their values were displayed in **Table 5.3**, page 198. Based on the possibility that the *ortho*-substituted groups may interact either with the hydrogen atom present on either of the β -carbons or the methylene group at position 2 or 5 in the N-methylpiperidin-4-one group (or equivalently in cyclopentanone or cyclohexanone) and interact or 'clash'. Consequently, compounds that contain an *ortho*-substituent group were removed from the data set and the remaining 19 compounds (**22a**, **22c-d**, **22f-g**, **22k**, **22m-p**, **22r-t**, **23b-c** and **23e-h**) analysed. Correlation analysis of $\log(1/IC_{50})$ vs clogP gave an R^2 value of 0.1071 whereas for $\log(1/IC_{50})$ vs δ -value of proton on the β -carbon of 1,4-diene-3-ones gave an improved R^2 value of 0.4513. The correlation coefficient values for $\log(1/IC_{50})$ vs δ -value or proton on the β -carbon of 1,4-diene-3-ones data set has shown a considerable increase in the correlation coefficient compared to the full data set. This indicates that *ortho*-substituents may have secondary effects related to the atom or atom 'clashes' with consequential distortion of the molecule. However the R^2 value of 0.4513 indicating that the correlation between biological activity and electrophilicity is still less than 50%, therefore further SAR was performed using reduced a data set.

Further SAR was conducted on a sub-group containing the bis-benzylidene derivatives of N-methylpiperidin-4-one (18 compounds, **22a-k** and **22m-t**). This has shown an improvement in

the correlation coefficient ($R^2 = 0.4138$) for the correlation plot between $\log(1/IC_{50})$ and clogP . On the other hand, the correlation analysis of $\log(1/IC_{50})$ vs the δ -value of proton on the β -carbon of bis-benzylidene derivatives of N-methylpiperidin-4-ones gave a good correlation coefficient ($R^2 = 0.6746$). This sub-set of data has shown significant improvement in the correlation and it clearly implies that the electrophilic property of bis-benzylidene derivatives of N-methylpiperidin-4-ones plays an important role in their inhibitory activity against *S. cerevisiae*.

Reanalysis of $\log(1/IC_{50})$ against clogP plot of bis-benzylidene derivatives of N-methylpiperidin-4-ones by removing *ortho*-substituted groups has shown a slight improvement in the correlation coefficient ($R^2 = 0.5312$) as compared to the SAR of data with *ortho*-substituted groups gave the $R^2 = 0.4138$. This possibly suggests some form of atomic 'bumping' causing distortion from the molecular plane may be occurring and *in silico* model building may prove useful in this context. Similarly SAR of bis-benzylidene derivatives of N-methylpiperidin-4-ones excluding compounds with *ortho*- groups gave a correlation coefficient of 0.6286, which was slightly lower than the R^2 value of compounds including *ortho*- groups. The reason for this decrease in R^2 is unclear.

However, the SAR analysis of $\log(1/AUC)$ against clogP or the δ -value of proton on the β -carbon gave a slightly lower correlation values for bis-benzylidene derivatives of N-methylpiperidin-4-ones whether analysed both with or without *ortho*-substituents, the R^2 being 0.3809 (including *ortho*-substituted compounds) or 0.5004 (excluding *ortho*-substituted compounds). Similarly the correlation coefficient values for $\log(1/AUC)$ vs δ -values of proton were 0.4493 (including *ortho*-substituents) and 0.4014 (excluding *ortho*-substituents). Differences between the correlation coefficient values of the SAR data of $\log(1/IC_{50})$ and

equivalent $\log(1/\text{AUC})$ is because the IC_{50} values obtained manually at the point of inflection (50%) of the dose-response curve whereas AUC includes a rectangle portion of the curve between two sets of concentrations.

Given the differences in the SAR results in *S. cerevisiae* of both $\log(1/\text{IC}_{50})$ and equivalent $\log(1/\text{AUC})$. A correlation plot of the two inhibitory parameters was performed to identify any possible differences between $\log(1/\text{AUC})$ and $\log(1/\text{IC}_{50})$. These two inhibitory parameters correlated significantly with each other. Cross-correlation of the IC_{50} with AUC was conducted on various subsets of data including: (1) the full data set of 31 compounds ($R^2 = 0.9371$), (2) compounds excluding *ortho*-substituents from full data set ($R^2 = 0.8906$), (3) the bis-benzylidene derivatives of N-methyl-piperidin-4-one including *ortho*-substituents ($R^2 = 0.9092$), (4) set 3 excluding compounds with *ortho*-substituents ($R^2 = 0.9102$) and (5) the bis-pyridylidene derivatives of N-methylpiperidin-4-one and cycloalkanone ($R^2 = 0.8989$). Given the high R^2 values between $\log(1/\text{AUC})$ and $\log(1/\text{IC}_{50})$, it is not obvious why the differences in the R^2 values for the previous data analysis are occurring.

In contrast SAR of bis-pyridylidene derivatives of N-methylpiperidin-4-one and cycloalkanones for $\log(1/\text{IC}_{50})$ vs clogP gave a correlation coefficient of 0.4790 whereas SAR of $\log(1/\text{IC}_{50})$ vs δ -value of the olefinic proton on the β -carbon gave a correlation coefficient of 0.1447. Similarly SAR of $\log(1/\text{AUC})$ against clogP of bis-pyridylidene derivatives of N-methylpiperidin-4-one and cycloalkanones gave an R^2 of 0.6416 while $\log(1/\text{AUC})$ vs clogP gave an R^2 of 0.3034. This demonstrates that the activity of pyridine containing compounds is influenced by solubility/lipophilicity rather than the electrophilic property of this class of compounds.

SAR studies in *S. cerevisiae* revealed that the antifungal activity of the 1,4-diene-3-ones is dependent on structural features including the presence of a heterocyclic moiety, the nature of the substituents attached to the aromatic rings and their associated effects particularly due to the electrophilicity of the β -carbon atom. High antifungal activity of 1,4-diene-3-ones against *S. cerevisiae* appears to be due to the presence of a strong electron-withdrawing group such as $-\text{CF}_3$, $-\text{OCF}_3$, $-\text{NO}_2$ or $-\text{Cl}$ on the aromatic ring of bis-benzylidene derivatives of N-methylpiperidin-4-one. In contrast, the presence of electron donating group (e.g. $-\text{CH}_3$) on the aromatic rings of bis-benzylidene derivatives of N-methylpiperidin-4-one leads to a decrease in the potency of the compounds. It has been reported previously in the QSAR study on chalcones that presence of that EDG on the aromatic rings of chalcones shown reduction in the antifungal activity (Sivakumar *et al.*, 2009).

5.5 Conclusions – Structure-activity relationship

Analysis of the various sub-sets of 1,4-diene-3-ones demonstrates that the electrophilic nature of the β -carbon on the compounds (**22a-k**, **22m-v**, **23a-h** and **24a-b**) is important in modulating the antifungal activity of this class of compounds (Sivakumar *et al.*, 2009). This is consistent with what has been observed with chalcones and another class of cysteine reactive enone compounds. SAR analysis of $\log(1/IC_{50})$ vs δ -values of proton on the β -carbon of bis-benzylidene derivatives of N-methylpiperidin-4-one gave a significantly higher correlation coefficient ($R^2 = 0.6746$) compared to the plot of $\log(1/IC_{50})$ vs clogP ($R^2 = 0.4138$). This suggests that the inhibitory activity of bis-benzylidene derivatives of N-methylpiperidin-4-one was influenced by the electronic rather than the lipophilic descriptor. The poor R^2 value of $\log(1/IC_{50})$ vs clogP suggests that other properties beside hydrophobicity are important for the activity of these compounds (**22a-k**, **22m-v**). This includes, but is not limited to the electrophilicity of the reacting carbon and volumetric constituents (not analysed). Based on the changes in R^2 values, when ortho-substituted compounds were removed from the data set it was believed that the improvement in R^2 was due to the removal of compounds that might give rise to stereo-chemical or volumetric bumping.

SAR of bis-pyridylidene derivatives of N-methylpiperidin-4-one and cycloalkanones exhibited hyperbolic curves for both plots in Figure 5.6 between $\log(1/IC_{50})$ vs δ -values of proton and $\log(1/IC_{50})$ vs clogP , their correlation coefficient values being 0.1447 and 0.4790 respectively. This indicates that the activity of the pyridyl derivatives were dependent on lipophilicity rather than electronic property. This speculatively suggests that the pyridyl group of compounds may be facilitating the targeting of multiple sites of the enzyme, multiple enzymes or causing some change(s) in cellular morphology.

Although improvement in the R^2 values were obtained when analysing subsets of compounds some (or even all) of this improvement may simply be due to the decrease in the size of the data set. In order to determine if such problem exist it would be necessary to study the distribution of individual residuals across the graphs and to perform more complex statistical analyses. Additionally further compounds would need to be synthesized in order to bring the data sets to the same size thus eliminating potential 'improvements' caused by different group sizes.

In conclusion, it has been identified that the two activity parameters, $\log(1/IC_{50})$ and $\log(1/AUC)$ correlate well with each other with excellent R^2 values for all data sets analysed. However the correlation analysis of $\log(1/IC_{50})$ vs clogP and $\log(1/IC_{50})$ vs δ -values of proton showed better fit of the data compared to the SAR of $\log(1/AUC)$ vs clogP and $\log(1/AUC)$ vs the δ -values of proton. This suggests that $\log(1/IC_{50})$ is a better parameter than $\log(1/AUC)$ when constructing SAR relationships for this class of compounds. Given that $\log(1/IC_{50})$ correlates well ($R^2 = 0.9371$) with $\log(1/AUC)$ for full data set of 1,4-diene-3-ones, the reason for the difference in correlation when comparing each inhibitory parameter with the δ -values of proton is unclear and requires further investigation.

Most of the sub-set of 1,4-diene-3-one analysed for SAR using either $\log 1/IC_{50}$ or $\log 1/AUC$ demonstrated decreased correlations suggesting that the 1,4-diene-3-one compounds may have poly-pharmacological effect (i.e. it may be affecting more than one system). However, SAR of the 1,4-diene-3-one compounds also suggests that the β -carbon electron density (or lack thereof) is a good predictor of potency.

CHAPTER SIX

GENERAL DISCUSSIONS AND CONCLUSIONS

6 General discussions and conclusions

Over the past twenty years, many pathogenic fungi have developed various forms of resistance to currently available clinically used antifungal agents (Chakrabarti, 2011; Cannon & Holmes, 2015; Schelenz *et al.*, 2016; Zhao *et al.*, 2016; Canela *et al.*, 2018). Although there has been an increase in the number of antifungal agents available both in a class (e.g. triazoles) or of novel classes (e.g. echinocandins), the choice of a suitable antifungal agent remains limited. This limitation is due to poor pharmacokinetics, pharmacodynamics and toxicological profiles of many of the presently used antifungal agents. There is thus an increased interest, and need, for the identification of novel drug targets within the mycota, along with the development of novel antifungal drug structures targeted to these targets.

Using various molecular biological techniques the fungal PM H⁺-ATPase has been identified as a potential antifungal drug target (Portillo, 2000). Although identified as a potential drug target some twenty years ago there has been, until recently, very limited attempts to develop drugs targeted to this enzyme (Seto-Young *et al.*, 1997; Dao *et al.*, 2016; Kjellerup *et al.*, 2017; Tung *et al.*, 2018). The PM H⁺-ATPase enzyme has been shown to be inhibited by various thiol-reactive compounds such as maleimides, omeprazole, curcumin, chalcones, ebselen, caffeic acid and other α,β -unsaturated carbonyls (Brooker & Slayman, 1982; Monk *et al.*, 1995; Manavathu *et al.*, 1999; Batovska *et al.*, 2007; Chan *et al.*, 2007; Dao *et al.*, 2016). An α,β -unsaturated carbonyl is electrophilic in nature and therefore it is readily attacked by a nucleophile. However the cysteine containing antioxidant glutathione commonly prevents damage to cellular components by reacting with electrophiles since it contains a sulfhydryl group which acts as a nucleophile and attacks the β -carbon of α,β -unsaturated carbonyl compounds (Das *et al.*, 2007).

The pharmaceutical and agrochemical industries have, over the last two decades, shown significant interest in bis(substituted-benzylidene)cycloalkanones as therapeutic and agrochemical agents (Amoozadeh *et al.*, 2011). It has also been identified that various enone compounds such as styryl ketones, dienones or curcumin exhibit low toxicity to mammalian cells (Manavathu *et al.*, 1999; Dao *et al.*, 2016; Kjellerup *et al.*, 2017). The aim of this study was to investigate compounds with the potential to inhibit the fungal PM H⁺-ATPase enzyme in the cell. Given the general safety of chalcones and related compounds (Dimmock *et al.*, 1998; Manavathu *et al.*, 1999) it was decided to synthesize a library of 1,4-diene-3-ones containing 33 symmetrical compounds (**22a-v**, **23a-h**, and **24a-c**). These compounds were synthesized as described in Chapter 2. Certain compounds in the library have a heterocyclic ring containing a nitrogen atom either in the aromatic ring present at either the *ortho*, *meta* or *para*-position or in the central piperidone ring. The presence of nitrogen atom has shown an increase in the amphipathicities of such compounds.

In this research work, 3,5-bis(3-nitrobenzylidene)-1-methylpiperidin-4-one (**22s**) and 3,5-bis(4-nitrobenzylidene)-1-methylpiperidin-4-one (**22t**) have been successfully synthesized using the method described by El-Subbagh *et al.*, (2000). The synthesis of 3,5-bis(2-nitrobenzylidene)-1-methylpiperidin-4-one has not previously been reported in the literature. In this study, various attempts were made to synthesize 3,5-bis(2-nitrobenzylidene)-1-methylpiperidin-4-one using variations of the Claisen-Schmidt reaction. However, we were unsuccessful in synthesizing this compound and the desired product was not obtained. The reasons for this are still unclear.

The inhibitory potencies of the synthesized compounds (**22a-v**, **23a-h** and **24a-c**) were investigated by conducting *in vitro* macro-broth susceptibility assays against *S. cerevisiae* and

C. albicans (described in Chapter-3). Significant levels of antifungal activity were seen for most of the compounds tested against *S. cerevisiae* (0.2 to 99% growth inhibition) over the range of concentration tested. However, compounds **22a-v**, **23a-h** and **24a-c** exhibited considerably less potency when screened against *C. albicans* although the levels of inhibition displayed still covered the range 0 to 99% inhibition.

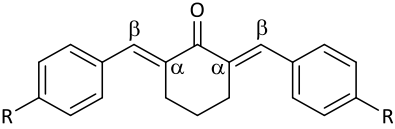
Certain compounds (**22c**, **22e**, **22f**, **22g**, **22m**, **22n**, **22o**, **22r**, **22s**, **22t**, **23b**, **23c** and **23e-h**) exhibited very good potency against *S. cerevisiae* with IC₅₀ values between 0.62 and 9.45 μM (**Table 3.1**, page 105). The higher potency of these compounds is due to the presence of EWG at either *meta* or *para*-position of the aromatic ring which increases the electrophilicity of the β-carbon thus making it more reactive to nucleophiles such as the sulfhydryl of cysteine which reacts via a Michael addition reaction (Dao *et al.*, 2016). In addition, compounds **23b**, **23c** and **23e-h** exhibited high potency due to the presence of pyridine ring. This increase in potency is probably due to an increase in solubility in both aqueous and organic systems and thus there is a probable increase in the bioavailability of these compounds although this remains to be confirmed (Moore *et al.*, 2014).

Other compounds (**22a**, **22b**, **22d**, **22p**, **22q**, **23a** and **23d**) were identified as moderate inhibitors of *S. cerevisiae* with their IC₅₀ values ranging from 10 to 100 μM. Most of the compounds in this group have electron-donating group attached to the aromatic rings which makes the β-carbon less electrophilic and therefore less reactive, except **22q**; iodo (EWG), **23a** and **23d** that contain pyridine rings. Compound **22q** is likely to be less effective than bromo or chloro equivalent isomers due to its higher electronegativity. In contrast, compounds **22h-l**, **22u-v** and **24a-b** exhibited lower inhibitory activity against *S. cerevisiae* growth (IC₅₀ values >100 μM).

The most potent compound identified from the 1,4-diene-3-ones library against *S. cerevisiae* was 3,5-bis(4-trifluoromethylbenzylidene)-1-methylpiperidin-4-one (**22n**) with the lowest IC₁₀, IC₂₅ and IC₅₀ values, these being 0.10, 0.22 and 0.62 μM, respectively. The second, third and fourth potent inhibitor of *S. cerevisiae* cells were **22f**, **22s** and **22m** with their IC₅₀ values of 1.21, 1.87 and 2.22 μM, respectively. The IC₅₀ values of compound **22f** and **22n** showing only a two-fold difference in their inhibitory potencies. The presence of a strong EWG (-CF₃) at the *para*-position of the aromatic ring of compound (**22n**) results in an increase in the electrophilicity of the β-carbon of this compound. Compound **22n** has three fluorine atoms whereas **22f** contain only a single chlorine atom on the aromatic ring, therefore the increase in the electrophilicity of the β-carbon is greater in **22n** than **22f**. Consequently **22n** shows higher potency than **22f**.

The inhibitory activity of the *para*-substituent groups on bis-benzylidene derivatives of N-methylpiperidin-4-one against *S. cerevisiae* were shown in **Table 6.1**, page 211. Compounds **22n**, **22p** and **22t** contain a strong electron-withdrawing group (EWG) at the *para*-position of the aromatic ring and their Hammett substituent constant (σ) values were 0.54, 0.35 and 0.78 respectively (Hansch & Leo, 1979). These compounds showed very good IC₅₀ values (0.62, 12.9 and 3.37 μM) which suggests a relationship between the strength of the EWGs, the associated electron densities at the β-carbon atoms of the compound and their antifungal potencies. Similarly, compound **22g** also gave a good IC₅₀ value (5.56 μM) which contains an EWG (-Cl) at the *para*-position of the aromatic ring. Compound **22g** has a low Hammett substituent constant (σ) value (0.23) compared to **22n**, **22p** and **22t**.

Table 6. 1. Comparison of the inhibitory activity of *para* substituted bis-benzylidene derivatives of *N*-methylpiperidin-4-ones against *S. cerevisiae*.

Compounds	R-substituents	Hammett's substituent constants (σ)	IC ₅₀ ± SD (μM)	AUC ± SD
				
22d	-OCH ₃	-0.27	27.9 ± 18.4	230 ± 16.1
22g	-Cl	+0.23	5.56 ± 8.01	160 ± 49.1
22k	-COOH	+0.73	218 ± 26.4	299 ± 14.4
22l	-CH ₃	-0.17	N/R	314 ± 10.5
22n	-CF ₃	+0.54	0.62 ± 0.26	104 ± 6.73
22p	-OCF ₃	+0.35	12.9 ± 0.91	180 ± 44.8
22t	-NO ₂	+0.78	3.37 ± 2.01	146 ± 48.5

Note: N/R represents that compound did not give 50% inhibition.

On the other hand compound **22k**, which has a moderate EWG at the *para*-position of the aromatic ring exhibited moderate inhibitory activity (IC₅₀ = 218 μM) although it has a very high σ value (0.73). In contrast, compound **22l** was unable to inhibit the 50% growth of *S. cerevisiae*. The presence of an electron-donating group (-CH₃) shows a plus inductive (+I) effect on the structure resulting in a lack of antifungal activity. Compound **22d** contains a methoxy group (weak EDG) which shows a negative inductive (-I) effect at the *para*-position and exhibited fairly good inhibitory activity against *S. cerevisiae* with IC₅₀ value of 27.9 μM. The increase in the activity of **22d** compare to **22l** is due to the presence of a methoxy group rather than a methyl group. This shows that the presence of oxygen has some influence on the inhibitory activity of this compound. Compound **22d** has clogP of 3.98 whereas **22l** has clogP of 4.67. Speculatively this could be due to an increase in the solubility of **22d** as well as a negative inductive (-I) effect since oxygen is more electronegative than carbon but a positive mesomeric (+M) effect due to the lone pair (Kerber, 2006).

This suggest a possible mechanism of action of bis-benzylidene derivatives of *N*-methylpiperidin-4-one is the interaction of olefinic carbon (β -carbon) with a sulfhydryl (-SH) groups present in a cysteine residue of the fungal PM H⁺-ATPase. The library of synthesized

1,4-diene-3-ones will all give rise to the Michael reactions. Due to the highest potency of compound **22n**, it was selected as an example for the Michael addition reaction mechanism with cysteine as shown in Figure 6.1.

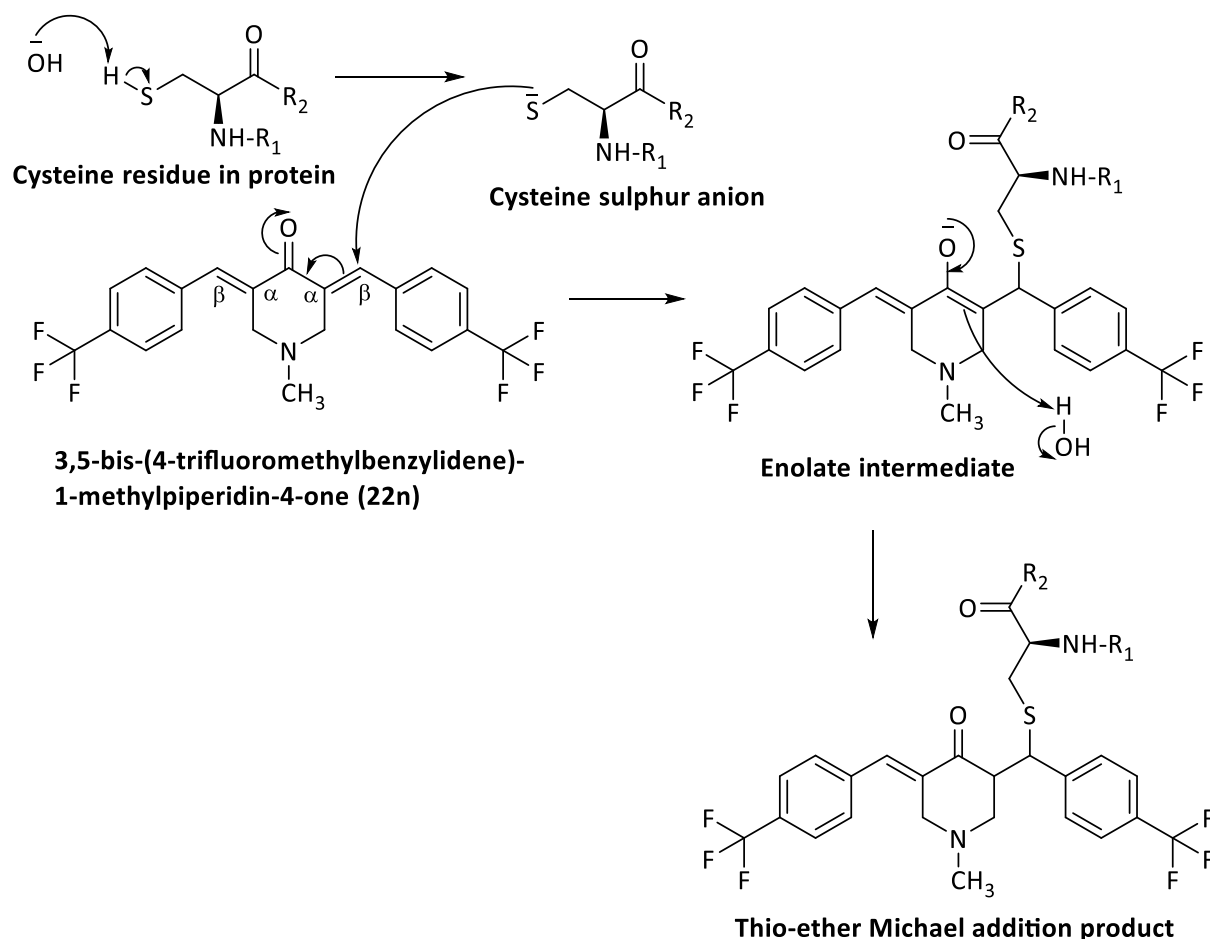


Figure 6. 1. A possible mechanism of cysteine and 3,5-(E)-bis-(4-trifluoromethylbenzylidene)-1-methylpiperidin-4-one (22n) reaction kinetics.

The sulfhydryl group (thiol, $-\text{SH}$) of a cysteine residue present in proteins such as the fungal plasma membrane H^+ -ATPase may form a thio-ether bond by reacting with the α,β -unsaturated carbonyl group of 3,5-bis-(4-trifluoromethylbenzylidene)-1-methylpiperidin-4-one (Figure 6.1). The SH group of cysteine acts as a nucleophile (S^-) while the β -carbon ($\text{HC}=\text{CHCO}$ group) of 3,5-bis-(4-trifluoromethylbenzylidene)-1-methylpiperidin-4-one acts as electrophile. The reaction of cysteine and 3,5-bis-(4-trifluoromethylbenzylidene)-1-

methylpiperidin-4-one forms a covalent C-S bond and the reaction could thus potentially cause an irreversible inhibition of the plasma membrane H⁺-ATPase as suggested by proton pumping experiments described in the chapter 4.

From the results of macro-broth susceptibility assays of 1,4-diene-3-ones against *C. albicans*, compounds **23f**, **23g** and **23h** exhibited the highest inhibitory activity with IC₅₀ values of 68.5, 57.6 and 50.7 μM respectively. The higher potency of these compounds is possible associated with some degree of promiscuous aggregation because their dose-response curves were steep and the associated Hill slopes were high (2.33, 1.45 and 2.21 respectively). Most of the compounds were unable to reach 90% inhibition of *C. albicans* growth. However a few compounds demonstrated >90% inhibition of *C. albicans* growth these being **22a**, **22f**, **23a-c**, **23f-h** and **24a** respectively.

In this study, the inhibitory activities of all compounds tested against *C. albicans* displayed significantly lower potency than miconazole nitrate (IC₅₀ = 0.04 μM). Although certain compounds (**22f**, **22m**, **22n**, **22o**, **22s**, and **22t**) exhibited good potencies against *S. cerevisiae* (IC₅₀; 1.21, 2.22, 0.62, 2.83, 1.87 and 3.37 μM) due to the presence of EWGs, their activity was limited against *C. albicans* (IC₅₀; 114, 525, 474, 549, 666 and 354 μM). This suggests that the inhibitory action of these compounds is probably specific to particular species (e.g. *S. cerevisiae*) although a range of fungal species need to be screened in order to confirm this conclusion.

The comparative potencies of various 1,4-diene-3-ones against *S. cerevisiae* and *C. albicans* were compared by using a discrimination ratio of their IC₅₀ and AUC values (**Table 6.2**, page 217). The threshold for discrimination ratio between 0 and 2 is generally considered to be good. Anything above this value suggests that a compound is less capable of targeting

multiple species. The discrimination ratio was obtained by dividing the antifungal activity of compounds against *C. albicans* with the antifungal activity of compounds against *S. cerevisiae*. The discrimination ratio based on the inhibitory action of compounds against *S. cerevisiae* and *C. albicans* vary significantly in terms of their IC_{50} values (0.06 to 764). However, the difference in the discrimination ratio is far less when comparing their AUC values (0.59 to 3.14). Compound **22n** exhibited highest potency against *S. cerevisiae* ($IC_{50} = 0.62 \mu\text{M}$) but gave moderate potency against *C. albicans* with the IC_{50} value of 474 μM therefore the ratio of its activity was very high (764.5) indicating that the activity of **22n** is limited to particular species. Additionally **22n** displayed the highest discrimination ratio (3.14) based on its AUC values.

The difference in the activities of compounds against *S. cerevisiae* and *C. albicans* is due to differences in the genetic or physiological profiles of these two species. A study conducted by Tebung, Choudhury, Tebbji, & Morschhäuser, (2016) described the difference between *S. cerevisiae* and *C. albicans*. They used ChIP-chip (Chromatin Immunoprecipitation Microarray) analysis to identify the transcriptional profiling of Ppr1 protein and found that in *S. cerevisiae* Ppr1 controls the building of pyrimidines whereas in *C. albicans* Ppr1 controls the degrading of purines. *S. cerevisiae* can exist either in haploid or diploid variants. In contrast *C. albicans* are dimorphic in nature means *C. albicans* can change from yeast to hyphae form under certain environmental conditions. Therefore it is possible that compounds showing good potency against *S. cerevisiae* may not show similar potency against *C. albicans*.

Compounds **22u** and **22v** displayed low discrimination ratios (1.24 and 0.85) which suggests they have the ability to target multiple species. However **22u** exhibited low inhibitory activities against both *S. cerevisiae* and *C. albicans* ($IC_{50} = 1290$ and $1604 \mu\text{M}$ respectively) whilst **22v** exhibited moderate activities against both *S. cerevisiae* and *C. albicans* ($IC_{50} = 263$

and 309 μM respectively). Similarly, compound **22a** has a discrimination ratio of 3.14, which can be considered reasonable. Compounds **22a**, **22u** and **22v** have un-substituted aromatic rings attached via di-methylene bridge to either piperidine, cyclopentyl or cyclohexyl ring. Higher potency of compounds **22a** and **22v** compared to **22u** suggests the influence of central six membered ring which adopts more a chair conformation which facilitate an increase in the reactivity of molecule to the target enzyme (H^+ -ATPase) whereas five membered ring compound ring is flatter and can't form chair conformation.

Compounds **22b**, **23f**, **23g** and **23h** gave the discrimination ratios of 9.91, 8.10, 10.4 and 8.11 respectively, which denotes these compounds have some capacity to inhibit multiple species however a 10-fold increase is required in the dose to inhibit the growth of *C. albicans* cells. On the other hand some compounds displayed discrimination ratio between 10 and 100; these being **22c**, **22d**, **22f**, **22g**, **22p**, **22q**, **22r**, **23a**, **23b**, **23c** and **23g** whereas other compounds (**22e**, **22m**, **22o**, **23d** and **23e**) displayed very high ratio (100-300) indicating *S. cerevisiae* cells were more susceptible to these group of compounds than *C. albicans* cells and probably could not be taken forward for further development.

Although the discrimination index of 1 is perfect by comparing one inhibitory parameter (IC_{50}) it is insufficient to decide whether to take this compound forward for future drug development or not. It would be useful to screen more species to cover a wide variety of types (e.g. yeasts or other forms) and that the discrimination ratio for all pairwise combinations or all other species compared to one standard species could be generated. Because a compound with a discrimination index of 1 is able to target multiple species, compounds with higher discrimination indexes are very specific to particular species tested.

Nevertheless, when comparing the discrimination ratio of the reference control compound miconazole nitrate based on their IC_{50} and AUC values, its 0.33 and 0.59, which shows a three-fold difference in its activity against *C. albicans* over *S. cerevisiae*. This confirms that miconazole is capable of targeting multiple species. Although this would normally not be a problem indeed it would be preferred because *C. albicans* is pathogenic whilst *S. cerevisiae* is only occasionally pathogenic. However, individuals suffering from various cancers or immunocompromised individuals are often susceptible to *S. cerevisiae* and it is becoming an opportunistic pathogen and an increase in the clinical dose may be needed. This could lead to toxicological problem depending on the therapeutic window of miconazole nitrate.

Table 6. 2. Discrimination ratio of the inhibitory activities of various 1,4-diene-3-ones against *S. cerevisiae* and *C. albicans*.

Compound	<i>C. albicans</i>		<i>S. cerevisiae</i>		Ratio of <i>C. albicans</i> / <i>S. cerevisiae</i>	
	IC ₅₀ (μM)	(AUC)	IC ₅₀ (μM)	(AUC)	(IC ₅₀)	(AUC)
22a	128	294	40.7	248	3.14	1.19
22b	532	341	53.7	249	9.91	1.37
22c	313	329	3.24	144	96.60	2.28
22d	1112	356	27.9	230	39.86	1.55
22e	1148	353	3.9	188	294.36	1.88
22f	114	288	1.21	97.3	94.21	2.96
22g	309	316	5.56	160	55.58	1.98
22h	N/R	368	154	269	*	1.37
22i	N/R	385	153	289	*	1.33
22j	N/R	383	124	258	*	1.48
22k	N/R	387	218	299	*	1.29
22l	N/R	389	N/R	314	*	1.24
22m	525	335	2.22	138	236.49	2.43
22n	474	327	0.62	104	764.52	3.14
22o	549	329	2.83	176	193.99	1.87
22p	409	314	12.9	180	31.71	1.74
22q	454	321	21.4	221	21.21	1.45
22r	243	302	7.64	196	31.81	1.54
22s	666	316	1.87	125	356.15	2.53
22t	354	319	3.37	146	105.04	2.18
22u	1604	372	1290	321	1.24	1.16
22v	263	327	309	314	0.85	1.04
23a	367	329	12.6	208	29.13	1.58
23b	238	320	8.84	194	26.92	1.65
23c	249	314	9.45	194	26.35	1.62
23d	2196	386	20.3	231	108.18	1.67
23e	1493	379	9.29	207	160.71	1.83
23f	68.5	279	8.46	194	8.10	1.44
23g	57.6	273	5.52	164	10.43	1.66
23h	50.7	261	6.25	178	8.11	1.47
24a	138	288	2233	315	0.06	0.91
24b	N/R	369	619	319	*	1.16
24c	334	312	N/R	328	*	0.95
4	0.04	25.3	0.12	43	0.33	0.59

Note: Data were displayed as the mean of three (*S. cerevisiae*) and two (*C. albicans*) individual experiments each conducted in duplicates. N/R represents compounds not reaching 50% inhibition. *means ratio not calculated.

Subsequent to these studies, it is necessary to identify the possible mechanisms of action of 1,4-diene-3-one compounds. It is possible that these compounds act on various cellular targets accessible either externally due to presence of EWG or certain compounds containing pyridine rings which may penetrate the cell membrane and cytoplasmically inhibit the H⁺-ATPase enzyme by forming a thio-ether bond with cysteine residue of H⁺-ATPase. Several authors have reported that NEM and other α,β -unsaturated carbonyls inhibited the H⁺-ATPase (Brooker & Slayman, 1982; Kongstad *et al.*, 2014; Tung *et al.*, 2018). The goal of this research work was to examine compounds with the ability to inhibit the fungal PM H⁺-ATPase enzyme.

Therefore, a library of 1,4-diene-3-ones was investigated to identify the possible mechanisms of action by measuring the glucose-induced acidification of the extracellular medium of *S. cerevisiae* using a modification of the method described by Ben-Josef *et al.*, (2000). Ben-Josef *et al.*, (2000) have studied the effect of CAN-296 (a complex carbohydrate isolated from the cell wall of *Mucor rouxii*) on *C. albicans*, *C. krusei*, *C. glabrata*, *C. guilliermondii* and *S. cerevisiae*. The effect of 1,4-diene-3-ones on H⁺-ATPase mediated proton pumping by intact cells of *S. cerevisiae* was conducted by measuring the change in pH of the external medium (detailed in Chapter 4). Interestingly within 10 minutes of medium acidification, the steady state of proton flux ($J_{H^+in} = J_{H^+out}$) has been achieved by bis-pyridylidene derivatives of N-methylpiperidin-4-one (**23a-c**, 60 μ M) while most of the other compounds from the library reached a steady state after about 15 mins after medium acidification was initiated. This suggests compounds (**23a-c**) penetrate the cell membrane and makes the membrane leaky thus inhibits the H⁺-ATPase.

Certain compounds with strong EWGs (**22f**; *meta*-chloro, **22g**; *para*-chloro and **22s**; *meta*-nitro, **22t**; *para*-nitro) exhibited good potency by inhibiting the H⁺ pumping ability of *S. cerevisiae*. The presence of a powerful EWG will make the compound more reactive to all nucleophiles however that external and PM nucleophiles/S_H groups will be the first to come into contact with the drug. As these compounds block the formation of transmembrane electrochemical proton gradient by inhibiting the PM H⁺-ATPase enzyme they were termed 'membrane active antifungal agents'. On the basis of SAR study of log (1/IC₅₀) vs δ -values of proton on the β -carbon plots of the initial activity it is believed that these compounds most likely interact with membrane associated cysteines possibly at or close to the omeprazole binding site. However further experiments need to be conducted to confirm this statement. These compounds form a covalent C-S bond with a cysteine residue within the protein which results in the inhibition of the H⁺-ATPase. In order uniquely prove this, it will be necessary to both purify and assay the enzyme along with determining the residue that is modified using e.g. MALDI-MS (Matrix-assisted laser desorption ionization mass spectrometry).

The bis-thienylidene derivatives of N-methylpiperidin-4-one and cycloalkanones (**24a**, **24b** and **24c**), and the bis-pyridylidene derivatives of cyclopentanone (**23d-f**) were not effective inhibitors of H⁺ pumping by *S. cerevisiae*. This result was consistent with the susceptibility assays against *S. cerevisiae* that also gave very poor inhibition for these above-mentioned compounds.

When comparing the inhibitory activity of compounds from susceptibility assays with the H⁺ extrusion assay there was some differences in their comparative potencies. For example, compounds (**22c**, **22m**, **22n** and **22o**) exhibited good potency against *S. cerevisiae* with low micromolar range of the IC₅₀ values. However these compounds were less effective at

inhibiting proton pumping by *S. cerevisiae*. A possible reason for this difference is due to variations in the time period of the experiment. The H⁺ extrusion assay was conducted only for 1.5 hours (60 mins pre-incubating cells with test compound followed by 30 mins of pH measurement subsequent to the addition of glucose) whereas the susceptibility assay was performed over a 24-hour duration. This difference in time period possibly gives rise to a greater ability to have multiple targeting effects.

The H⁺ extrusion assay is associated with the initial part of metabolism prior to the significant production of glycolytic intermediates while the macro-broth susceptibility assay occurs over 24 hours (Roos & Luckner, 1984). Therefore the compounds have more time to interact with other enzymes in the growth assay. It is possible that some compounds need a longer time period to interact with cellular constituents to exhibit their full potency which may be due to a polypharmacological effect rather than to targeting a single enzyme.

In this study, certain compounds have displayed good potency against *S. cerevisiae* in macro-broth susceptibility assay, exhibiting IC₅₀ values in the low μM range (1-10 μM). However, when compared to miconazole they were still considerably less active.

A 60 μM (one point) assay is a standard protocol for primary screening of compound libraries in drug discovery and on this basis the inhibitory activity of a library of 1,4-diene-3-ones on H⁺ pumping of *S. cerevisiae* was investigated. A 60 μM concentration is also commonly employed in single concentration high throughput screening systems (McGovern *et al.*, 2002). Only a few compounds gave full inhibition of H⁺ pumping by *S. cerevisiae* within 10 mins of pump activation.

Low IC₅₀ values for compounds **22f**, **22m**, **22n** and **22s** against *S. cerevisiae* in macro-broth susceptibility assays make the pharmacophore (1,4-diene-pentan-3-one) a useful fragment to

integrate into a more site-targeted molecule. Additionally certain compounds with pyridine rings such as **23a**, **23b** and **23c** exhibited the highest capacity to inhibit H⁺ pumping in *S. cerevisiae*. Additionally, in macro-broth susceptibility assays, these compounds exhibited good activity against *S. cerevisiae* (IC₅₀ = 12.6, 8.84 and 9.45 μM respectively) but only low to moderate activity against *C. albicans* (IC₅₀ = 367, 238 and 249 μM). This suggests that the pyridine (or pyrazine or pyrimidine) ring structure might be a useful fragment to include in future molecules due to their ability to increase the amphipathic nature of the molecule and, even possibly with the pyrimidine structure, to increase specificity towards ATP binding proteins.

The current studies reveal that the presence of an amphipathic group, such as pyridine, in 1,4-diene-3-ones gives rise to an increase in the solubility of the compounds. It can reasonably be suggested that the ability of the 1,4-diene-3-ones to act as antifungals by inhibiting the growth of yeast (*S. cerevisiae*) and to inhibit the efflux of protons from the cell is associated with their inhibitory effects on the PM H⁺-ATPase. It is therefore useful to compare the antifungal activities of these compounds with their electrophilic and lipophilic properties. This can be achieved by performing both basic and complex structure-activity studies.

The preliminary structure-activity analysis of 1,4-diene-3-ones indicated that the electrophilic nature of the β-carbon of compounds (generated from data containing all or subsets of 31 compounds; **22a-k**, **22m-v**, **23a-h** and **24a-b**) is a significant contributor for its antifungal activity. The structure-activity analysis of various bis-benzylidene derivatives of N-methylpiperidin-4-one suggested that the potency of this group of compounds (**22a-k** and **22m-v**) is dependent on their electronic property rather than their lipophilic property. The presence of strong EWGs at either *meta* or *para*-position increases the electrophilicity of the

β -carbon of these compounds (**22a**, **22c-d**, **22f-g**, **22k**, **22m-p** and **22r-t**). However, SAR analysis of bis-pyridylidene derivatives of both N-methylpiperidin-4-one and cycloalkanones (**23a-h**) indicated that potencies of these compounds is dependent on their lipophilic rather than the electrophilic property. This could be possibly due to lower clogP values of this group of compounds or less data points included in SAR (8 compounds were analysed, which is very low) or that the data obtained for this group of compounds are unexpected and may be aberrant (Hansch & Leo, 1979).

The results obtained from this study suggests that the interaction of the synthesized compound with the fungal plasma membrane is, by itself, insufficient for complete inhibition of the H⁺-ATPase enzyme. However, these 1,4-diene-3-ones can be considered as lead compounds which will aid further optimization towards highly selective H⁺-ATPase inhibitors as a new class of antifungal agents and aiding in the drug design process. Compounds containing the 1,4-diene-3-one pharmacophore targeting the membrane segment would not have to cross the plasma membrane. Hence these compounds will not be susceptible to the action of multidrug resistance pumps such as ABC efflux pump, which act to pump drugs out from the cell. Alternatively molecules or drugs which have a better aqueous or organic solubility profile, along with a high specificity for the nucleotide binding site of the H⁺-ATPase would be a useful development.

In conclusion, this work has produced a set of probes which has helped to define some of the parameters required to design a molecule targeting the plasma membrane H⁺-ATPase and which could possibly be included in such a future covalent drug acting to possibly eliminate a fungal infection.

CHAPTER SEVEN

SPECULATIONS ON FUTURE WORK AND DEVELOPMENT

7 Speculations on future work and development

The encouraging results from this study suggest it may be useful to synthesize further compounds. These could include structures asymmetric around the 1,4-diene-3-one pharmacophore and/ or to introduce such structures into site-targeted compounds such as molecules targeted to the nucleotide-binding site or to the omeprazole binding site of the H⁺-ATPase. For example, introduction of the most potent group (e.g. -CF₃) on one side of the aromatic ring whilst also introducing a nitrogen-containing aromatic ring (e.g. pyridine) on the other side of the 1,4-diene-3-one pharmacophore could be useful. Such changes could potentially increase both the overall solubility and permeability of the compound across the plasma membrane and the specificity towards nucleotide binding sites thus hopefully its potency against the H⁺-ATPase.

A potential problem of using this pharmacophore (1,4-diene-3-one) is that it may not be sufficiently specific to the fungal plasma membrane H⁺-ATPase. Therefore, other possibilities include altering the pharmacophore such that it can have different levels of reactivity to different cysteine sulfhydryls. For example, it might be possible to synthesize some compounds which could possibly initially act as prodrugs, which are then activated to an enone by a reverse Michael reaction to form the active drug which would finally react at the target site. It might therefore be possible to synthesize some compounds which could act as reverse Michael reactors, which can act as prodrugs facilitating the generation of an α,β -unsaturated enone from a compound which already contains a carbonyl group but having a good leaving group beta to the carbonyl, such as chloro or trimethyl ammonium (Figure 7.1).

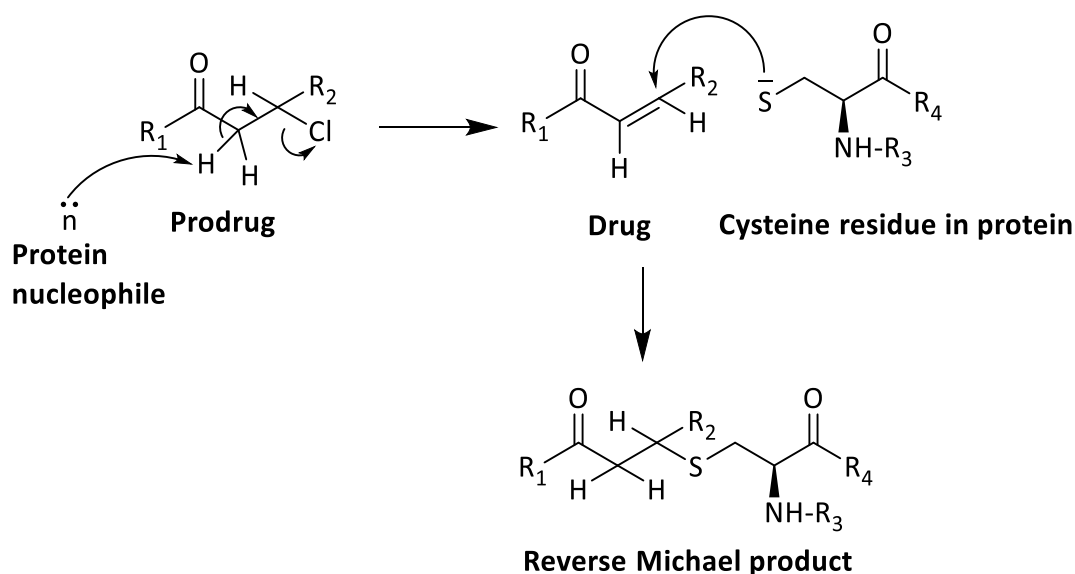


Figure 7. 1. A potential example of the mechanism for a reverse Michael reaction.

Moreover, compounds containing the 1,4-diene-3-one pharmacophore have the potential to target sulfhydryl (-SH) groups at multiple sites of interaction on the ATPase, such as the omeprazole binding site in the membrane segment (M₁/M₂) as well as the nucleotide binding site.

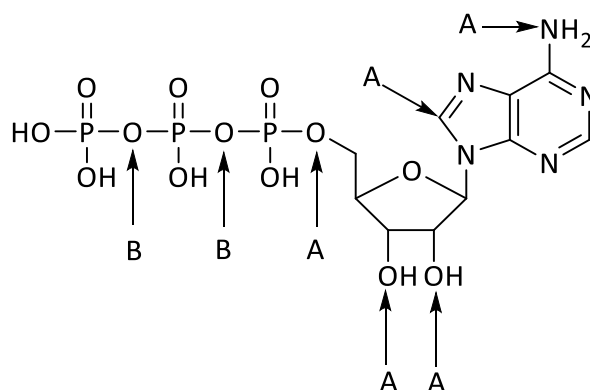
Additionally, it would be useful to model the plasma membrane H⁺-ATPase enzyme in 3D and to prepare both open and closed (E₁/E₂) models using the Ca²⁺-ATPase or other P-type ATPases of known 3D structures (Griffiths and Kirton, unpublished data).

Molecular modelling coupled with developing further quantitative structure-activity relationships will need to be performed in order to improve the preliminary pharmacophore model. *In silico* compound screening against 3D structures of the open (E₁) and closed (E₂) forms of the H⁺-ATPase and other P-type ATPases such as Na⁺/K⁺, Ca²⁺, Cu²⁺ and H⁺/K⁺-ATPase could be performed in order to maximise the levels of discrimination between the PMA H⁺-ATPase and other P-type ATPase enzyme. Hopefully this would help to minimise the potential toxicity of future molecules.

There is also need to consider the potential effects of novel compounds on membrane stability particularly within the host cells and to study the action of the compounds on lipid and membrane stability. Moreover, it is essential to perform further experiments to examine the integrity of the cytoplasmic membrane in the presence of 1,4-diene-3-ones in the intact cells by studying the leakage rate of fluorescent molecules such as Rhodamine 123 from preloaded cells with or without drug over time (De Cesco *et al.*, 2017).

In both the design and screening of future compounds, it would be useful to have significant amount of easily produced H⁺-ATPase enzyme. Although this enzyme has been extracted and purified previously from various fungi and plants, yields were not high (Ben-Josef *et al.*, 2000; Dao *et al.*, 2016). Previous attempts by other workers to produce the whole recombinant protein in *Escherichia coli* were unsuccessful (Rosano & Ceccarelli, 2014). This could possibly be due the ATPase acting as a toxic protein due to the high rates of ATP hydrolysis and thus pumping protons out of the *E. coli* cell (Rosano & Ceccarelli, 2014). This could potentially deplete the ATP concentration, especially at high ATPase expression levels. However, recent work has shown that it is possible to express the cytoplasmic ATP hydrolysing domain as a soluble recombinant protein in *E. coli* (Dylan Patel and D. Griffiths, unpublished data). This may potentially lead to a high throughput screening system based on a soluble ATPase fragment.

Finally, it may be possible to improve the specificity or selectivity by including a phosphoramidate structure (Figure 7.2). Such structures are found in drugs used in the treatment of osteoporosis (Gledhill *et al.*, 2007). More recently various diphenylphosphane derivatives of antifungal drugs has been synthesized having both oxyphosphate (P=O) or thiophosphate (P=S) centres (de Almeida *et al.*, 2019).



Where, **A** = Potential points of attachment of (di)enone structure and thus being close to the nucleotide binding site cysteine.

B = Potential points of introducing a phosphoramidate structure.

Figure 7. 2. A potential example of attachment of dienone or phosphoramidate to the ATP.

A study by Kappler & Hampton (1990) has shown that it is possible to actually design ATP analogs by introducing non-hydrolysable groups that would potentially increase the selectivity for different enzymes such as thymidine kinase, adenylate kinase, pyruvate kinase or methionine adenosyltransferase, etc. This can be achieved either by replacing/modifying the nitrogen atom on the adenine ring of ATP or by modifying the triphosphate group to introduce either phosphoramidate or replacing the oxygen with CH₂ or NH groups. The phosphoramidate structure of ATP molecule are not hydrolysable so in theory, if 1,4-diene-3-one pharmacophore were coupled with one or other of two hydroxyl groups in the ribose (via a dehydration reaction). Alternatively either (di)enone or reverse Michael group could be introduced at positions labelled 'A' in Fig 7.2 where they might be placed would depend on the relationship of the nucleotide binding site cysteine to the various parts of the ATP molecule.

Bibliography

- Abbott, A. B., & Odds, F. C. (1989). Abrogation by glucose of the ATP suppression induced by miconazole in *Candida albicans*. *Journal of Antimicrobial Chemotherapy*, *24*(6), 905–919.
- Agarwal, R., & Gupta, D. (2011). Severe asthma and fungi: Current evidence. *Medical Mycology*, *49*(SUPPL. 1), S150-157.
- Akins, R. A. (2005). An update on antifungal targets and mechanisms of resistance in *Candida albicans*. *Medical Mycology*, *43*(4), 285–318.
- Ameen, M. (2010). Epidemiology of superficial fungal infections. *Clinics in Dermatology*, *28*(2), 197–201.
- Amoozadeh, A., Rahmani, S., Dutkiewicz, G., Salehi, M., Nemati, F., & Kubicki, M. (2011). Novel Synthesis and Crystal Structures of Two α , α' -bis-Substituted benzylidene cyclohexanones: 2,6-bis-2-nitro(benzylidene)cyclohexanone and 2,6-bis-4-methyl(benzylidene)cyclohexanone. *Journal of Chemical Crystallography*, *41*(9), 1305–1309.
- Andrés, M. T., & Fierro, J. F. (2010). Antimicrobial mechanism of action of transferrins: Selective inhibition of H⁺-ATPase. *Antimicrobial Agents and Chemotherapy*, *54*(10), 4335–4342.
- Andriole, V. T. (2000). Current and future antifungal therapy: new targets for antifungal therapy. *International Journal of Antimicrobial Agents*, *16*(3), 317–321.
- Ashley, E. S. D., Lewis, R., Lewis, J. S., Martin, C., & Andes, D. (2006). Pharmacology of systemic antifungal agents. *Clinical Infectious Diseases*, *43*(Suppl 1), S28–S39.
- Axelsen, K. B., & Palmgren, M. G. (1998). Evolution of substrate specificities in the P-Type ATPase superfamily. *Journal of Molecular Evolution*, *46*(1), 84–101.
- Baell, J. B., & Holloway, G. A. (2010). New substructure filters for removal of pan assay interference compounds (PAINS) from screening libraries and for their exclusion in bioassays. *Journal of Medicinal Chemistry*, *53*(7), 2719–2740.
- Baell, J., & Walters, M. A. (2014). Chemical con artists foil drug discovery. *Nature*, *513*(7519), 481–483.
- Barf, T., & Kaptein, A. (2012). Irreversible protein kinase inhibitors: Balancing the benefits and risks. *Journal of Medicinal Chemistry*, *55*, 6243–6262.
- Batovska, D., Parushev, S., Slavova, A., Bankova, V., Tsvetkova, I., Ninova, M., & Najdenski, H. (2007). Study on the substituents' effects of a series of synthetic chalcones against the yeast *Candida albicans*. *European Journal of Medicinal Chemistry*, *42*(1), 87–92.
- Becher, B., & Muller, V. (1994). Delta mu Na⁺ drives the synthesis of ATP via an delta mu Na(+)-translocating F₁F₀-ATP synthase in membrane vesicles of the Archaeon *Methanosarcina mazei* Gö1. *Journal of Bacteriology*, *176*(9), 2543–2550.
- Ben-Josef, A. M., Manavathu, E. K., Platt, D., & Sobel, J. D. (2000). Proton translocating ATPase mediated fungicidal activity of a novel complex carbohydrate: CAN-296. *International Journal of Antimicrobial Agents*, *13*(4), 287–295.
- Bhattacharya, S., Esquivel, B. D., & White, T. C. (2018). Overexpression or deletion of

- ergosterol biosynthesis genes alters doubling time, response to stress agents, and drug susceptibility in *Saccharomyces cerevisiae*. *MBio*, *9*(4), e-01291-18.
- Bidaud, A. L., Chowdhary, A., & Dannaoui, E. (2018). *Candida auris*: An emerging drug resistant yeast – A mini-review. *Journal de Mycologie Medicale*.
- Brooker, R. J., & Slayman, W. (1982). Inhibition of the plasma membrane [H⁺]-ATPase of *Neurospora crassa* by *N*-Ethylmaleimide. *Journal of Biological Chemistry*, *257*(20), 12051–12055.
- Brown, G. D., Denning, D. W., Gow, N. A. ., Levitz, S. M., Netea, M. G., & White, T. C. (2012). Hidden Killers: Human fungal infections. *Science Translational Medicine*, *4*(165), 165rv13.
- Buckley, H. R. (1989). Identification of yeasts. In E. G. V Evans & M. D. Richardson (Eds.), *Medical Mycology: A practical approach* (pp. 97–99). Oxford: Oxford University Press.
- Caballero, J., & Fernández, M. (2006). Linear and nonlinear modeling of antifungal activity of some heterocyclic ring derivatives using multiple linear regression and Bayesian-regularized neural networks. *Journal of Molecular Modeling*, *12*(2), 168–181.
- Canela, H. M. S., Cardoso, B., Vitali, L. H., Coelho, H. C., Martinez, R., & Ferreira, M. E. da S. (2018). Prevalence, virulence factors and antifungal susceptibility of *Candida* spp. isolated from bloodstream infections in a tertiary care hospital in Brazil. *Mycoses*, *61*(1), 11–21.
- Cannon, R. D., & Holmes, A. R. (2015). Learning the ABC of oral fungal drug resistance. *Molecular Oral Microbiology*, *30*(6), 425–437.
- Casey, R. P., Thelen, M., & Azzi, A. (1980). Dicyclohexylcarbodiimide binds specifically and covalently to cytochrome c oxidase while inhibiting its H⁺-translocating activity. *Journal of Biological Chemistry*, *255*(9), 3994–4000.
- Chakrabarti, A. (2011). Drug resistance in fungi – an emerging problem. *Regional Health Forum*, *15*(1), 97–103.
- Chakraborty, B., Sengupta, J., & Mukherjee, R. (2013). Structural insights into the mechanism of translational inhibition by the fungicide sordarin. *Journal of Computer-Aided Molecular Design*, *27*(2), 173–184.
- Chan, G., Hardej, D., Santoro, M., Lau-Cam, C., & Billack, B. (2007). Evaluation of the antimicrobial activity of ebselen: role of the yeast plasma membrane H⁺-ATPase. *Journal of Biochemical and Molecular Toxicology*, *21*(5), 252–264.
- Chen, Z.-H., Zheng, C.-J., Sun, L.-P., & Piao, H.-R. (2010). Synthesis of new chalcone derivatives containing a rhodanine-3-acetic acid moiety with potential anti-bacterial activity. *European Journal of Medicinal Chemistry*, *45*(12), 5739–5743.
- Chène, P. (2002). ATPases as drug targets: Learning from their structure. *Nature Reviews Drug Discovery*, *1*(9), 665–673.
- Cherry, J. M., Hong, E. L., Amundsen, C., Balakrishnan, R., Binkley, G., Chan, E. T., ... Wong, E. D. (2012). *Saccharomyces* Genome Database: The genomics resource of budding yeast. *Nucleic Acids Research*, *40*(D1), 1–6.
- Chowdhary, A., Voss, A., & Meis, J. F. (2016). Multidrug-resistant *Candida auris*: ‘new kid on the block’ in hospital-associated infections? *Journal of Hospital Infection*, *94*(3), 209–212.

- Clausen, J. D., Bublitz, M., Arnou, B., Olesen, C., Andersen, J. P., Møller, J. V., & Nissen, P. (2016). Crystal structure of the vanadate-inhibited Ca²⁺-ATPase. *Structure*, *24*(4), 617–623.
- Cowen, L. E., Sanglard, D., Howard, S. J., Rogers, P. D., & Perlin, D. S. (2015). Mechanisms of antifungal drug resistance. *Cold Spring Harbor Perspectives in Medicine*, *5*(7), a019752.
- Dadar, M., Tiwari, R., Karthik, K., Chakraborty, S., Shahali, Y., & Dhama, K. (2018). *Candida albicans* - Biology, molecular characterization, pathogenicity, and advances in diagnosis and control – An update. *Microbial Pathogenesis*, *117*(February), 128–138.
- Dadi, P. K., Ahmad, M., & Ahmad, Z. (2009). Inhibition of ATPase activity of *Escherichia coli* ATP synthase by polyphenols. *International Journal of Biological Macromolecules*, *45*(1), 72–79.
- Dahal, U. P., Gilbert, A. M., Obach, R. S., Flanagan, M. E., Chen, J. M., Garcia-Irizarry, C., ... Young, J. A. (2016). Intrinsic reactivity profile of electrophilic moieties to guide covalent drug design: *N*- α -acetyl-L-lysine as an amine nucleophile. *Medicinal Chemistry Communications*, *7*(5), 864–872.
- Dalton, S. E., Dittus, L., Thomas, D. A., Convery, M. A., Nunes, J., Bush, J. T., ... Campos, S. (2018). Selectively targeting the kinome-conserved lysine of PI3K δ as a general approach to covalent kinase inhibition. *Journal of the American Chemical Society*, *140*(3), 932–939.
- Dao, T. T., Sehgal, P., Tung, T. T., Møller, J. V., Nielsen, J., Palmgren, M., ... Fuglsang, A. T. (2016). Demethoxycurcumin is a potent inhibitor of P-Type ATPases from diverse kingdoms of life. *PLoS ONE*, *11*(9), 1–19.
- Das, U., Alcorn, J., Shrivastav, A., Sharma, R. K., De Clercq, E., Balzarini, J., & Dimmock, J. R. (2007). Design, synthesis and cytotoxic properties of novel 1-[4-(2-alkylaminoethoxy)phenylcarbonyl]-3,5-bis(arylidene)-4-piperidones and related compounds. *European Journal of Medicinal Chemistry*, *42*(1), 71–80.
- Das, U., Doroudi, A., Das, S., Bandy, B., Balzarini, J., De Clercq, E., & Dimmock, J. R. (2008). *E,E*-2-Benzylidene-6-(nitrobenzylidene)cyclohexanones: Syntheses, cytotoxicity and an examination of some of their electronic, steric, and hydrophobic properties. *Bioorganic and Medicinal Chemistry*, *16*(11), 6261–6268.
- de Almeida, R. F. M., Santos, F. C., Marycz, K., Alicka, M., Krasowska, A., Suchodolski, J., ... Starosta, R. (2019). New diphenylphosphane derivatives of ketoconazole are promising antifungal agents. *Scientific Reports*, *9*(1), 1–14.
- De Cesco, S., Kurian, J., Dufresne, C., Mittermaier, A. K., & Moitessier, N. (2017). Covalent inhibitors design and discovery. *European Journal of Medicinal Chemistry*, *138*, 96–114.
- Deacon, J. W. (2013). *Fungal Biology* (4th ed.). Oxford: John Wiley & Sons.
- DeLean, A., Munson, P. J., & Rodbard, D. (1978). Simultaneous analysis of families of sigmoidal curves: application to bioassay, radioligand assay, and physiological dose-response curves. *American Journal of Physiology*, *235*(2), E97-102.
- Di Santo, R. (2010). Natural products as antifungal agents against clinically relevant pathogens. *Natural Product Reports*, *27*(7), 1084–1098.
- Dimmock, J. R., Arora, V. K., Semple, H. A., Lee, J. S., Allen, T. M., & Kao, G. Y. (1992). 3,5-bis-arylidene-1-methyl-4-piperidone methohalides and related compounds with activity

- against L 1210 cells and DNA binding properties. *Die Pharmazie*, *47(4)*, 246–248.
- Dimmock, J. R., Kandepu, N. M., Hetherington, M., Quail, J. W., Pugazhenti, U., Sudom, A. M., ... Balzarini, J. (1998). Cytotoxic activities of Mannich bases of chalcones and related compounds. *Journal of Medicinal Chemistry*, *41(7)*, 1014–1026.
- Dong, F., Jian, C., Zhenghao, F., Kai, G., & Zuliang, L. (2008). Synthesis of chalcones via Claisen–Schmidt condensation reaction catalyzed by acyclic acidic ionic liquids. *Catalysis Communications*, *9(9)*, 1924–1927.
- Duchowicz, P. R., Vitale, M. G., Castro, E. A., Fernández, M., & Caballero, J. (2007). QSAR analysis for heterocyclic antifungals. *Bioorganic & Medicinal Chemistry*, *15(7)*, 2680–2689.
- Edmond, M. B., Wallace, S. E., McClish, D. K., Pfaller, M. A., Jones, R. N., & Wenzel, R. P. (1999). Nosocomial bloodstream infections in United States hospitals: A three-year analysis. *Clinical Infectious Diseases : An Official Publication of the Infectious Diseases Society of America*, *29(2)*, 239–244.
- El-Subbagh, H. I., Abu-Zaid, S. M., Mahran, M. A., Badria, F. A., & Al-Obaid, A. M. (2000). Synthesis and biological evaluation of certain α,β -unsaturated ketones and their corresponding fused pyridines as antiviral and cytotoxic agents. *Journal of Medicinal Chemistry*, *43(15)*, 2915–2921.
- Emami, S., Ghobadi, E., Saednia, S., & Hashemi, S. M. (2019). Current advances of triazole alcohols derived from fluconazole: Design, in vitro and in silico studies. *European Journal of Medicinal Chemistry*, *170*, 173–194.
- Fonyo, A. (1979). Inhibitors of mitochondrial transport. *Pharmacology and Therapeutics*, *7(3)*, 627–645.
- Fothergill, A. W. (2012). *Antifungal susceptibility testing: clinical laboratory and standards institute (CLSI) methods*. In *Interactions of Yeasts, Moulds, and Antifungal Agents* (pp. 65–74). Totowa, NJ: Humana Press.
- Francois, K., Devlieghere, F., Standaert, A. R., Geeraerd, A. H., Cools, I., Van Impe, J. F., & Debevere, J. (2005). Environmental factors influencing the relationship between optical density and cell count for *Listeria monocytogenes*. *Journal of Applied Microbiology*, *99(6)*, 1503–1515.
- Galgiani, J. N., & Stevens, D. A. (1976). Antimicrobial susceptibility testing of yeasts: a turbidimetric technique independent of inoculum size. *Antimicrobial Agents and Chemotherapy*, *10(4)*, 721–726.
- Ghannoum, M. A., & Rice, L. B. (1999). Antifungal agents : mode of action, mechanisms of resistance and correlation of these mechanisms with bacterial resistance. *Clinical Microbiology Reviews*, *12(4)*, 501–517.
- Giacometti, A., Cirioni, O., Barchiesi, F., Del Prete, M. S., Caselli, F., & Scalise, G. (2000). In vitro susceptibility tests for cationic peptides: Comparison of broth microdilution methods for bacteria that grow aerobically. *Antimicrobial Agents and Chemotherapy*, *44(6)*, 1694–1696.
- Giannetti, A. M., Koch, B. D., & Browner, M. F. (2008). Surface plasmon resonance based assay for the detection and characterization of promiscuous inhibitors. *Journal of Medicinal Chemistry*, *51*, 574–580.

- Giraud, F., Guillon, R., Logé, C., Pagniez, F., Picot, C., Le Borgne, M., & Le Pape, P. (2009). Synthesis and structure-activity relationships of 2-phenyl-1-[(pyridinyl- and piperidinylmethyl)amino]-3-(1H-1,2,4-triazol-1-yl)propan-2-ols as antifungal agents. *Bioorganic & Medicinal Chemistry Letters*, *19*(2), 301–304.
- Gledhill, J. R., Montgomery, M. G., Leslie, A. G. W., & Walker, J. E. (2007). Mechanism of inhibition of bovine F₁-ATPase by resveratrol and related polyphenols. *Proceedings of the National Academy of Sciences of the United States of America*, *104*(34), 13632–13637.
- Gottschalk, P. G., & Dunn, J. R. (2005). The five-parameter logistic: A characterization and comparison with the four-parameter logistic. *Analytical Biochemistry*, *343*(1), 54–65.
- Groll, A. H., De Lucca, A. J., & Walsh, T. J. (1998). Emerging targets for the development of novel antifungal therapeutics. *Trends in Microbiology*, *6*(3), 117–124.
- Guinea, J. (2014). Global trends in the distribution of *Candida* species causing candidemia. *Clinical Microbiology and Infection*, *20*, 5–10.
- Hamada, Y. (2018). Role of Pyridines in Medicinal Chemistry and Design of BACE1 Inhibitors Possessing a Pyridine Scaffold. In *Pyridine* (pp. 9–26). IntechOpen.
- Hansch, C., & Fujita, T. (1964). ρ - σ - π Analysis. A Method for the Correlation of Biological Activity and Chemical Structure. *Journal of the American Chemical Society*, *86*(8), 1616–1626.
- Hansch, C., & Leo, A. J. (1979). Electronic Parameters. In *Substituent constants for correlation analysis in chemistry and biology* (pp. 1–8). New York: John Wiley & Sons.
- Haruta, M., Gray, W. M., & Sussman, M. R. (2015). Regulation of the plasma membrane proton pump (H⁺-ATPase) by phosphorylation. *Current Opinion in Plant Biology*, *28*, 68–75.
- Hawksworth, D. L. (2001). The magnitude of fungal diversity: the 1.5 million species estimate revisited. *Mycological Research*, *105*(12), 1422–1432.
- Hay, R. (2017). Superficial fungal infections. *Medicine (United Kingdom)*, *45*(11), 707–710.
- Helmerhorst, E. J., Murphy, M. P., Troxler, R. F., & Oppenheim, F. G. (2002). Characterization of the mitochondrial respiratory pathways in *Candida albicans*. *Biochimica et Biophysica Acta*, *1556*(1), 73–80.
- Hussain, I. A. (2014). *M.Sc. Thesis - The Synthesis and Biological Evaluation of Novel Nitrogen containing 6 and 7 membered ring Heterocyclic Compounds*. Hatfield, Hertfordshire: University of Hertfordshire.
- Ingólfsson, H. I., Thakur, P., Herold, K. F., Hobart, E. A., Ramsey, N. B., Periole, X., ... Andersen, O. S. (2014). Phytochemicals perturb membranes and promiscuously alter protein function. *ACS Chemical Biology*, *9*(8), 1788–1798.
- Isham, N., & Ghannoum, M. A. (2010). Antifungal activity of miconazole against recent *Candida* strains. *Mycoses*, *53*(5), 434–437.
- Jackson, P. A., Widen, J. C., Harki, D. A., & Brummond, K. M. (2017). Covalent modifiers: A chemical perspective on the reactivity of α,β -unsaturated carbonyls with thiols via Hetero-Michael addition reactions. *Journal of Medicinal Chemistry*, *60*(3), 839–885.
- Kabir, M. A., Hussain, M. A., & Ahmad, Z. (2012). *Candida albicans*: A model organism for studying fungal pathogens. *International Scholarly Research Network Microbiology*, *2012*, 1–15.

- Kappler, F., & Hampton, A. (1990). Approaches to Isozyme-Specific inhibitors. 17. Attachment of a Selectivity-Inducing substituent to a multisubstrate adduct. Implications for facilitated design of potent, Isozyme-Selective inhibitors. *Journal of Medicinal Chemistry*, *33*(9), 2545–2551.
- Karathia, H., Vilaprinyo, E., Sorribas, A., & Alves, R. (2011). *Saccharomyces cerevisiae* as a model organism: A comparative study. *PloS One*, *6*(2), 1256–1271.
- Kathiravan, M. K., Salake, A. B., Chothe, A. S., Dudhe, P. B., Watode, R. P., Mukta, M. S., & Gadhwe, S. (2012). The biology and chemistry of antifungal agents: A review. *Bioorganic and Medicinal Chemistry*, *20*(19), 5678–5698.
- Katritzky, A. R., Slavov, S. H., Dobchev, D. A., & Karelson, M. (2008). QSAR modeling of the antifungal activity against *Candida albicans* for a diverse set of organic compounds. *Bioorganic & Medicinal Chemistry*, *16*(14), 7055–7069.
- Katz, D. B., & Sussman, M. R. (1987). Inhibition and labeling of the plant plasma membrane H⁺-ATPase with *N*-Ethylmaleimide. *Plant Physiology*, *83*(4), 977–981.
- Kerber, R. C. (2006). If It's Resonance, What Is Resonating? *Journal of Chemical Education*, *83*(2), 223–227.
- Khan, N., Shreaz, S., Bhatia, R., Ahmad, S. I., Muralidhar, S., Manzoor, N., & Khan, L. A. (2012). Anticandidal activity of curcumin and methyl cinnamaldehyde. *Fitoterapia*, *83*(3), 434–440.
- Kim, D., Shin, W. S., Lee, K. H., Kim, K., Park, J. Y., & Koh, C.-M. (2002). Rapid differentiation of *Candida albicans* from other *Candida* species using its unique germ tube formation at 39 °C. *Yeast*, *19*(11), 957–962.
- Kjellerup, L., Gordon, S., Cohrt, K. O., Brown, W. D., Fuglsang, A. T., & Winther, A.-M. L. (2017). Identification of antifungal H⁺-ATPase inhibitors with effect on the plasma membrane potential. *Antimicrobial Agents and Chemotherapy*, *61*(7), e00032-17.
- Kongstad, K. T., Wubshet, S. G., Johannesen, A., Kjellerup, L., Winther, A. L., Jager, A. K., & Staerk, D. (2014). High-Resolution screening combined with HPLC-HRMS-SPE-NMR for identification of fungal plasma membrane H⁺-ATPase inhibitors from plants. *Journal of Agricultural and Food Chemistry*, *62*(24), 5595–5602.
- Kozel, T. R., & Wickes, B. (2014). Fungal diagnostics. *Cold Spring Harbor Perspectives in Medicine*, *4*(4), a019299.
- Krantz, A., Copp, L. J., Coles, P. J., Smith, R. A., & Heard, S. B. (1991). Peptidyl (acyloxy)methyl ketones and the quiescent affinity label concept: The departing group as a variable structural element in the design of inactivators of cysteine proteinases. *Biochemistry*, *30*(19), 4678–4687.
- Krishnan, S., Miller, R. M., Tian, B., Mullins, R. D., Jacobson, M. P., & Taunton, J. (2014). Design of reversible, cysteine-targeted michael acceptors guided by kinetic and computational analysis. *Journal of the American Chemical Society*, *136*(36), 12624–12630.
- Lagisetty, P., Vilekar, P., Sahoo, K., Anant, S., & Awasthi, V. (2010). CLEFMA-an anti-proliferative curcuminoid from structure-activity relationship studies on 3,5-bis(benzylidene)-4-piperidones. *Bioorganic & Medicinal Chemistry*, *18*(16), 6109–6120.
- Lecchi, S., & Slayman, C. W. (2004). Yeast plasma membrane H⁺-ATPase: Model system for

- studies of structure, function, biogenesis and regulation. In *Handbook of ATPases: Biochemistry, Cell Biology, Pathophysiology* (pp. 1–24).
- Lehmann, P. F., Lin, D., & Lasker, B. A. (1992). Genotypic identification and characterization of species and strains within the genus *Candida* by using random amplified polymorphic DNA. *Journal of Clinical Microbiology*, *30*(12), 3249–3254.
- Leonard, N. J., & Locke, D. M. (1955). γ -Pyridones by isomerization. Substituted 1-methyl-3,5-dibenzyl-4-pyridones. *Journal of the American Chemical Society*, *77*(7), 1852–1855.
- Leonova, E. S., Makarov, M. V., Rybalkina, E. Y., Nayani, S. L., Tongwa, P., Fonari, A., & Odinets, I. L. (2010). Structure-cytotoxicity relationship in a series of N-phosphorus substituted E,E-3,5-bis(3-pyridinylmethylene)- and E,E-3,5-bis(4-pyridinylmethylene)piperid-4-ones. *European Journal of Medicinal Chemistry*, *45*, 5926–5934.
- Leonova, Evgeniya S, Makarov, N. S., Fonari, A., Lucero, R., Perry, J. W., Sammeth, D. M., & V.Timofeeva, T. (2013). Synthesis, structure, and one- and two-photon absorption properties of N-substituted 3,5-bisarylidenepropenpiperidin-4-ones. *Journal of Molecular Structure*, *1037*, 288–293.
- Lepesheva, G. I., & Waterman, M. R. (2004). CYP51-the omnipotent P450. *Molecular and Cellular Endocrinology*, *215*(1–2), 165–170.
- Li, Y., Metcalf, B. J., Chochua, S., Li, Z., Walker, H., Tran, T., ... Beall, B. W. (2019). Genome-wide association analyses of invasive pneumococcal isolates identify a missense bacterial mutation associated with meningitis. *Nature Communications*, *10*(1), 1–11.
- Liao, Y., Chen, M., Thomas, H., Yang, R., & Liao, W. (2013). Epidemiology of opportunistic invasive fungal infections in China: Review of literature. *Chinese Medical Journal*, *126*(2), 361–368.
- Lipinski, C. A., Lombardo, F., Dominy, B. W., & Feeney, P. J. (1997). Experimental and computational approaches to estimate solubility and permeability in drug discovery and development settings. *Advanced Drug Delivery Reviews*, *23*(1–3), 3–25.
- Logan-Smith, M. J., Lockyer, P. J., East, J. M., & Lee, A. G. (2001). Curcumin, a molecule that inhibits the Ca^{2+} -ATPase of sarcoplasmic reticulum but increases the rate of accumulation of Ca^{2+} . *Journal of Biological Chemistry*, *276*(50), 46905–46911.
- Lopez, S. N., Castelli, M. V., Zacchino, S. A., Domínguez, J. N., Lobo, G., Charris-Charris, J., ... Enriz, R. D. (2001). In vitro antifungal evaluation and structure–activity relationships of a new series of chalcone derivatives and synthetic analogues, with inhibitory properties against polymers of the fungal cell wall. *Bioorganic & Medicinal Chemistry*, *9*(8), 1999–2013.
- Ma, X., Lv, X., & Zhang, J. (2018). Exploiting polypharmacology for improving therapeutic outcome of kinase inhibitors (KIs): An update of recent medicinal chemistry efforts. *European Journal of Medicinal Chemistry*, *143*, 449–463.
- Mager, D. E. (2006). Quantitative structure-pharmacokinetic/pharmacodynamic relationships. *Advanced Drug Delivery Reviews*, *58*(12–13), 1326–1356.
- Mahmoud, Y. A. (2005). Curcumin modulation of Na,K-ATPase: Phosphoenzyme accumulation, decreased K^+ occlusion, and inhibition of hydrolytic activity. *British Journal of Pharmacology*, *145*(2), 236–245.

- Manavathu, E. K., Dimmock, J. R., Vashishtha, S. C., & Chandrasekar, P. H. (1999). Proton-pumping-ATPase-targeted antifungal activity of a novel conjugated styryl ketone. *Antimicrobial Agents and Chemotherapy*, *43*(12), 2950–2959.
- Manavathu, E. K., Vashishtha, S. C., Alangaden, G. J., & Dimmock, J. R. (1998). In vitro antifungal activity of some Mannich bases of conjugated styryl ketones. *Canadian Journal of Microbiology*, *44*(1), 74–79.
- Martins, C. V. B., Da Silva, D. L., Neres, A. T. M., Magalhães, T. F. F., Watanabe, G. A., Modolo, L. V., ... De Resende, M. A. (2009). Curcumin as a promising antifungal of clinical interest. *Journal of Antimicrobial Chemotherapy*, *63*(2), 337–339.
- Mazon, M. J., Eraso, P., & Portillo, F. (2015). Specific phosphoantibodies reveal two phosphorylation sites in yeast Pma1 in response to glucose. *FEMS Yeast Research*, *15*(5), 1–9.
- McCarthy, M. W., Kontoyiannis, D. P., Cornely, O. A., Perfect, J. R., & Walsh, T. J. (2017). Novel agents and drug targets to meet the challenges of resistant fungi. *The Journal of Infectious Diseases*, *216*(3), S474–S483.
- McGovern, S. L., Caselli, E., Grigorieff, N., & Shoichet, B. K. (2002). A common mechanism underlying promiscuous inhibitors from virtual and high-throughput screening. *Journal of Medicinal Chemistry*, *45*(8), 1712–1722.
- Meyer, H. H. (1901). Zur theorie der alkoholnarkose. Der einfluss wechselnder temperature auf wirkungsstärke und theilungscoefficient der narcotica. *Archiv Fur Experimentelle Pathologie Und Pharmakologie*, *46*, 338–346.
- Milo, R., & Phillips, R. (2015). *Cell biology by the numbers*. Garland Science.
- Mishra, N. N., Prasad, T., Sharma, N., Payasi, A., Prasad, R., Gupta, D. K., & Singh, R. (2007). Pathogenicity and drug resistance in *Candida albicans* and other yeast species. A review. *Acta Microbiologica et Immunologica Hungarica*, *54*(3), 201–235.
- Monk, B. C., Mason, A. B., Abramochkin, G., Haber, J. E., Seto-Young, D., & Perlin, D. S. (1995). The yeast plasma membrane proton pumping ATPase is a viable antifungal target. I. Effects of the cysteine-modifying reagent omeprazole. *Biochimica et Biophysica Acta*, *1239*(1), 81–90.
- Monk, B. C., & Perlin, D. S. (1994). Fungal plasma membrane proton pumps as promising new antifungal targets. *Critical Reviews in Microbiology*, *20*(3), 209–223.
- Moore, D. (2003). *Fungal Morphogenesis*. Cambridge University Press.
- Moore, T. W., Zhu, S., Randolph, R., Shoji, M., & Snyder, J. P. (2014). Liver S9 fraction-derived metabolites of curcumin analogue UBS109. *ACS Medicinal Chemistry Letters*, *5*(4), 288–292.
- Mora-Montes, H. M., & Gacser, A. (2016). Editorial: Recent advances in the study of the host-fungus interaction. *Frontiers in Microbiology*, *7*, 1694.
- Murakami, S., Kijima, H., Isobe, Y., Muramatsu, M., Aihara, H., Otomo, S., ... Ai Chun-bo, A. (1990). Effect of salvianolic acid A, a depside from roots of *salvia miltiorrhiza*, on gastric H⁺, K⁺-ATPase. *Planta Medica*, *56*(4), 360–363.
- Nakhjiri, M., Safavi, M., Alipour, E., Emami, S., Atash, A., Jafari-Zavareh, M., ... Shafiee, A. (2012). Asymmetrical 2,6-bis(benzylidene)cyclohexanones: Synthesis, cytotoxic activity

- and QSAR study. *European Journal of Medicinal Chemistry*, 50, 113–123.
- Neelofar, K., Shreaz, S., Rimple, B., Muralidhar, S., Nikhat, M., & Khan, L. A. (2011). Curcumin as a promising anticandidal of clinical interest. *Canadian Journal of Microbiology*, 57(3), 204–210.
- Nelson, K. M., Dahlin, J. L., Bisson, J., Graham, J., Pauli, G. F., & Walters, M. A. (2017). The Essential Medicinal Chemistry of Curcumin. *Journal of Medicinal Chemistry*, 60(5), 1620–1637.
- Odds, F. C. (1988). *Candida and candidosis: a review and bibliography* (2nd Ed). Bailliere Tindall; London.
- Odds, F. C. (1992). Antifungal susceptibility testing of *Candida* spp. by relative growth measurement at single concentrations of antifungal agents. *Antimicrobial Agents and Chemotherapy*, 36(8), 1727–1737.
- Odds, F. C., & Abbott, A. B. (1984). Relative inhibition factors—a novel approach to the assessment of antifungal antibiotics in vitro. *Journal of Antimicrobial Chemotherapy*, 13, 31–43.
- Odds, Frank C, Brown, A. J. P., & Gow, N. A. R. (2003). Antifungal agents: Mechanisms of action. *Trends in Microbiology*, 11(6), 272–279.
- Ottillie, S., Goldgof, G. M., Cheung, A. L., Walker, J. L., Vigil, E., Allen, K. E., ... Durrant, J. D. (2018). Two inhibitors of yeast plasma membrane ATPase 1 (Sc Pma1p): toward the development of novel antifungal therapies. *Journal of Cheminformatics*, 10(6), 1–9.
- Overton, C. E. (1991). *Studies of Narcosis*. Chapman and Hall, London.
- Palmgren, M. G., & Nissen, P. (2011). P-type ATPases. *Annual Review of Biophysics*, 40, 243–266.
- Parker, S. (2009). *Molds, Mushrooms & Other Fungi*. Capstone: Compass Point Books.
- Pati, H. N., Das, U., Das, S., Bandy, B., De Clercq, E., Balzarini, J., ... Dimmock, J. R. (2009). The cytotoxic properties and preferential toxicity to tumour cells displayed by some 2,4-bis(benzylidene)-8-methyl-8-azabicyclo[3.2.1] octan-3-ones and 3,5-bis(benzylidene)-1-methyl-4-piperidones. *European Journal of Medicinal Chemistry*, 44(1), 54–62.
- Pemán, J., & Zaragoza, R. (2010). Current diagnostic approaches to invasive candidiasis in critical care settings. *Mycoses*, 53(5), 424–433.
- Pérez-Torrado, R., & Querol, A. (2016). Opportunistic strains of *Saccharomyces cerevisiae*: A potential risk sold in food products. *Frontiers in Microbiology*, 6(JAN), 1–5.
- Perlin, D. S., Brown, C. L., & Habern, J. E. (1988). Membrane potential defect in hygromycin of *Saccharomyces* B-resistant pmal mutants. *The Journal of Biological Chemistry*, 263(34), 18118–18122.
- Perlin, D. S., Latchney, L. R., & Senior, A. E. (1985). Inhibition of *Escherichia coli* H⁺-ATPase by venturicidin, oligomycin and ossamycin. *Biochimica et Biophysica Acta (BBA) - Bioenergetics*, 807(3), 238–244.
- Petrov, V. V., & Slayman, C. W. (1995). Site-directed mutagenesis of the yeast PMA1 H⁺-ATPase. *Journal of Biological Chemistry*, 270(48), 28535–28540.
- Piraccini, B. M., & Tosti, A. (2019). Ciclopirox hydroxypropyl chitosan: Efficacy in mild-to-

- moderate Onychomycosis. *Skin Appendage Disorders*, 5(1), 13–19.
- Polak, A., & Scholer, H. J. (1975). Mode of action of 5-Fluorocytosine and mechanisms of resistance. *Chemotherapy*, 21(3,4), 113–130.
- Portillo, F. (2000). Regulation of plasma membrane H⁺-ATPase in fungi and plants. *Biochimica et Biophysica Acta (BBA) - Reviews on Biomembranes*, 1469(1), 31–42.
- Portillo, F., & Gancedo, C. (1984). Mode of action of miconazole on yeasts: Inhibition of the mitochondrial ATPase. *European Journal of Biochemistry*, 143(2), 273–276.
- Portillo, F., & Serrano, R. (1989). Growth control strength and active site of yeast plasma membrane ATPase studied by site-directed mutagenesis. *European Journal of Biochemistry*, 186(3), 501–507.
- Pouliot, M., & Jeanmart, S. (2016). Pan Assay Interference Compounds (PAINS) and other promiscuous compounds in antifungal research. *Journal of Medicinal Chemistry*, 59(2), 497–503.
- Prinz, H. (2010). Hill coefficients, dose-response curves and allosteric mechanisms. *Journal of Chemical Biology*, 3(1), 37–44.
- Rahman, A. F. M., Ali, R., Jahng, Y., & Kadi, A. A. (2012). A facile solvent free Claisen-Schmidt reaction: Synthesis of α,α' -bis-(substituted-benzylidene)cycloalkanones and α,α' -bis-(substituted-alkylidene)cycloalkanones. *Molecules*, 17(1), 571–583.
- Rautenbach, M., Gerstner, G. D., Vlok, N. M., Kulenkampff, J., & Westerhoff, H. V. (2006). Analyses of dose-response curves to compare the antimicrobial activity of model cationic α -helical peptides highlights the necessity for a minimum of two activity parameters. *Analytical Biochemistry*, 350(1), 81–90.
- Richardson, M. D., & Warnock, D. W. (2012). *Fungal infection: Diagnosis and Management* (4th ed.). West Sussex, UK: Wiley-Blackwell.
- Rogers, T. R. (2006). Antifungal drug resistance : limited data , dramatic impact ? *International Journal of Antimicrobial Agents*, 27, 7–11.
- Roos, W., & Luckner, M. (1984). Relationships between proton extrusion and fluxes of ammonium ions and organic acids in *Penicillium cyclopium*. *Journal of General Microbiology*, 130(4), 1007–1014.
- Rosano, G. L., & Ceccarelli, E. A. (2014). Recombinant protein expression in *Escherichia coli*: Advances and challenges. *Frontiers in Microbiology*, 5, 172.
- Sahu, P. K., Sahu, P. K., Gupta, S. K., Thavaselvam, D., & Agarwal, D. D. (2012). Synthesis and evaluation of antimicrobial activity of 4H-pyrimido[2,1-b]benzothiazole, pyrazole and benzylidene derivatives of curcumin. *European Journal of Medicinal Chemistry*, 54, 366–378.
- Sangamwar, A. T., Deshpande, U. D., & Pekamwar, S. S. (2008). Antifungals: Need to search for a new molecular target. *Indian Journal of Pharmaceutical Sciences*, 70(4), 423–430.
- Sardi, J. C. O., Scorzoni, L., Bernardi, T., Fusco-Almeida, A. M., & Mendes Giannini, M. J. S. (2013). *Candida* species: Current epidemiology, pathogenicity, biofilm formation, natural antifungal products and new therapeutic options. *Journal of Medical Microbiology*, 62(1), 10–24.
- Sardi, J. de C. O., Gullo, F. P., Freires, I. A., Pitanguí, N. de S., Segalla, M. P., Fusco-Almeida, A.

- M., ... Mendes-Giannini, M. J. S. (2016). Synthesis, antifungal activity of caffeic acid derivative esters, and their synergism with fluconazole and nystatin against *Candida* spp. *Diagnostic Microbiology and Infectious Disease*, *86*(4), 387–391.
- Schaad, L. J., & Hess, B. A. (1974). Huckel theory and aromatically. *Journal of Chemical Education*, *51*(10), 640.
- Schelenz, S., Hagen, F., Rhodes, J. L., Abdolrasouli, A., Chowdhary, A., Hall, A., ... Fisher, M. C. (2016). First hospital outbreak of the globally emerging *Candida auris* in a European hospital. *Antimicrobial Resistance and Infection Control*, *5*(1), 1–7.
- Schultz, C., Bossolani, M. P., Torres, L. M. B., Lima-Landman, M. T. R., Lapa, A. J., & Souccar, C. (2007). Inhibition of the gastric H⁺,K⁺-ATPase by plectrinone A, a diterpenoid isolated from *Plectranthus barbatus* Andrews. *Journal of Ethnopharmacology*, *111*(1), 1–7.
- Schwilden, H., & Schuttler, J. (2008). The site of anaesthetic action. In B. W. Urban (Ed.), *Modern Anesthetics. Handbook of Experimental Pharmacology* (pp. 7–10). Springer, Berlin, Heidelberg.
- Scorzoni, L., Paula, A. C. A. De, Marcos, C. M., Assato, P. A., Melo, W. C. M. A. De, Oliveira, H. C. De, ... Fusco-almeida, A. M. (2017). Antifungal Therapy: New Advances in the Understanding and Treatment of Mycosis. *Frontiers in Microbiology*, *8*(36), 1–23.
- Seidler, J., McGovern, S. L., Doman, T. N., & Shoichet, B. K. (2003). Identification and prediction of promiscuous aggregating inhibitors among known drugs. *Journal of Medicinal Chemistry*, *46*(21), 4477–4486.
- Serrano, R. (1980). Effect of ATPase inhibitors on the proton pump of respiratory-deficient yeast. *European Journal of Biochemistry*, *105*, 419–424.
- Serrano, Ramon. (1983). In vivo glucose activation of the yeast plasma membrane ATPase. *FEBS Letters*, *156*(1), 11–14.
- Serrano, Ramon. (1993). Structure, function and regulation of plasma membrane H⁽⁺⁾-ATPase. *FEBS Letters*, *325*(1,2), 108–111.
- Seto-Young, D., Monk, B. C., Mason, A. B., & Perlin, D. S. (1997). Exploring an antifungal target in the plasma membrane H⁺-ATPase of fungi. *Biochimica et Biophysica Acta*, *1326*(2), 249–256.
- Sexton, J. A., Brown, V., & Johnston, M. (2007). Regulation of sugar transport and metabolism by the *Candida albicans* Rgt1 transcriptional repressor. *Yeast*, *24*, 847–860.
- Shao, P. L., Huang, L. M., & Hsueh, P. R. (2007). Recent advances and challenges in the treatment of invasive fungal infections. *International Journal of Antimicrobial Agents*, *30*(6), 487–495.
- Sharma, M., Manoharlal, R., Puri, N., & Prasad, R. (2010). Antifungal curcumin induces reactive oxygen species and triggers an early apoptosis but prevents hyphae development by targeting the global repressor TUP1 in *Candida albicans*. *Bioscience Reports*, *30*(6), 391–404.
- Sheehan, D. J., Hitchcock, C. A., & Carol, M. (1999). Current and emerging azole antifungal agents. *Clinical Microbiology Reviews*, *12*(1), 40–79.
- Singh, J., Petter, R. C., Baillie, T. A., & Whitty, A. (2011). The resurgence of covalent drugs. *Nature Reviews Drug Discovery*, *10*(4), 307–317.

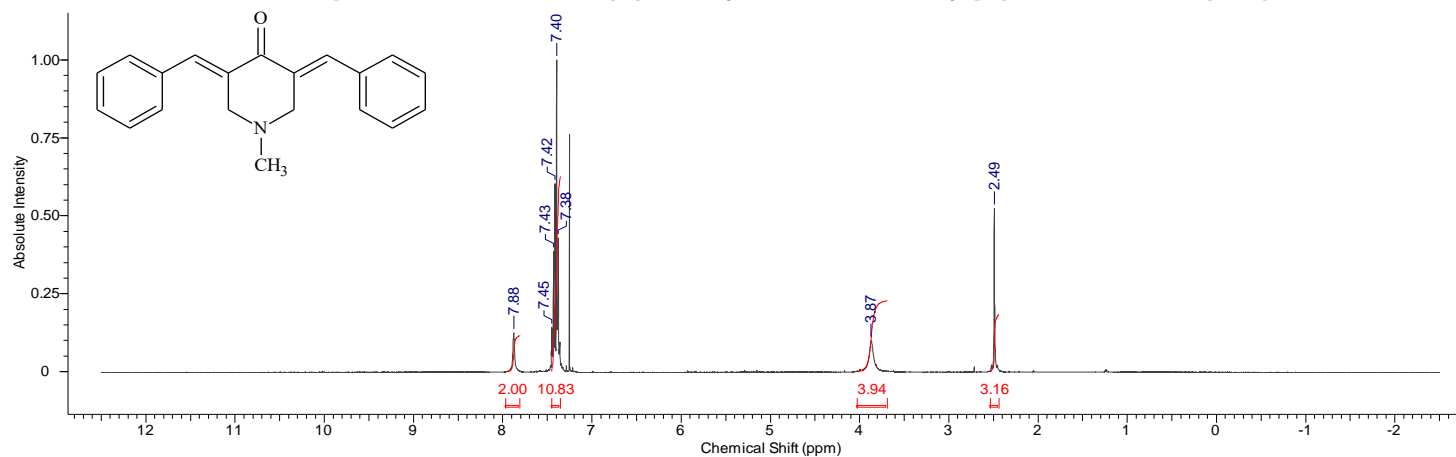
- Sivakumar, P. M., Muthu Kumar, T., & Doble, M. (2009). Antifungal activity, mechanism and QSAR studies on chalcones. *Chemical Biology & Drug Design*, *74*(1), 68–79.
- Škedelj, V., Tomašić, T., Mašič, L. P., & Zega, A. (2011). ATP-binding site of bacterial enzymes as a target for antibacterial drug design. *Journal of Medicinal Chemistry*, *54*(4), 915–929.
- Soteropoulos, P., Vaz, T., Santangelo, R., Paderu, P., Huang, D. Y., Tamás, M. J., & Perlin, D. S. (2000). Molecular characterization of the plasma membrane H⁺-ATPase, an antifungal target in *Cryptococcus neoformans*. *Antimicrobial Agents and Chemotherapy*, *44*(9), 2349–2355.
- Sudfeld, C. R., Dasenbrook, E. C., Merz, W. G., Carroll, K. C., & Boyle, M. P. (2010). Prevalence and risk factors for recovery of filamentous fungi in individuals with cystic fibrosis. *Journal of Cystic Fibrosis*, *9*(2), 110–116.
- Sullivan, D. J., Henman, M. C., Moran, G. P., O'Neill, L. C., Bennett, D. E., Shanley, D. B., & Coleman, D. C. (1996). Molecular genetic approaches to identification, epidemiology and taxonomy of non-albicans *Candida* species. *Journal of Medical Microbiology*, *44*(6), 399–408.
- Tebung, W. A., Choudhury, B. I., Tebbji, F., & Morschhäuser, J. (2016). Rewiring of the Ppr1 Zinc cluster transcription factor from purine catabolism to pyrimidine biogenesis in the Saccharomycetaceae. *Current Biology*, *26*(13), 1677–1687.
- Tung, T.-T., Dao, T. T., Junyent, M. G., Palmgren, M., Günther-Pomorski, T., Fuglsang, A. T., ... Nielsen, J. (2018). LEGO-inspired drug design: unveiling of the novel class of benzo[d]thiazole containing a 3,4-dihydroxyphenyl moiety as plasma membrane H⁺-ATPase inhibitors. *ChemMedChem*, *13*(1), 37–47.
- Ursu, O., Costescu, A., Diudea, M. V., & Parv, B. (2006). QSAR modeling of antifungal activity of some heterocyclic compounds. *Croatia Chemica Acta*, *79*(3), 483–488.
- Van Burik, J.-A. H., Ratanatharathorn, V., Stepan, D. E., Miller, C. B., Lipton, J. H., Vesole, D. H., ... Walsh, T. J. (2004). Micafungin versus fluconazole for prophylaxis against invasive fungal infections during neutropenia in patients undergoing hematopoietic stem cell transplantation. *Clinical Infectious Diseases*, *39*(10), 1407–1416.
- Vatsadze, S. ., Manaenkova, M. ., Sviridenkova, N. ., Zyk, N. ., Krut'ko, D. ., Churakov, A. ., ... Lang, H. (2006). Synthesis and spectroscopic and structural studies of cross-conjugated dienones derived from cyclic ketones and aromatic aldehydes. *Russian Chemical Bulletin, International Edition*, *55*(7), 1184–1194.
- Walker, M. E., Nguyen, T. D., Liccioli, T., Schmid, F., Kalatzis, N., Sundstrom, J. F., ... Jiranek, V. (2014). Genome-wide identification of the Fermentome; genes required for successful and timely completion of wine-like fermentation by *Saccharomyces cerevisiae*. *BMC Genomics*, *15*(1), 552.
- Winslow, J. W. (1981). The reaction of sulfhydryl groups of sodium and potassium ion-activated adenosine triphosphatase with *N*-ethylmaleimide. The relationship between ligand-dependent alterations of nucleophilicity and enzymatic conformational states. *The Journal of Biological Chemistry*, *256*(18), 9522–9531.
- Wu, J., Zhang, Y., Cai, Y., Wang, J., Weng, B., Tang, Q., ... Yang, S. (2013). Discovery and evaluation of piperid-4-one-containing mono-carbonyl analogs of curcumin as anti-inflammatory agents. *Bioorganic & Medicinal Chemistry*, *21*(11), 3058–3065.

- Yap, C. W., & Chen, Y. Z. (2005). Quantitative structure-pharmacokinetic relationships for drug distribution properties by using general regression neural network. *Journal of Pharmaceutical Sciences*, *94*(1), 153–168.
- Yatime, L., Buch-Pedersen, M. J., Musgaard, M., Morth, J. P., Winther, A. M. L., Pedersen, B. P., ... Fedosova, N. (2009). P-type ATPases as drug targets: Tools for medicine and science. *Biochimica et Biophysica Acta (BBA) - Bioenergetics*, *1787*(4), 207–220.
- Yoshinaka, K., Kumanogoh, H., Nakamura, S., & Maekawa, S. (2004). Identification of V-ATPase as a major component in the raft fraction prepared from the synaptic plasma membrane and the synaptic vesicle of rat brain. *Neuroscience Letters*, *363*(2), 168–172.
- Zafar, A., Pilkington, L. I., Haverkate, N. A., Van Rensburg, M., Leung, E., Kumara, S., ... Reynisson, J. (2018). Investigation into improving the aqueous solubility of the thieno[2,3-b]pyridine anti-proliferative agents. *Molecules*, *23*(1), 1–14.
- Zakheim, G. A., Goldberg, J. E., Motosko, C. C., Cohen, B. E., & Ho, R. S. (2019). Sexual dysfunction in men taking systemic dermatologic medication: A systematic review. *Journal of the American Academy of Dermatology*, *81*(1), 163–172.
- Zentz, F., Valla, A., Le Guillou, R., Labia, R., Mathot, A.-G., & Sirot, D. (2002). Synthesis and antimicrobial activities of N-substituted imides. *Il Farmaco*, *57*(5), 421–426.
- Zhang, L., Xiao, M., Watts, M. R., Wang, H., Fan, X., Kong, F., & Xu, Y. C. (2015). Development of fluconazole resistance in a series of *Candida parapsilosis* isolates from a persistent candidemia patient with prolonged antifungal therapy. *BMC Infectious Diseases*, *15*(1), 1–7.
- Zhang, Y.-Q., Gamarra, S., Garcia-Effron, G., Park, S., Perlin, D. S., & Rao, R. (2010). Requirement for ergosterol in V-ATPase function underlies antifungal activity of azole drugs. *PLoS Pathogens*, *6*(6), 1–13.
- Zhao, Y., Nagasaki, Y., Kordalewska, M., Press, E. G., Shields, R. K., Nguyen, M. H., ... Perlin, D. S. (2016). Rapid detection of FKS-associated echinocandin resistance in *Candida glabrata*. *Antimicrobial Agents and Chemotherapy*, *60*(11), 6573–6577.
- Zhao, Z., Liu, Q., Bliven, S., Xie, L., & Bourne, P. E. (2017). Determining cysteines available for covalent inhibition across the human kinome. *Journal of Medicinal Chemistry*, *60*(7), 2879–2889.
- Zhong, X., & Guidotti, G. (1999). A yeast Golgi E-type ATPase with an unusual membrane topology. *Journal of Biological Chemistry*, *274*(46), 32704–32711.

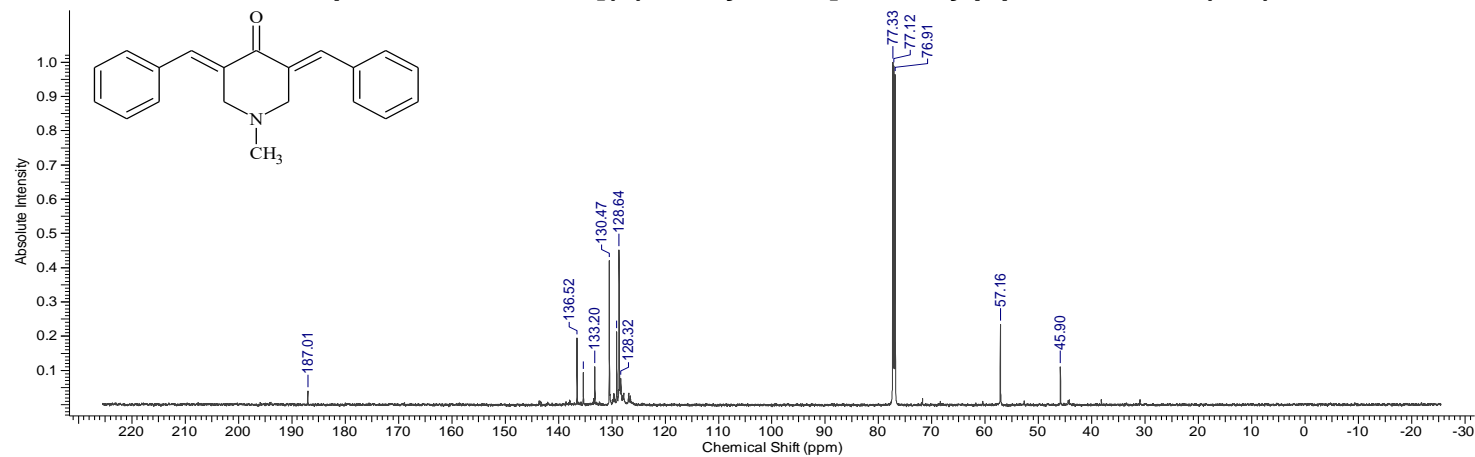
Appendix 1 - Full spectra of synthesized dienones

Compound 22a

Proton spectrum of 3,5-bis[(E)-benzylidene]-1-methylpiperidin-4-one (22a)

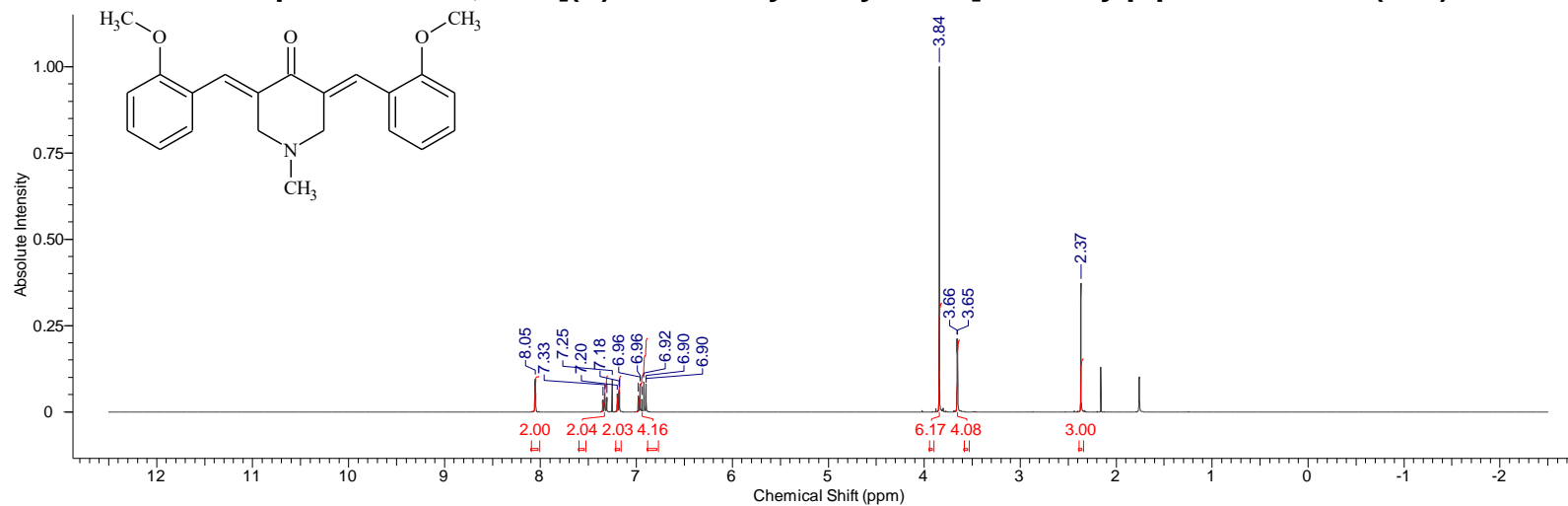


Carbon spectrum of 3,5-bis[(E)-benzylidene]-1-methylpiperidin-4-one (22a)

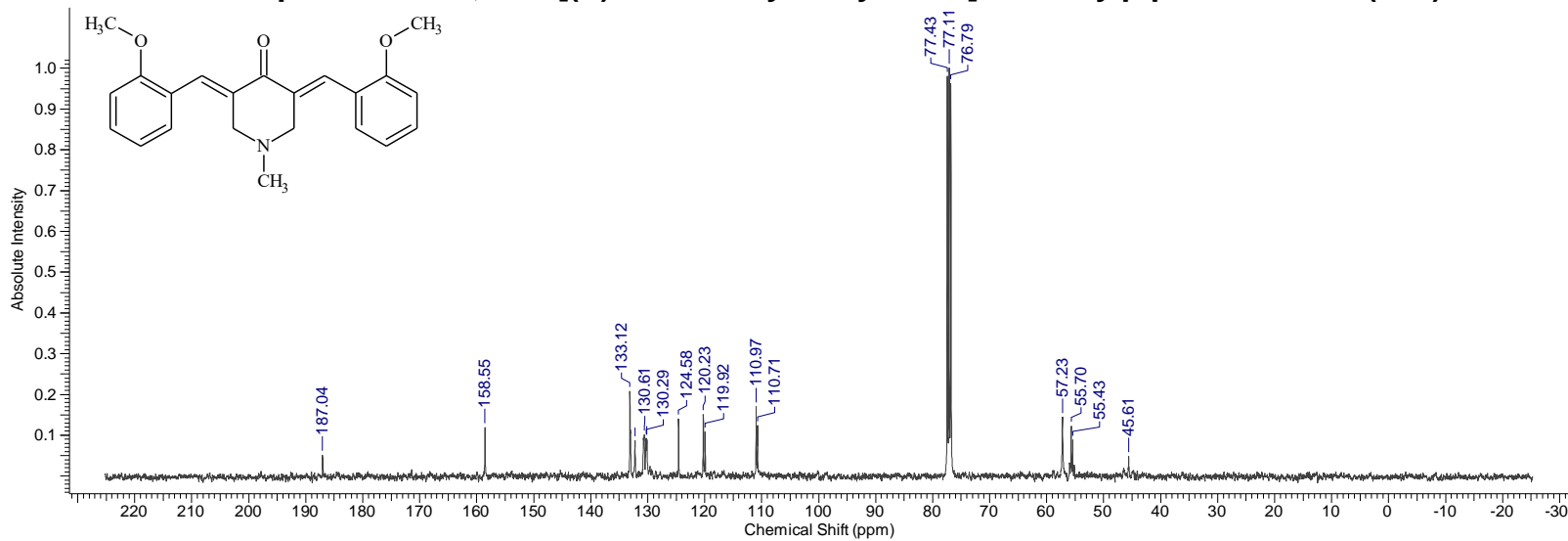


Compound 22b

Proton spectrum of 3,5-bis[(E)-2-methoxybenzylidene]-1-methylpiperidin-4-one (22b)

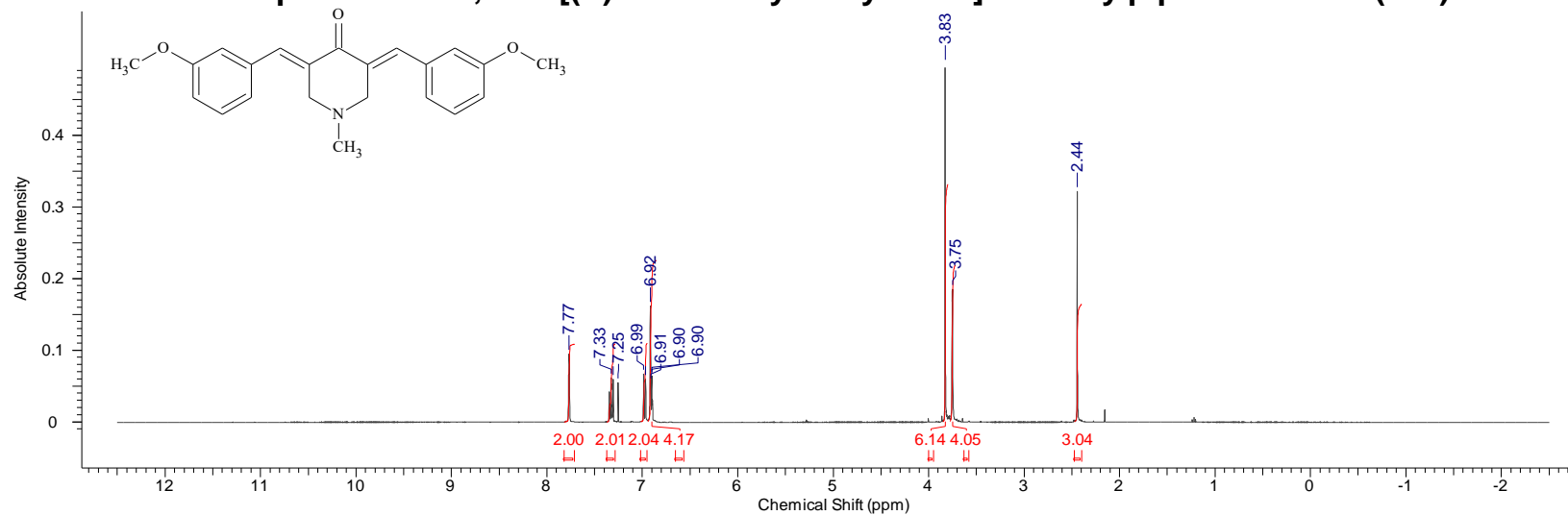


Carbon spectrum of 3,5-bis[(E)-2-methoxybenzylidene]-1-methylpiperidin-4-one (22b)

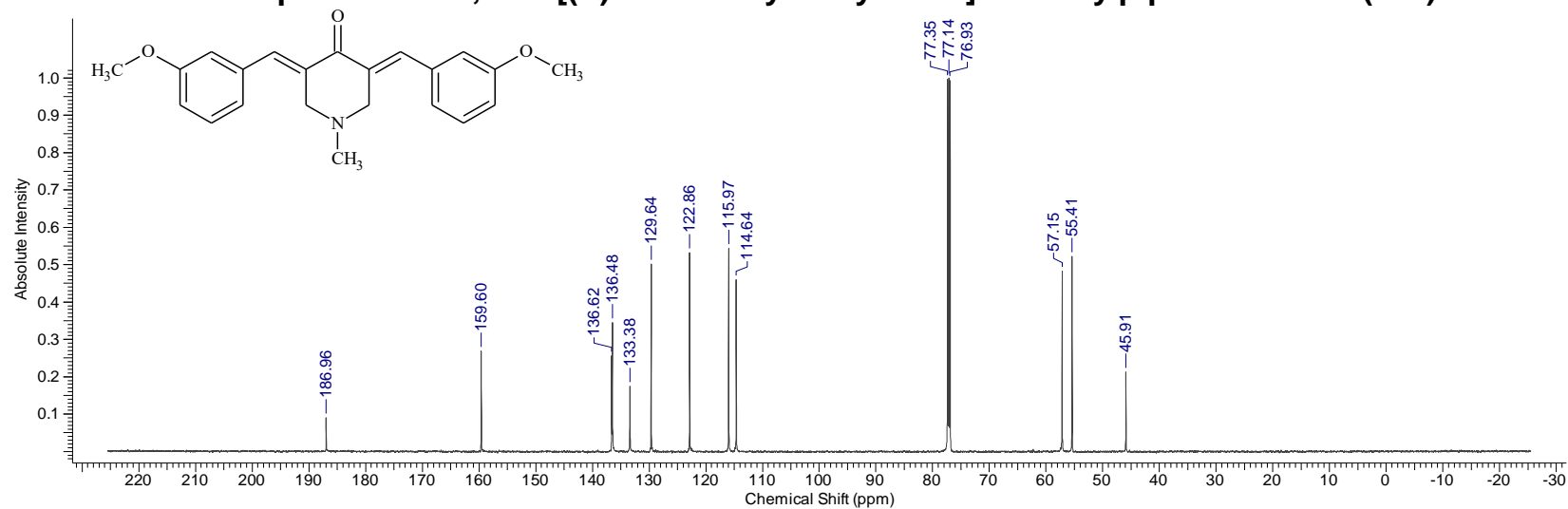


Compound 22c

Proton spectrum of 3,5-bis[(E)-3-methoxybenzylidene]-1-methylpiperidin-4-one (22c)

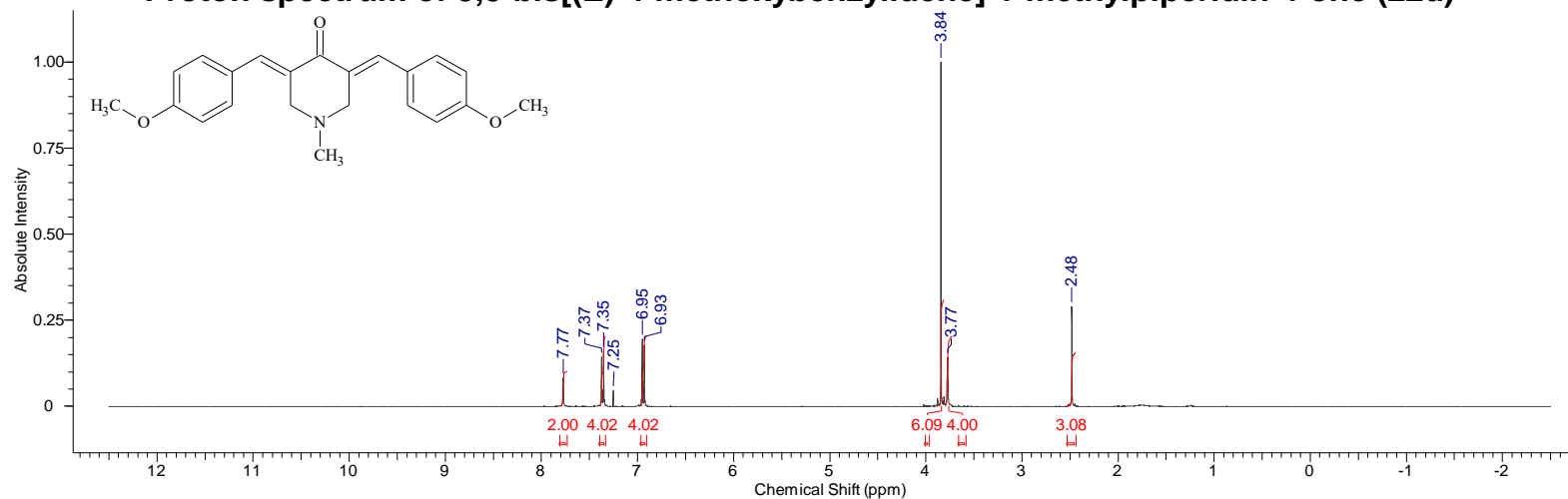


Carbon spectrum of 3,5-bis[(E)-3-methoxybenzylidene]-1-methylpiperidin-4-one (22c)

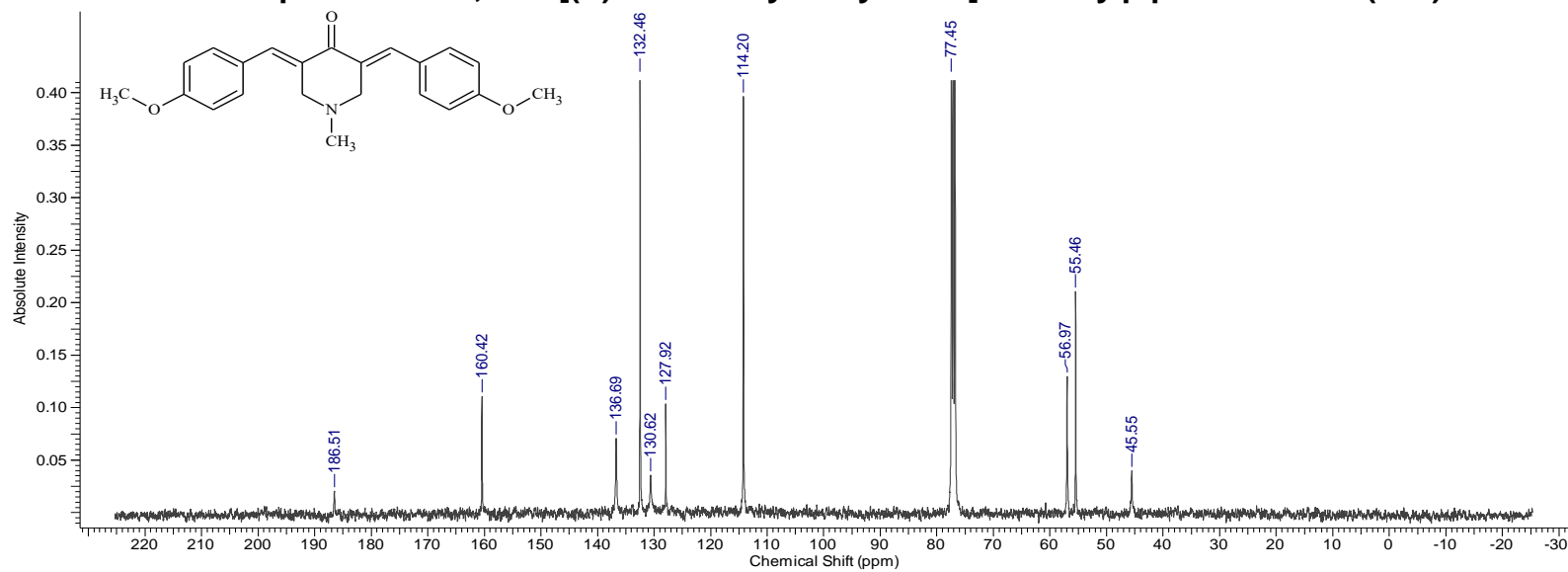


Compound 22d

Proton spectrum of 3,5-bis[(E)-4-methoxybenzylidene]-1-methylpiperidin-4-one (22d)

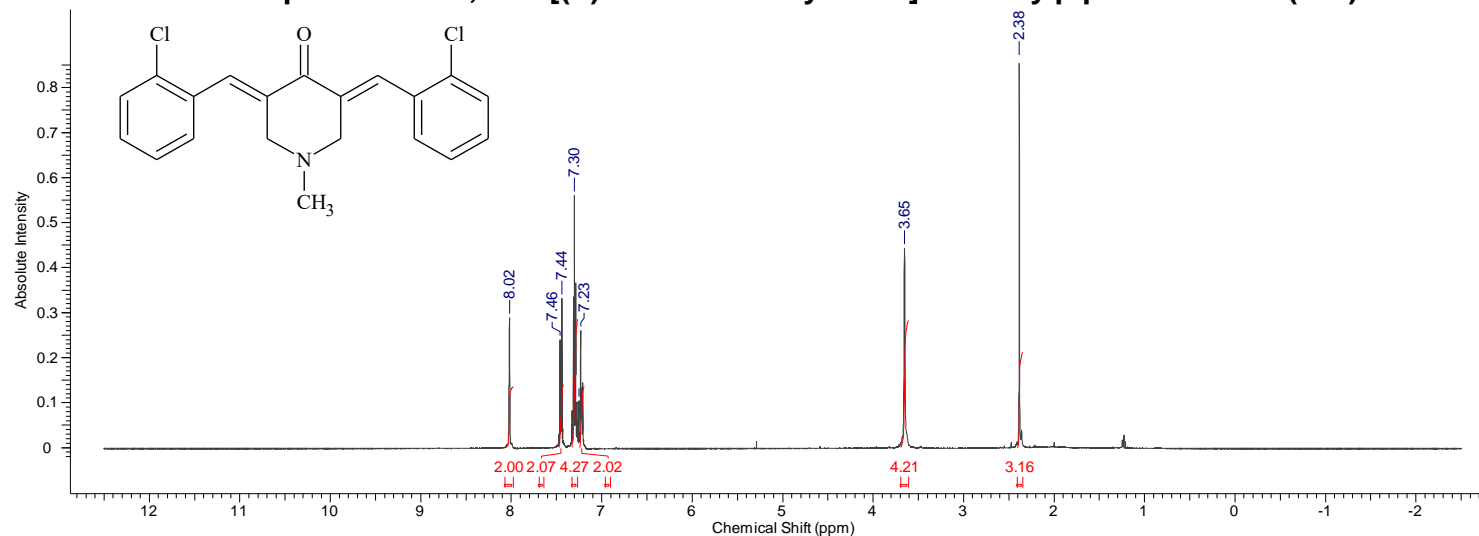


Carbon spectrum of 3,5-bis[(E)-4-methoxybenzylidene]-1-methylpiperidin-4-one (22d)

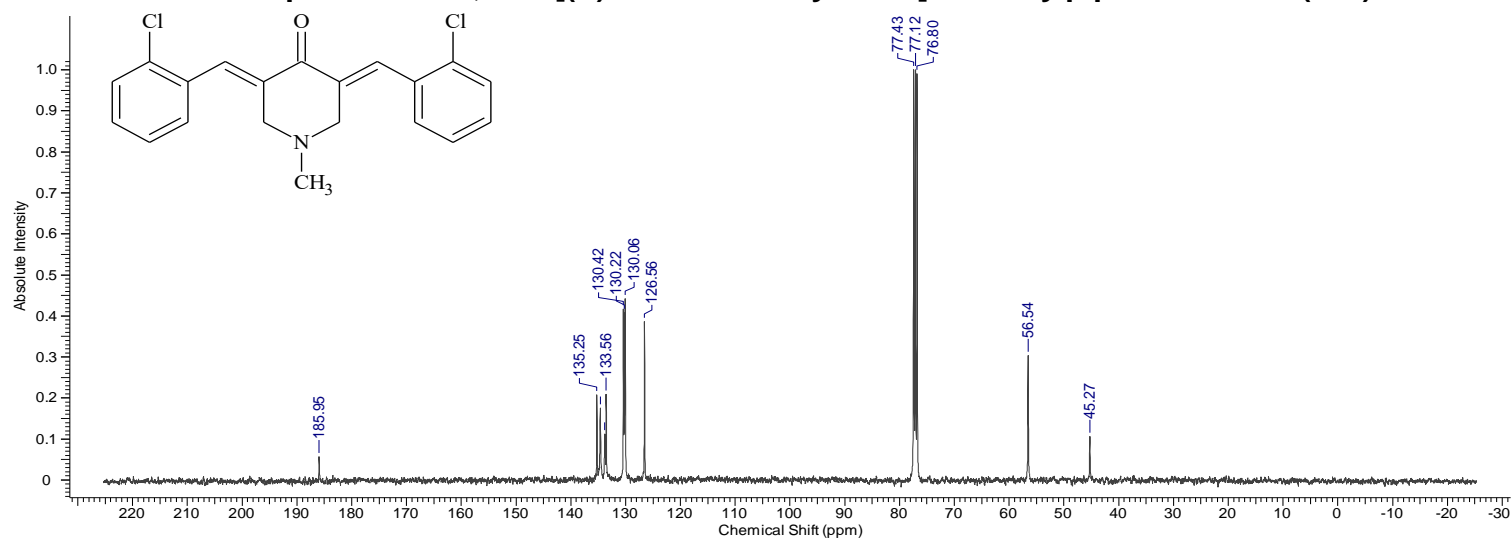


Compound 22e

Proton spectrum of 3,5-bis[(E)-2-chlorobenzylidene]-1-methylpiperidin-4-one (22e)

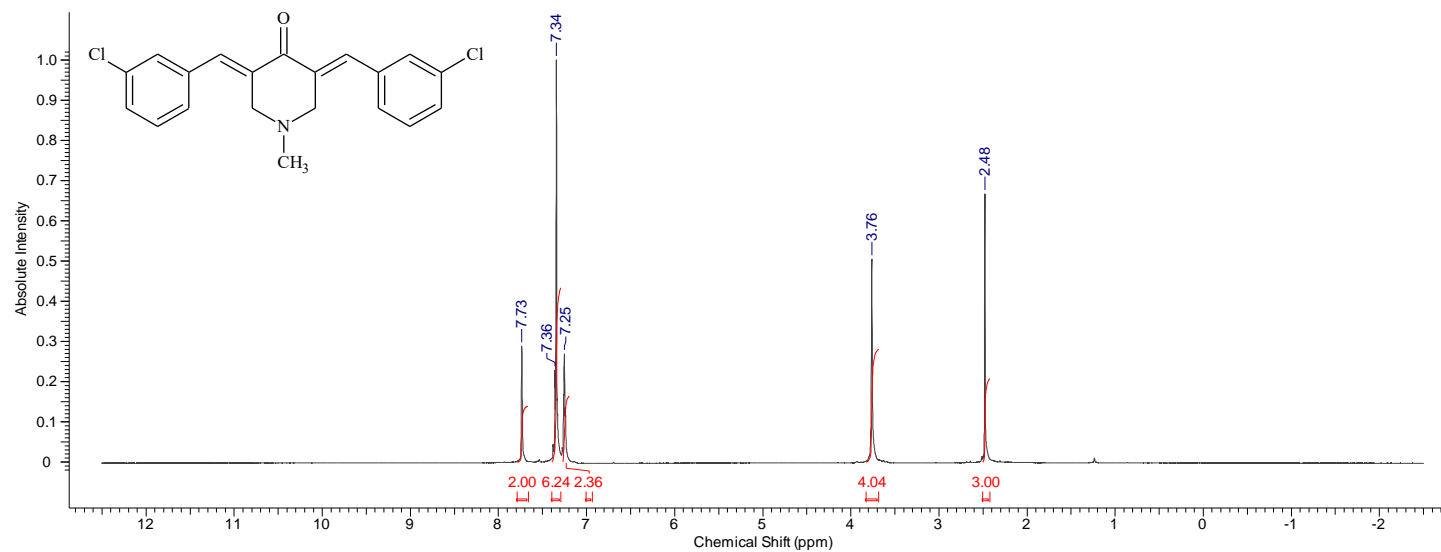


Carbon spectrum of 3,5-bis[(E)-2-chlorobenzylidene]-1-methylpiperidin-4-one (22e)

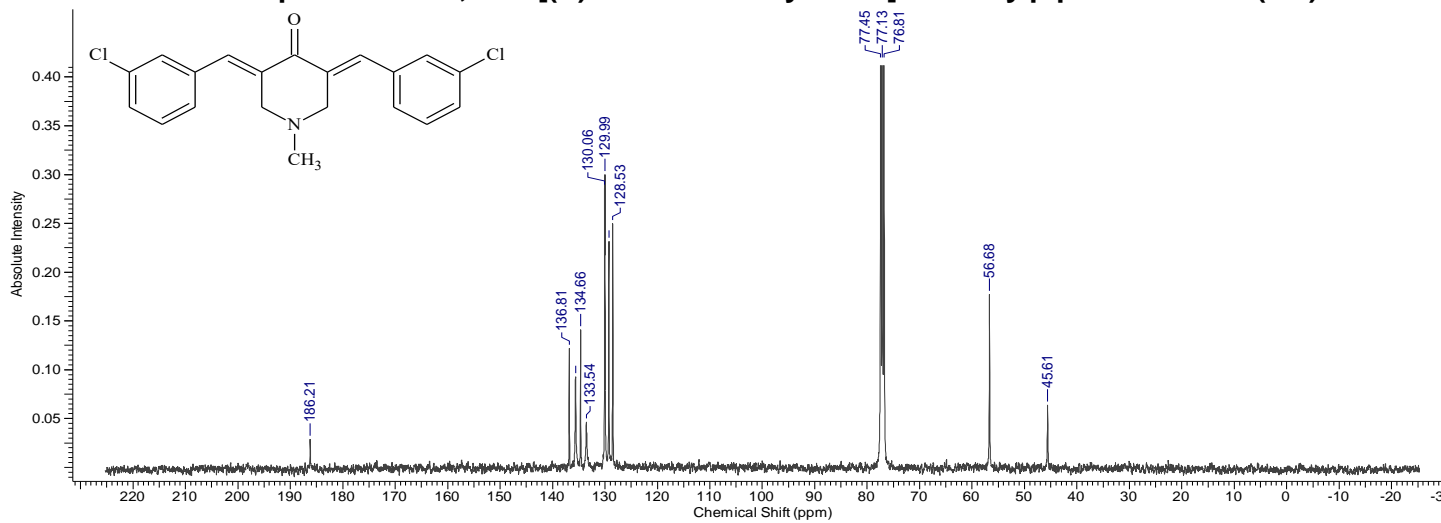


Compound 22f

Proton spectrum of 3,5-bis[(E)-3-chlorobenzylidene]-1-methylpiperidin-4-one (22f)

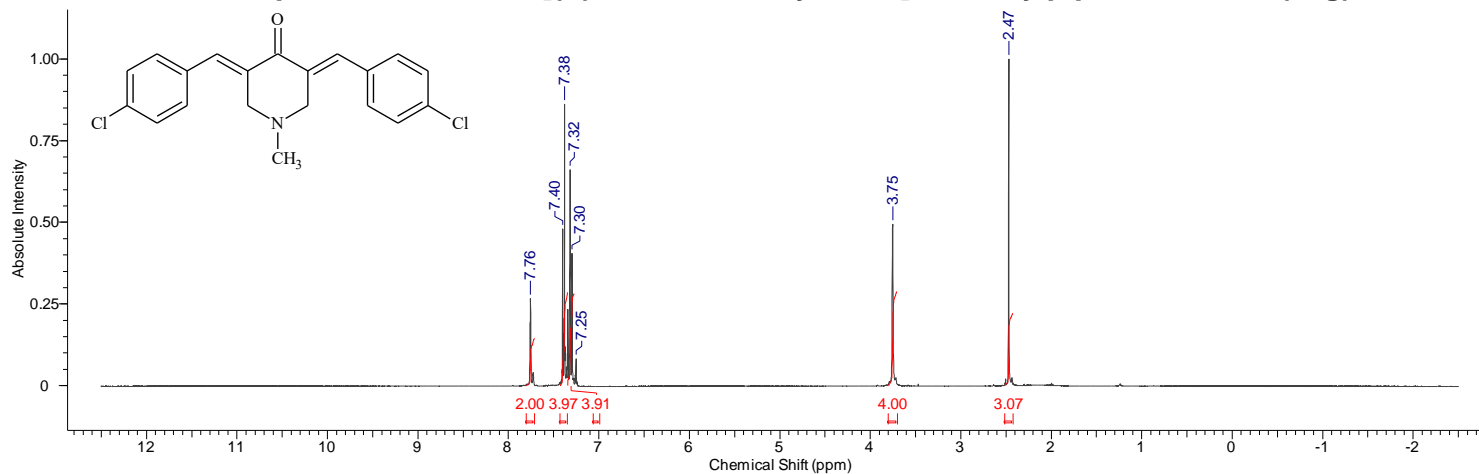


Carbon spectrum of 3,5-bis[(E)-3-chlorobenzylidene]-1-methylpiperidin-4-one (22f)

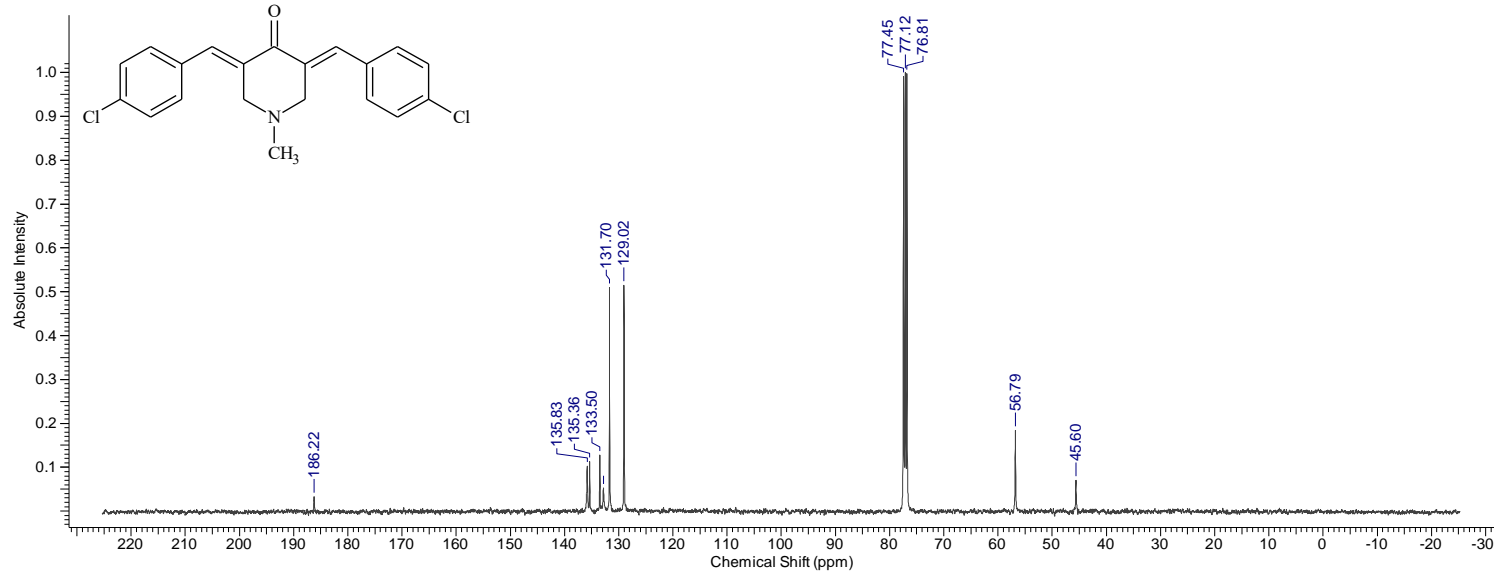


Compound 22g

Proton spectrum of 3,5-bis[(E)-4-chlorobenzylidene]-1-methylpiperidin-4-one (22g)

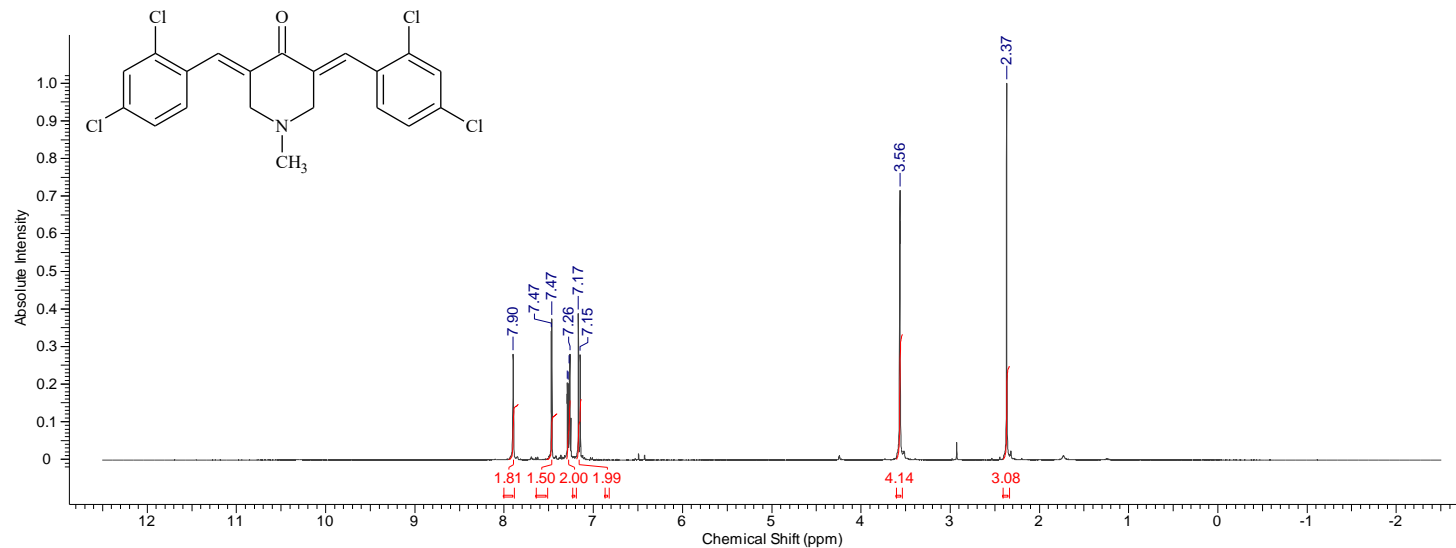


Carbon spectrum of 3,5-bis[(E)-4-chlorobenzylidene]-1-methylpiperidin-4-one (22g)

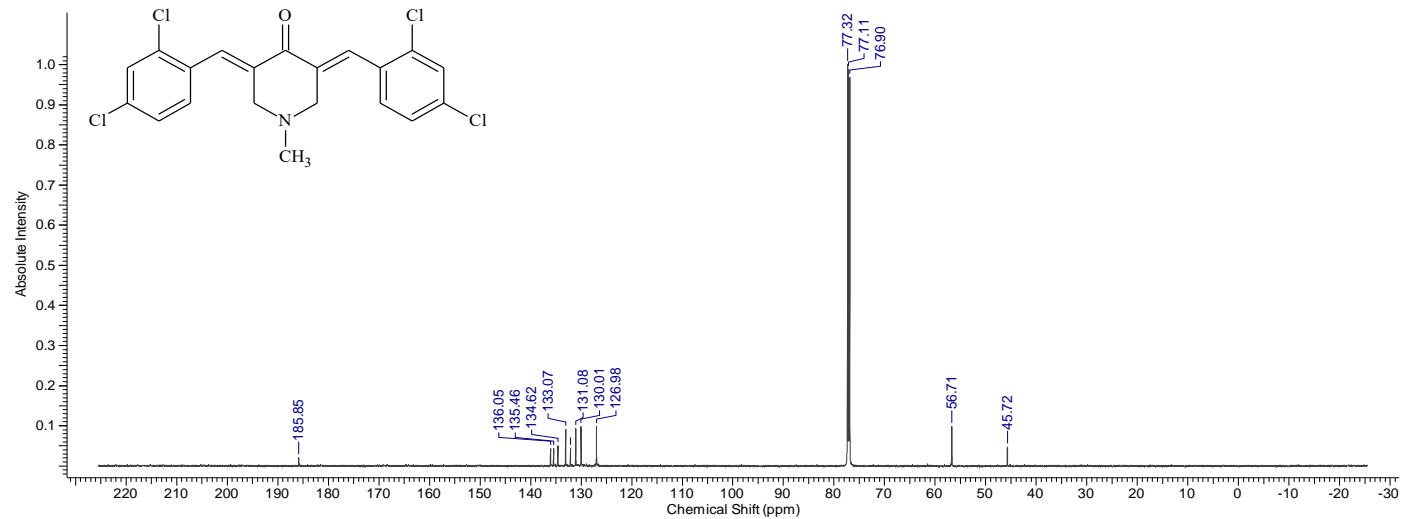


Compound 22h

Proton spectrum of 3,5-bis[(E)-2,4-dichlorobenzylidene]-1-methylpiperidin-4-one (22h)

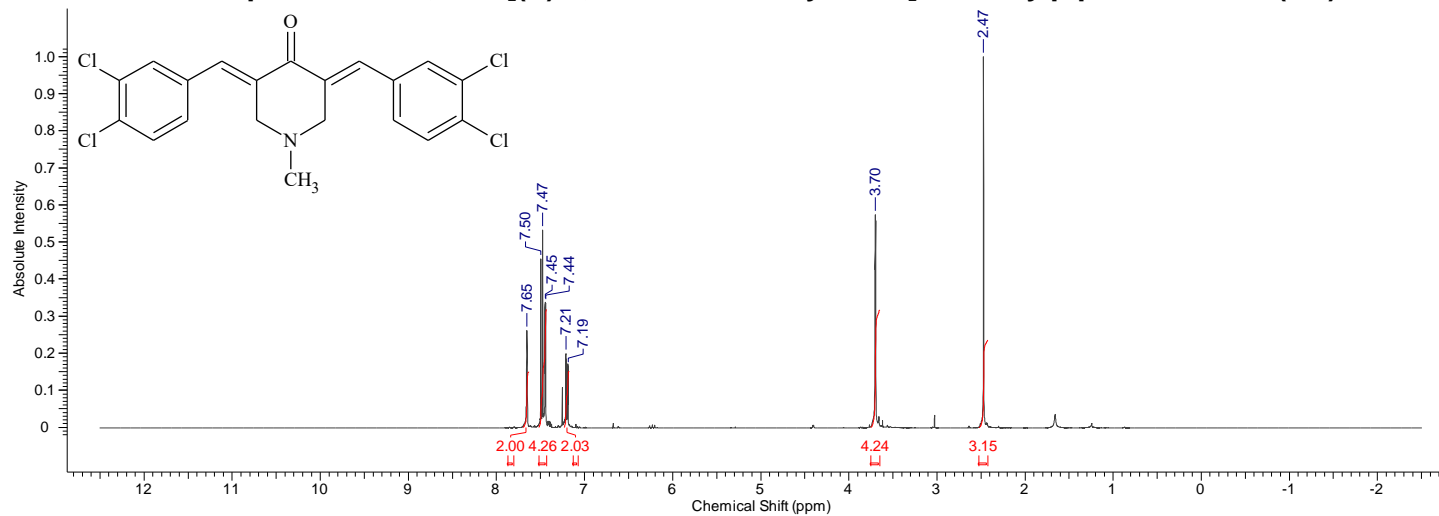


Carbon spectrum of 3,5-bis[(E)-2,4-dichlorobenzylidene]-1-methylpiperidin-4-one (22h)

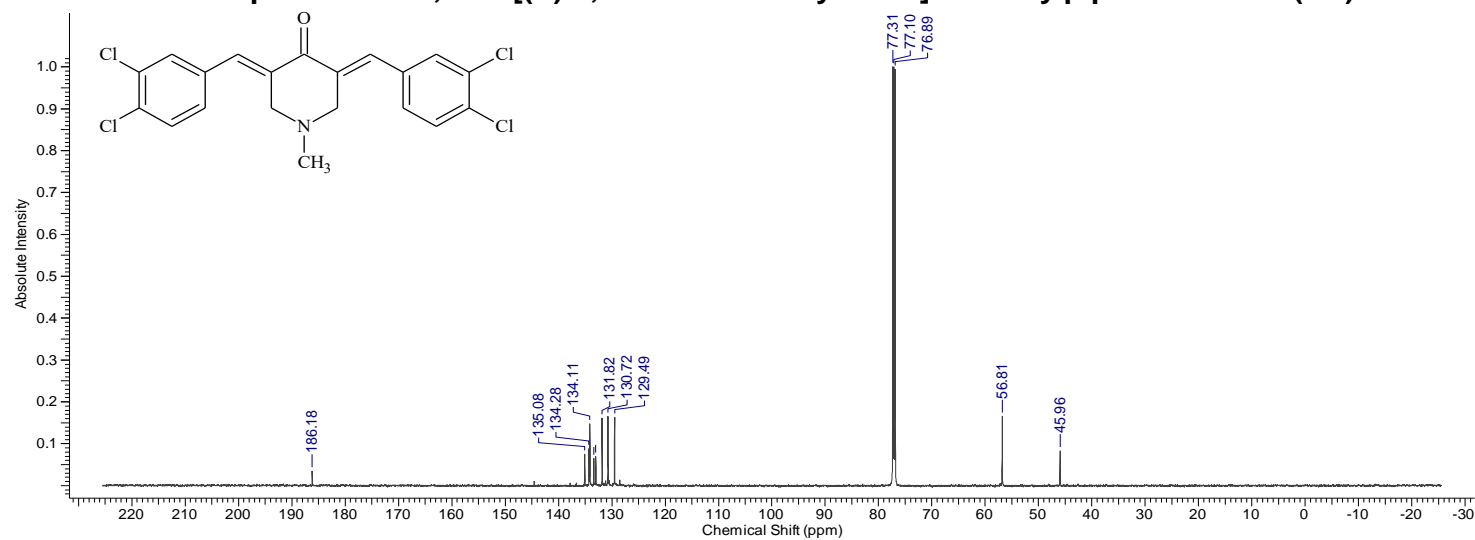


Compound 22i

Proton spectrum of 3,5-bis[(E)-3,4-dichlorobenzylidene]-1-methylpiperidin-4-one (22i)

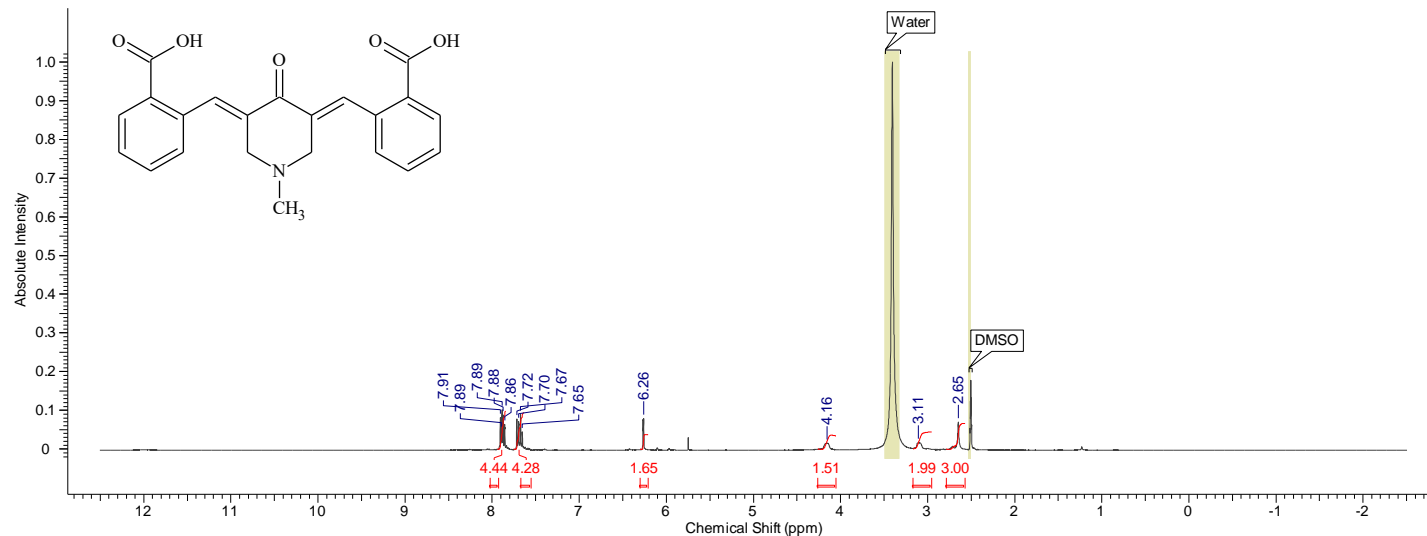


Carbon spectrum of 3,5-bis[(E)-3,4-dichlorobenzylidene]-1-methylpiperidin-4-one (22i)

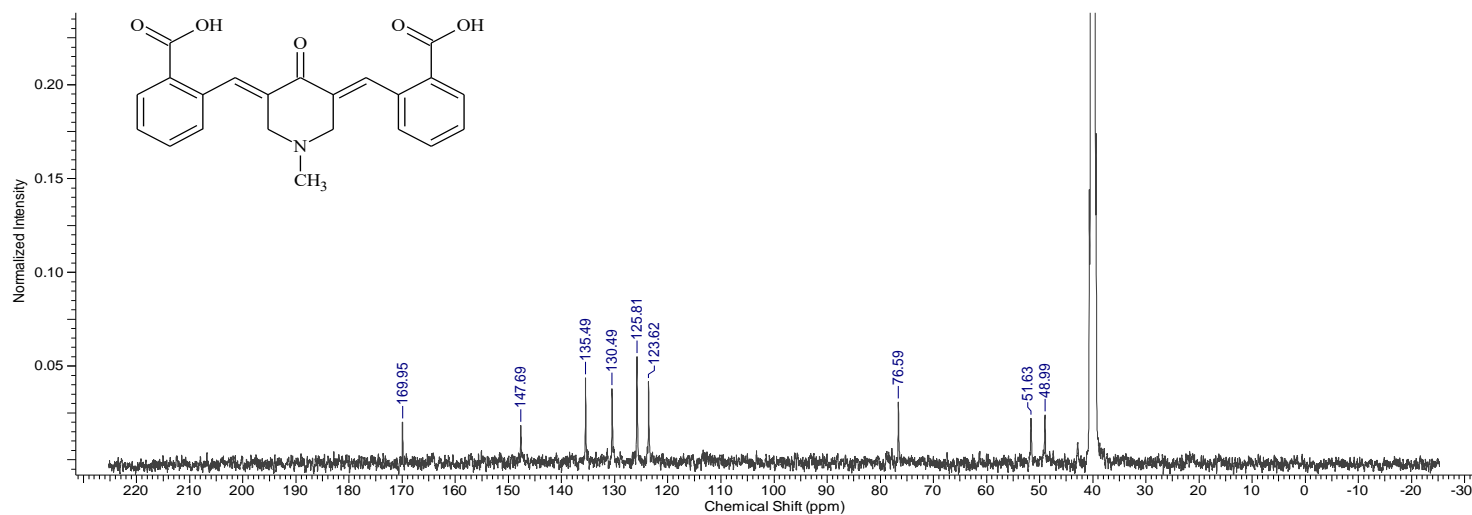


Compound 22j

Proton spectrum of 2,2'-((1E,1'E)-(1-methyl-4-oxopiperidine-3,5-diylidene)bis(methaneylylidene))dibenzoic acid (22j)

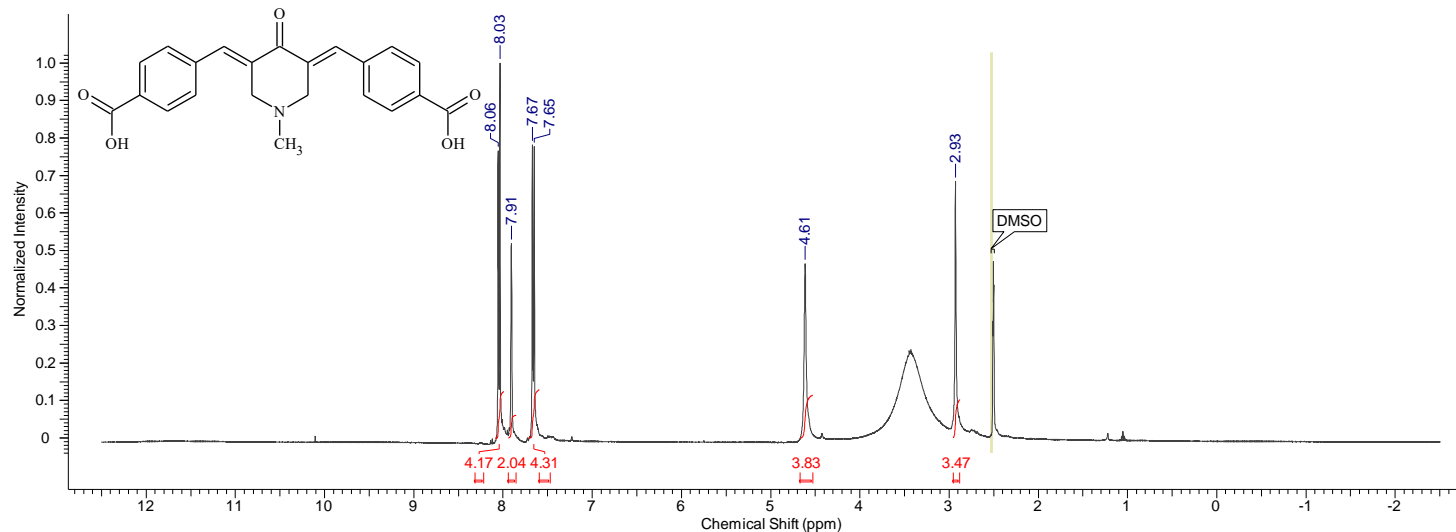


Carbon spectrum of 2,2'-((1E,1'E)-(1-methyl-4-oxopiperidine-3,5-diylidene)bis(methaneylylidene))dibenzoic acid (22j)

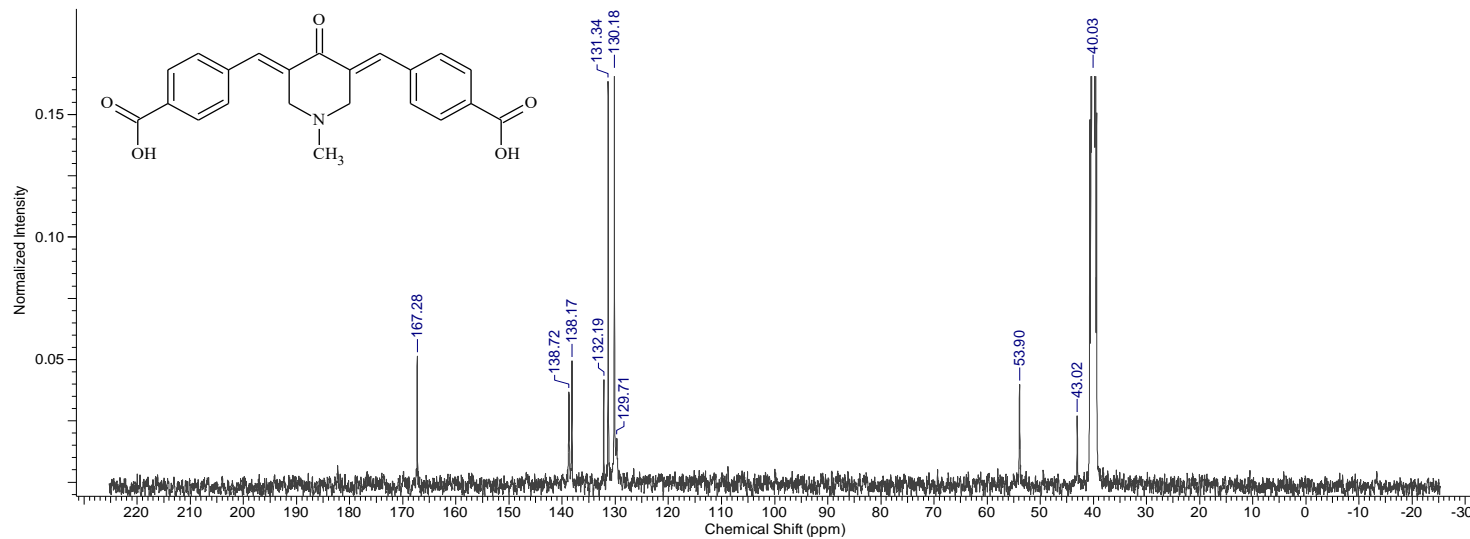


Compound 22k

Proton spectrum of 4,4'-((1E,1'E)-(1-methyl-4-oxopiperidine-3,5-diylidene)bis(methaneylylidene))dibenzoic acid (22k)

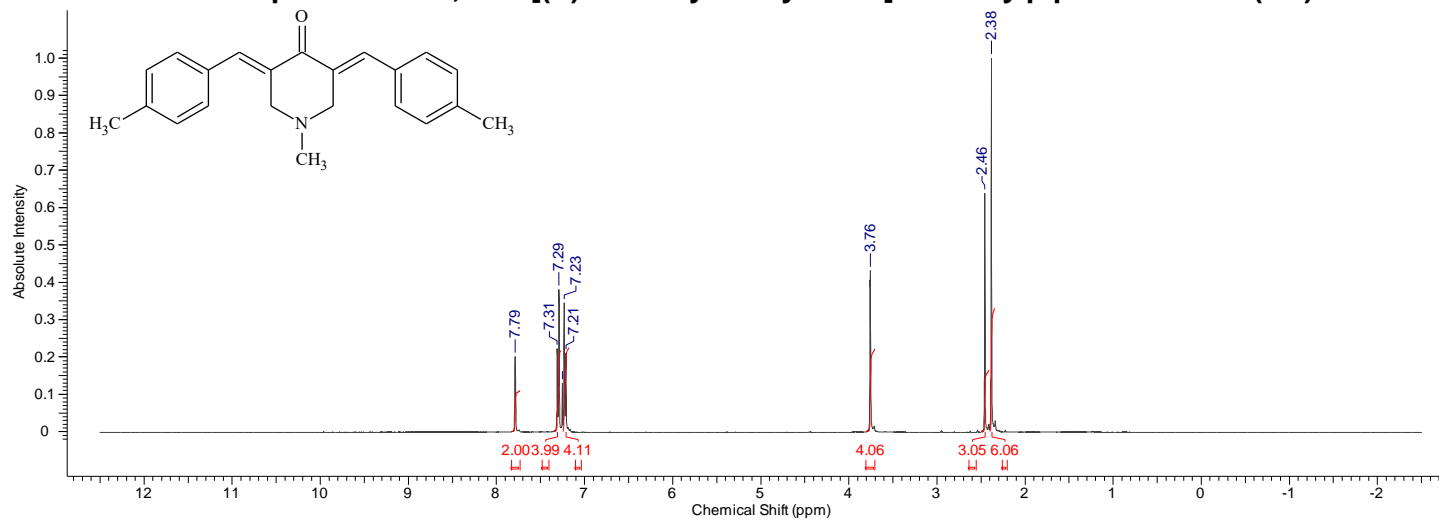


Carbon spectrum of 4,4'-((1E,1'E)-(1-methyl-4-oxopiperidine-3,5-diylidene)bis(methaneylylidene))dibenzoic acid (22k)

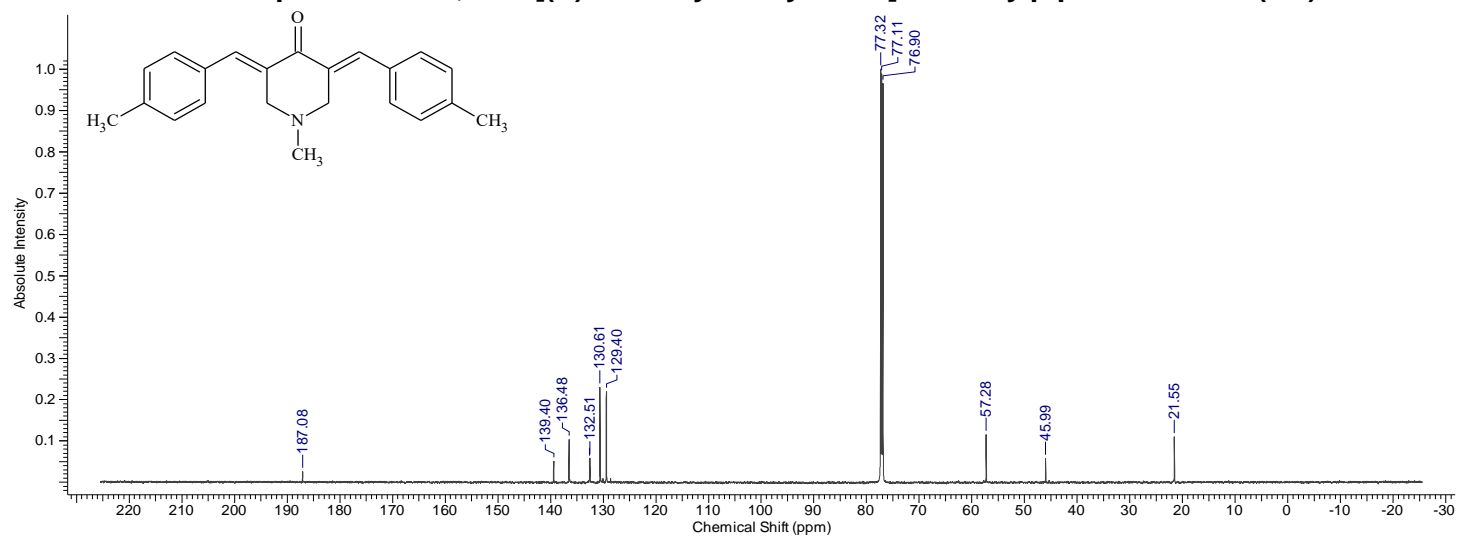


Compound 22I

Proton spectrum of 3,5-bis[(E)-4-methylbenzylidene]-1-methylpiperidin-4-one (22I)

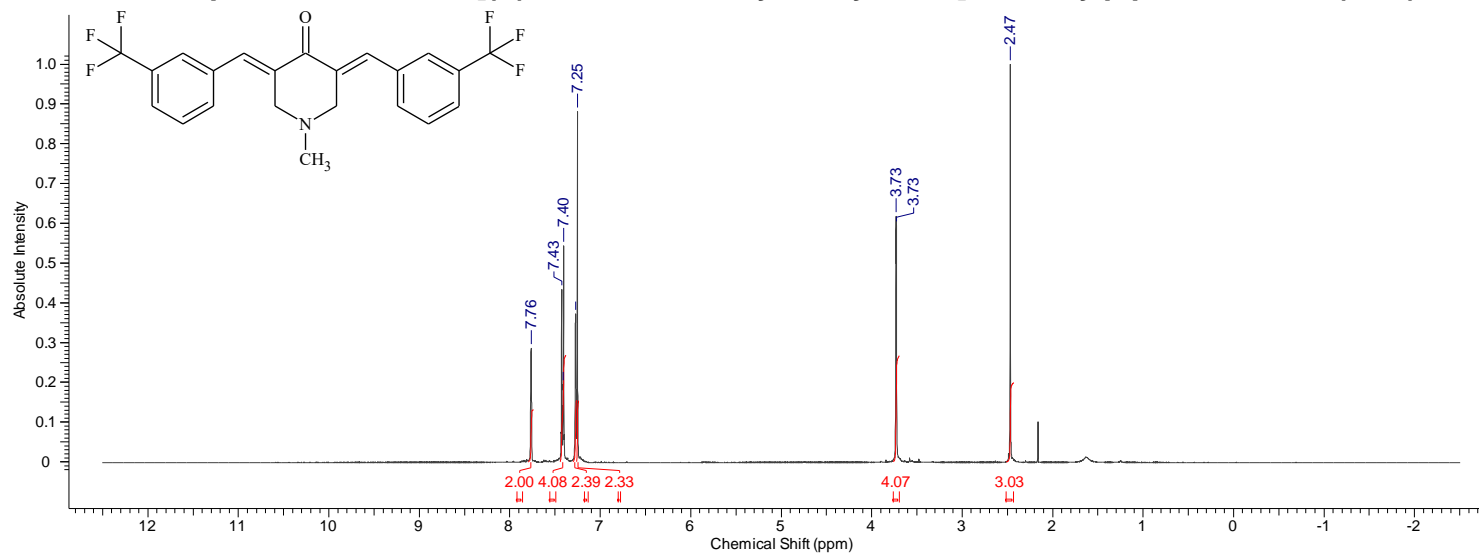


Carbon spectrum of 3,5-bis[(E)-4-methylbenzylidene]-1-methylpiperidin-4-one (22I)

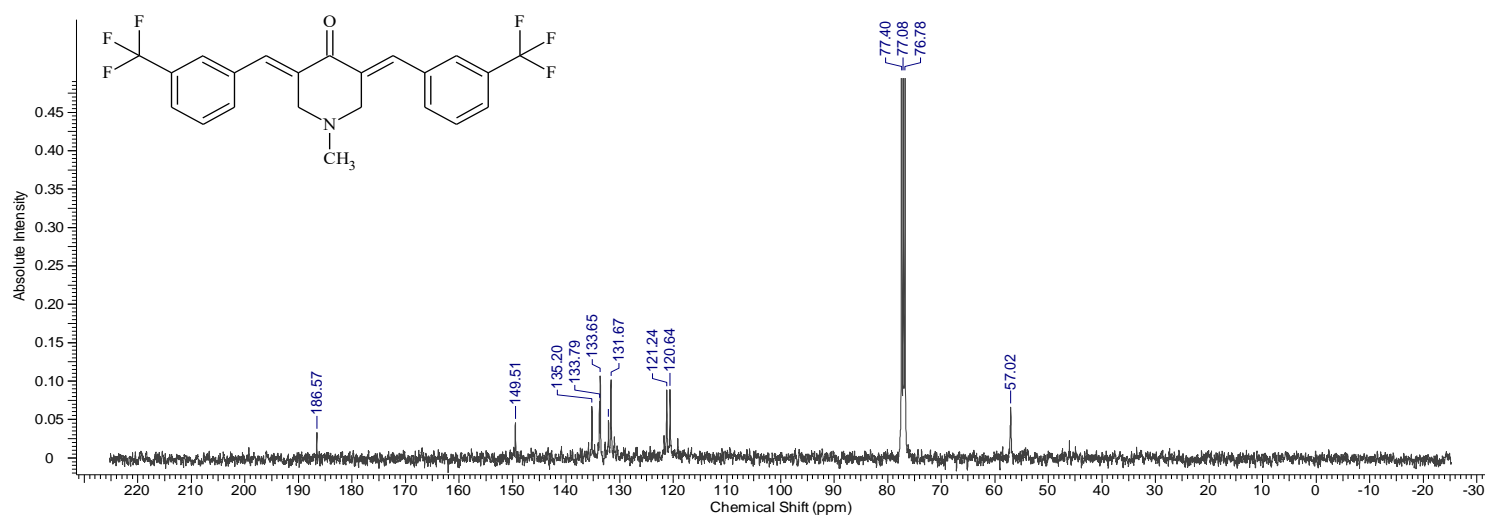


Compound 22m

Proton spectrum of 3,5-bis[(E)-3-trifluoromethylbenzylidene]-1-methylpiperidin-4-one (22m)

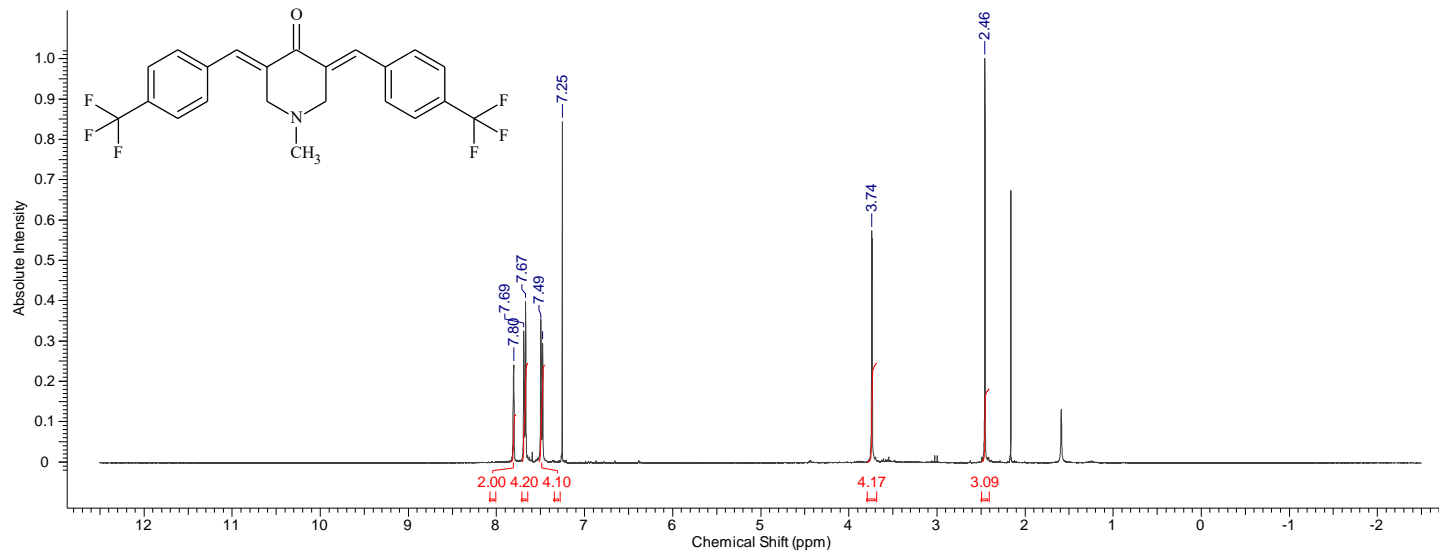


Carbon spectrum of 3,5-bis[(E)-3-trifluoromethylbenzylidene]-1-methylpiperidin-4-one (22m)

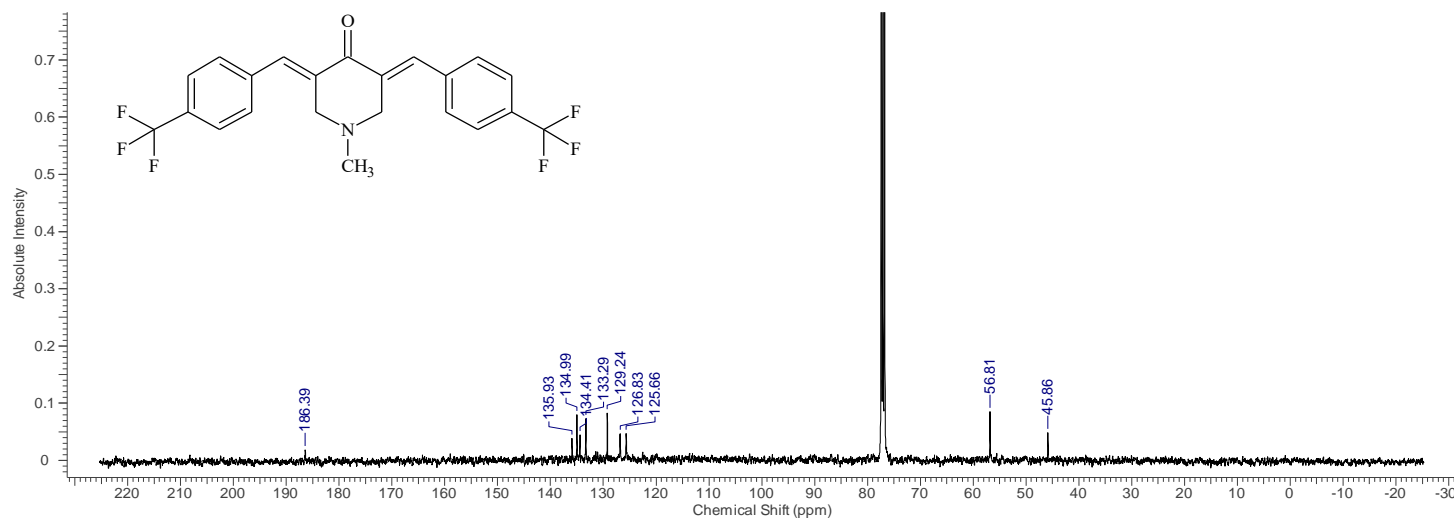


Compound 22n

Proton spectrum of 3,5-bis[(E)-4-trifluoromethylbenzylidene]-1-methylpiperidin-4-one (22n)

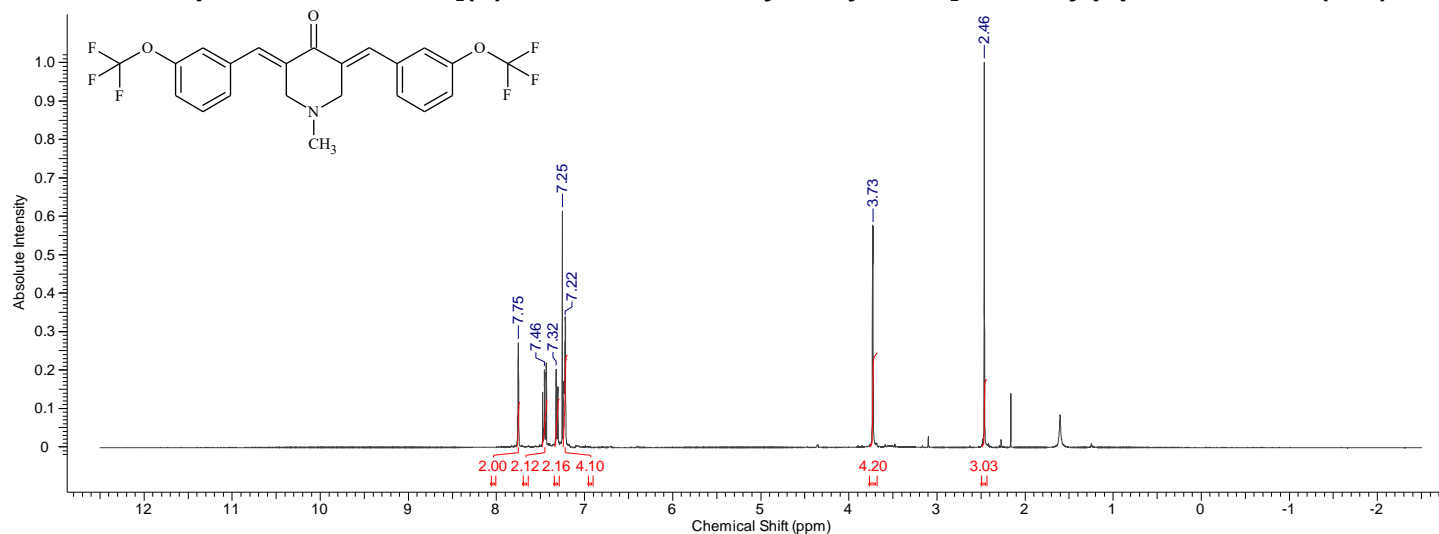


Carbon spectrum of 3,5-bis[(E)-4-trifluoromethylbenzylidene]-1-methylpiperidin-4-one (22n)

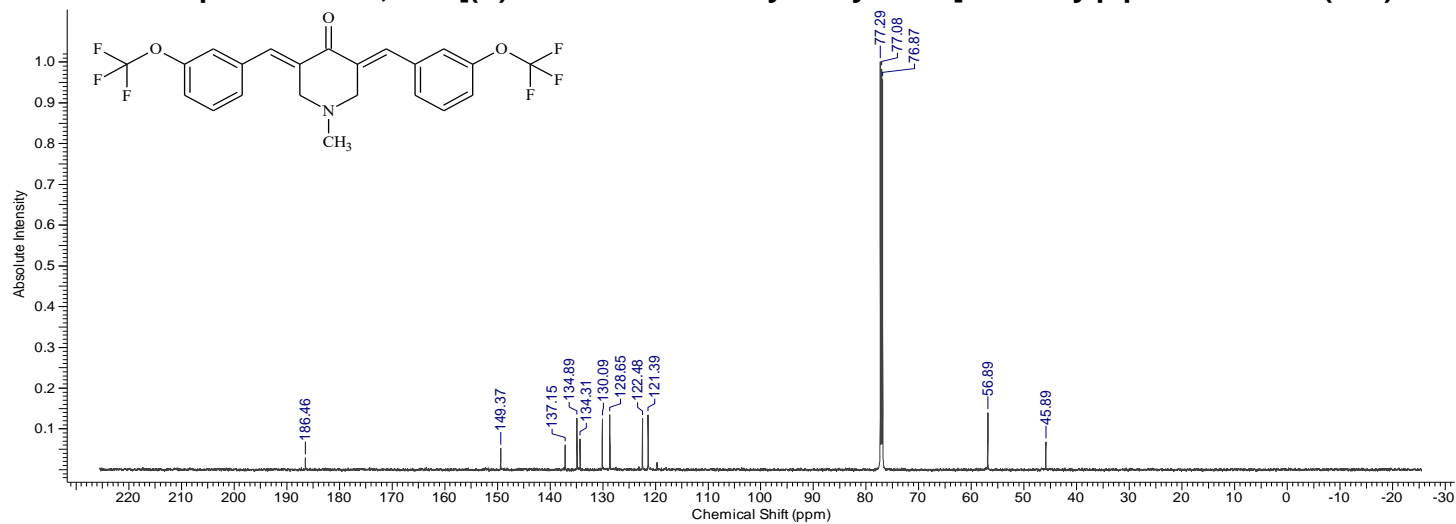


Compound 22o

Proton spectrum of 3,5-bis[(E)-3-trifluoromethoxybenzylidene]-1-methylpiperidin-4-one (22o)

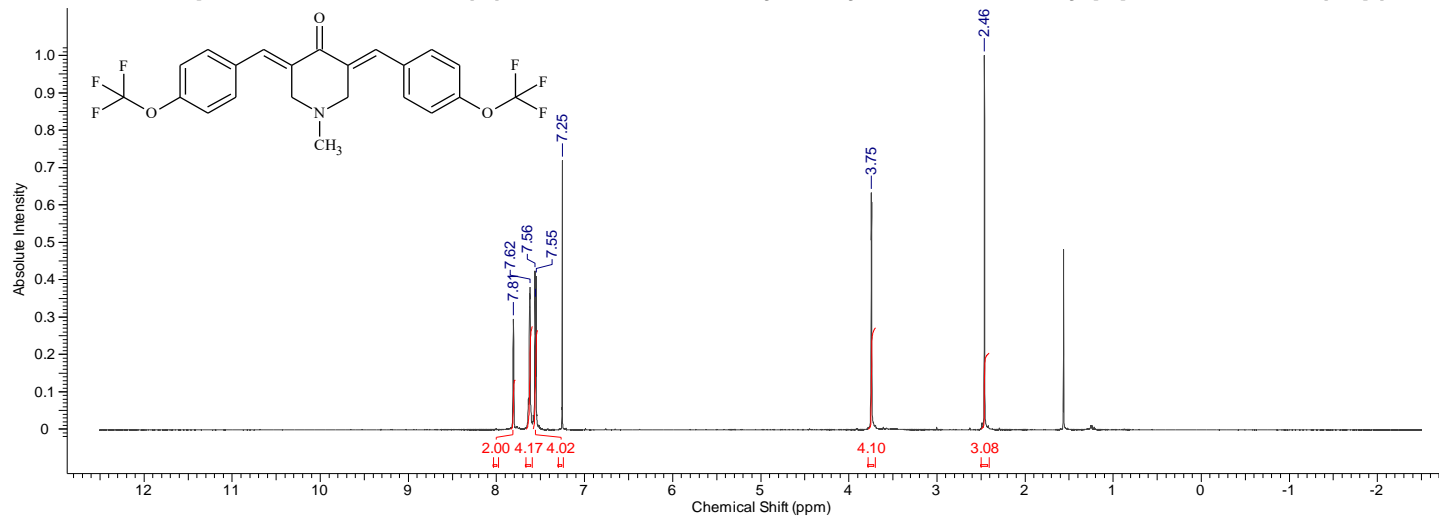


Carbon spectrum of 3,5-bis[(E)-3-trifluoromethoxybenzylidene]-1-methylpiperidin-4-one (22o)

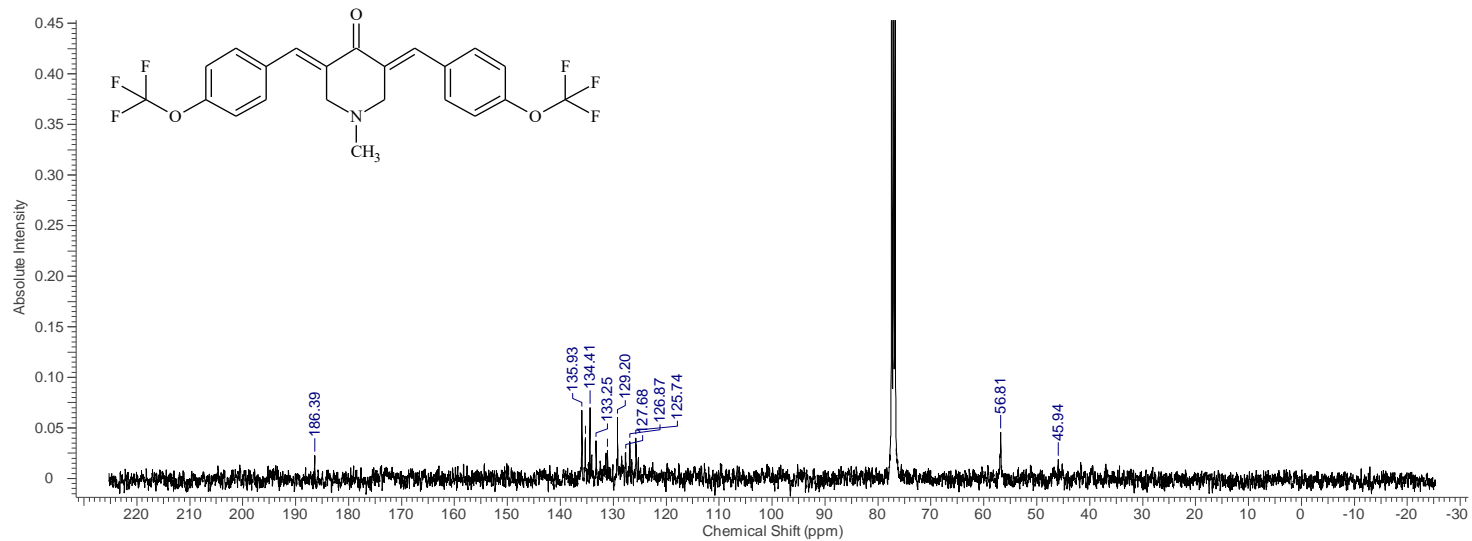


Compound 22p

Proton spectrum of 3,5-bis[(E)-4-trifluoromethoxybenzylidene]-1-methylpiperidin-4-one (22p)

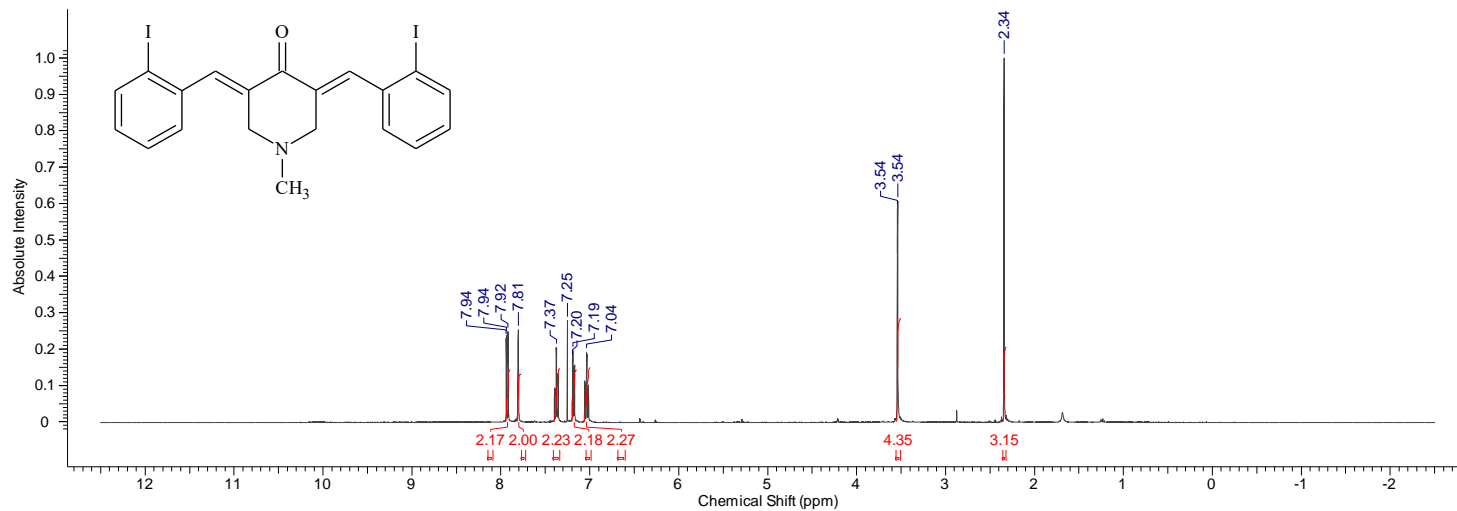


Carbon spectrum of 3,5-bis[(E)-4-trifluoromethoxybenzylidene]-1-methylpiperidin-4-one (22p)

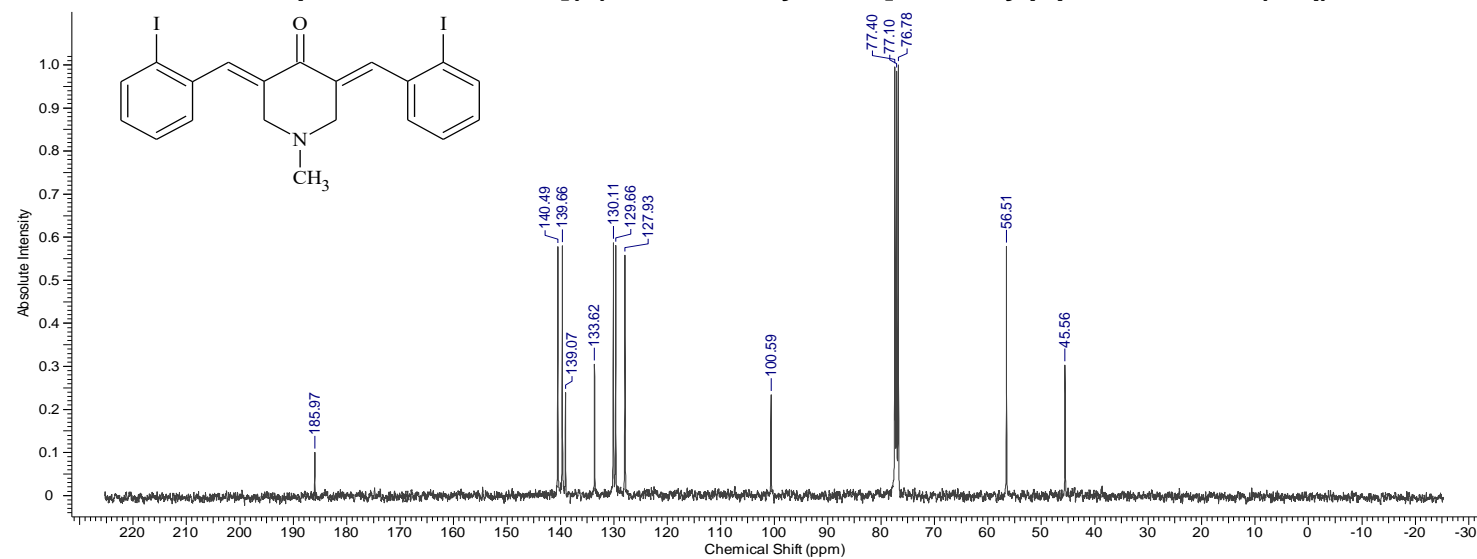


Compound 22q

Proton spectrum of 3,5-bis[(E)-2-iodobenzylidene]-1-methylpiperidin-4-one (22q)

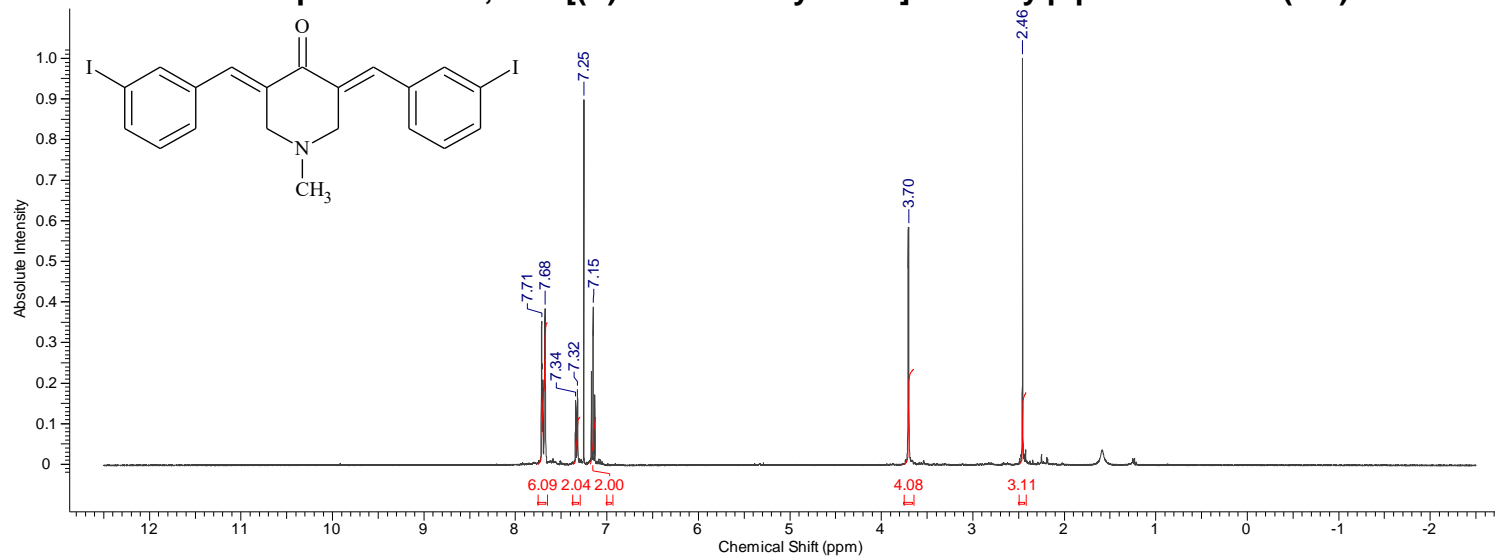


Carbon spectrum of 3,5-bis[(E)-2-iodobenzylidene]-1-methylpiperidin-4-one (22q)

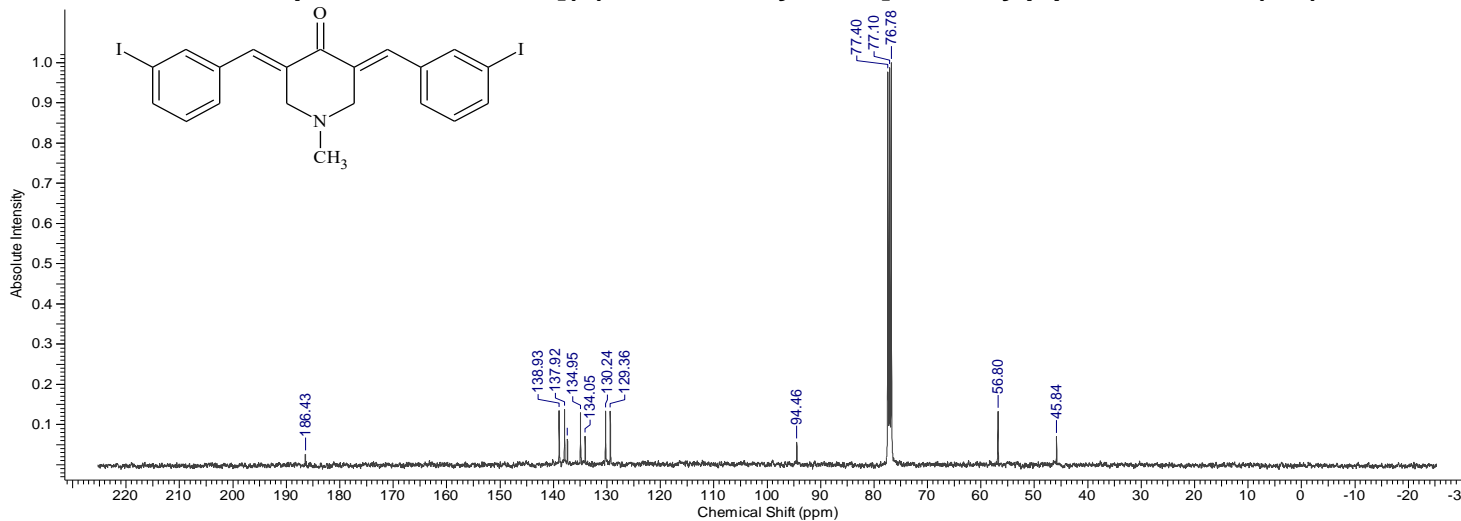


Compound 22r

Proton spectrum of 3,5-bis[(E)-3-iodobenzylidene]-1-methylpiperidin-4-one (22r)

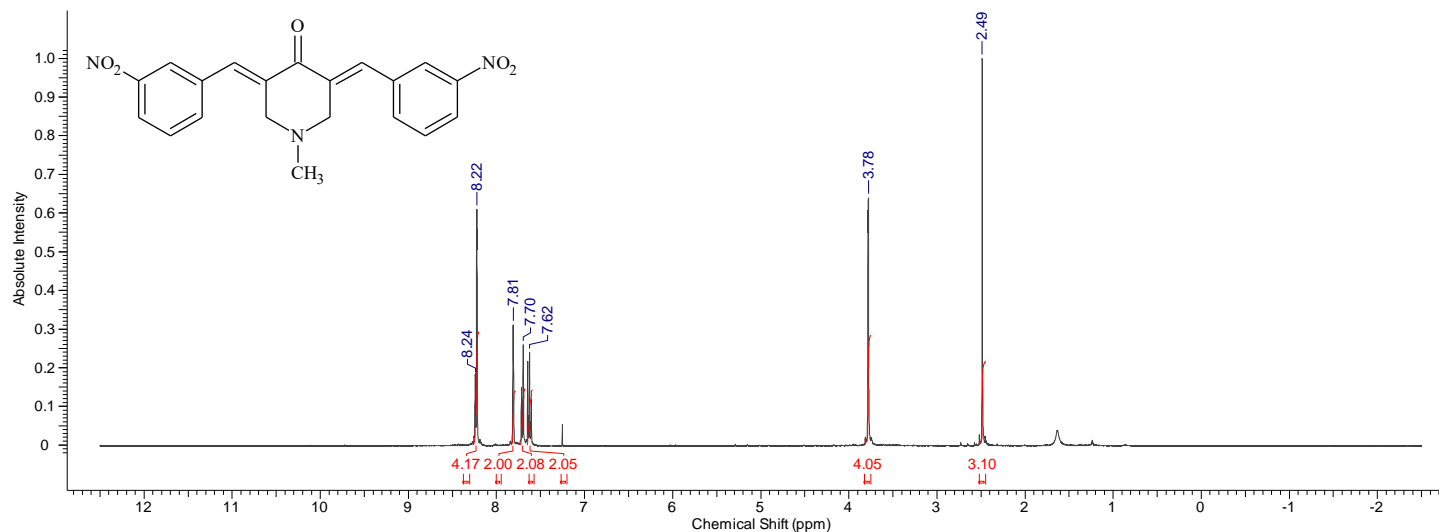


Carbon spectrum of 3,5-bis[(E)-3-iodobenzylidene]-1-methylpiperidin-4-one (22r)

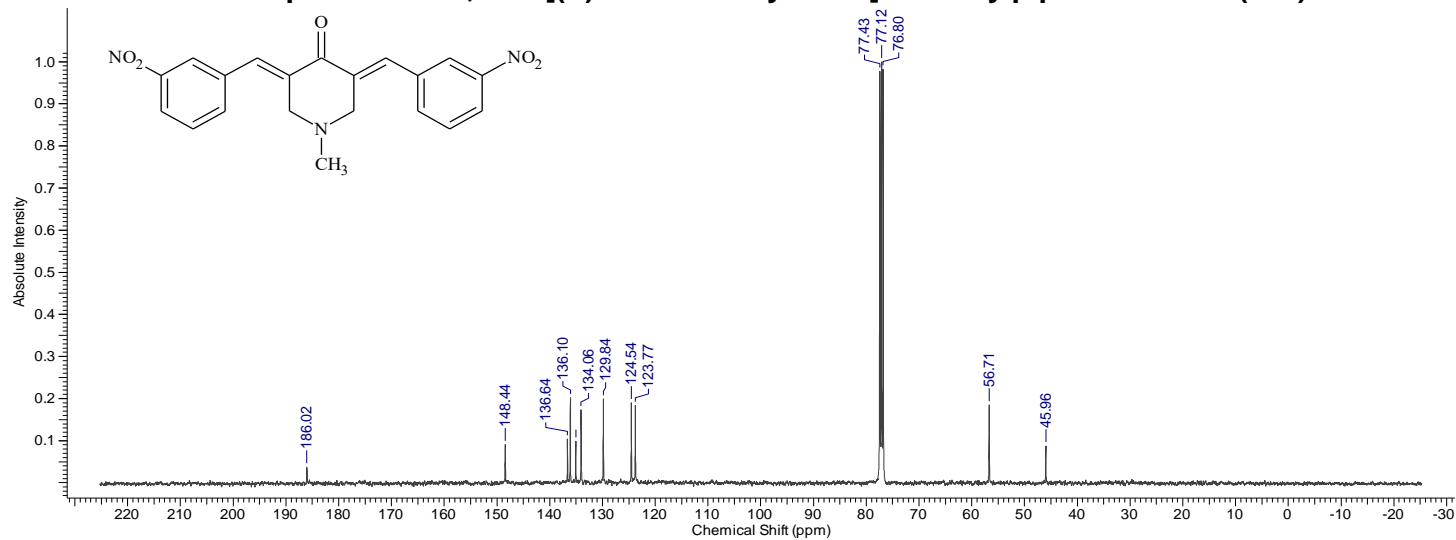


Compound 22s

Proton spectrum of 3,5-bis[(E)-3-nitrobenzylidene]-1-methylpiperidin-4-one (22s)

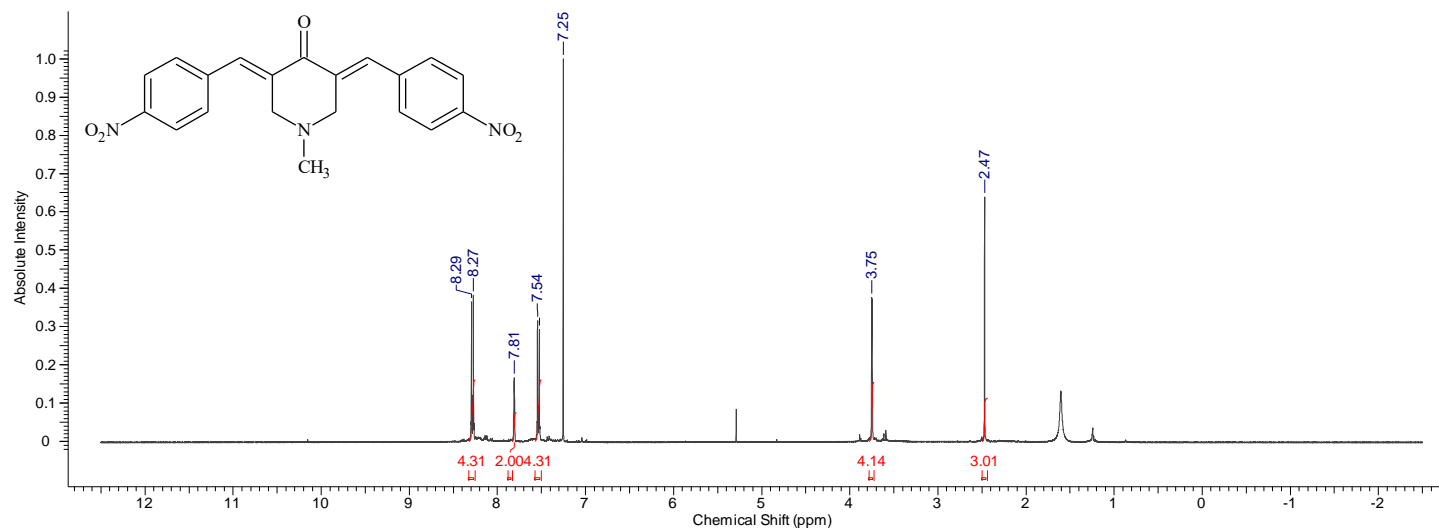


Carbon spectrum of 3,5-bis[(E)-3-nitrobenzylidene]-1-methylpiperidin-4-one (22s)

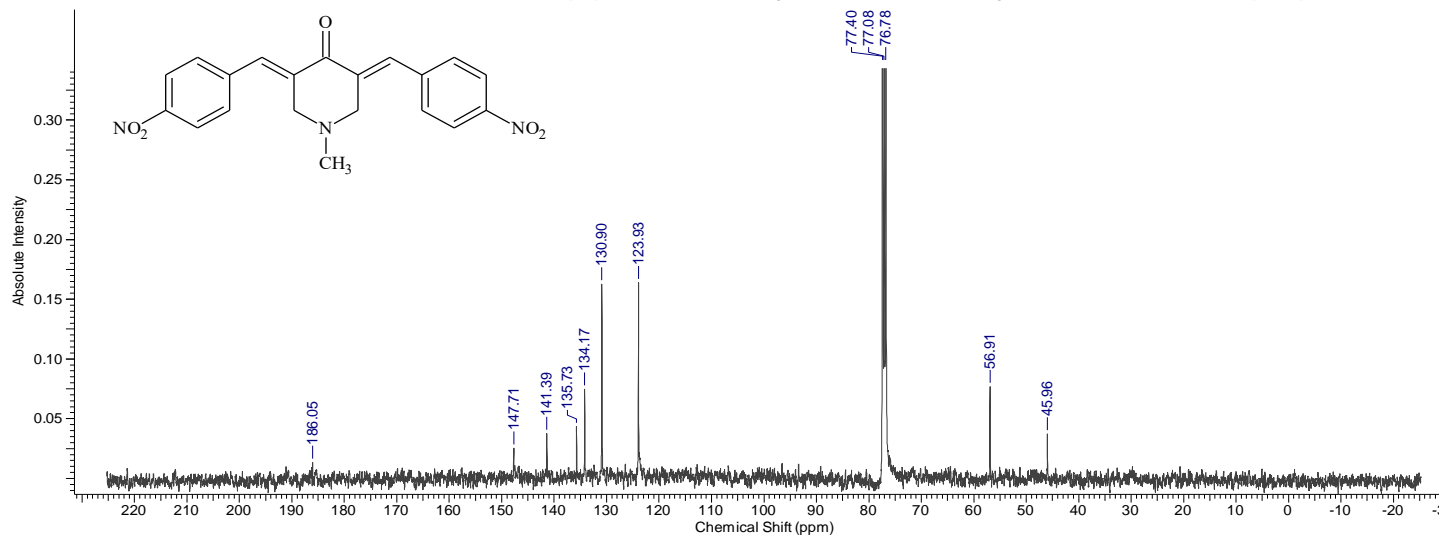


Compound 22t

Proton spectrum of 3,5-bis[(E)-4-nitrobenzylidene]-1-methylpiperidin-4-one (22t)

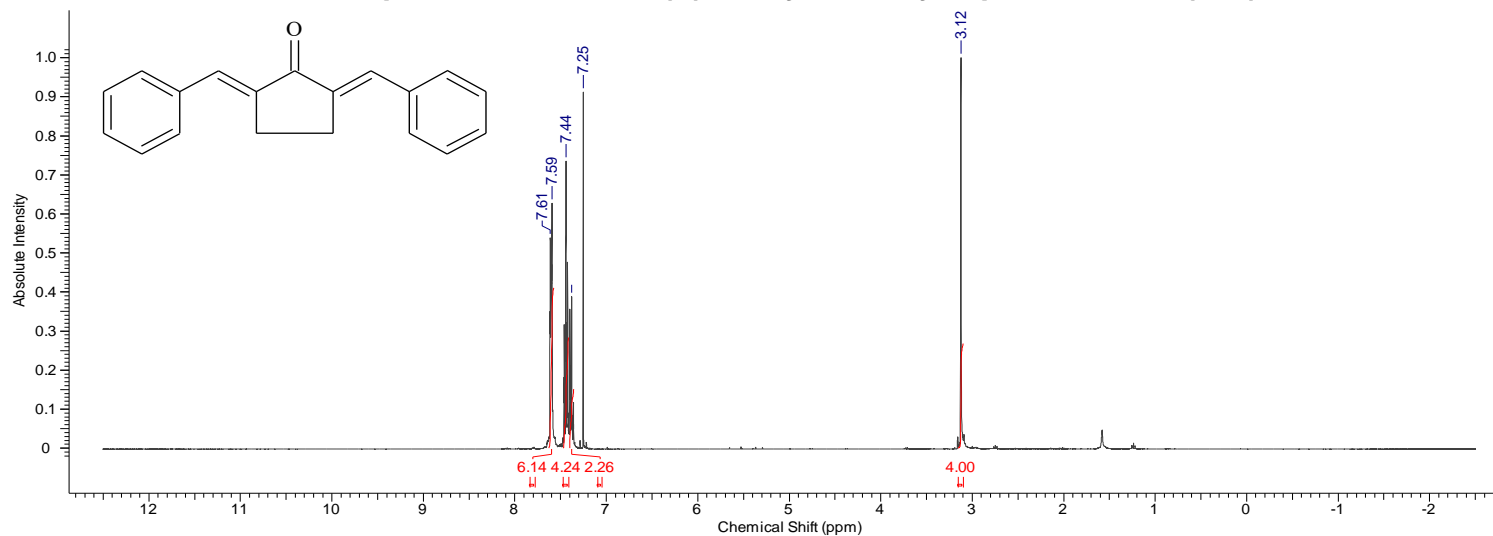


Carbon spectrum of 3,5-bis[(E)-4-nitrobenzylidene]-1-methylpiperidin-4-one (22t)

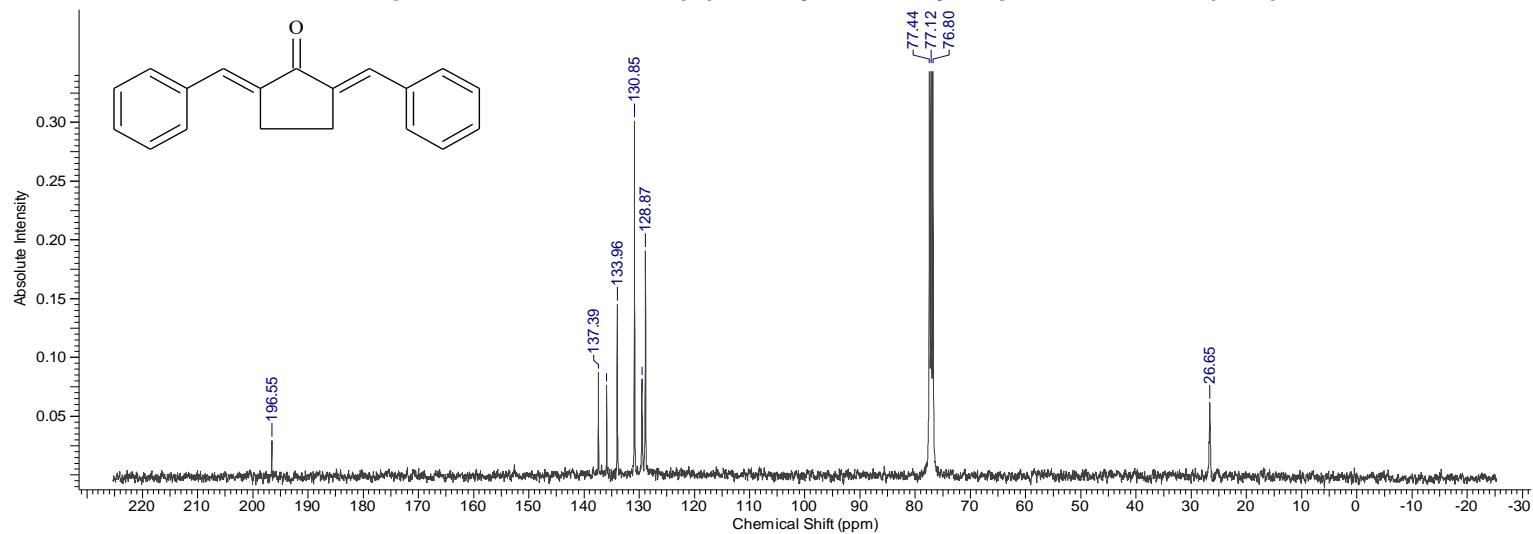


Compound 22u

Proton spectrum of 2,5-bis[(E)-benzylidene]cyclopentan-1-one (22u)

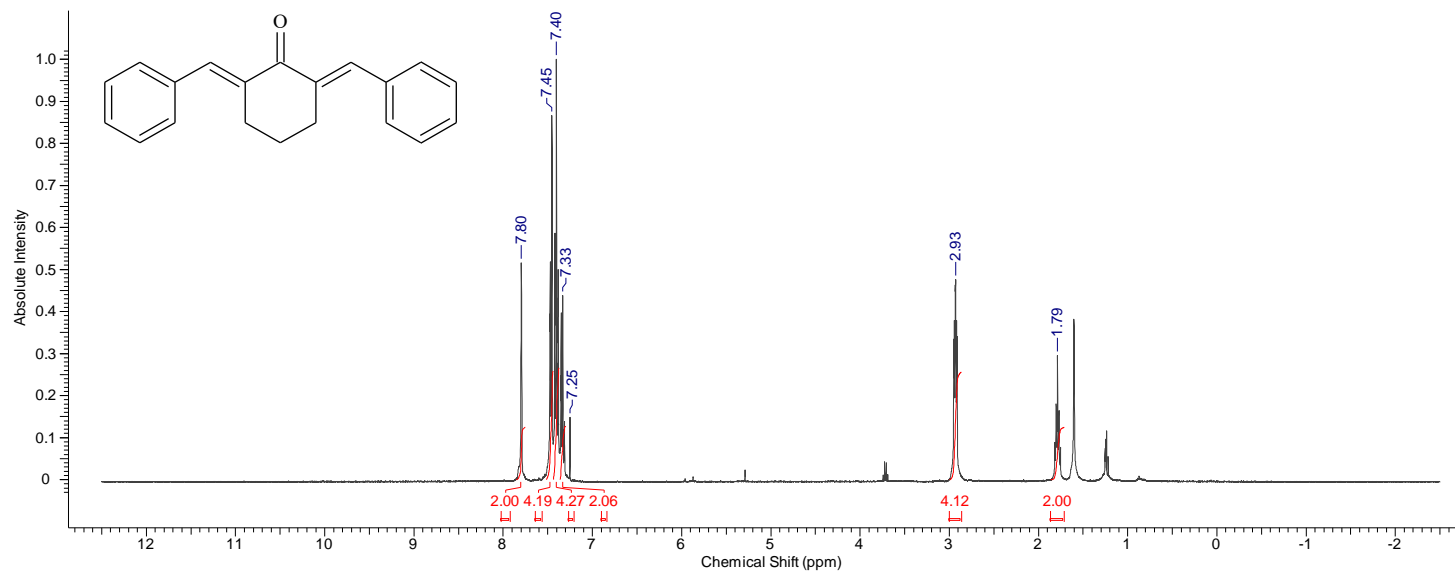


Carbon spectrum of 2,5-bis[(E)-benzylidene]cyclopentan-1-one (22u)

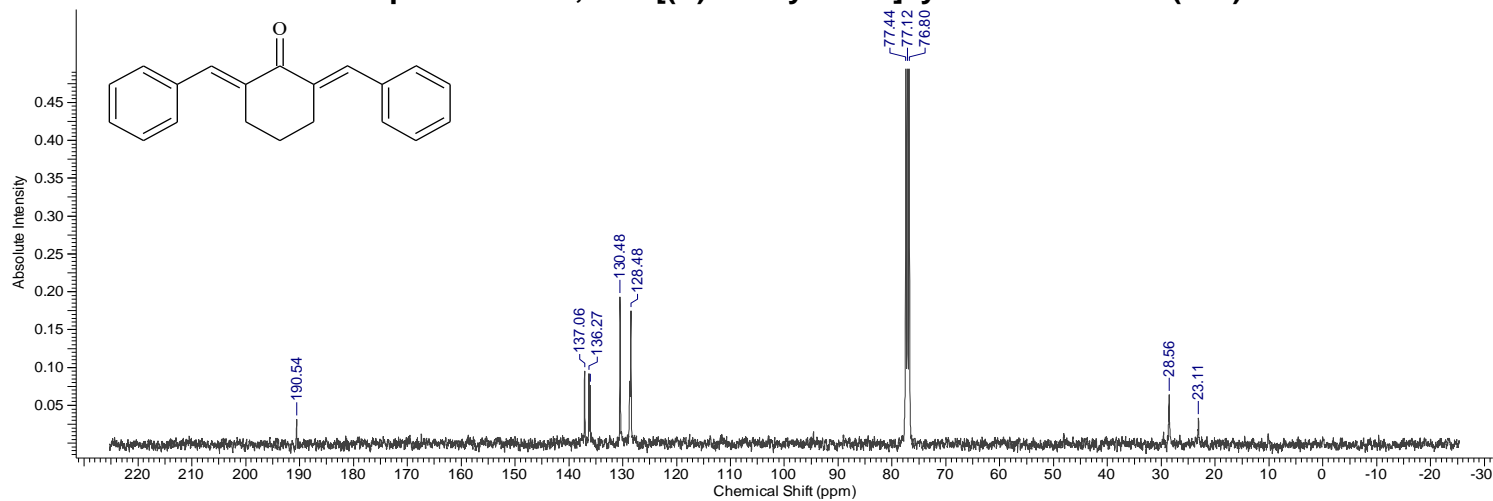


Compound 22v

Proton spectrum of 2,6-bis[(E)-benzylidene]cyclohexan-1-one (22v)

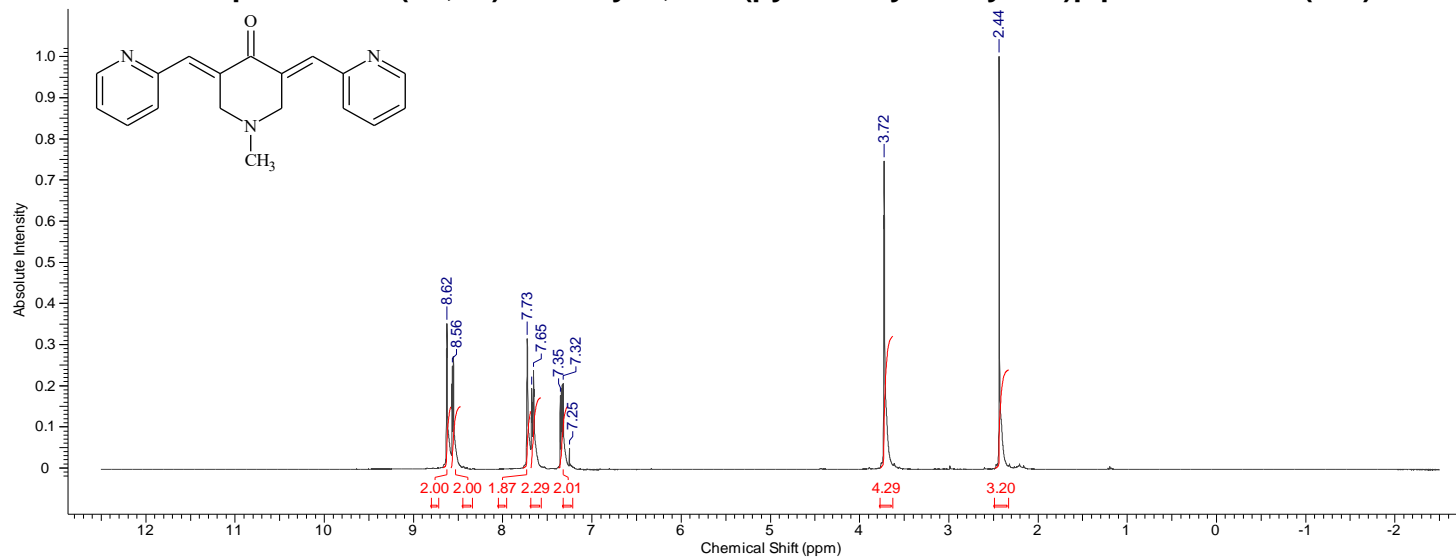


Carbon spectrum of 2,6-bis[(E)-benzylidene]cyclohexan-1-one (22v)

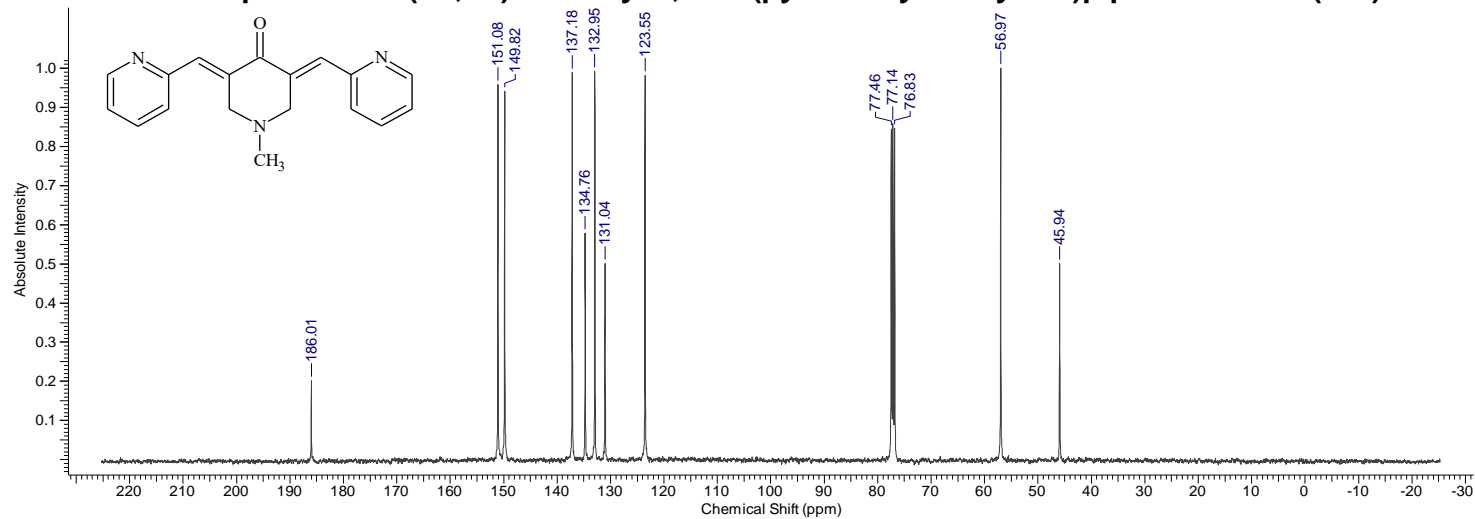


Compound 23a

Proton spectrum of (3E,5E)-1-methyl-3,5-bis(pyridin-2-ylmethylene)piperidin-4-one (23a)

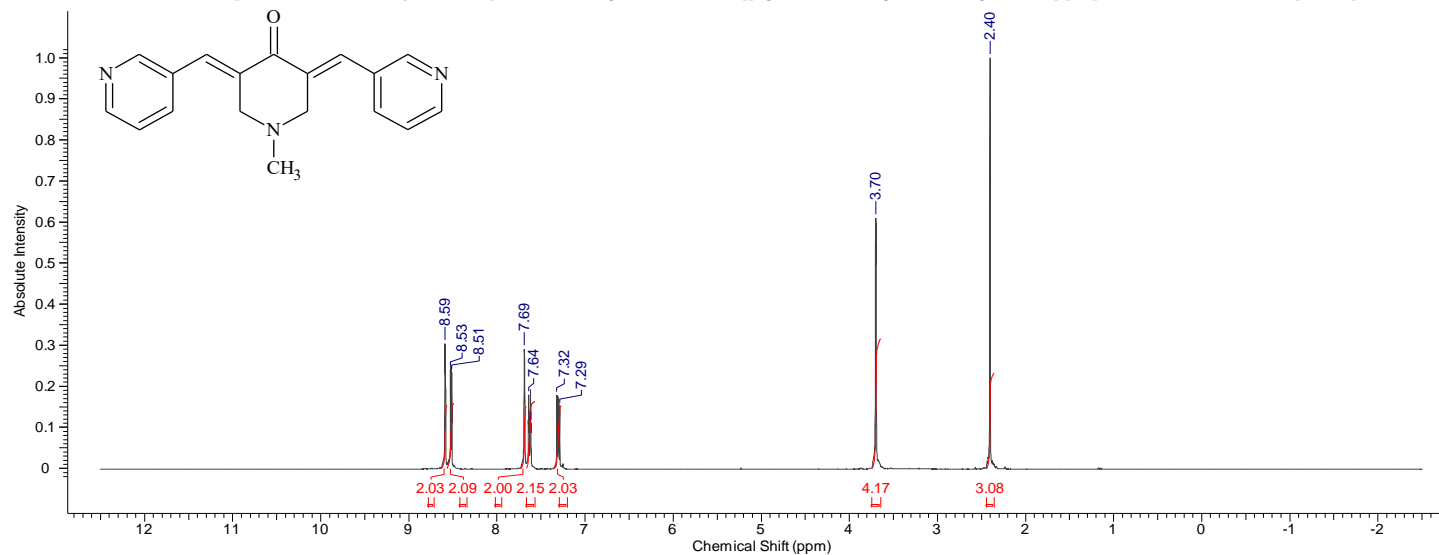


Carbon spectrum of (3E,5E)-1-methyl-3,5-bis(pyridin-2-ylmethylene)piperidin-4-one (23a)

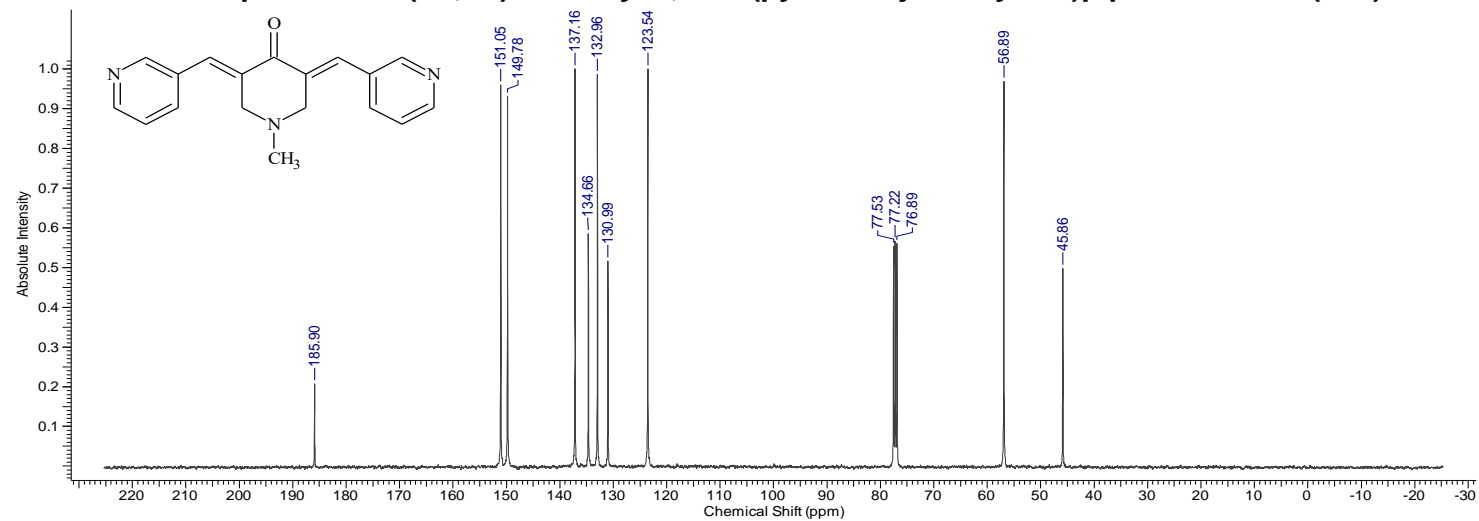


Compound 23b

Proton spectrum of (3E,5E)-1-methyl-3,5-bis(pyridin-3-ylmethylene)piperidin-4-one (23b)

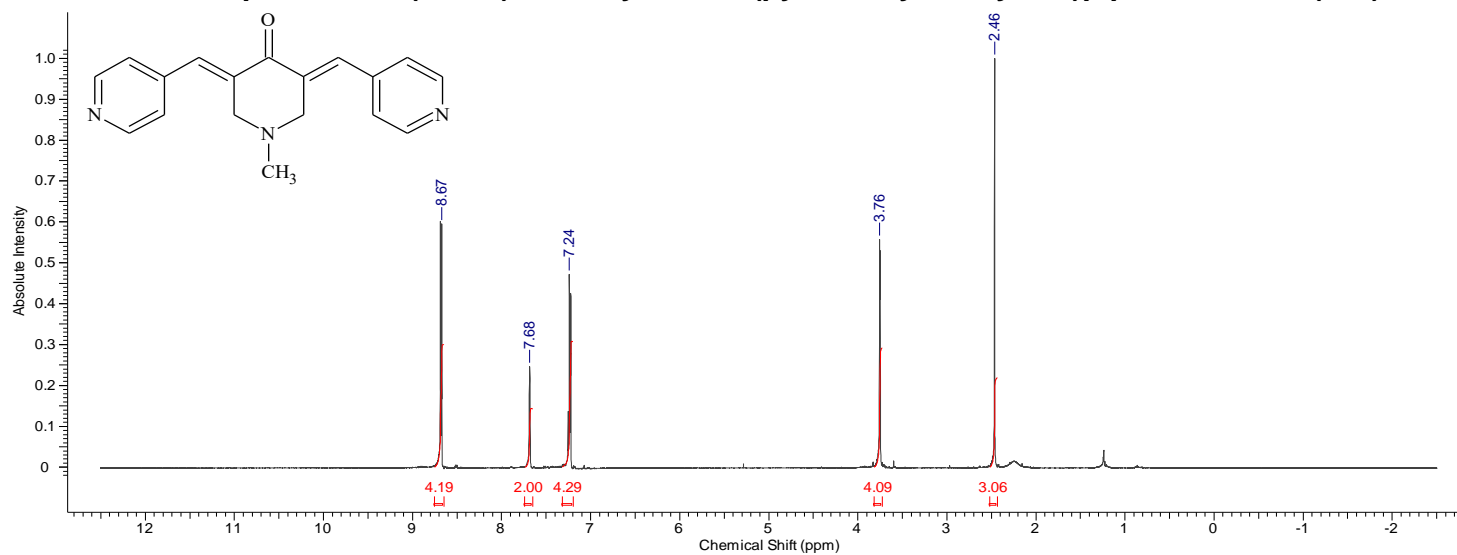


Carbon spectrum of (3E,5E)-1-methyl-3,5-bis(pyridin-3-ylmethylene)piperidin-4-one (23b)

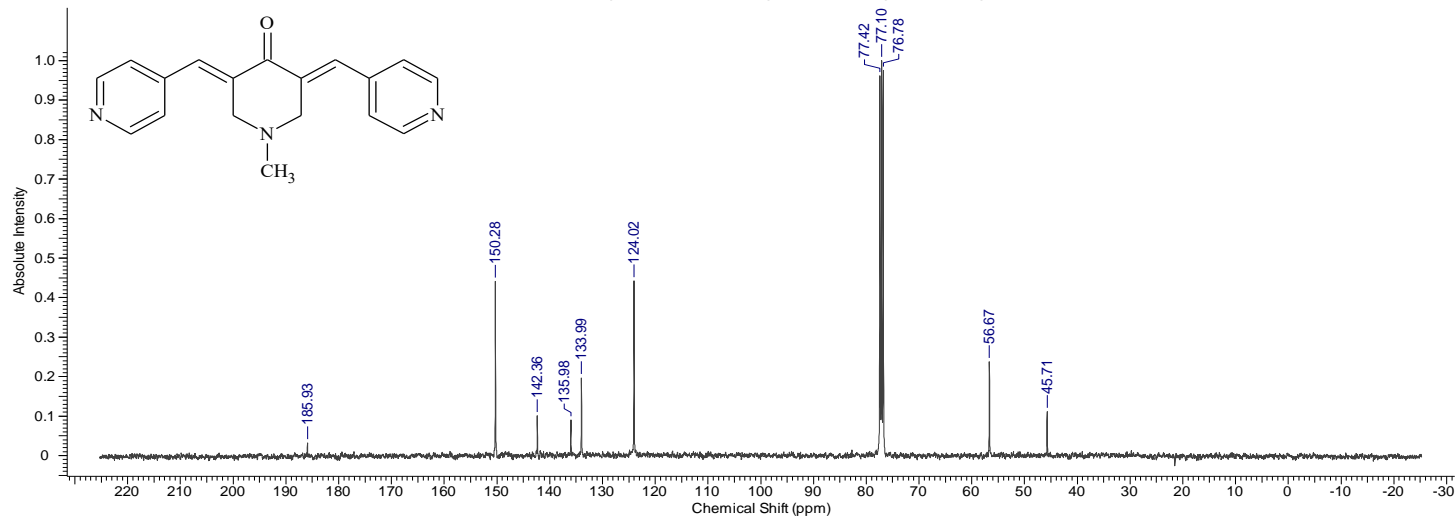


Compound 23c

Proton spectrum of (3E,5E)-1-methyl-3,5-bis(pyridin-4-ylmethylene)piperidin-4-one (23c)

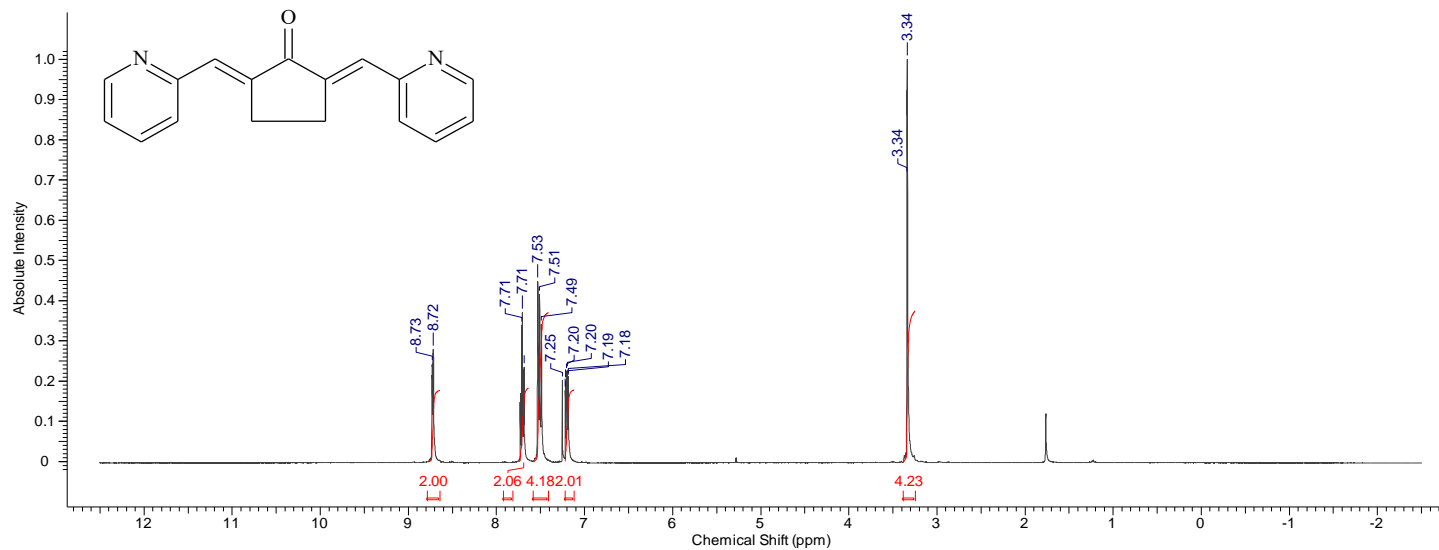


Carbon spectrum of (3E,5E)-1-methyl-3,5-bis(pyridin-4-ylmethylene)piperidin-4-one (23c)

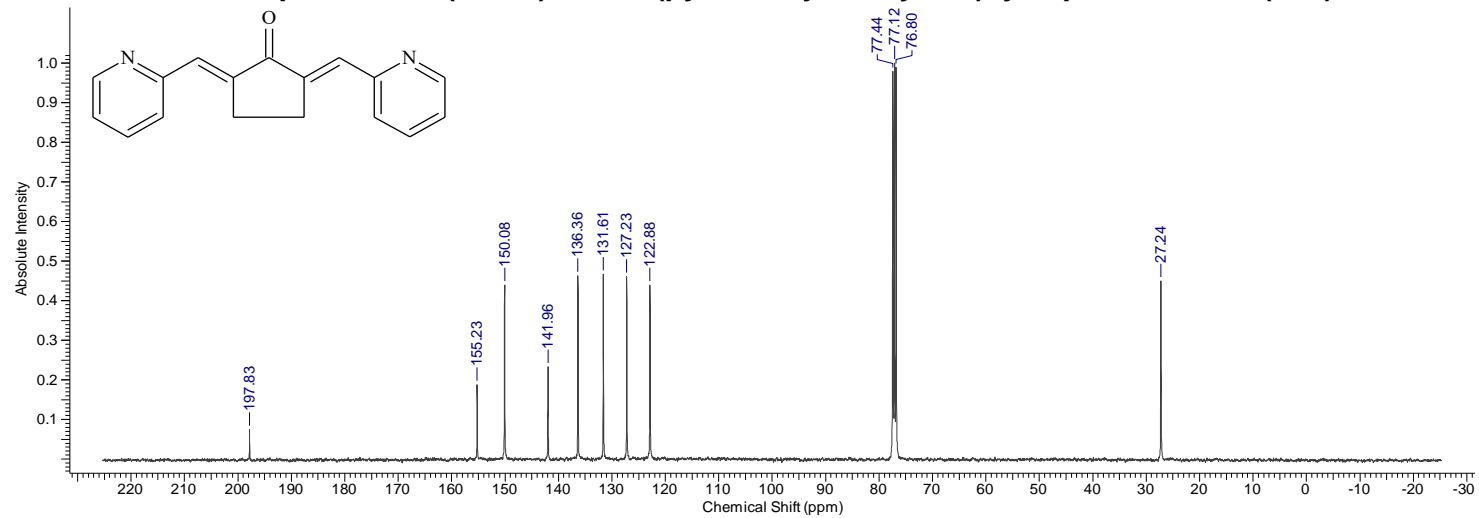


Compound 23d

Proton spectrum of (2E,5E)-2,5-bis(pyridin-2-ylmethylene)cyclopentan-1-one (23d)

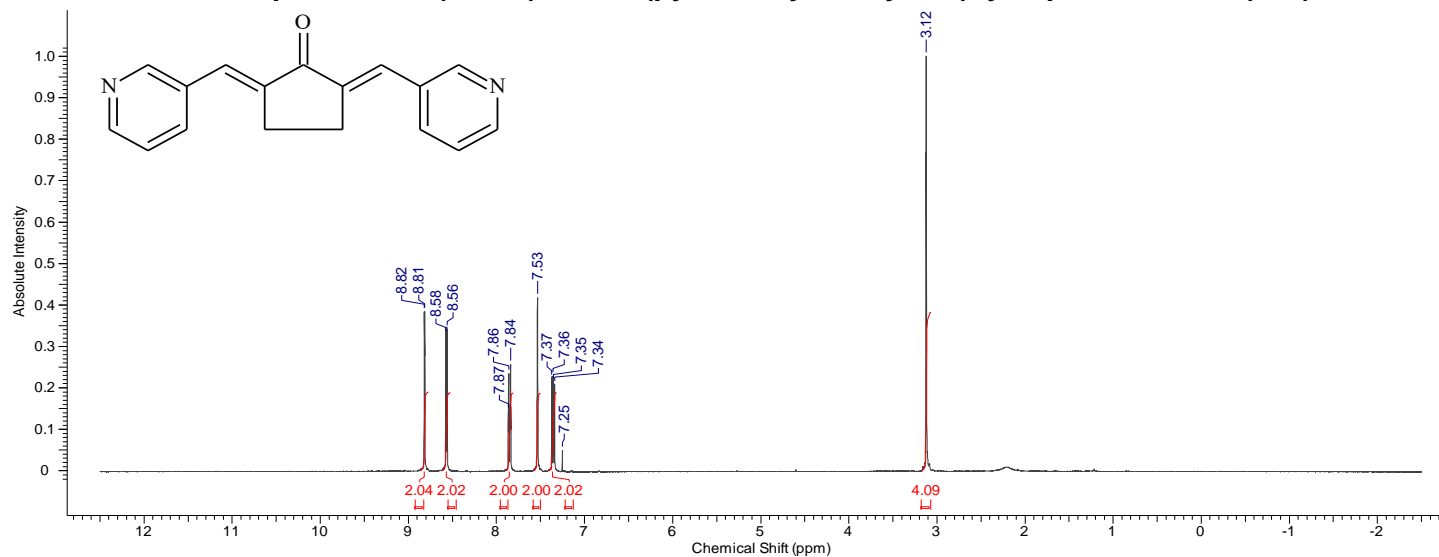


Carbon spectrum of (2E,5E)-2,5-bis(pyridin-2-ylmethylene)cyclopentan-1-one (23d)

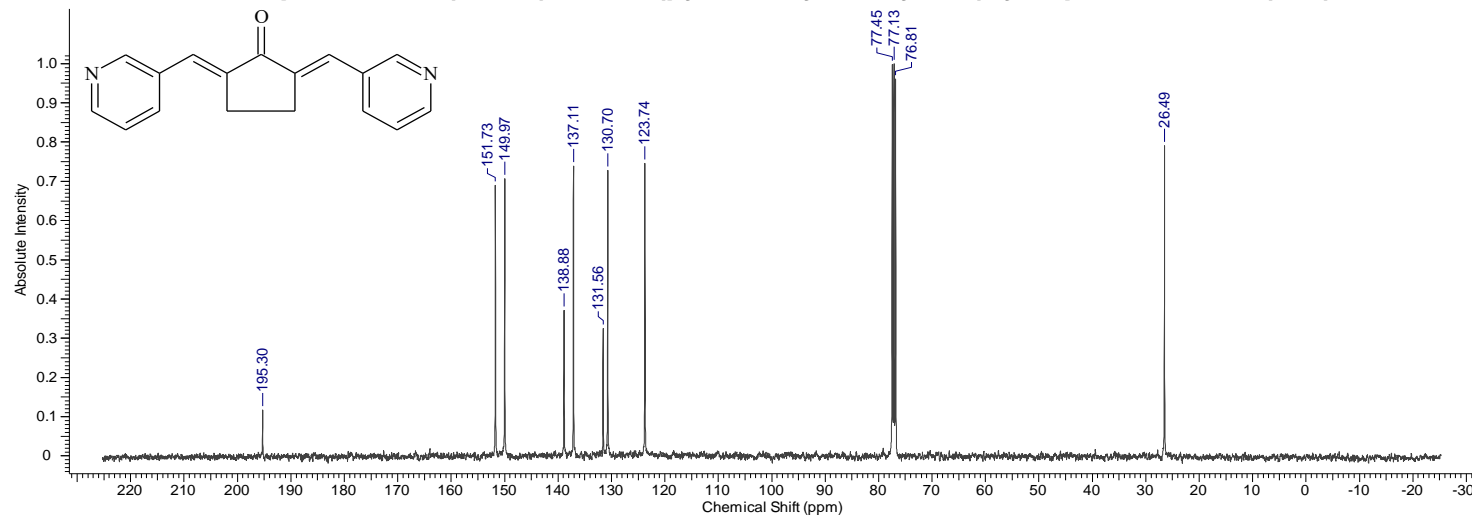


Compound 23e

Proton spectrum of (2E,5E)-2,5-bis(pyridin-3-ylmethylene)cyclopentan-1-one (23e)

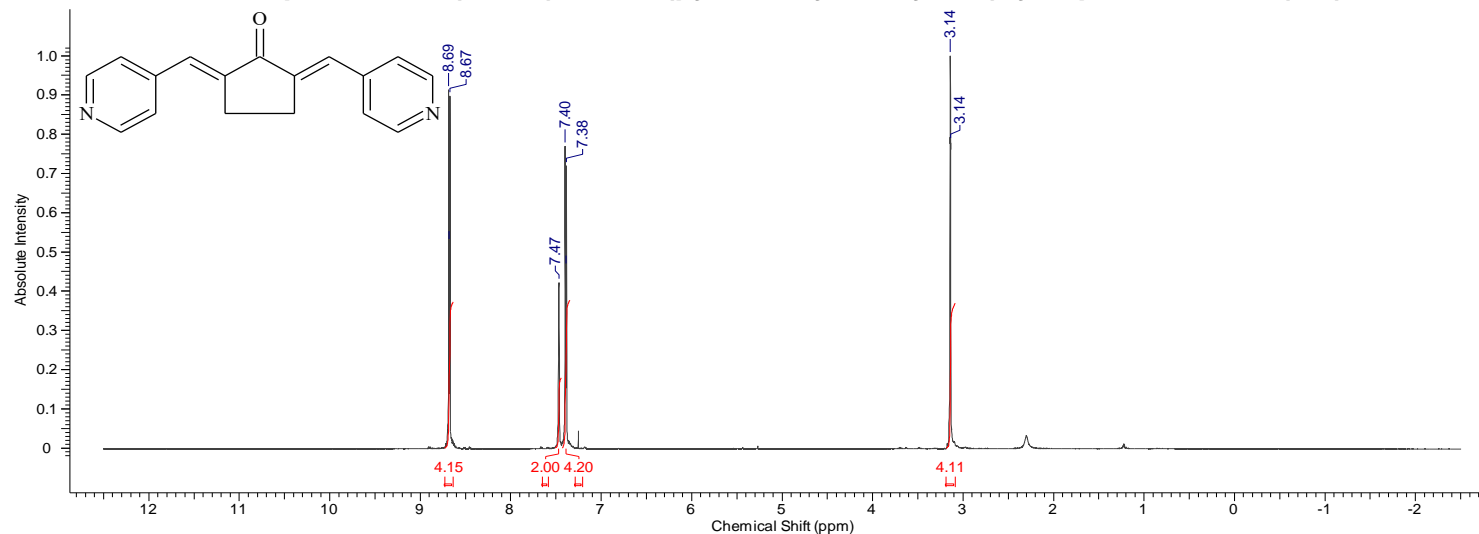


Carbon spectrum of (2E,5E)-2,5-bis(pyridin-3-ylmethylene)cyclopentan-1-one (23e)

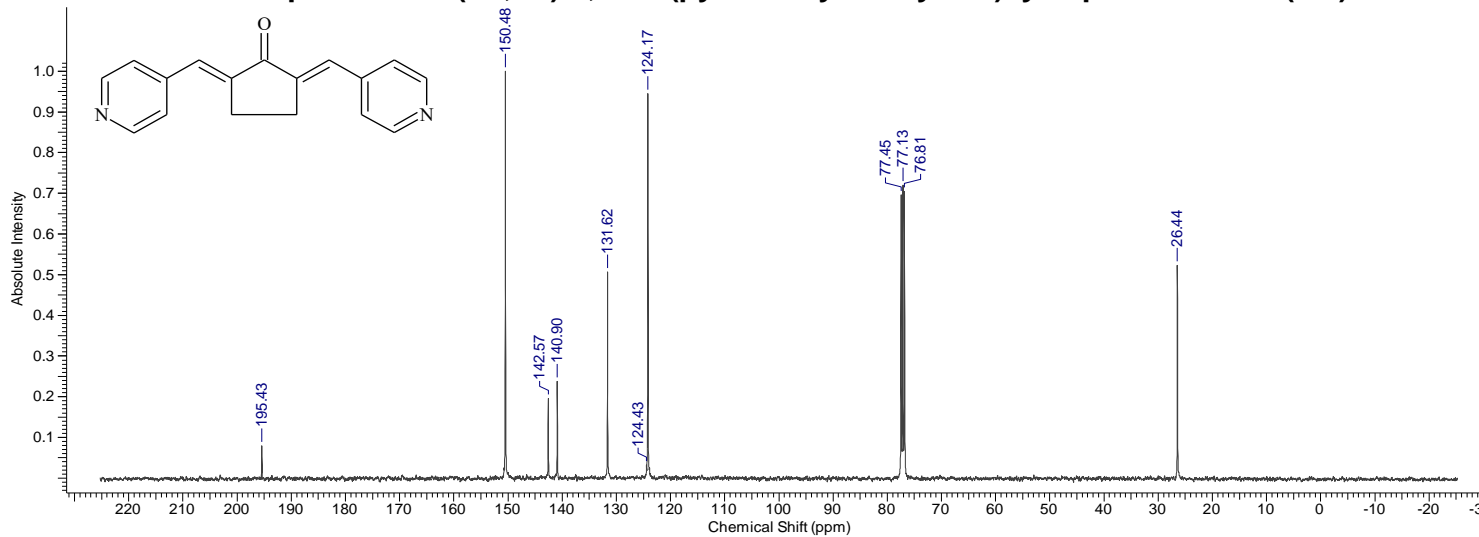


Compound 23f

Proton spectrum of (2E,5E)-2,5-bis(pyridin-4-ylmethylene)cyclopentan-1-one (23f)

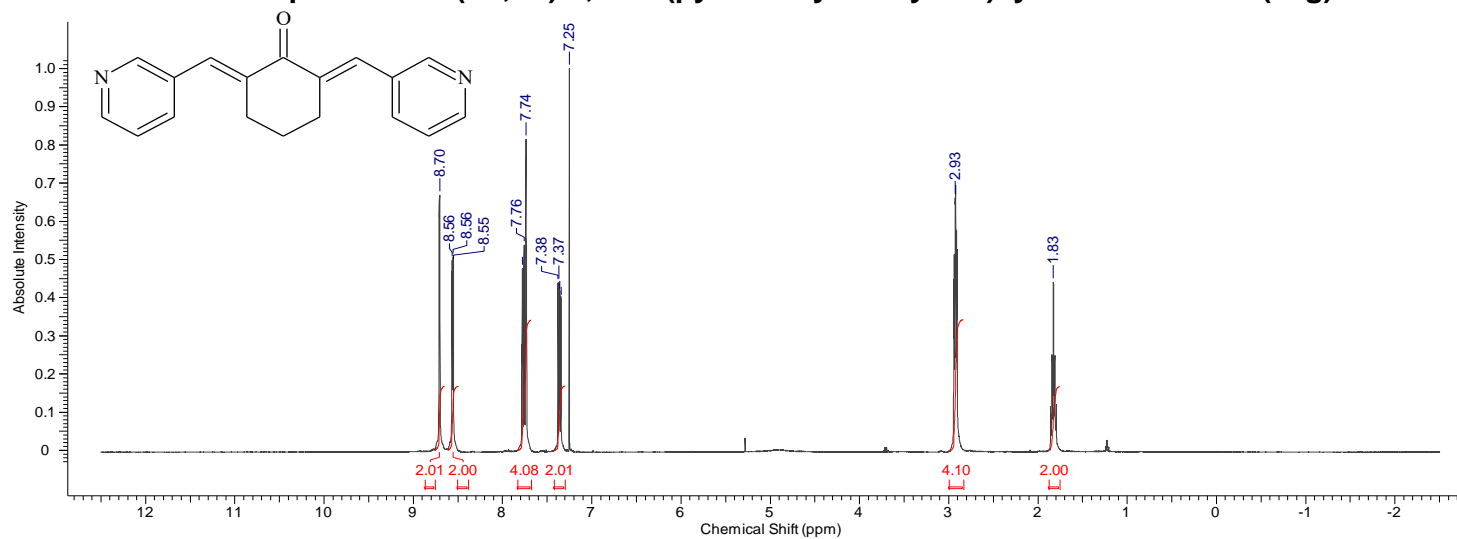


Carbon spectrum of (2E,5E)-2,5-bis(pyridin-4-ylmethylene)cyclopentan-1-one (23f)

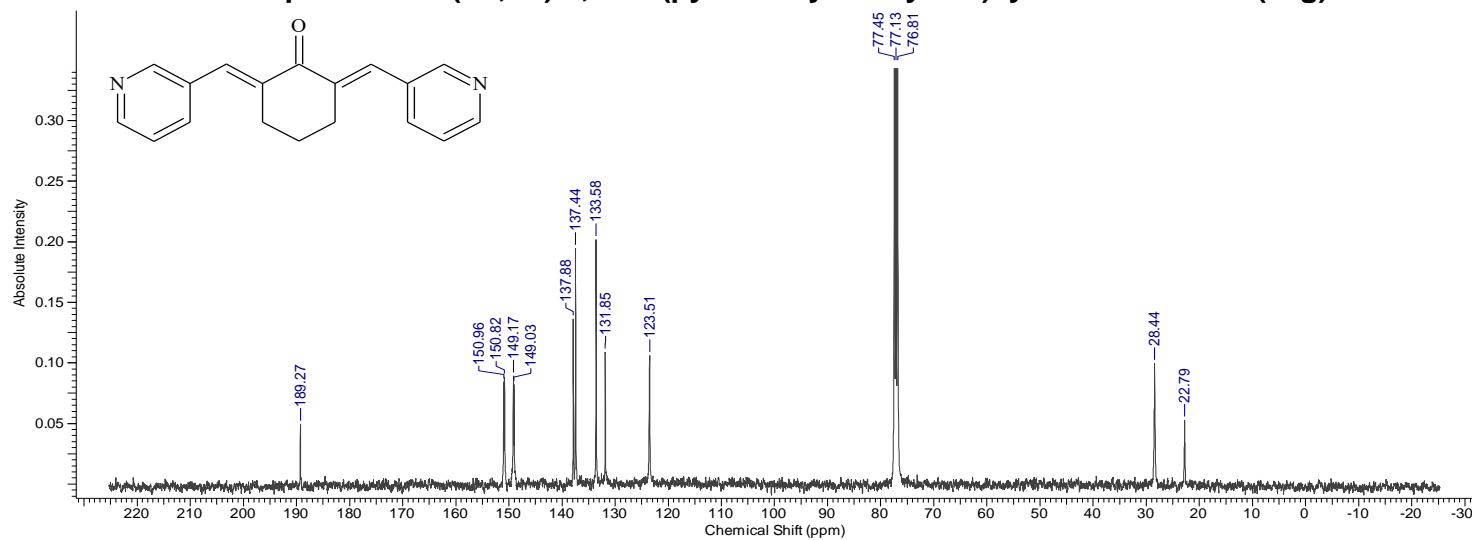


Compound 23g

Proton spectrum of (2E,6E)-2,6-bis(pyridin-3-ylmethylene)cyclohexan-1-one (23g)

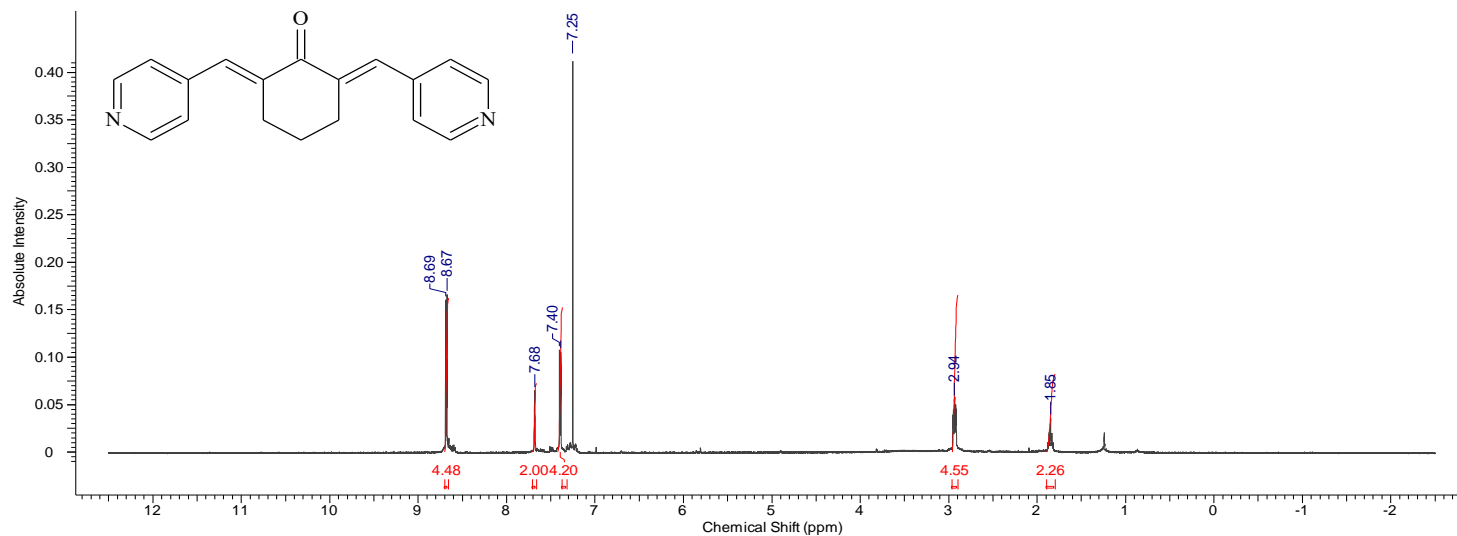


Carbon spectrum of (2E,6E)-2,6-bis(pyridin-3-ylmethylene)cyclohexan-1-one (23g)

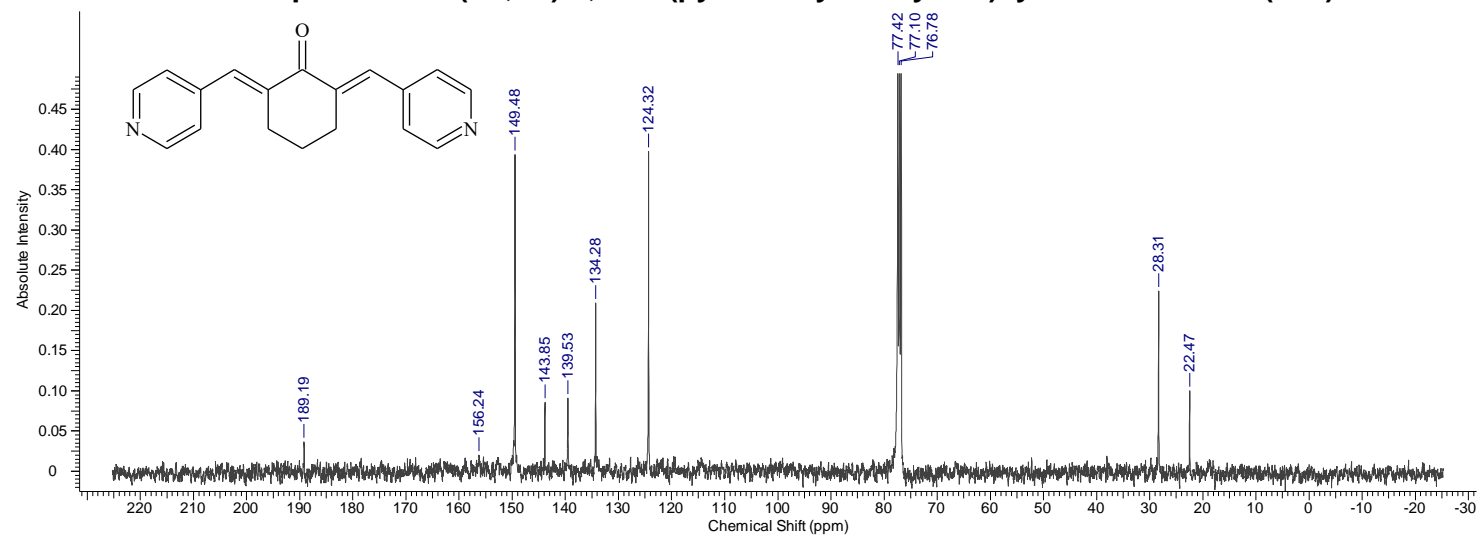


Compound 23h

Proton spectrum of (2E,6E)-2,6-bis(pyridin-4-ylmethylene)cyclohexan-1-one (23h)

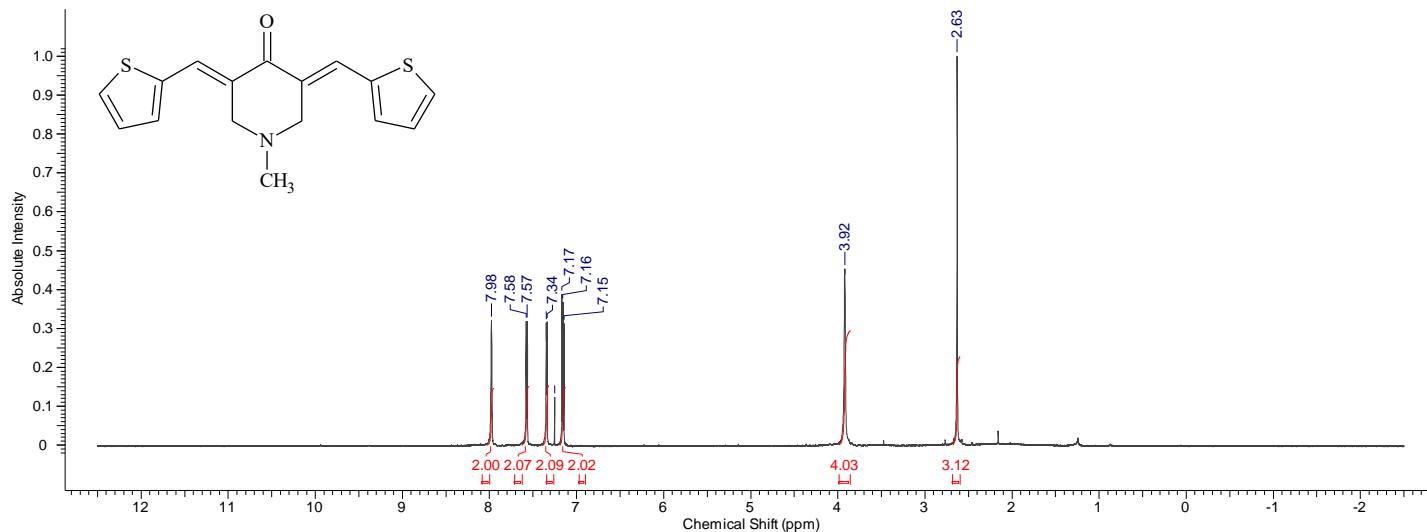


Carbon spectrum of (2E,6E)-2,6-bis(pyridin-4-ylmethylene)cyclohexan-1-one (23h)

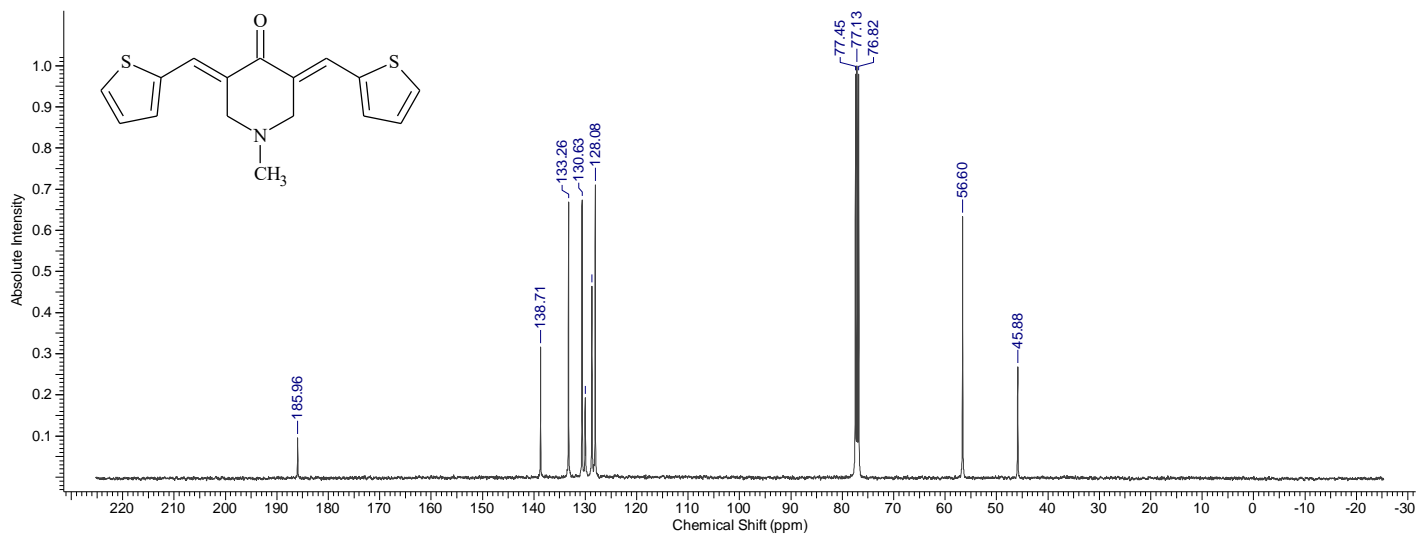


Compound 24a

Proton spectrum of (3E,5E)-1-methyl-3,5-bis(thiophen-2-ylmethylene)piperidin-4-one (24a)

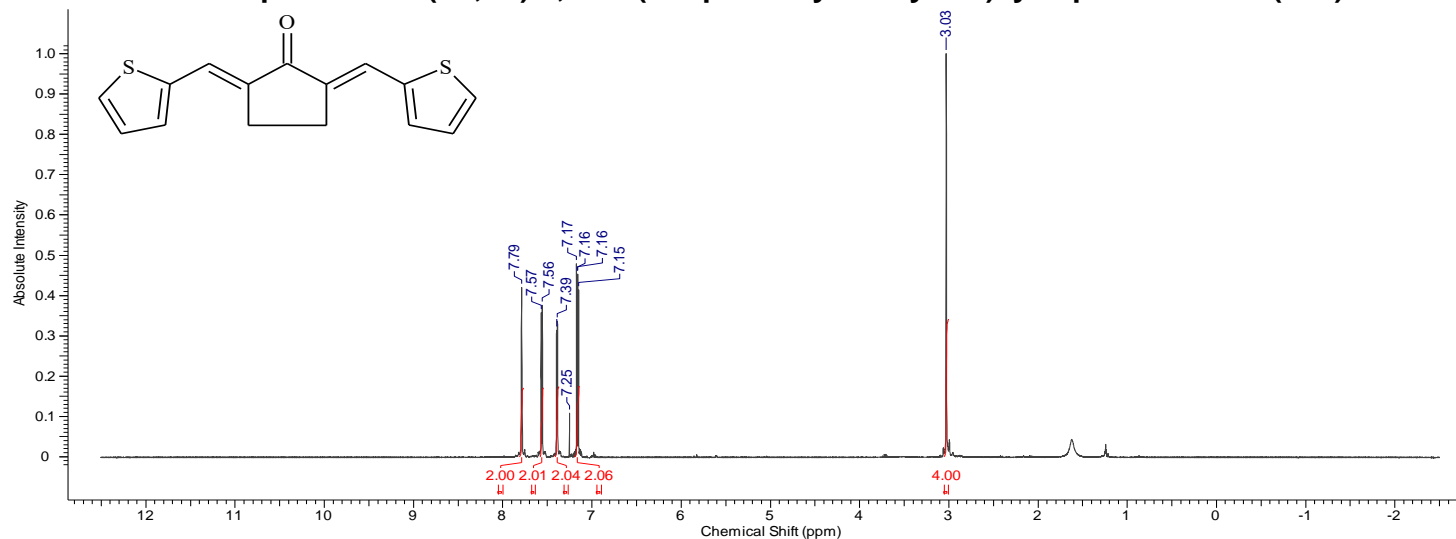


Carbon spectrum of (3E,5E)-1-methyl-3,5-bis(thiophen-2-ylmethylene)piperidin-4-one (24a)

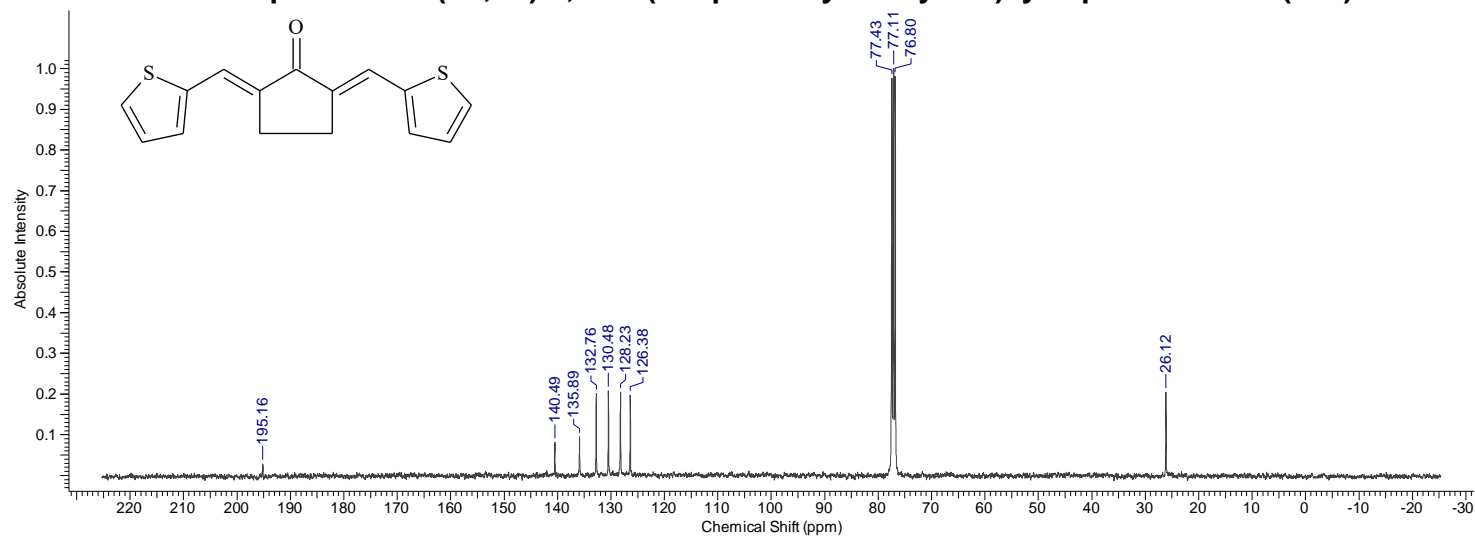


Compound 24b

Proton spectrum of (2E,5E)-2,5-bis(thiophen-2-ylmethylene)cyclopentan-1-one (24b)

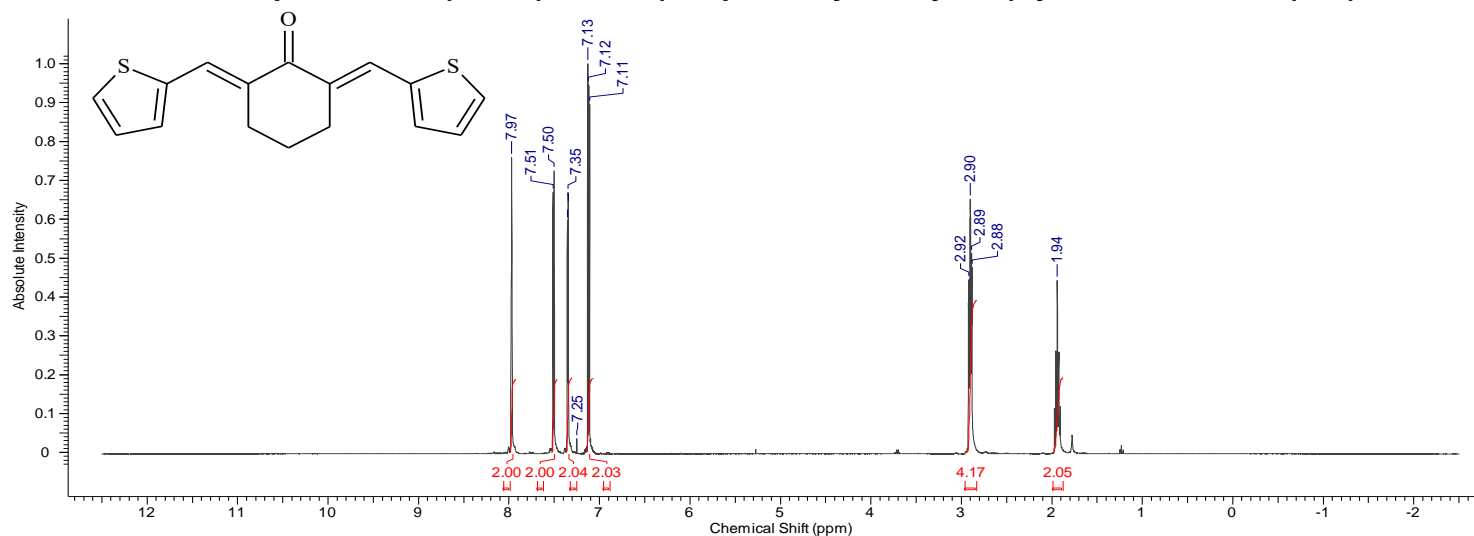


Carbon spectrum of (2E,5E)-2,5-bis(thiophen-2-ylmethylene)cyclopentan-1-one (24b)

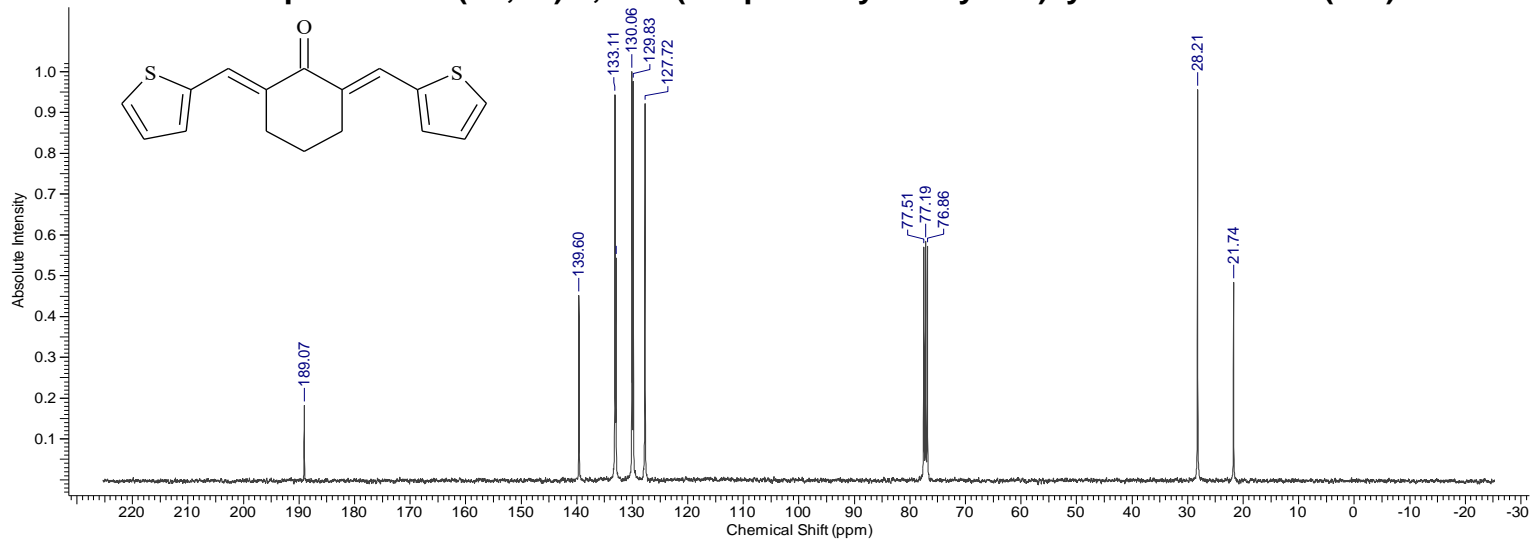


Compound 24c

Proton spectrum of (2E,6E)-2,6-bis(thiophen-2-ylmethylene)cyclohexan-1-one (24c)

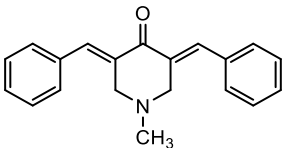
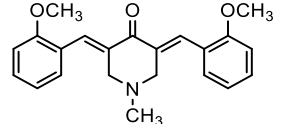
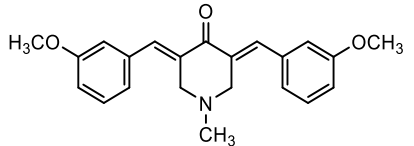
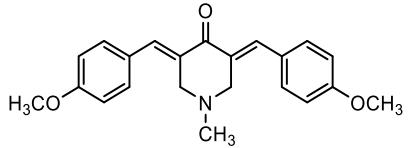
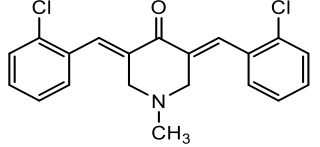
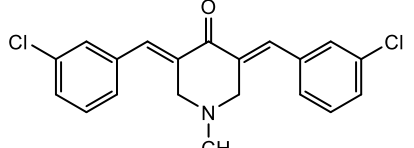
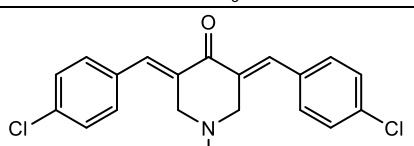
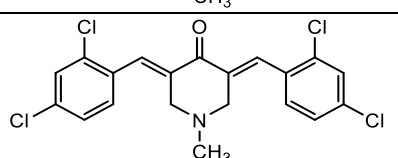
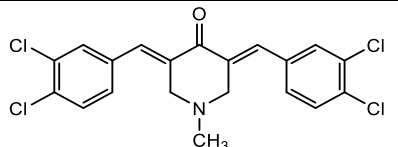


Carbon spectrum of (2E,6E)-2,6-bis(thiophen-2-ylmethylene)cyclohexan-1-one (24c)



Appendix 2 List of synthesized 1,4-diene-3-ones with their chemical names, structures and molecular weight

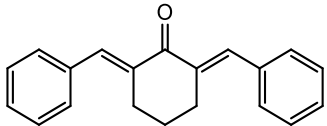
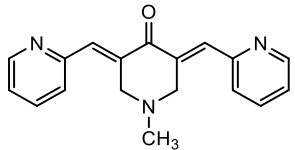
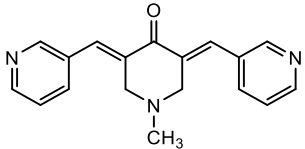
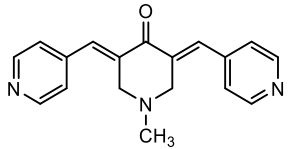
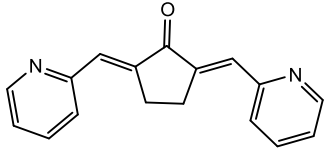
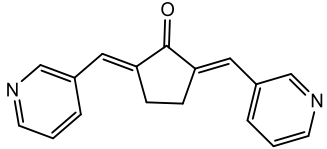
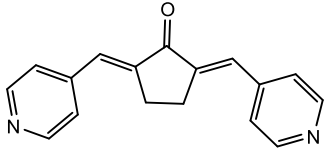
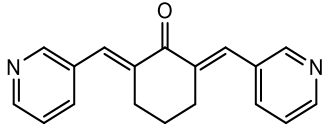
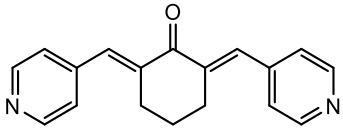
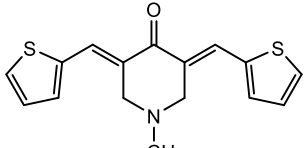
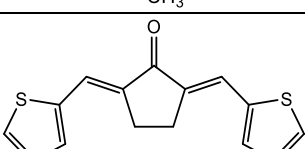
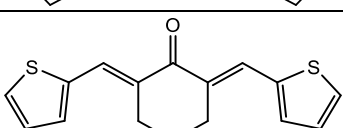
Table 7. 1. Appendix. List of synthesized 1,4-diene-3-ones with detailed information about their chemical structures, chemical names and molecular weight.

Compound numbers	Compound structures	Chemical names	Molecular weight
22a		3,5-bis[(E)-(benzylidene)]-1-methylpiperidin-4-one	289.37
22b		3,5-bis[(E)-(2-methoxybenzylidene)]-1-methylpiperidin-4-one	349.43
22c		3,5-bis[(E)-(3-methoxybenzylidene)]-1-methylpiperidin-4-one	349.43
22d		3,5-bis[(E)-(4-methoxybenzylidene)]-1-methylpiperidin-4-one	349.43
22e		3,5-bis[(E)-(2-chlorobenzylidene)]-1-methylpiperidin-4-one	358.26
22f		3,5-bis[(E)-(3-chlorobenzylidene)]-1-methylpiperidin-4-one	358.26
22g		3,5-bis[(E)-(4-chlorobenzylidene)]-1-methylpiperidin-4-one	358.26
22h		3,5-bis[(E)-(2,4-dichlorobenzylidene)]-1-methylpiperidin-4-one	427.15
22i		3,5-bis[(E)-(3,4-dichlorobenzylidene)]-1-methylpiperidin-4-one	427.15

Appendix 2 Chemical information of synthesized 1,4-diene-3-ones

22j		2,2'-((1 <i>E</i> ,1' <i>E</i>)-(1-methyl-4-oxopiperidine-3,5-diylidene)bis(methaneylylidene))-dibenzoic acid	377.41
22k		4,4'-((1 <i>E</i> ,1' <i>E</i>)-(1-methyl-4-oxopiperidine-3,5-diylidene)bis(methaneylylidene))-dibenzoic acid	377.41
22l		3,5-bis[(<i>E</i>)-(4-methylbenzylidene)]-1-methylpiperidin-4-one	317.43
22m		3,5-bis[(<i>E</i>)-(3-trifluoromethylbenzylidene)]-1-methylpiperidin-4-one	425.37
22n		3,5-bis[(<i>E</i>)-(4-trifluoromethylbenzylidene)]-1-methylpiperidin-4-one	425.37
22o		3,5-bis[(<i>E</i>)-(3-trifluoromethoxybenzylidene)]-1-methylpiperidin-4-one	457.30
22p		3,5-bis[(<i>E</i>)-(4-trifluoromethoxybenzylidene)]-1-methylpiperidin-4-one	457.30
22q		3,5-bis[(<i>E</i>)-(2-iodobenzylidene)]-1-methylpiperidin-4-one	540.84
22r		3,5-bis[(<i>E</i>)-(3-iodobenzylidene)]-1-methylpiperidin-4-one	540.84
22s		3,5-bis[(<i>E</i>)-(3-nitrobenzylidene)]-1-methylpiperidin-4-one	379.04
22t		3,5-bis[(<i>E</i>)-(4-nitrobenzylidene)]-1-methylpiperidin-4-one	379.04
22u		2,5-bis[(<i>E</i>)-(benzylidene)]cyclopentan-1-one	260.12

Appendix 2 Chemical information of synthesized 1,4-diene-3-ones

22v		2,6-bis[(<i>E</i> -benzylidene)]cyclohexan-1-one	274.14
23a		(<i>3E,5E</i>)-1-methyl-3,5-bis(pyridin-2-ylmethylene)piperidine-4-one	291.35
23b		(<i>3E,5E</i>)-1-methyl-3,5-bis(pyridin-3-ylmethylene)piperidine-4-one	291.35
23c		(<i>3E,5E</i>)-1-methyl-3,5-bis(pyridin-4-ylmethylene)piperidine-4-one	291.35
23d		(<i>2E,5E</i>)-2,5-bis(pyridin-2-ylmethylene)cyclopentan-1-one	262.31
23e		(<i>2E,5E</i>)-2,5-bis(pyridin-3-ylmethylene)cyclopentan-1-one	262.31
23f		(<i>2E,5E</i>)-2,5-bis(pyridin-4-ylmethylene)cyclopentan-1-one	262.31
23g		(<i>2E,6E</i>)-2,6-bis(pyridin-3-ylmethylene)cyclohexan-1-one	276.33
23h		(<i>2E,6E</i>)-2,6-bis(pyridin-4-ylmethylene)cyclohexan-1-one	276.33
24a		(<i>3E,5E</i>)-1-methyl-3,5-bis(thiophen-2-ylmethylene)piperidin-4-one	301.42
24b		(<i>2E,5E</i>)-2,5-bis(thiophen-2-ylmethylene)cyclopentan-1-one	272.38
24c		(<i>2E,6E</i>)-2,6-bis(thiophen-2-ylmethylene)cyclohexan-1-one	286.41

Communications

Publication

Patel Dhruvnesh V, Bassin, Jatinder P and Griffiths, David G. (2017) *Synthesis and evaluation of novel antifungal agents targeted to the plasma membrane H⁺-ATPase (2017)*. British Journal of Pharmacy, 2(2). pp. 29-40. <https://doi.org/10.5920/bjpharm.2017.28>. [Abstract].

Oral Presentation

Dhruvnesh V. Patel, Jatinder P. Bassin, David G. Griffiths. Synthesis and evaluation of novel antifungal agents targeted to the plasma membrane H⁺-ATPase (2017). *School of Life and Medical Sciences Research Conference*, University of Hertfordshire, Hatfield.

Posters

Dhruvnesh V. Patel, Jatinder P. Bassin, David G. Griffiths. Synthesis and evaluation of dienones as novel antifungal agents (2018). *RSC – Chemical Biology meets Drug Discovery*, GSK Medicines Research Centre, Stevenage.

Dhruvnesh V. Patel, Jatinder P. Bassin, David G. Griffiths. Synthesis and evaluation of novel antifungal agents targeted to the plasma membrane H⁺-ATPase (2017). *The JPAG Pharmaceutical Analysis Postgraduate Research & Careers Symposium*, Royal Society of Chemistry, Burlington House, London.

Dhruvnesh V. Patel, Jatinder P. Bassin, David G. Griffiths. Synthesis and evaluation of novel antifungal agents targeted to the plasma membrane H⁺-ATPase (2017). *APS International PharmSci Conference*, University of Hertfordshire, Hatfield.

Dhruvnesh V. Patel, Jatinder P. Bassin, David G. Griffiths. Synthesis and evaluation of novel antifungal agents targeted to the plasma membrane H⁺-ATPase (2017). *The 2nd Symposium on Transporters in Drug Discovery and Development*, Royal Society of Chemistry, Burlington House, London.

Dhruvnesh V. Patel, Jatinder P. Bassin, David G. Griffiths. Design and synthesis of benzylidene, pyridylidene and thienylidene derivatives of N-methylpiperidin-4-one and other cycloalkanones as potential antifungal agents (2016). *RSC - Chemical Biology & Bio-organic Group Meeting*, The University of Nottingham, Nottingham.

Dhruvnesh V. Patel, Jatinder P. Bassin, Stewart B. Kirton, David G. Griffiths. Design and synthesis of benzylidene, pyridylidene and thienylidene derivatives of N-methylpiperidin-4-one and other cycloalkanones as potential antifungal agents (2016). *School of Life and Medical Sciences Research Conference*, University of Hertfordshire, Hatfield.

Dhruvnesh V. Patel, Idhnan A. Hussain, Jatinder P. Bassin, Stewart B. Kirton, David G. Griffiths. Growth inhibition of *Saccharomyces cerevisiae* by benzylidene and pyridylidene derivatives of N-methylpiperidin-4-one and other cycloalkanones (2015). *School of Life and Medical Sciences Research Conference*, University of Hertfordshire, Hatfield.

Dhruvnesh V. Patel, Idhnan A. Hussain, Jatinder P. Bassin, Stewart B. Kirton, Jennifer J. Young, David G. Griffiths. Synthesis and antifungal testing of benzylidene derivatives of piperidone (2014). *APS International PharmSci Conference*, University of Hertfordshire, Hatfield.